Cortical Adaptation and Frequency Selectivity: From Single Neurons to Evoked Potentials

By Oscar Woolnough BEng MSc

Thesis submitted to the University of Nottingham for the degree of Doctor of Philosophy

September 2016

Abstract

Adaptation is a reduction in a neural response to a sensory stimulus resulting from repeated presentation of the stimulus and is an important aspect of sensory neural coding. This phenomenon is sensitive to changes in parameters of the repeating stimuli and the adaptation will be greatest when the stimuli are identical and diminish with changes in stimulus parameters between repetitions.

In the auditory system it has been shown the specificity of cortical adaptation relates primarily to the frequency of a stimulus, with wider frequency separations between sequentially presented stimuli resulting in a reduced level of adaptation. This frequency specific adaptation has been measured at multiple scales, in EEG recordings in humans and at the single unit level in animals but the results from each implicate different underlying neural mechanisms.

This thesis attempts to elucidate some of those differences by investigating the effects of the differences in methodology between the studies, the inter-species differences in adaptation characteristics and the effects of anaesthesia on sensory neural processing. This touches upon the forward and inverse modelling problems in computational neuroscience and also the issues with relating results from EEG in awake humans with single neuron recordings in anaesthetised animals.

The thesis starts by building on previous work looking at whether the frequency selectivity of adaptation can be changed by the temporal properties of the adapting stimuli. It was found that a sharpening of frequency selectivity of adaptation could be induced by using multiple repeated adapters but not with single onset, prolonged duration adapters. This repetition induced sharpening was also shown to act independently of attention despite there being an attentionally induced sharpening effect on adaptation.

This EEG adaptation tuning was explained by an extension of a computational model previously proposed to explain stimulus specific adaptation and oddball responses in single neurons. The model was a two-layer network with independently adapting synapses and is able to quantitatively reproduce the observed non-monotonic adaptation and sharpening of tuning observed in our EEG responses, and the effects of repeated and prolonged adapters.

To further investigate this then this study was replicated in an anaesthetised animal model with recordings directly from auditory cortex. This study showed none of the repetition induced sharpening effects and dramatically quantitatively different adaptation results compared to the human studies.

To help explain these results then recordings were made in awake guinea pigs with chronically implanted intracranial EEG electrodes and invasive depth electrodes to discover whether these differences were a result of species or anaesthesia. These experiments start to explain some of the discrepancies seen before, with adaptation time constants orders of magnitude different to those in humans and differences in their innate frequency selectivity.

Alongside this then the effects of anaesthesia on the results were investigated under a range of anaesthetic regimes including opiates, NMDA antagonists and GABA potentiators. It was shown that anaesthetic choice has substantial effects on sensory signalling, temporal processing and cross-modal interactions which result in multifaceted effects on the characteristics of adaptation.

This thesis builds on previous work on the plasticity of frequency selectivity of adaptation in auditory cortex and helps to characterise this phenomenon and explain its mechanisms. This work also highlights the difficulties of directly relating studies and findings between humans and animal studies of the auditory system, demonstrating the magnitude of difference in temporal and frequency processing between species and also shows the substantial changes in sensory processing induced by anaesthesia and modulated by anaesthetic choice.

Contents

List of Abbreviations

A1	Primary Auditory Cortex
ABR	Auditory Brainstem Response
ACh	Acetylcholine
AEP	Auditory Evoked Potential
AM	Amplitude Modulated
AP	Action Potential
ASSR	Auditory Steady State Response
BF	Best Frequency
CF	Characteristic Frequency
CN	Cochlear Nucleus
CSD	Current Source Density
CSI	Common Stimulus Specific Adaptation Index
DMT	Dimethyltryptamine
ECoG	Electrocorticography
EEG	Electroencephalography
fAHP	Fast Afterhyperpolarisation
FFT	Fast Fourier Transform
FSA	Frequency Specific Adaptation
GABA	γ-Aminobutyric acid
GP	Guinea Pig
IAI	Inter-Adapter Interval
IC	Inferior Colliculus
ICA	Independent Component Analysis
iEEG	Intracranial Electroencephalography
ISI	Inter-Stimulus Interval
KS	Kolmogorov-Smirnov
LFP	Local Field Potential
LOC	Loss of Consciousness
mAHP	Middle-duration Afterhyperpolarisation
MGB	Medial Geniculate Body
MI	Mutual Information
MMN	Mismatch Negativity
MU	Multi-Unit
MUA	Multi-Unit Activity
NE	Norepinephrine
NMDA	*N*-Methyl-D-aspartic acid
PSTH	Post Stimulus Time Histogram
RF	Receptive Field
RIS	Repetition Induced Sharpening
sAHP	Slow Afterhyperpolarisation
SC	Synchronisation Coefficient

SD	Standard Deviation
SE	Standard Error
SI	Stimulus Specific Adaptation Index
SNR	Signal to Noise Ratio
SOA	Stimulus Onset Asynchrony
SSA	Stimulus-Specific Adaptation
STP	Short Term Plasticity

Chapter 1

General Introduction

Adaptation is a reduction in a neural response to a sensory stimulus resulting from repeated presentation of the stimulus. This phenomenon is sensitive to changes in parameters of the repeating stimuli and the adaptation will be greatest when the stimuli are identical and diminish with changes in stimulus parameters between repetitions.

In the auditory system it has been shown the specificity of cortical adaptation relates primarily to the frequency of a stimulus, with wider frequency separations between sequentially presented stimuli resulting in a reduced level of adaptation. This adaptation has been measured at multiple scales, in EEG recordings (Briley and Krumbholz, 2013) and at the single unit level (Scholes et al., 2011). Three main models of the neural basis of adaptation have been proposed, the Fatigue model, Sharpening model and Facilitation model (Grill-Spector et al., 2006) which are further elaborated on later (Section 1.2.2).

Briley and Krumbholz (2013) used computational models of neuronal firing to simulate the human EEG data they had collected, comparing both the Fatigue and Sharpening models of adaptation. They found that for single adapters the Fatigue based computational model showed a close agreement with the data whereas the Sharpening model did not. However with multiple adapters they needed to add a Sharpening characteristic to the Fatigue model to maintain a good fit.

The study by Scholes et al. (2011) measured single neuron responses to adapting stimuli in guinea pigs which found evidence of a small number of units showing Fatigue, some showing an adapter frequency specific

suppression, termed frequency specific adaptation (FSA), and no evidence of either Sharpening or Facilitation. The FSA response does not fit with any of the three proposed models as they all suggest changes to neural responses are dependent on the neuron's characteristic frequency (CF), though the FSA response is independent of unit CF.

The reasons for the differences in prediction have not yet been discovered and could be related to a multitude of factors. For example, the different recording methodologies of EEG and single units, as well as differences in stimulus presentation paradigms, inter-species differences between humans and guinea pigs and the comparison of awake and anaesthetised recordings may be causing these differences.

The aim of this project is to attempt to elucidate these differences by using comparative electrophysiology in humans and an animal model, and making simultaneous multi-scale neural recordings of cortical adaptation within an animal model. This will touch upon the forward and inverse modelling problems in computational neuroscience and also the issues with comparing results from EEG in awake humans with single neuron recordings in anaesthetised animals. The studies in this thesis will broadly cover three main themes:

- How does adaptation affect frequency selectivity in auditory cortex?
- How can we relate invasive studies of auditory cortex in animals to human EEG potentials?
- To what degree does anaesthesia disrupt auditory processing in the brain?

This chapter will cover a review of pertinent literature to this thesis, starting with details of the practicalities and biophysics underlying common electrophysiological measurement techniques. This is followed by a review of the characteristics and proposed mechanisms behind auditory adaptation and

then a summary of the known effects of general anaesthesia on auditory neural processing.

1.1 Electrophysiological Recordings

Electrophysiological neural activity can be recorded from multiple scales, representing single neurons, local circuits or whole functional systems. Recording from each of these scales relies on different electrical principles and requires different techniques.

1.1.1 Single Unit recording

Recordings of cortical spiking activity are done by inserting small surface area microelectrodes into the cortex. Commonly used probe types include wire electrodes, which will have a single exposed recording site at their tip with the rest of the wire coated in an insulating material, and silicon electrodes, which will have multiple recording sites along a thin silicon shank. To avoid picking up local field potentials but to maintain the rapid voltage changes of the spikes typically the recordings are band-pass filtered between 300-3000 Hz. When recording in cortex it is incredibly difficult to make intracellular recordings due to poor visibility through the cortex, so instead extracellular potentials are typically monitored. This results in recordings of this type typically picking up the activity of several neighbouring neurons.

Using spike sorting algorithms, it is often possible to attribute individual spikes to the individual neurons that generated them by looking at the temporal and amplitude parameters of the action potentials. This is possible as neurons show an all-or-nothing response to firing, meaning all action potentials from a given neuron will be roughly the same magnitude and morphology. By parameterising the recorded spikes' properties from a multi-unit electrode, such as spike amplitude and the relative latencies of their peaks, troughs and inflection points, and submitting them to dimensionality reduction and cluster analysis it is possible to distinguish between the units being recorded from (Quiroga and Panzeri, 2009; Buzsáki et al., 2012; Marblestone et al., 2013).

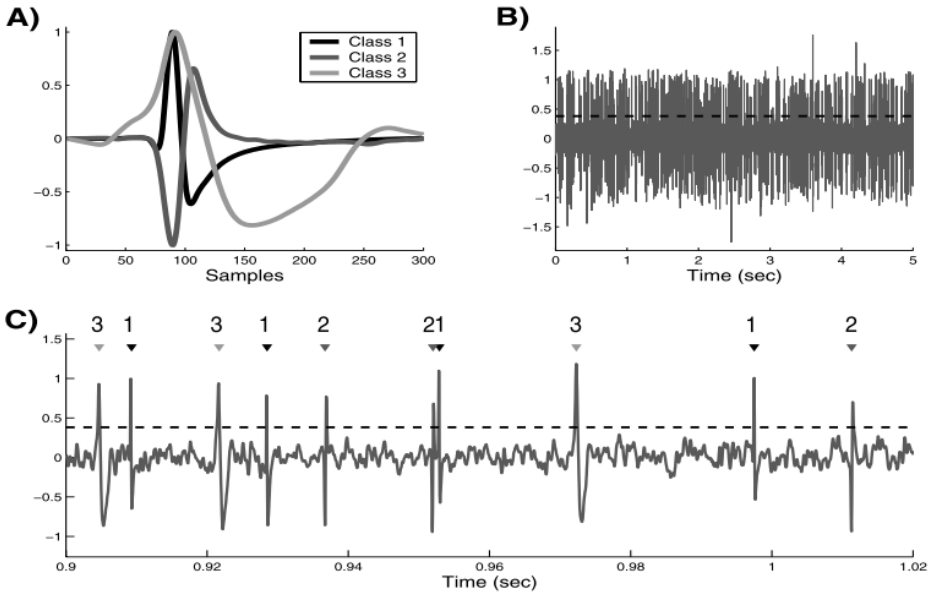

Figure 1.1: Simulated spike sorting dataset showing three spike morphologies (A) embedded in noise (B,C). Spike events can be detected by a constant threshold (dashed line) and attributed to multiple units by using a spike sorting algorithm (Quiroga et al., 2004)

By using the spike morphology and peak latencies it is also possible to putatively designate units as excitatory pyramidal cells or inhibitory interneurons. This method was developed from experiments in somatosensory and prefrontal cortex where it was demonstrated that spike duration of pyramidal cells (0.86 ± 0.17ms) was significantly different to that of inhibitory cells (0.43 ± 0.27ms). They found by plotting the half-amplitude duration against the trough to peak time of a unit's spike shape it was possible to define discrete clusters of excitatory and inhibitory cells (Barthó et al., 2004).

Analysis of spike trains typically looks into the changing spiking rates of individual neurons in response to a certain stimuli but it is currently theorised that neurons can work on a rate-place code, with the timing of the spikes adding information along with the overall rate.

1.1.2 Local Field Potentials (LFPs)

Local field potentials are the summation of extracellular currents of small populations of neurons, usually recorded from within the cortex. They can be recorded simultaneously with single unit activity by low pass filtering the raw

recorded signal with a cut-off of 300 Hz to remove the spiking activity but to retain the neural oscillatory activity representing a wider area of effect than the recorded single units.

The amplitude, polarity and morphology of individual neuron's contributions to local field potentials depends heavily on the location of the recording electrode relative to the neuron (Figure 1.2). The dominating source of the extracellular currents are synaptic input and return currents, with input currents representing a negative voltage deflection and return currents a positive one.

The neuron's structure will also affect its contribution as pyramidal cells, such as the one in figure 1.2, have an open-field structure with a substantial spatial separation between the synapses and the soma leading to a large area of effect. This is in comparison to stellate cells which have a roughly spherical shape with little separation between synapses and soma resulting in little separation between synaptic input currents and somatic return currents, leading to them having a closed-field structure, only producing a very local net current change (Einevoll et al., 2013). In the cortex, pyramidal cells are excitatory, glutamatergic neurons and stellate cells are inhibitory, GABAergic neurons which results in the LFP signals being dominated by the activity of the excitatory pathway with little input from the inhibitory pathways.

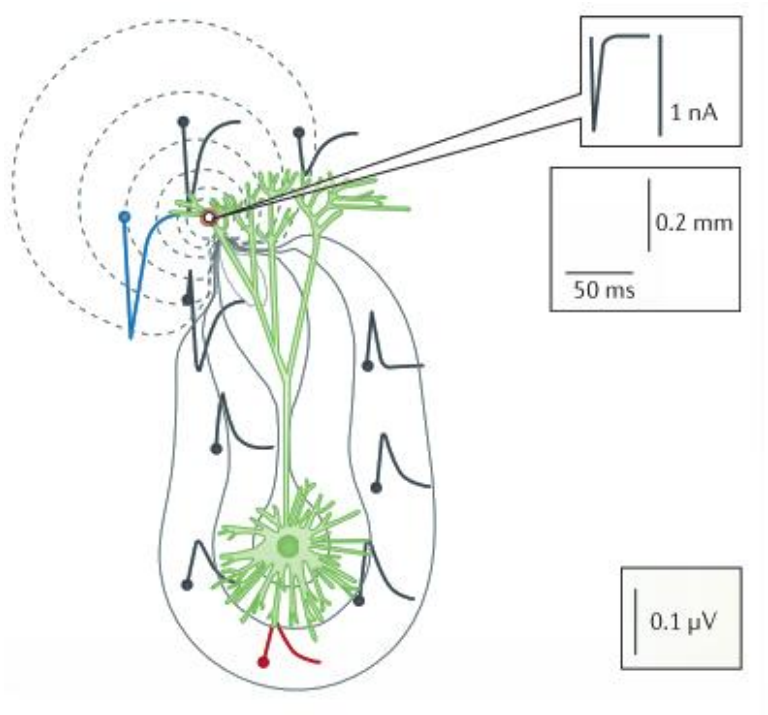

Figure 1.2: A reconstructed neuron from visual cortex showing simulated local field potentials following stimulation by a single excitatory synapse at an apical branch, demonstrating the variability of recorded LFPs with electrode location (Einevoll et al., 2013).

The cortex is arranged in a layered structure starting with the deepest Layer VI, at the interface between the cortex and the thalamus, to the most superficial Layer I at the cortical surface. Each layer comprises a different cytoarchitecture with varying pyramidal cell morphologies and variable pyramidal to stellate cell ratios. Primary auditory cortex is organised in a columnar structure with each column having a preferred frequency which will lead to a maximal neural response. These columns are arranged in a tonotopic gradient across the cortex. In response to auditory stimulation neural signalling will progress vertically through the column, with the middle layers receiving input from the medial geniculate body (MGB) before relaying to the higher, supragranular layers then back down to the deeper, infragranular layers (Linden and Schreiner, 2003).

Using this knowledge about the functional organisation of the cortex we can use a common analysis technique performed on LFPs recorded with depth

electrodes, current source density (CSD) analysis. CSD is calculated as the second spatial derivative of the measured voltage (Equation 1.1).

$$CSD = \frac{V(z+h) - 2V(z) + V(z-h)}{h^2} \tag{1.1}$$

Where $V(z)$ is the measured voltage at depth z, and h is the distance between electrodes.

This analysis shows the rate of change in current between two electrodes, representing how active the neurons between the recording sites are. Current sources are associated with net local outward transmembrane currents whereas sinks represent local transmembrane current flows into the neurons (Kajikawa and Schroeder, 2011). This allows inferences to be made about which cortical layers respond most strongly to the presented stimuli more than purely measuring response amplitudes.

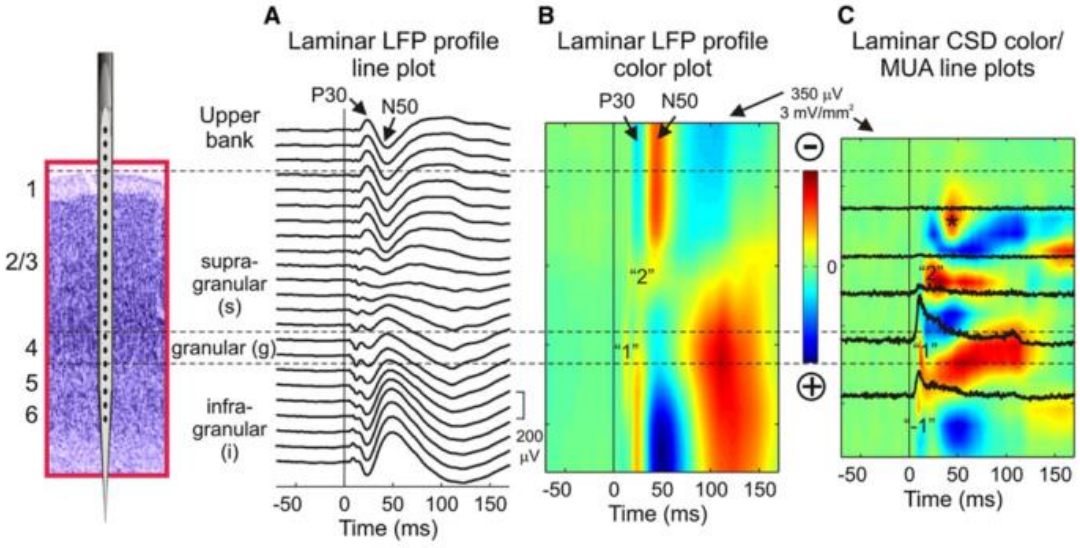

Figure 1.3: Recorded LFP traces from macaque A1 in response to a pure tone stimuli. Presented as raw voltage traces (A) and as an interpolated colour plot (B). C shows the CSD analysis results representing extracellular current sinks in red and current sources in blue (Kajikawa and Schroeder, 2011)

1.1.3 Electroencephalography (EEG)

Electroencephalography is a non-invasive method of recording neural population dynamics in the brain. It records the far-field effects of the current dipoles established by neural activity.

One requirement for producing a meaningfully large EEG potential is synchronicity. As the scalp-recorded potential is summing the potentials of the individual neurons, a large number of them must fire near simultaneously for their compound action to be detected at the surface.

Due to the generation of EEG dipoles by the vector sum of ion current flow around neurons the vector direction must also be considered. Only neurons with spatial alignment of their current flows will be able to produce meaningful far field potentials as otherwise the current vectors will cancel and will be unable to be detected at a far field level. This results in certain structures producing stronger EEG signals than others, for example the auditory nerve consists of around 30,000 parallel nerve fibres, firing near simultaneously in a compound action potential, whereas in the thalamus there is much less spatial organisation which will result in a much smaller contribution (Eggermont, 2007). This also results in the ability to detect strong correlates of cortical activity as excitatory pyramidal cells form mini-column structures in cortical layers II to VI. Though this does mean that due to the comparatively disordered structure in cortical layer I that it makes it harder to record signals from via EEG.

Another comparable technique used is electrocorticography (ECoG) which uses many of the same principles as EEG but is recorded intracranially. As such this gives it a better spatial resolution than EEG and access to the gamma brainwave frequency bands (>30Hz) which are usually filtered out by the low pass filter characteristics of the skull (Pfurtscheller and Cooper, 1975). ECoG is recorded via planar electrode arrays that will be placed onto the surface of the cortex, either epidurally or subdurally.

1.1.4 Summary

Each of these recording methodologies will look at a different neural scale, recording either single functional units, local populations or a global population response.

Relating between this methodologies is often complicated as forward modelling from single units to LFPs or EEG is heavily dependent on the spatial organisation of the neurons contributing to the signal. Additionally to be able to assume the response of a population, a sufficiently large population of neurons must be sampled to assess their response properties and how their signals will combine.

Inverse modelling is even more fraught with problems with EEG and LFPs picking up an incomplete picture of the population, either due to spatial orientation of the cortical surface, lack of spatial organisation within the cortex or physical properties of the cells. This leads to certain cortical areas, layers or cell types not contributing to the recordings although they are vital to the underlying computations.

This thesis attempts to find better methodologies for relating single unit and EEG recordings of adaptation by first comparing the responses of EEG measured in humans and an animal model then looking at multiple neural scales within the animal model to correlate the activity.

1.2 Neural Adaptation

Adaptation is a ubiquitous phenomenon in human and animal sensory systems, presenting as a modulation in a neural response after repeated presentation of a stimulus.

While the mechanisms behind adaptation are not fully understood the phenomenon itself can be useful as a research tool for other percepts such as pitch. As pitch and frequency are so intrinsically linked it is not possible to directly search for pitch sensitive neurons in auditory cortex in non-invasive

studies but instead by showing that a response can adapt to stimuli with identical pitch but no frequency overlap then the two can be disentangled (Briley et al., 2013). This method uses adaptation's feature selectivity as only neurons that respond to both stimuli should adapt.

1.2.1 Generation and Characteristics

Adaptation in the auditory system can be measured at all levels of the auditory pathway, with different stimulus conditions needed to adapt out each level. It has been shown through forward masking experiments in auditory nerve fibres that by using a masking tone before a probe tone that there will be a frequency dependant suppression of activity. When the masker and probe frequencies are close in frequency there will be greater suppression with the effect decaying with larger separation. This effect also shows a recovery over time with larger inter-stimulus intervals (ISIs) allowing a release from adaptation. In chinchilla auditory nerve this was shown to have a time constant of 37ms (Harris and Dallos, 1979). It is theorised this effect is related to depletion of neurotransmitter reserves in auditory nerve fibres following repeated discharge.

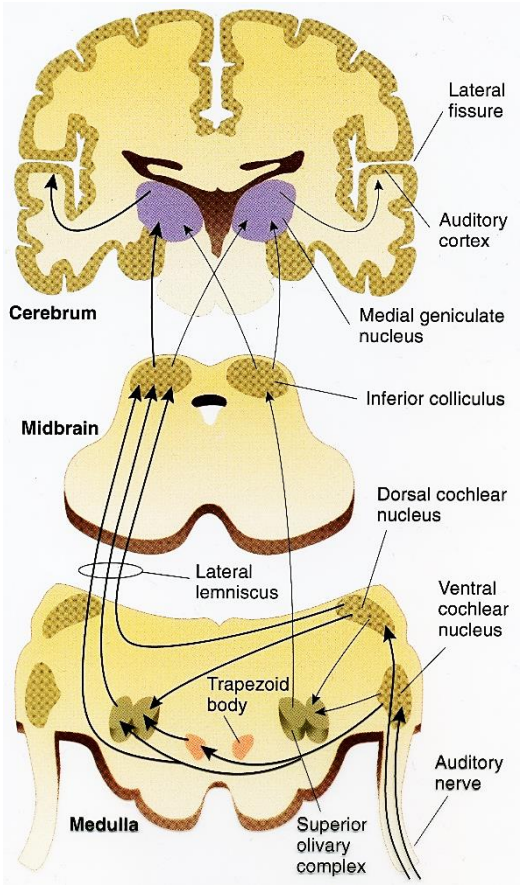

Figure 1.4: Schematic diagram of the ascending auditory pathway (Carlson, 2006)

Using near-field potentials in cochlear nucleus (CN) it was shown that in response to trains of 100μs duration clicks presented at rates of 100-1000 clicks per second, the neural response reduced to 30% of its initial level within 20ms of train onset (Loquet et al., 2003). Adaptation in the CN has also been

demonstrated in single units and is shown to act at multi-second timescales, be frequency selective and occur in both Bushy cells and Multipolar cells (Pressnitzer et al., 2008). The timescales and frequency selectivity of these responses have been shown to correlate well to the perceptual build-up of auditory streaming.

Forward suppression has been shown to affect single neurons in the inferior colliculus (IC) in rats, with around 60% of recorded neurons showing a significant suppression of activity. This suppression was independent of the adapter tone duration and was more strongly correlated with the stimulus onset asynchrony (SOA), the time between the onset of the adapter and probe. The recovery time constants of these neurons were not homogenous or parametrically distributed, with a mean of 271.4ms and median of 72.8ms (Finlayson, 1999). This study also showed that different cell types, as indexed by their post-stimulus time histogram (PSTH), responded differently to the adapter-probe stimuli. Their 'Transient' cells, cells showing an onset response and little sustained activity, were most strongly and reliably supressed whereas their 'Pauser/Buildup' cells, showing both onset and sustained activity, demonstrated facilitation to the same stimuli.

The IC has been shown to adapt not just to frequency of the stimuli but also to the sound level (Dean et al., 2005). It was shown that responses of single neurons would change their rate-level response functions based on the mean and variance of the sound level of the preceding stimulus. These changes in response properties increased the level of available information about the sound levels around the mean sound level the system was adapted to. This is an example of one of the functional benefits of adaptation, allowing accurate coding of sound level along a large dynamic range.

In the cortex, adaptation has been shown to last in the order of seconds, causing a suppression of firing activity in individual neurons (Calford and Semple, 1995; Bartlett and Wang, 2005; Wehr and Zador, 2005; Brosch and Scheich, 2008). Cortical neurons have also been shown to demonstrate facilitation, an

enhancement in the response size to a probe stimuli, seen in some neurons when stimulated with a pair of same frequency tones (Wehr and Zador, 2005) or when the adapter is ±1 octave separated from a probe played at the best frequency (BF) of the recorded neuron (Brosch and Schreiner, 2000; Brosch and Scheich, 2008). This can also be seen in isolated rat auditory cortex slices when exposed to paired-pulse stimulation. In this preparation electrical stimulation is applied to brain slice and the evoked potentials were measured, showing the response to the second of two pulses would show a larger response than the first, with a maximal response at 200-300ms gap between the pulses. This was attributed to a release from GABAergic inhibition in the later pulse (Metherate and Ashe, 1994).

Another property found in cortical neurons is lateral inhibition, the suppression of activity a neuron by adapting tones outside the limits of its excitability response area. Lateral inhibition was shown in 38% of the total population of sampled neurons and was seen in 77% of the total neurons with non-monotonic rate-level functions. Further experiments showed that even when the adapter was within the response area of the neuron that the spiking rate in response to the adapter showed little correlation with the degree of suppression of the probe response. This suggests adaptation is not simply a post-discharge habituation (Calford and Semple, 1995).

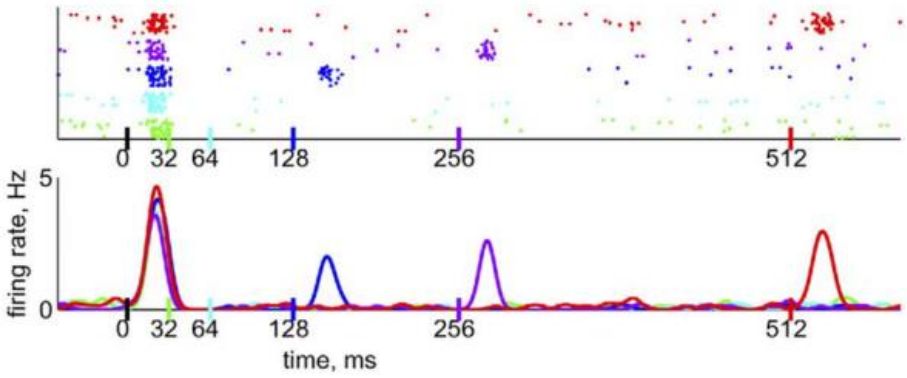

Figure 1.5: Single unit spiking activity in rat auditory cortex measured in response to an adapter-probe sequence with varying inter-stimulus interval (ISI), showing full suppression of firing for ISIs of 64ms or less and gradually increasing firing rates for probe tones with longer ISIs (Wehr and Zador, 2005)

These effects can also be seen in EEG recordings as a suppression in the size of auditory evoked potentials (AEPs).

Lanting *et al.* (2013) performed a parametric analysis of the effects of the temporal properties of adapting tones on a probe tone of the same frequency using EEG in humans. They varied the adapter duration, stimulus onset asynchrony (SOA), inter-stimulus interval (ISI), number of preceding adapters and the rate those adapters were presented. In their results they showed recovery from adaptation as the adapter and probe were moved apart in time, resulting in a recovery time constant of ~1200ms. This time constant was not fixed however and appeared to be a function of the number of adapters, showing a time constant of ~750ms when 4 adapters were used. They also showed monotonically increasing adaptation with increasing adapter duration, saturating from around 475ms adapter duration.

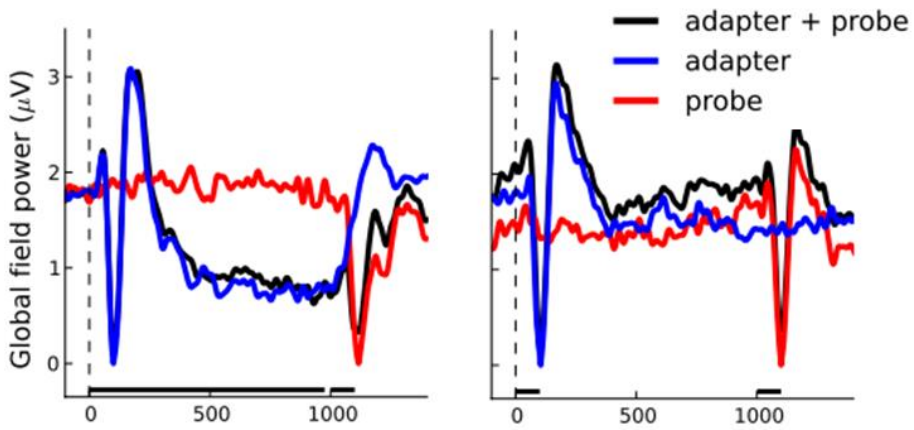

Figure 1.6: EEG-measured auditory evoked potentials (AEPs) during an adapter-probe sequence showing a significantly smaller AEP in response to the second (probe) tone. Black bars show when the 1 kHz tone is being presented. (Lanting et al., 2013)

Another study of adaptation in human EEG was performed by Briley and Krumbholz (2013), this time looking at frequency selectivity of adaptation. They were attempting to discover the effects of adapter SOA and number of adapters on the frequency selectivity of adaptation and these parameters could be used to alter the degree of selectivity.

In their first experiment they varied the adapter-probe SOA while varying the adapter-probe frequency difference. This showed that for SOAs of 125 to 1000ms there was no change in frequency selectivity of the adaptation response, just changes in the overall degree of adaptation. In their second experiment they used varying numbers of adapters with a fixed SOA of 500ms. This time they found an effect on the frequency selectivity, with greater number of preceding adapters increasing the selectivity. This was due to an increase in adaptation for small frequency separations and greater release from adaptation with wide separations (Figure 1.7).

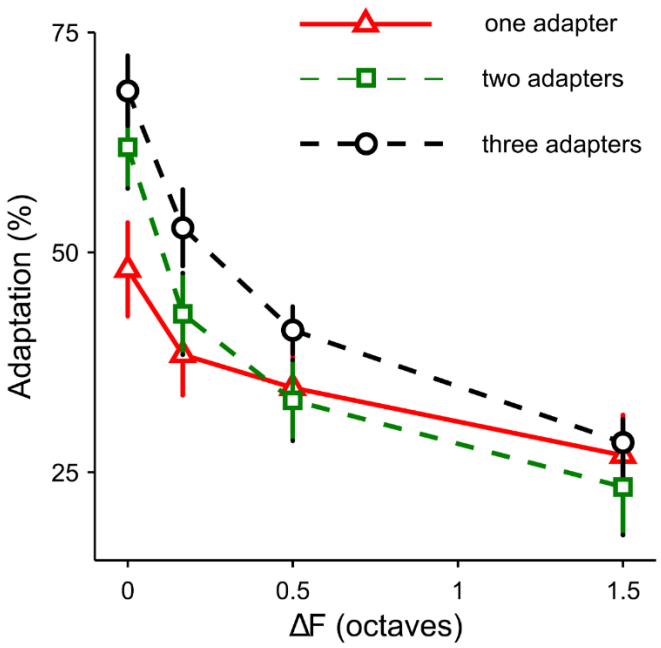

Figure 1.7: EEG-measured adaptation frequency tuning from an adapter-probe sequence showing an increase in frequency selectivity with increasing number of preceding adapters. Adapted from (Briley and Krumbholz, 2013)

Two main methods of probing auditory adaptation are used. The preceding research presented is via adapter-probe sequences, sometimes referred to as forward suppression, but adaptation can also be measured through oddball paradigms, usually referred to as stimulus specific adaptation (SSA). Oddball paradigms were initially used for the generation of mismatch negativity (MMN) responses, a phenomenon resulting in a negative voltage deflection at a latency of 280-420ms in humans following an unexpected stimulus (Duncan

et al., 2009). The oddball paradigm uses a continuous sequence of tones presented as a Bernoulli process with a standard with a high probability of occurring (P>0.7) and a deviant with a low probability of appearing (P<0.3).

Two main measures are used to quantify adaptation in oddball sequences, stimulus specific adaptation index (SI) and the common SI (CSI) (Ulanovsky et al., 2003). SI gives a measure of the degree of adaptation at a given frequency by comparing the magnitudes of the responses when presented as either the standard or deviant stimulus.

$$SI_i = \frac{d(f_i) - s(f_i)}{d(f_i) + s(f_i)} \tag{1.2}$$

Where $d(f_i)$ is the magnitude of the deviant response at a given frequency and $s(f_i)$ is the magnitude of the standard response at the same frequency. This is expanded on by the CSI which requires an alternated oddball where the standard and deviant stimuli parameters are switched between two runs so each frequency is used as both a standard and deviant. This allows the calculation of the more frequency independent CSI.

$$CSI = \frac{d(f_1) + d(f_2) - s(f_1) - s(f_2)}{d(f_1) + d(f_2) + s(f_1) + s(f_2)} \tag{1.3}$$

For the SI and CSI metrics a value significantly different to zero represents the presence of stimulus specific adaptation (SSA).

Oddball evoked SSA has been shown to exist in structures from the IC and higher in the auditory pathway (Ayala et al., 2015). One group, using 25ms duration pure tone stimuli presented at 4-20 tones per second, found no evidence of SSA in CN when measured at a single unit level (Ayala et al., 2013). The same group showed when using 75ms duration tones at a presentation rate of 4 tones per second that an SSA response could be elicited in inferior colliculus (IC), but not in CN. Higher on the auditory pathway, the medial geniculate body (MGB) demonstrates SSA (Anderson et al., 2009) with trains

of 75ms tones presented with 50-425ms inter-stimulus interval (Antunes et al., 2010). It is unsurprising the IC is the first structure in the pathway to show SSA, as the IC is also the first structure to integrate together multiple frequency response regions of the cochlea, contributing to the frequency selective nature of SSA.

In one study SSA in the MGB was found to be independent of the auditory cortex, as cortical inactivation via cooling did not affect the CSI in MGB neurons (Antunes and Malmierca, 2011) however another study published the same year suggests that corticofugal feedback is integral to SSA in the MGB as pharmacological deactivation of the cortex led to the abolishment of SSA (Bauerle et al., 2011). This means it is unclear if SSA acts through the corticofugal pathway giving feedback control from higher structures.

The adapter-probe method, which will be the primary method used in this thesis, has several advantages over the oddball method. This method allows a greater freedom to investigate the effect of parameters of the adapting stimulus than an oddball paradigm. For example it allows a greater ability to probe the frequency selectivity of the adaptation response by varying the frequency separation between the adapter and probe tones. It also provides much greater control over the temporal properties of the adapting stimuli such as duration or repeat rate.

1.2.2 Proposed Mechanisms

While there are several leading hypotheses about the mechanisms of adaptation there is, as yet, no comprehensive model of the underlying biological processes.

One early hypothesis put forward for the mechanism of adaptation in auditory neurons was long-lasting GABAergic inhibition but this has since been disproved (Wehr and Zador, 2005). It was found that inhibitory conductances of rat auditory cortical neurons, evoked by a click stimulus, typically last in the order of 100ms but adaptation of the probe response still continued with inter-

stimulus intervals of over 500ms. This demonstrates that inhibition plays little role in adaptation beyond 100ms. The authors however suggest synaptic depression, a form of short term plasticity (STP), as a potential alternative mechanism.

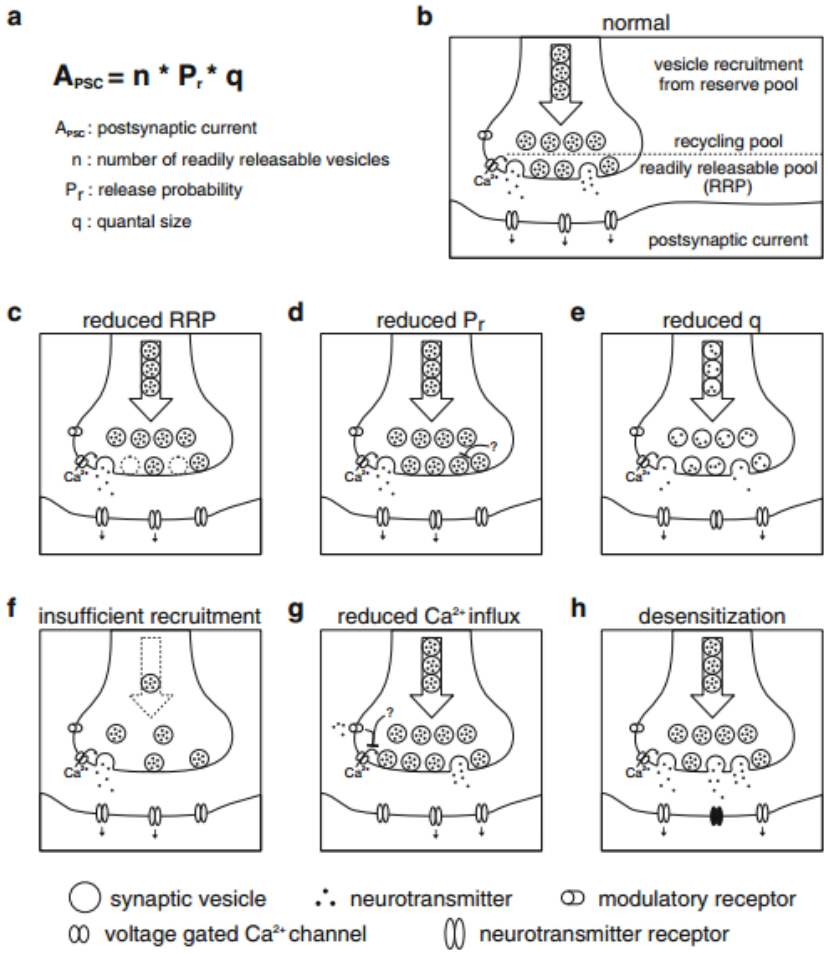

Figure 1.8: Mechanisms of short term plasticity (STP). The amplitude of a postsynaptic current response A_{PSC} is described as the product of three parameters (a), namely the number n of readily releasable vesicles, the probability Pr to release a vesicle and the amount of neurotransmitter per vesicle, q. Changes in the three parameters leads to STP. The figure also illustrates the normal state of an active synapse, including different vesicle pools (b) and six scenarios where n, Pr, and q are changed. Five of them (c–g) are presynaptic and one (h) is postsynaptic (Friauf et al., 2015)

As shown in figure 1.8 there are a multitude of potential STP mechanisms that could result in a reduction in firing rate. These include a depletion of readily available vesicles in the presynaptic neuron, an insufficient supply of

neurotransmitter for the vesicles or a desensitisation of postsynaptic receptors.

Another potential mechanism that has been suggested is afterhyperpolarisation. This is a phenomenon seen at the single neuron level characterised by a hyperpolarisation of the neuron's membrane potential after sustained stimulation. By hyperpolarising the cell it will increase the response threshold needed to evoke an action potential. This desensitisation of the neurons could be a contributing factor to the build-up of adaptation, most notably at short latencies. This will occur through three separate processes mediated by potassium and calcium channels with different timescales. Fast afterhyperpolarisation (fAHP) will recover in a millisecond timescale, middle-duration afterhyperpolarisation (mAHP) will last for a few tens of milliseconds and slow afterhyperpolarisation (sAHP) will continue for several seconds following intense stimulation (Schwindt et al., 1988).

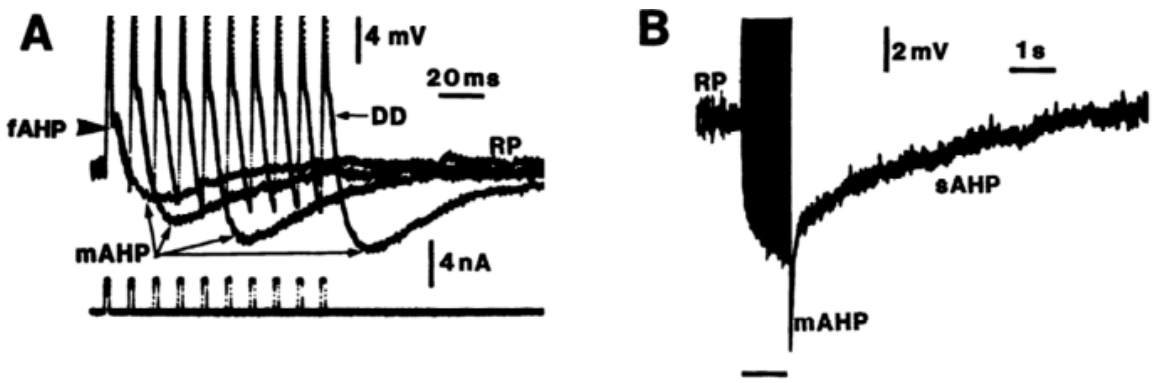

Figure 1.9: Demonstrations of the three types of afterhyperpolarisation. A: Superimposed responses of a cell to multiple short current bursts presented at 100Hz indicating the areas of fast and middle-duration AHP. B: Longer duration stimulation by 100Hz current bursts results in the generation of sAHP which will continue for several seconds after stimulation offset (Schwindt et al., 1988)

Three leading models of adaptation, based around experimental data from multiple sensory systems, were reviewed by Grill-Spector et al. (2006), each with different implications for tuning at the single neuron level. Firstly the Fatigue model, based around STP, suggests that all neurons initially responsive

to a stimulus will show a reduction in firing rate relative to the strength of their initial response. A prediction of this model is that neurons tuned closely to the stimulus will be adapted most strongly (Figure 1.10a).

Secondly the Sharpening model which suggests that the receptive fields of neurons closely tuned to the frequency of the stimulus will show a narrowing of their frequency receptive fields resulting in a sharpening of the frequency representation in the cortex. This model predicts that neurons optimally tuned to the repeating stimulus will show little suppression but those with receptive fields (RFs) close to the stimulus frequency will sharpen their selectivity (Figure 1.10b).

Lastly the Facilitation model predicts that processing of repeated stimuli will speed up processing of the stimuli leading to shorter latencies or durations of firing. This model suggests no change to frequency selectivity at a single neuron level (Figure 1.10c). Due to multiple experiments showing a lack of evidence in the auditory system for any of the effects predicted by this model (Scholes et al., 2011; Briley and Krumbholz, 2013) then it can be disregarded.

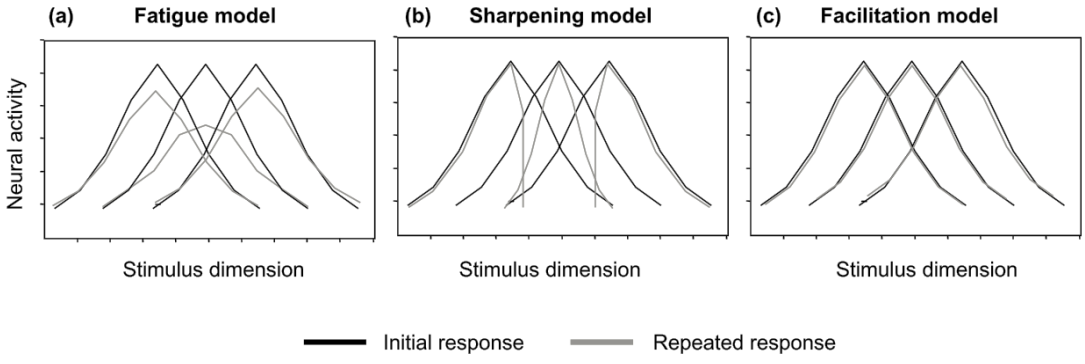

Figure 1.10: Schematic effects of changes to neural receptive fields following repeated adapters according to the three proposed Grill-Spector models (Grill-Spector et al., 2006)

As previously discussed, in the experiments of Scholes et al. (2011) a single unit behaviour independent of these phenomena appeared, FSA. Unlike the three previous models, FSA is an effect that is not dependant on the CF of the unit being adapted but primarily on the frequency of the adapting stimulus, causing a reduction in responsiveness around the adapter frequency while

leaving the rest of the receptive field intact (Figure 1.11). This response could potentially represent the preferential adaptation and fatiguing of afferent synapses tuned around the frequency of the adapter.

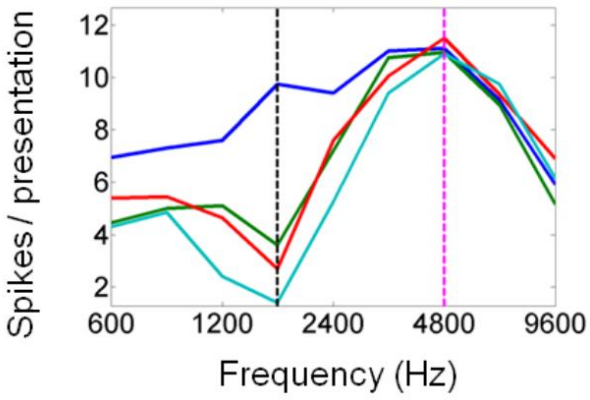

Figure 1.11: Adaptation of a multi-unit response with multiple repeated adapters showing suppression of the unadapted response (blue) around the adapter frequency (black). Unit characteristic frequency (CF) is shown in magenta (Scholes, 2009).

These simple models of adaptation effects on single neurons will work well for peripheral structures in the sensory pathway. However, adaptation of single neurons in higher regions of the sensory pathway may not be as simple as those near the periphery as adaptation effects can be inherited and compounded. These fatigue, sharpening and FSA effects seen may be first order effects, caused by direct effects of adaptation, or may be a combination of direct adaptation effects and the implications of receiving inputs of adapted neurons earlier in the processing pathway (Solomon and Kohn, 2014). This means that the effects of adaptation must be considered at both the single unit and network levels.

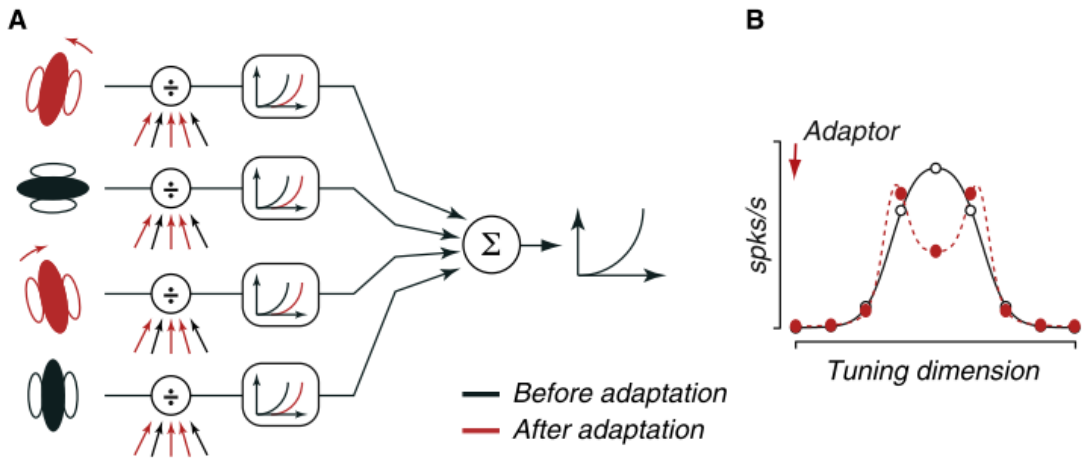

Figure 1.12: Schematic of a generic, hierarchical sensory processing pathway showing that a combination of fatigue and FSA type neurons (A) can combine their properties to create more exotic response suppression types (B) (Solomon and Kohn, 2014)

1.2.3 Proposed Functions

One theory proposed about the function of adaptation is tied in with Barlow's efficient coding hypothesis (Barlow and Foldiak, 1989). This hypothesis states that sensory neural systems will attempt to encode stimuli as optimally efficiently as possible, with as few spikes fired as possible (Wark et al., 2007). This would result in adaptation being a computational phenomenon, as a result of the brain attempting to more efficiently encode high probability stimuli.

This potential computational mechanism has been probed by several methods. Studies in rat barrel cortex have shown that at single unit, local cluster and larger network levels that adaptation will increase the derived level of mutual information (MI) in the system while decreasing the overall spike count representing a decrease in metabolic demand (Adibi et al., 2013a, 2013b). In chicken auditory nerve it was found that while adaptation degraded the rate coding reliability, thereby decreasing the amount of information, it maintained its spike timing precision while phase locked to a signal (Avissar et al., 2007).

Another facet of efficient coding is the reduction of redundancy and correlation in neural coding. Under normal conditions the cortex will show a highly redundant coding strategy, with multiple neurons encoding overlapping

information, and also a modest degree of inter-neuron correlation. Both redundancy and correlation are computationally inefficient (Barlow and Foldiak, 1989) and adaptation has been suggested as a method of redundancy reduction and de-correlation of the neural representation of external stimuli. It should be noted however that coding efficiency benefits have been proposed for strategies incorporating decreases (Barlow and Foldiak, 1989; Chechik et al., 2006; Kohn, 2007; Chen et al., 2012) and increases (Abbott and Dayan, 1999; Adibi et al., 2013b; Franke et al., 2015) in inter-neural correlations as while a sparse code is more computationally efficient it is also more prone to disruption by noisy signals.

Another proposed function of adaptation is as a novelty detection mechanism (Ulanovsky et al., 2003). With the high probability stimuli presenting suppressed responses, in relative terms the response to novel stimuli will be enhanced, supposedly increasing detectability or discriminability.

It has also been suggested that adaptation acts as a mechanism of population homeostasis. In visual cortex it was shown that adaptation will allow the neural population to maintain a stable level of activity over time, without a subset of neurons showing prolonged over-activity, despite being presented with a biased stimulus set over-representing one particular stimulus (Benucci et al., 2013).

1.2.4 Links to Mismatch Negativity

Mismatch negativity (MMN) is characterised by a negative voltage deflection present in the neural response to a low probability (deviant) stimulus in a sequence relative to when presented as a high probability (standard) stimuli. It is treated as the correlate of a neural process concerned with detecting violations or deviations from an established pattern. This phenomenon shows analogous responses in auditory, visual, somatosensory and olfactory modalities.

In humans auditory MMN usually shows a latency of around 150-250ms after the onset of the change from expectation with shorter latencies seen for larger changes (Näätänen et al., 2007). It is heavily debated whether a true MMN can be elicited in non-human animals.

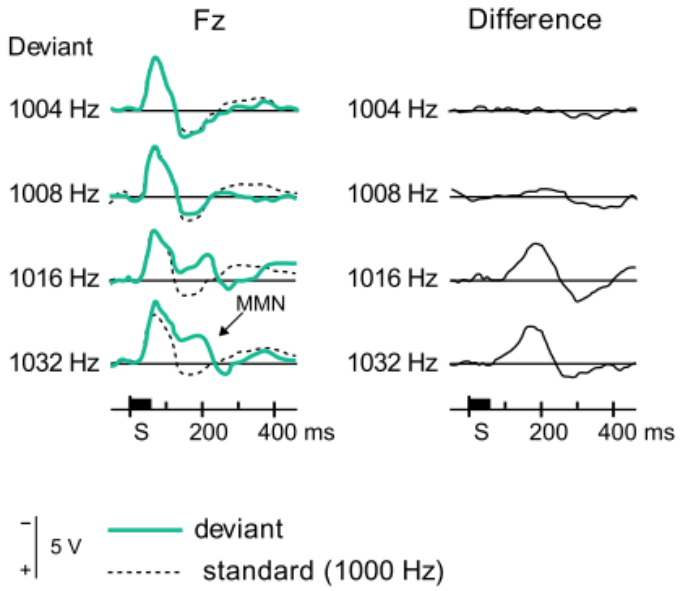

Figure 1.13: After presenting an oddball stimulus set the neural responses to the high (standard) and low (deviant) probability stimuli can be compared (left). Traditionally the MMN shows as a negative deflection in the voltage trace in response to the deviant when compared to the standard response (right). (Näätänen et al., 2007)

Opinion is still split on the interconnectedness of adaptation and the MMN with some papers claiming the MMN can be explained independently of adaptation (Lieder et al., 2013) and some claiming MMN is explainable entirely as a consequence of adaptation (May and Tiitinen, 2010).

1.2.5 Summary

Adaptation is a reduction in a neural response to a sensory stimulus resulting from repeated presentation of the stimulus. In the auditory system this response is selective to changes in frequency

All structures in the ascending auditory pathway show some form of adaptation response, each responding to different adapter temporal

parameters. In general this means more peripheral structures needing faster adapter rates to begin adapting.

The main mechanisms behind adaptation are thought to be dominated by afterhyperpolarisation at short latencies and short term potentiation (STP) at longer latencies, acting together to reduce the responsiveness of individual neurons to stimulation.

This thesis looks into the functional effects of adaptation on frequency tuning in auditory cortex, attempting to find if adaptation will confer any functional benefits to frequency selectivity. This is done by assessing the effects on population responses in human EEG recording before attempting to find underlying neural mechanisms from smaller scale recordings in our animal model.

1.3 Anaesthetics

In this report there will be assessments of the effects of anaesthetics on the representation of basic sensory stimuli in sensory cortical areas. While there have been studies of some anaesthetics on some of these phenomena there are still many commonly used anaesthetics for which their effects on these recordings has not been investigated.

This is especially important when considering anaesthetic choice for recordings, as will be shown below, some studies have shown significant changes to these phenomena under some anaesthetics which could make them unsuitable for use in auditory research. For single neuron recordings this is very relevant as the majority of recordings are made under anaesthesia. If there is a significant change to the population response the individual neuron responses may not be a good representation of those in the awake animal and therefore any perceived correlates to less invasive recordings made in awake animals or humans may not be valid.

1.3.1 Mechanisms of Action

Given electrophysiological data on their effects, the main current theory on the mechanism by which anaesthetics cause a loss of consciousness is their modulation of ligand-gated ion channels. This can be through various pathways, for example ketamine is an NMDA antagonist which noncompetitively binds to NMDA receptors decreasing the activity of excitatory neurons. This is in contrast to propofol, which potentiates $GABA_A$ activity, thereby increasing the activity of inhibitory GABAergic interneurons. Urethane is a long-acting injectable anaesthetic but does not show as strong affinity for any single ion channel as many other anaesthetics but instead shows a distributive effect, potentiating and antagonising channels to a much smaller degree than other anaesthetics with specific target channels.

	Conc.	$GABA_A$	NMDA	AMPA	Glycine	nACh
Ketamine	10μM	0%	-80%	0%	0%	-20-50%
Propofol	1μM	>+100%	-3%	0%	+10%	0%
Pentobarbital	50μM	>+100%	-9%	-50%	+17%	-50-80%
Urethane	10mM	+23%	-10%	-18%	+33%	+15%
Ethanol	50mM	+10%	-40%	-40%	+40%	+30%
Isoflurane	150μM	+100%	-20%	-10%	+90%	-60%
Halothane	0.25mM	>+100%	0%	-20-50%	>+100%	-80-100%
Nitrous Oxide	0.58 atm	+30%	-30%	-20%	+30%	-30%

Table 1.1: The effects of commonly used non-opiate anaesthetics on the activity of the major classes of ligand-gated ion channels. Measured under voltage clamp conditions at approximately clinical doses, compared to baseline activity. Increases of >50% are shown in green and decreases of <-50% are highlighted in red. Data compiled from (Sanna et al., 1995; Yamakura and Harris, 2000; Yamakura et al., 2001; Hara and Harris, 2002)

Opioid derivatives target opioid receptors, G protein-coupled receptors with the opioid as their ligand. Fentanyl is a commonly used opioid derivative and when combined with an anti-psychotic, is used as a neuroleptanalgesic in veterinary medicine. Fentanyl preferentially binds with the μ-opioid receptor which will in turn cause a reduction in the amount of intracellular calcium

thereby inhibiting the ability of the neuron to release neurotransmitter vesicles.

A common problem when attempting to determine the mechanism of action of anaesthetics is the lack of published electrophysiological data. For example fentanyl/fluanisone is a common neuroleptanalgesic combination in veterinary anaesthesia however there is no published data on the mechanism of action of fluanisone. Looking more broadly to the butyrophenone class of drugs that fluanisone belongs to, butyrophenones are anti-psychotic drugs with some, like droperidol and haloperidol, having a high affinity for dopamine receptor D_2 and some antihistaminic and anticholinergic activity. They also appear to show an inhibitory effect on NMDA receptors (Shim et al., 1999).

Given the multiple modes of action of these anaesthetics there is still no general consensus on the exact mechanism of how they achieve loss of consciousness especially when considering other classes of anaesthetics like the α-2 agonists xylazine and medetomidine, which are hypothesised to work by feedback inhibition of noradrenaline (Khan et al., 1999), or xenon, which acts as an anaesthetic despite being an inert, monatomic gas.

1.3.2 Effects on Cortical Auditory Evoked Potentials

An auditory evoked potential (AEP) is the summed electrical response of a population of neurons to an auditory stimuli. As the power of the response from AEPs is reasonably small compared to the background neural activity the signal needs to be averaged over many stimulus presentations. This will attempt to eliminate the effects of the background activity as the AEP response will be almost equal at each presentation though the background activity will be more random (Eggermont, 2007).

Anaesthetics have been shown to significantly affect EEG recorded cortical AEPs, to the extent of AEPs being proposed as a measure of depth of anaesthesia in surgery (Horn et al., 2009). This is usually studied using volatile anaesthetics such as sevoflurane, as in most surgeries requiring general

anaesthesia inhalable anaesthetics are used for maintaining unconsciousness. Sevoflurane shows a progressive suppression of AEPs with increasing concentration (Schwender et al., 1995; Schneider et al., 2005; Horn et al., 2009). These recordings however may not be measuring suppression of AEPs directly at a cortical level, as would be required as a direct correlate of consciousness, but may be produced by effects acting peripherally at the level of the cochlea or brainstem (See section 1.3.3) that have been inherited by structures higher on the auditory pathway.

Several studies have looked into the effects of opiates such as fentanyl on auditory evoked potentials, showing minimal effects on latency, an effective low pass filtering of the power spectrum (Schwender et al., 1993) and a non-monotonically increasing amplitude with increasing concentration (Antunes et al., 2003). In Antune *et al.*'s study, amplitude increased immediately following an intravenous bolus of fentanyl and the effect dissipated within 10 minutes. This effect may be prolonged with intraperitoneal injection as there is a longer absorption time though it may also show a reduced amplitude increase without the concentration peaks from intravenous bolus injections.

Propofol's effect on AEPs has also been studied and a linear relationship was shown between the dose of propofol given to the patients and the N1 amplitude measured in humans (Simpson et al., 2002). From a baseline N1 response amplitude of -3.81±0.54 μV it shrank to -0.51±0.42 μV at the point of loss of consciousness. The authors showed that the N1 amplitude was a better predictor of unconsciousness than the estimated blood concentration of propofol.

1.3.3 Effects on Auditory Brainstem Response

The auditory brainstem response (ABR) is an evoked response measured from the auditory brainstem and is used as a non-invasive method of measuring hearing thresholds. ABRs can be invoked during sleep, under anaesthesia, in animals and in human foetuses from the end of the second trimester (Burkard

and Don, 2007) so are a robust and widely used tool for screening for hearing loss. Hearing loss detected by ABRs implicates a disorder of the ear or brainstem. Hearing threshold under ABRs is usually measured as the first amplitude at which an ABR can be reliably discerned within the averaged epochs. ABR hearing threshold has been shown to correlate well with results obtained via audiometry but without the need for subject participation so is commonly used as a tool for screening for hearing in new-borns and animals.

It has been shown that ketamine produces a small (<5 dB) increase in ABR measured hearing threshold in gerbils (Smith and Mills, 1989) and mice (van Looij et al., 2004; Cederholm et al., 2012), representing reasonably negligible effects of ketamine on ABR thresholds. This is comparable to fentanyl which was found to have no statistically significant effect on the auditory brainstem response up to doses of 50µg/kg in humans (Samra et al., 1984).

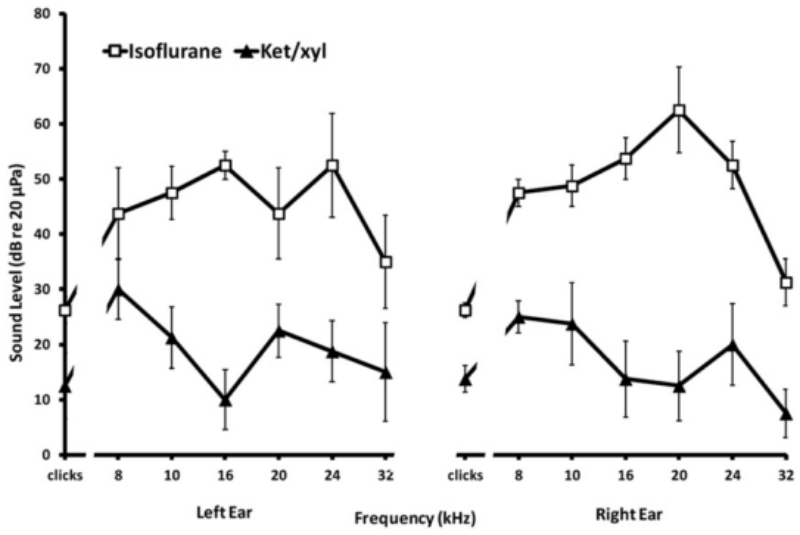

Figure 1.14: Hearing threshold, calculated from click and pure tone evoked ABRs in rat, under isoflurane or ketamine/xylazine anaesthesia (Ruebhausen et al., 2012).

Isoflurane however seems to have a profound effect on ABRs, dramatically reducing their amplitude. This reduction in amplitude is analogous to a 20-48dB increase in hearing threshold by the level of the auditory brainstem (Figure 1.14) (Ruebhausen et al., 2012). By comparison, despite having very

similar ion channel affinities, pentobarbital only relates to a ~15dB threshold increase measured at the level of the cortex (Feng et al., 2009).

It has also been demonstrated that recordings under isoflurane do not display a stable threshold hearing level, as shown by Cederholm et al. (2012), where isoflurane's initial 15 dB increase in ABR threshold further increased another 15-20 dB after 1 hour under anaesthesia.

Halothane also shows significant effects on the ABR amplitude, with the ratio of the amplitudes of peaks V and I under 0.6% halothane being 55.4% less than under nitrous oxide representing an attenuation of the response. This is in comparison to a 75.8% decrease in V/I amplitude ratio under 0.8% isoflurane anaesthesia relative to 79% N_2O (Sloan et al., 2010).

Isoflurane's effect on hearing threshold appears not to be occurring solely at the auditory brainstem itself. As shown in figure 1.14, there is an increased threshold for click-evoked activity at the level of the auditory nerve.

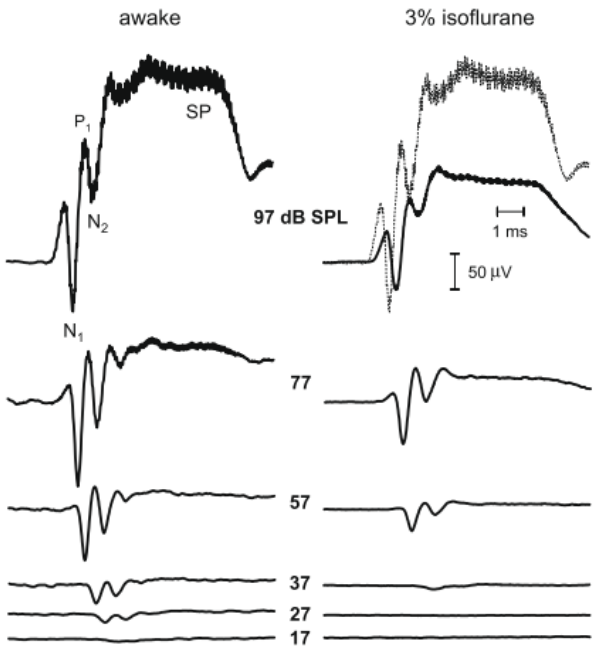

Figure 1.15: Compound action potential (CAP) recordings from guinea pig auditory nerve in response to click stimuli showing a reduction in measured hearing threshold under 3% isoflurane anaesthesia, representing, on average, a 14-17 dB increase in threshold (Stronks et al., 2010)

Cederholm *et al.* (2012) concluded that as isoflurane has negligible effects on cochlear nerve conduction and a reduction in nerve recruitment at the level of the cochlea that isoflurane may be hyperpolarising cochlear spiral ganglion cells. This was supported by the negligible effect of isoflurane on otoacoustic emissions (OAEs), which suggests an insignificant effect of isoflurane on outer hair cells.

In contrast they found that despite the comparatively stable ABR recordings under ketamine anaesthesia it significantly changed the measured OAEs during the 1 hour recording session but with negligible change to the cochlear output. This suggests that ketamine has an effect on the outer hair cells that is compensated for before being transmitted through the auditory nerve.

From these results it appears isoflurane, and potentially other volatile anaesthetics, may be unsuitable for auditory research as with the hearing threshold shift, even before transduction into the auditory nerve, any stimulus will be significantly attenuated. With a high variability of degree of suppression, even within subject between ears and a variation over time, this is not an effect that can easily be compensated for. Ketamine and fentanyl however show minimal effects on the ABR and while ketamine may affect the outer hair cells, this effect does not appear to translate into an altered CAP or ABR response.

1.3.4 Effects on Oscillatory Activity

Oscillatory activity in EEG refers to the typical rhythmic electrical activity of the brain. As opposed to AEPs, the oscillatory activity can be recorded at rest with no external stimuli. Due to the low pass filter characteristics of the skull (Pfurtscheller and Cooper, 1975) most extracranial recordings of this activity are limited to <30Hz oscillations whereas intracranial recordings have access to a wider frequency range.

As table 1.2 shows, the main correlations between frequency activity and neural state is the level of alertness, with higher frequency bands showing

higher amplitude with greater level of alertness in subjects. This has made it an attractive prospect for monitoring patients under anaesthesia, as it could provide a passive, non-invasive, quantitative measure of depth of anaesthesia.

Band	Frequency	Location	Related Neural State
Delta (δ)	<4 Hz	Frontal	Slow Wave Sleep
Theta (θ)	4-7 Hz	Unattended Brain Regions	Drowsiness
Alpha (α)	8-13 Hz	Posterior	Relaxation
Beta (β)	13-30 Hz	Symmetrical Distribution	Alert, Active
Gamma (γ)	30-100< Hz	Somatosensory Cortex	Multimodal Stimulus Processing

Table 1.2: Comparison of frequency bands of EEG oscillatory activity

One such attempt to try to use statistics of oscillatory activity to discriminate between the conscious and unconscious states was by Schneider *et al.* in 2005 who attempted to find the best parameters within the EEG oscillations to use with a discrimination algorithm to monitor patients during surgery to ensure maintained unconsciousness (Table 1.3).

Parameter	Consciousness, Mean ± SD	Unconsciousness, Mean ± SD	P_K ± SE
Median frequency 8–30 Hz	17.44 ± 2.55	14.95 ± 1.86	0.78 ± 0.03
Absolute power 21–30 Hz	59.87 ± 111.79	16.43 ± 26.62	0.77 ± 0.03
2nd Derivative: variance	$3.86 \times 10^{10} \pm 6.98 \times 10^{10}$	$1.31 \times 10^{10} \pm 1.82 \times 10^{10}$	0.73 ± 0.03
2nd Derivative: mean absolute amplitude	$1.28 \times 10^{5} \pm 8.68 \times 10^{4}$	$7.90 \times 10^{4} \pm 4.41 \times 10^{4}$	0.72 ± 0.03
2nd Derivative: root mean square	$1.60 \times 10^{5} \pm 1.07 \times 10^{5}$	$9.94 \times 10^{4} \pm 5.46 \times 10^{4}$	0.72 ± 0.03
2nd Derivative: crest factor	3.26 ± 0.40	3.65 ± 0.61	0.29 ± 0.03
Relative power 21–30 Hz	9.92 ± 12.36	3.90 ± 5.62	0.71 ± 0.03
1st Derivative: root mean square	$1.22 \times 10^{3} \pm 685.78$	915.21 ± 424.67	0.65 ± 0.03
First time-derivative order-proxy	6.97 ± 0.48	6.70 ± 0.46	0.65 ± 0.03
Morphology	877.06 ± 226.27	766.61 ± 181.13	0.64 ± 0.03
Approximate entropy	0.25 ± 0.12	0.20 ± 0.09	0.64 ± 0.03
2nd Derivative: form factor	1.25 ± 0.02	1.26 ± 0.03	0.38 ± 0.03
Lempel-Ziv complexity	0.14 ± 0.05	0.12 ± 0.04	0.62 ± 0.03
Kurtosis	$-3.90 \times 10^{5} \pm 2.44 \times 10^{6}$	$-3.91 \times 10^{5} \pm 1.68 \times 10^{6}$	0.58 ± 0.03
Normed kurtosis	0.03 ± 0.40	−0.03 ± 0.42	0.57 ± 0.03
Root mean square	22.16 ± 12.66	21.13 ± 13.07	0.56 ± 0.03
Spectral entropy	2.37 ± 0.65	2.31 ± 0.57	0.55 ± 0.03
Skewness	$-496.32 \pm 9.01 \times 10^{3}$	$206.22 \pm 7.23 \times 10^{3}$	0.54 ± 0.04

Table 1.3: Measured EEG oscillation parameters of conscious and anaesthetised patients, under sevoflurane/remifentanil or propofol/remifentanil. P_K is the probability of the parameter being able to distinguish correctly between the conscious and unconscious states, with chance level at 0.5. Adapted from (Schneider et al., 2005).

This transition in brain states has also been shown in EEG recordings in humans by recording during induction of anaesthesia to show the effects of

loss of consciousness (LOC) on oscillatory activity. Their results appear to show a reasonably abrupt shift of oscillatory activity at the point of LOC with a large increase in signal power in the alpha, theta and delta bands that disappears upon return of consciousness.

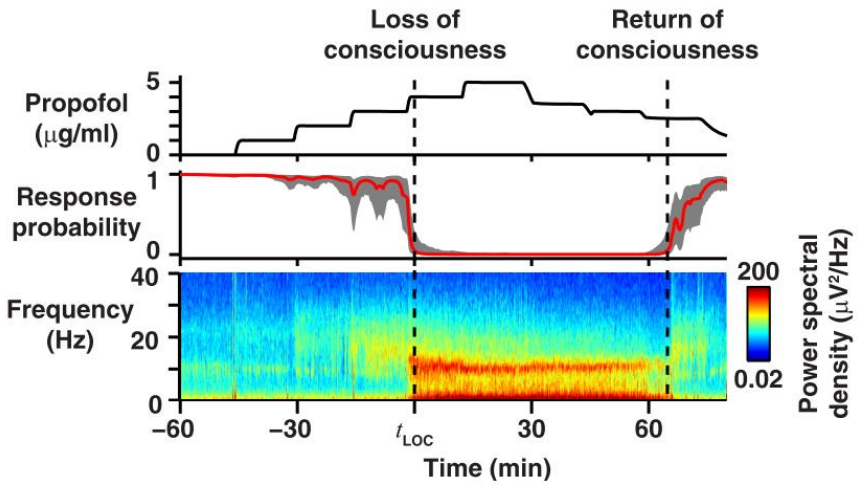

Figure 1.16: Changes in EEG recordings during administration of increasing doses of intravenous propofol showing a rapid increase in low frequency activity at loss of consciousness, determined from a lack of response to a cueing sound (Mukamel et al., 2014)

Anaesthetic induced LOC has also been investigated using electrodes implanted in patients with intractable epilepsy, recording LFPs and unit activity from the temporal gyrus (Lewis et al., 2012). These recordings also showed increases in low frequency power but limited to the delta band.

These low frequency oscillations are accompanied by phase locking of neural firing, with 46.6% of their spikes occurring at the $\pi/2$ phase around the trough of the slow oscillations. 67.2% of their 183 units showed significant phase coupling behaviour. This constraint of brief firing periods leads to a disruption of information processing which, compounded with the low frequency oscillations in disparate brain areas being out of phase, limits the brain's capacity for long range, inter-area signalling.

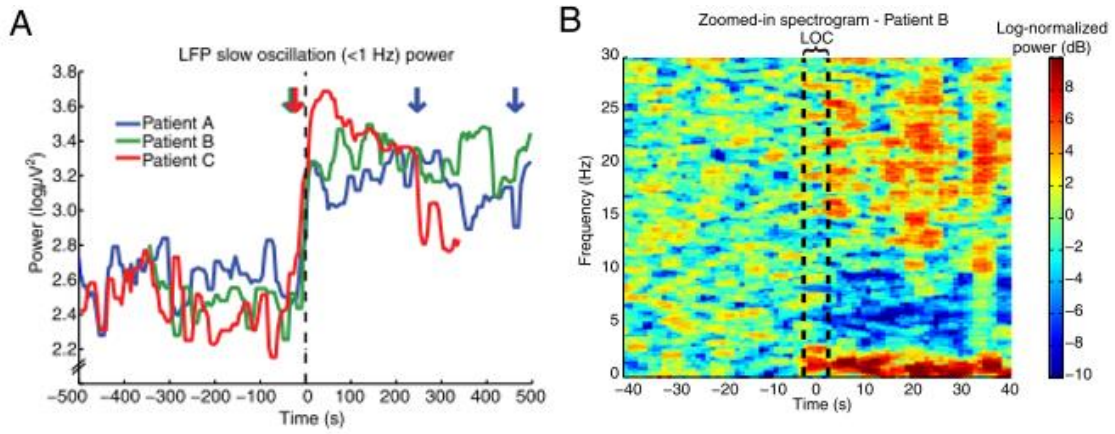

Figure 1.17: A: Signal power of low delta band oscillations in human ECoG recordings sharply increases following propofol-induced loss of consciousness (LOC). B: LFP oscillations in human temporal gyrus show a significant increase in delta band oscillations following propofol-induced LOC (Lewis et al., 2012)

1.3.5 Effects on Single Unit Recordings

As shown in the previous sections, anaesthesia can have significant effects on the population response to external stimuli and to the baseline activity of the brain at rest. Evidently this entails significant changes of firing behaviour at the single neuron level.

At the most basic level, anaesthesia will affect the spontaneous and evoked firing rates of neurons. For example, GABA will decrease net spontaneous spiking activity and gabazine, a GABA antagonist, increases firing rate of recorded single units (Duque et al., 2014). As with the effects of anaesthesia on oscillatory activity, the modulation from awake to anaesthetised modes appears to be a fast transition at LOC (Figure 1.18).

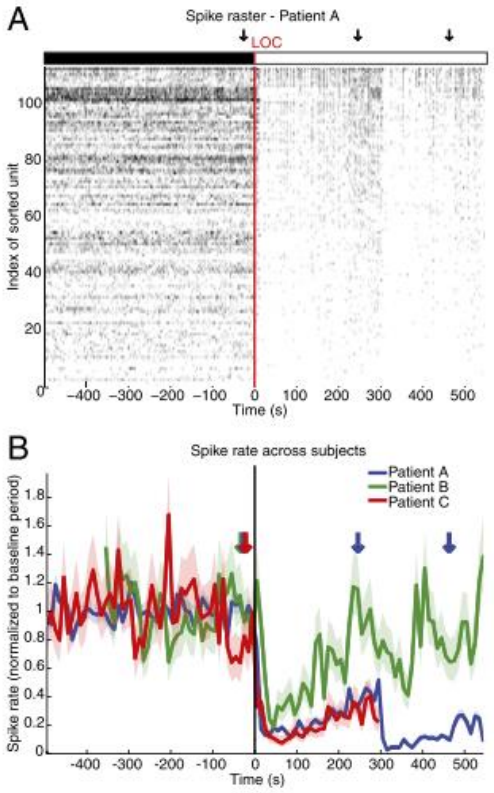

Figure 1.18: Spike raster plot (A) and normalised spike rates (B) of single unit activity in human temporal gyrus, showing a sharp drop in spike rate following propofol-induced LOC (Lewis et al., 2012)

These trends are also seen in single unit recordings of evoked activity. Figure 1.19 shows spike raster tuning profiles of isolated single units in auditory cortex before and after systemic administration of ketamine and pentobarbital showing overall reductions in responsiveness to pure tone stimuli.

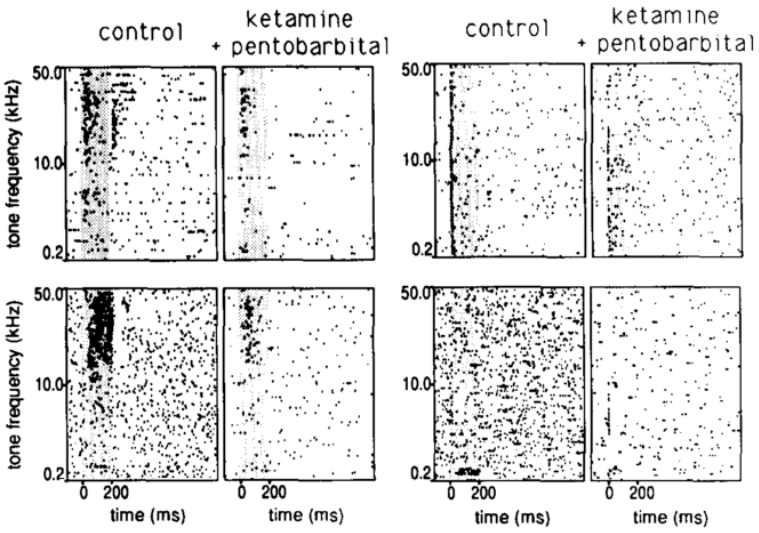

Figure 1.19: Spike rasters for four representative units, showing responses for frequencies from 0.2-50kHz under 80% N_2O (control) and after administration of ketamine and pentobarbital (Zurita et al., 1994)

This study also showed dramatic shifts in basic response characteristics of the neurons for example onset and offset excitation and sustained inhibition or excitation. This study is also rare within literature looking at the effects of anaesthesia on auditory processing in that they compare between multiple anaesthetics and a control condition. For example, under pure ketamine 50% of their neurons gained sustained excitation characteristics compared to their control condition whereas under pentobarbital alone nearly 100% of units lost their sustained excitation.

Another notable modulation of single unit activity with anaesthesia is their frequency tuning curves. Figure 1.20 demonstrates three common effects of GABA based anaesthesia on frequency tuning curves with the primary effects being a loss of responsiveness or a sharpening of frequency tuning. Gaese *et al.* (2001) observed that neurons that lost responsiveness to tones under anaesthesia showed low spontaneous rates under awake conditions than those units that had remained responsive. They also observed that while the anaesthesia demonstrated an overall sharpening effect there was no significant changes in threshold.

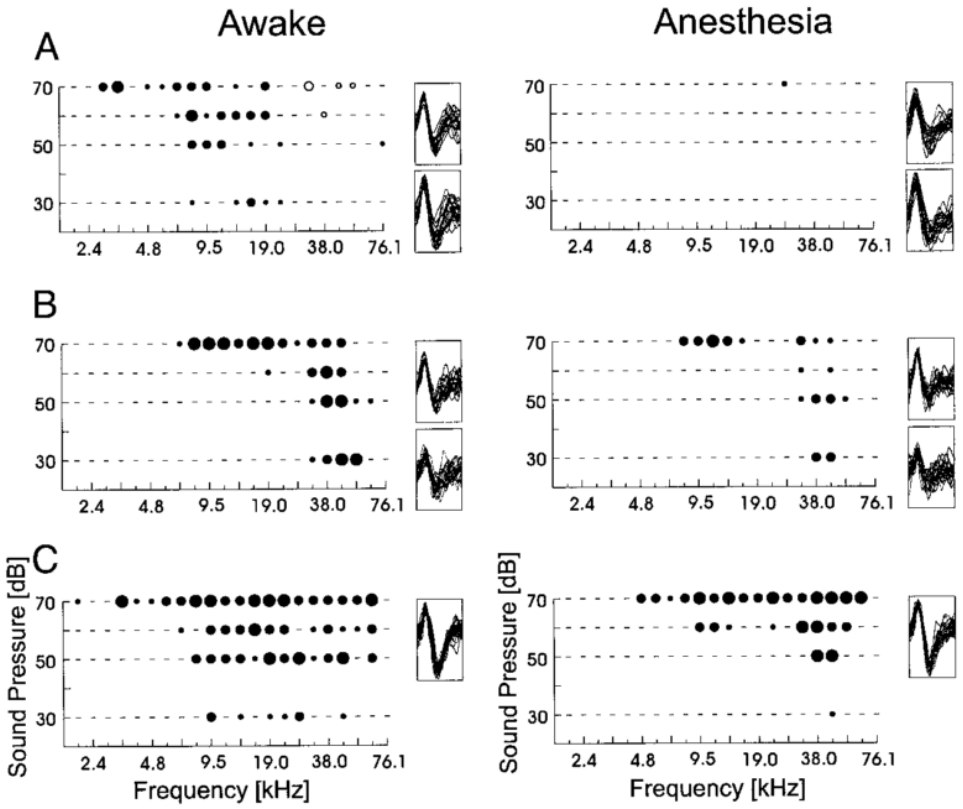

Figure 1.20: Changes in single unit tuning before and after systemic administration of Equithesin, a GABA potentiating anaesthetic combination of pentobarbital and chloral hydrate. Units show loss of responsiveness (A), sharpening of response area (B) or loss of sections of response area (C) (Gaese et al., 2001)

It appears the effects on unit tuning are not limited to just NMDA and GABA modulators and other classes of neuromodulators, such cholinergic and noradrenergic, will have effects. For example acetylcholine (Ach) shows sharpening and increased gain characteristics, lowering the response threshold, and norepinephrine (NE) which shows increased sharpening and reduced gain (Edeline, 2012).

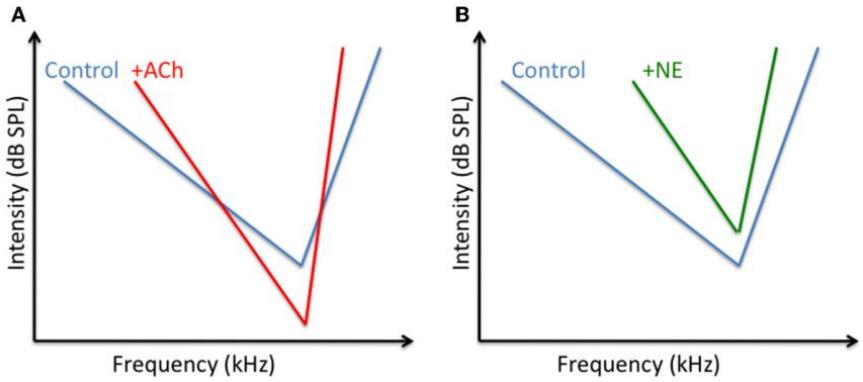

Figure 1.21: Changes in single unit tuning before and after iontophoretic administration of acetylcholine (ACh, A) or norepinephrine (NE, B). Units exposed to ACh show a reduction in response threshold around CF and a sharpening of response area whereas those administered NE show a combined sharpening and threshold increase (Edeline, 2012)

1.3.6 Effects on Mismatch Negativity

Given the frequent links between MMN and adaptation (Section 1.2.4) it is worth investigating the effects of anaesthesia on MMN as a potential indicator of the effects of anaesthesia on adaptation.

Effects of anaesthetics on MMN responses have previously been reported, with ketamine, propofol (Simpson et al., 2002; Heinke et al., 2004) and ethanol (Jääskeläinen et al., 1996) in humans attenuating the MMN response.

Ketamine has been used extensively alongside MMN as an NMDA antagonist model of schizophrenia and has been shown to significantly attenuate the MMN response in humans (Umbricht et al., 2000; Heekeren et al., 2008; Gunduz-Bruce et al., 2012), monkeys (Javitt et al., 1996) and mice (Ehrlichman et al., 2008).

Propofol was shown to completely abolish the MMN response, even in some subjects with sub-anaesthetic doses who were still conscious and responding to commands (Simpson et al., 2002). The authors suggest that there is a concentration of propofol, less than that needed to produce unconsciousness, which will inhibit the subject's ability to form new short term sensory memories thereby removing the ability to perform change detection.

As discussed before, ketamine, propofol and ethanol all reduce MMN amplitude but each has a very different effect on the ion channels with the individual effects of NMDA blockade or $GABA_A$ potentiation and more general global effects over all channels causing loss of MMN (Figure 1.22). One study used a serotonin agonist, dimethyltryptamine (DMT), which, like ketamine, is used for animal models of schizophrenia but this showed no effect on MMN amplitude (Heekeren et al., 2008).

Given that natural sleep will also reduce the magnitude of the MMN response (Sculthorpe et al., 2009) it may just be the loss of alertness that causes the reduction in MMN. This may be supported by the effects of attention on the MMN response. However these increases and decreases through attentional modulation only tend to affect the frontal generator of the MMN response whereas under sub-anaesthetic doses of ketamine (Heekeren et al., 2008), increasing sedation under propofol (Simpson et al., 2002; Heinke et al., 2004) and in subjects exposed to ethanol (Jääskeläinen et al., 1996), both the frontal and temporal MMN generators are affected.

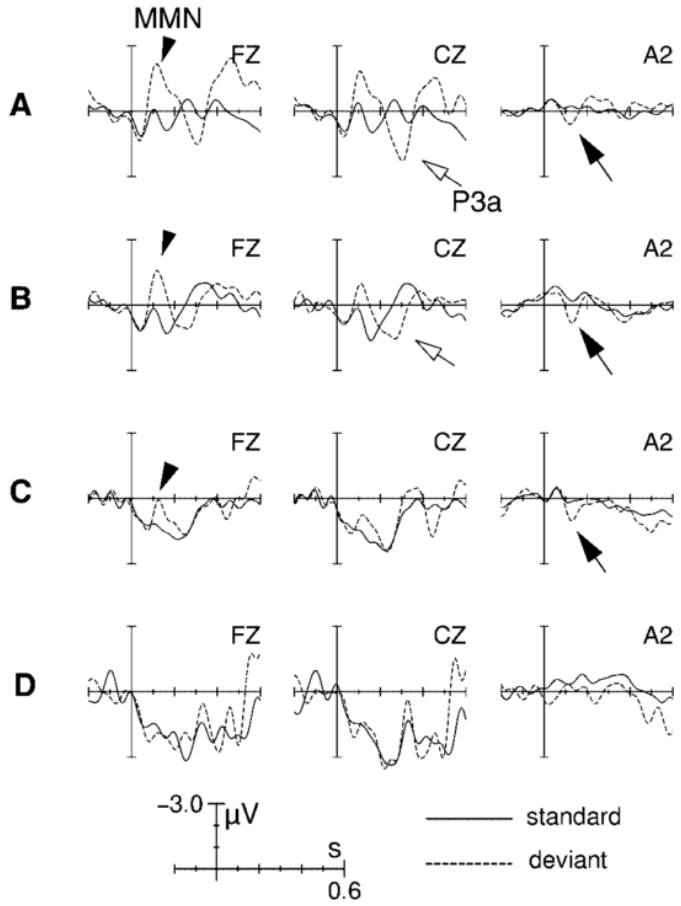

Figure 1.22: Effects of propofol anaesthesia on frequency deviant MMN recorded with an oddball paradigm, under 4 levels of anaesthesia. A: Awake. B: Light sedation. C: Deep sedation. D: Unconsciousness. The MMN and P3A responses highlighted diminish with increasing levels of propofol and are abolished once unconscious (Heinke et al., 2004)

1.3.7 Potential Effects on Adaptation

Recently there have been several studies looking at the effects of neuromodulators on adaptation but primarily on SSA, using oddball protocols.

Two studies have looked directly at the effects of GABA modulation on oddball SSA in the MGB (Duque et al., 2014) and IC (Pérez-González et al., 2012) of the rat. Both studies used the GABA channel antagonist gabazine and Duque *et al.*'s study also used GABA as an agonist. Duque et al.'s single unit recordings showed that 79% of their neurons exhibited a change in SSA magnitude following iontophoretic application of the drugs. 45% showed reduced levels of SSA in the presence of gabazine and 57% showed a greater degree of SSA

following application of GABA. GABA also showed a significant reduction of the time constants for the onset of adaptation (Duque et al., 2014). This appears to show that SSA is at least partially mediated by GABA activity.

The effects of the cholinergic system on SSA have also investigated. Using iontophoresis of ACh and muscarinic and nicotinic channel antagonists in IC (Ayala and Malmierca, 2015; Ayala et al., 2015). While there is a visible trend in their data showing a small modulation of CSI for a subset of the recorded neurons, trending toward a decreased CSI with cholinergic activation, at a population level this displays a very small effect size, especially when compared to GABAergic modulation.

Using an adapter-probe approach, Wehr and Zador (2005) used whole-cell, blind patch-clamping techniques to get recordings of synaptic conductances of cortical neurons in rat auditory cortex. Click stimuli were used to elicit a response from the neurons and the resulting conductances were measured (Figure 1.23A). It was found that a combination of pentobarbital and ketamine produced substantial changes to the evoked conductances compared to ketamine alone, with a dramatically increased amplitude of both excitatory and inhibitory currents and an increase of the inhibitory time constant. The authors also found that pentobarbital, a GABA potentiator, increased the degree of adaptation of their cells (Figure 1.23B). This effect is likely either indirectly related or unrelated to the changes in inhibitory conductance, due to the previously discussed finding of this study of the mismatch of the time course of inhibitory conductances and adaptation.

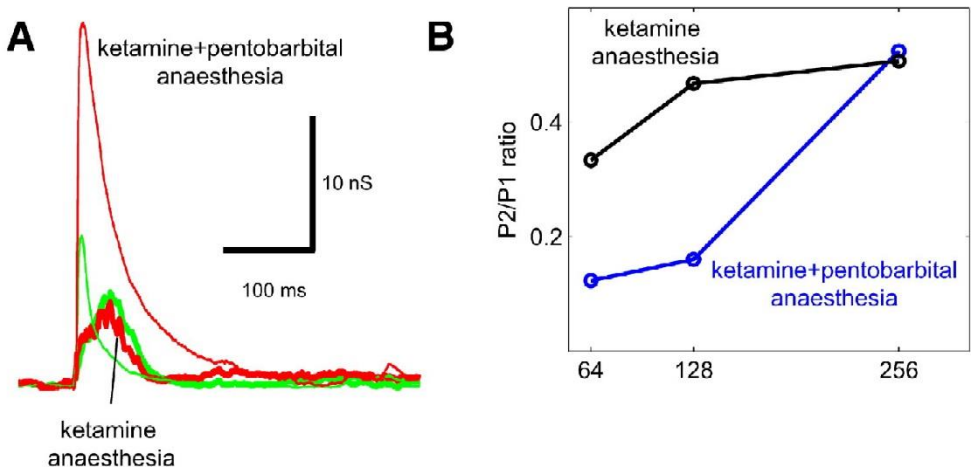

Figure 1.23: Pentobarbital anaesthesia prolonged inhibitory synaptic conductances and increased suppression compared to ketamine. (A) Excitatory (green) and inhibitory (red) synaptic conductances evoked by a click under ketamine (heavy lines). After pentobarbital administration the inhibitory conductance of the cell was greatly increased and prolonged (thin lines). Duration of inhibition increased from <100 to >200ms. (B) P2/P1 ratio (Ratio of adapted to unadapted response amplitude) before (black) and after (blue) pentobarbital for this cell. Forward suppression was greatly enhanced by pentobarbital for intervals up to 128ms showing a greater degree of adaptation (Wehr and Zador, 2005).

1.3.8 Summary

Anaesthesia is widely used in in vivo studies of sensory neural processing. Previous studies of the effects of systemic general anaesthesia on neurons in the auditory cortex have shown significant changes to frequency tuning and responses to basic features within the stimulus such as onsets and offsets. Studies of this nature have typically used a single anaesthetic agent, comparing awake and anaesthetised states, and it remains unclear to what extent the choice of anaesthetic agent will affect basic response properties of neurons to sensory stimulation.

This thesis investigates the effects of anaesthesia on coding of sensory stimuli in the cortex, looking at the effects on both evoked potentials and neural spiking activity. The implications for studying basic stimulus features, frequency tuning and temporal processing under multiple anaesthetic agents are studied in an attempt to find the pitfalls of running sensory coding experiments under anaesthesia and how to attempt to avoid them.

Chapter 2

Parameters Affecting Adaptation in Human Auditory Cortex

2.1 Introduction

As discussed in section 1.1, a previous study showed that the selectivity of adaptation frequency tuning of auditory evoked potentials (AEPs) from human auditory cortex sharpened with increasing number of preceding adapters (Briley and Krumbholz, 2013). This is important as it could likely reflect an underlying plastic change in the tuning of auditory cortical neurons with short term exposure to external stimuli. It is unclear from the results of this experiment how generalised this effect is and what aspects of the adapter could generate this sharpening. In the previous experiment, this increase in frequency selectivity was shown to occur with increasing the number of adapting tones which will result in both an increased physical exposure to the adapting sound and an increased number of tone onsets. Here we attempt to disentangle these two parameters and characterise their effects on adaptation and frequency selectivity.

When measuring electrophysiological responses to auditory stimuli the evoked potentials can be classed into different latency bands relative to onset time. The short latency (0-20ms) response represents potentials from the auditory nerve and brainstem, mid-latency (20-50ms) produced by the sub-cortical pathway and the long latency response (50-300ms) which represents the cortical response to the stimuli. The standard cortical AEP, representing the average summed activity of the population of neurons in the cortex sensitive to a particular stimulus, can typically be described as a 3 peak waveform in humans and many other mammals (Figure 2.1). In humans the P1 peak (~50ms) localises to generators in the medial and central parts of

Heschl's gyrus, thought to reflect primary auditory cortex however the N1 (~100ms) has been localised more laterally in Herschl's gyrus and into planum temporale and is therefore thought to be representative of more non-primary regions (Liegeois-Chauvel et al., 1994). The P2 (~160ms) has a wider source spread, across planum temporale and Brodmann area 22 which contains further non-primary auditory regions and association areas (Godey et al., 2001).

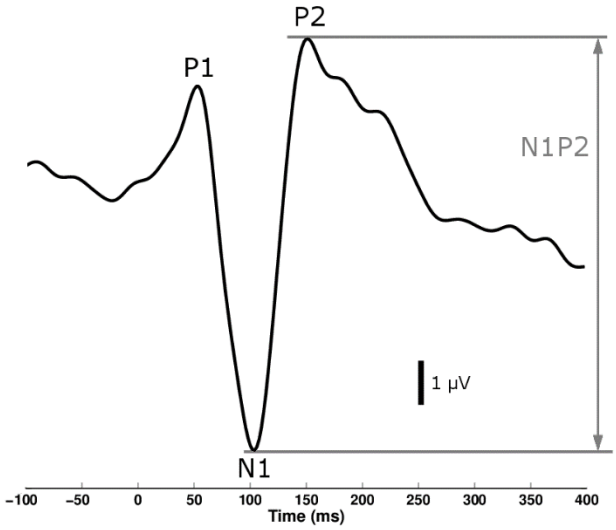

Figure 2.1: Example EEG-recorded, cortical AEP in response to a 100ms, 1 kHz pure tone presentation showing the three main stationary points and the definition of the N1-P2 amplitude

The N1-P2 amplitude was chosen as our measure of the AEP size. Our piloting showed robust adaptation effects between conditions using this, compared to the P1-N1 amplitude which showed no significant trends between any conditions. Some published work uses just the N1 or P2 amplitude but that encounters problems of ensuring a stable pre-stimulus baseline, increasing measurement noise. It has also been shown, due to the opposing polarities and overlapping time courses of the N1 and P2, the two components can partially cancel each other out (Makeig et al., 1997).

To calculate the degree of adaptation the adapted AEP amplitude has to be compared with that of the unadapted response (Equation 2.1).

$$\% \, Adaptation = \left(1 - \frac{Adapted}{Unadapted}\right) * 100 \qquad (2.1)$$

The frequency specificity of the response is a description of the degree of release from adaptation resulting from a frequency separation between adapter and probe. Increased frequency selectivity of this response results in larger release from adaptation from smaller frequency separations.

To investigate which adapter temporal factors could potentially modulate this increase in frequency selectivity we first ran a range of pilot tests to identify any parameters of interest.

2.2 Pilot Data

The pilot tests were designed to test a wide range of temporal parameter variations on the degree of adaptation measured, to discover the most important factors in the establishment of adaptational sharpening. Through the pilots the variables tested were (i) adapter duration, (ii) number of adapter onsets, (iii) inter-adapter interval (IAI) and (iv) inter-stimulus interval (ISI).

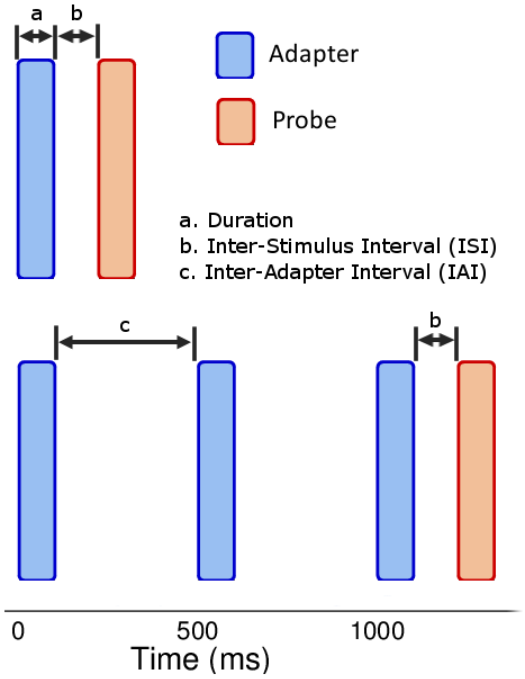

Figure 2.2: Schematic of the adapter-probe parameters varied in the pilot tests

The probe tone was chosen to be a 100ms, 1 kHz, 70dB SPL tone. In human studies 1 kHz is typically used as it gives a roughly maximal AEP amplitude. 100ms duration was used as the N1-P2 complex appears to integrate the energy of the tone over the first ~72ms of the presentation (Woods, 1995) so we wanted a stimulus longer than this integration window for maximum recruitment of neurons. ISIs of greater than

100ms were chosen to attempt to minimise the effects of sub-cortical adaptation contributing to the cortical measurements and to forego the need for using subtraction waveforms to account for overlapping adapter and probe AEPs (Lanting et al., 2013).

2.2.1 Method

EEG Data Acquisition: Auditory evoked potentials were recorded with a 32-channel EEG amplifier system (BrainAmp DC, Brain Products, Gilching, Germany) and an EEG cap fitted with 4 Ag/AgCl ring electrodes positioned for recording at Cz, linked mastoid reference electrodes at TP9&10 and grounded on the central forehead at AFz. Skin-to-electrode impedances were kept below 5 kΩ. The data were recorded continuously at a sampling rate of 500Hz and band-pass filtered online between 0.1 and 250Hz. Participants watched a self-chosen silent movie with subtitles through the recordings to remain alert. The participants were seated on a comfortable chair in a double-walled, electrically insulated, sound-attenuating booth (Industrial Acoustics Company, Winchester, United Kingdom).

Stimulus Presentation: All stimuli were generated digitally at a sampling rate of 24.414 kHz by RPvdsEx (Tucker Davis Technologies, Alchua, FL), digital-to-analog converted with a 24-bit amplitude resolution using TDT System 3 (RP2.1 Real-Time Processor, HB7 Headphone Amplifier, Tucker Davis Technologies) and presented diotically through Sennheiser HD280 headphones. The adapter and probe stimuli were gated on and off with 10ms cosine squared ramps and presented at an RMS level of 70dB SPL. They were presented in discrete trials of 3000ms duration with a pseudorandom, uniformly distributed ±200 cents jitter about the centre frequency to minimise longer term adaptation effects.

Parameter Variations: To test the specificity of the responses, frequency separations of 0-1800 cents frequency separation were used (1200 cents = 1 octave). Four parameters were varied between different conditions; adapter

duration, number of adapter repetitions, inter-adapter interval (IAI), the gap between adapter presentations, and ISI, the gap between the end of the adapter sequence and the probe presentation.

Analysis: Unless otherwise stated, statistical results are presented as mean ± standard error (SE). AEPs were obtained by averaging over all 100 repeats of each condition, aligned by first adapter onset. AEP peaks were determined visually and adaptation percentage was calculated for each subject using equation 2.1, using the N1-P2 amplitude as the amplitude measure.

2.2.2 Results

The results of these pilots suggested that both duration and number of repetitions could be important for the onset of sharpening, with both factors producing a significantly greater release from adaptation between 0-1800 cents than the 100ms adapter condition. This is far more evident in the short ISI condition (Figure 2.4, Left). These effects also change with increasing number of adapters, with 9 adapters showing greater frequency selectivity than 3.

From the results of these pilots it was decided the first human experiments should be focussing on the effects of adapter repetitions and duration, using a 125ms ISI between the adapter and probe. The adapter presentation rate does not appear to have a large effect on the frequency selectivity from these results so will not be a primary focus of our study but will still be investigated.

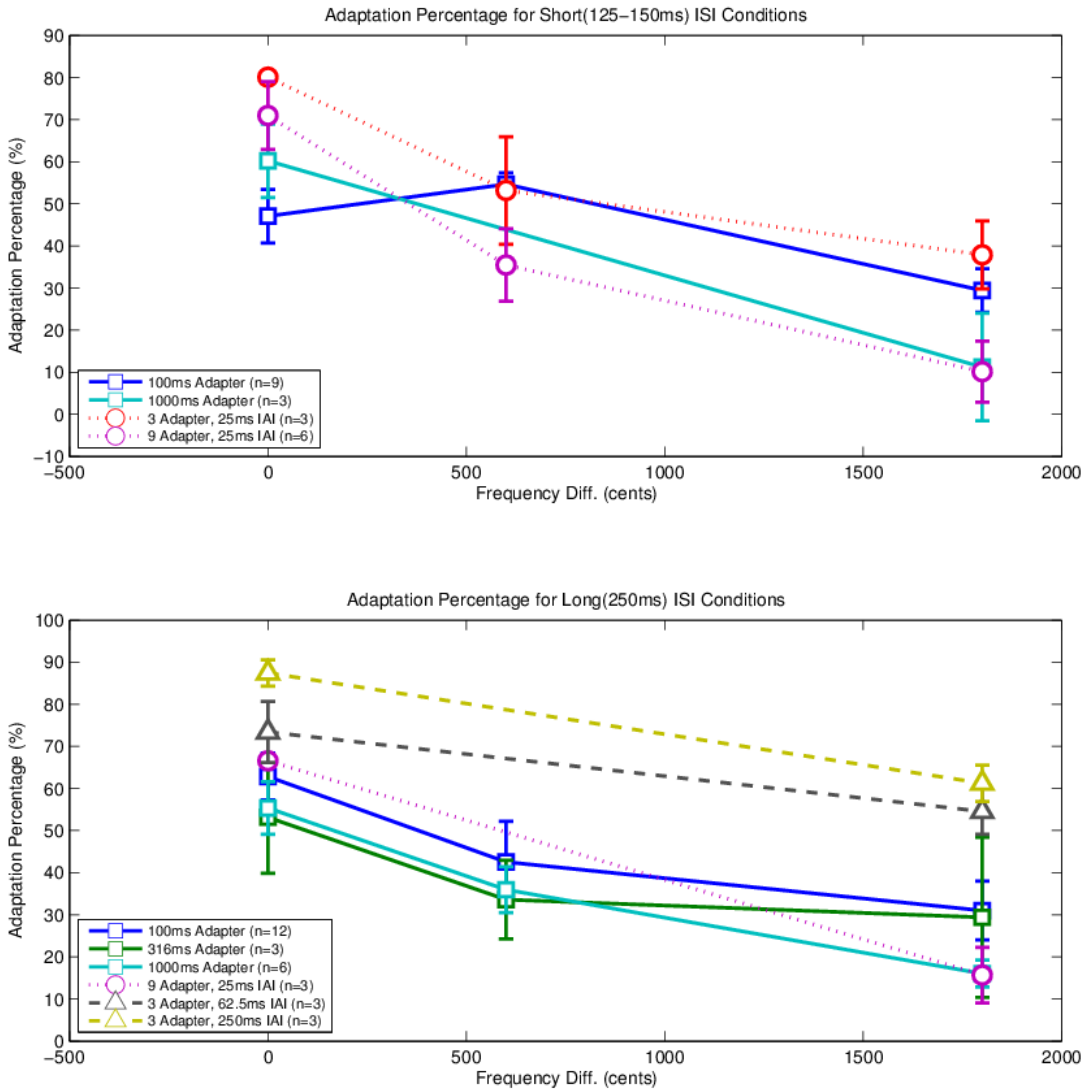

Figure 2.3: Effects of adapter parameter variations on adaptation percentage for short (top) and long (bottom) ISI conditions

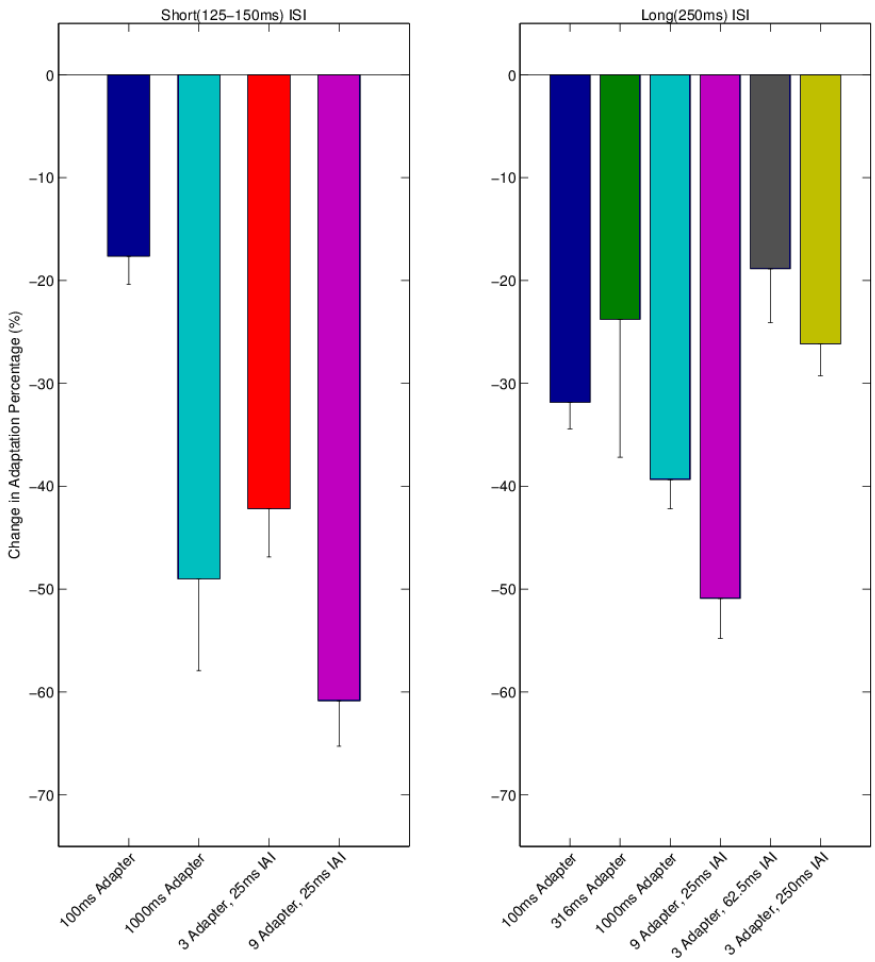

Figure 2.4: Change in adaptation percentage between 0 and 1800 cent frequency separation for the different stimulus temporal conditions and for the short (left) and long (right) ISI versions

2.3 Experiment 1

From the results of the pilots it was shown both tone duration and number of preceding adapters potentially contribute to the onset of sharpening. These effects were most prominent at short probe ISIs (~125ms) so these parameters were used to further investigate this sharpening. To create an analogous comparison between duration and multiple adapters the conditions were split into single onset, variable duration adapters and multiple onset adapters with the same first onset to last offset duration. Additional conditions were also included to investigate the effect of the presentation rate of the multiple adapters to see if the sharpening effects remain the same at slower presentation rates.

2.3.1 Method

Participants: 18 participants (13 male, 18-27 years, median 21 years) took part in the experiment after giving written, informed consent. All participants had normal hearing (pure tone thresholds below 20 dB HL between 0.25-8kHz) in both ears and no history of neurological or audiological disease. The experimental procedures used were approved by the School of Psychology Ethics Committee of the University of Nottingham and conformed to the Human Subjects Guidelines of the Helsinki Declaration (Version 6, 2008). They were not formally pre-registered online in accordance with the 2014 amendment to the declaration.

EEG Data Acquisition: The technical setup is identical to that used in the pilot studies (Section 2.2.1) except that a full 32 electrode EEG configuration was used in the standard 10-20 arrangement.

Stimulus Presentation: All stimuli were pure tones, presented diotically at an RMS level of 70 dB SPL and gated on and off with 10ms cosine squared ramps, identical to the pilots. Probe stimuli were 100ms 1 kHz tones, jittered within ±200 cents to minimise longer term adaptation effects and presented 125ms after adapter offset. Stimuli were presented in discrete trials of 3000ms duration.

Parameters: Adapter stimuli were either a varying number of repeating 100ms tones with either 25ms or 400ms inter-adapter interval (IAI) or continuous tones with an identical onset to offset duration as the repeating conditions. Each of the 6 temporal conditions (Figure 2.5) was presented with an adapter-probe frequency separation of either 0, 600 or 1800 cents resulting in 18 conditions. Stimuli were presented to the participants in 5 blocks, each containing 20 repeats of each condition in a pseudorandom order.

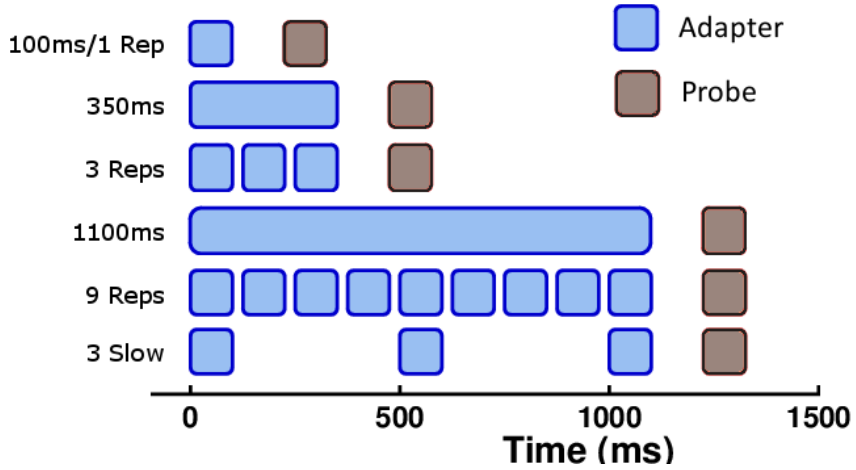

Figure 2.5: Schematic diagram of the 6 temporal conditions tested showing the adapter (blue) and probe (brown) durations and repetitions

Preprocessing: The data were 1) re-referenced to paired mastoid electrodes (TP9&10), 2) band-pass filtered between 0.1-35 Hz using a -48 dB/oct zero-phase infinite impulse response filter, 3) segmented into 2600ms epochs ranging from 100ms before to 2500ms after the first adapter onset, and 4) baseline-corrected to the 100ms pre-stimulus period. Epochs containing unusually large potentials across many electrodes (joint probability ≥3.5 SD) were rejected automatically. All epochs rejected this way were band-pass filtered between 1 and 35 Hz and subjected to independent component analysis (ICA). The ICA components were calculated for these rejected epochs.

The original epoched data were again tested and any epochs outside 2.5 SD from the joint probability mean were rejected. The remaining data were band-pass filtered between 0.1 and 35 Hz and artefacts related to eye blinks, lateral eye movements or electrocardial activity were removed using the ICA components calculated previously from the rejected epochs.

Waveforms from individual subject electrode Czs were primarily used for analysis but the overall trends of the data were also confirmed by global field power and all-subject grand average waveforms. AEPs were obtained by averaging over all remaining repeats of each condition, aligned by first adapter onset. AEP peaks were determined visually as the maximal amplitude

inflection points within the expected latency windows. Adaptation percentage was determined for each subject using equation 2.1, using the N1-P2 amplitude as the amplitude measure. The unadapted N1-P2 was taken as the mean of the N1-P2 amplitudes of the 100ms adapter and the first adapter of the 3 slow adapter condition in the 0 cents condition.

Analysis: Unless otherwise stated, statistical results are presented as mean ± SE. ANOVAs were undertaken in SPSS 22. All repeated measures ANOVAs were Greenhouse-Geisser corrected for violation of sphericity. All other statistics were done in Matlab.

2.3.2 Results

The adaptation percentages derived from the individual subject AEPs were initially tested by a three-way repeated measures ANOVA with factors frequency separation, duration and single vs multiple onsets (Figure 2.6). This test showed significant interaction between number of onsets and the frequency separation ($F_{(1.7,28.8)}$=7.88, P=0.003), indicative of changes in frequency tuning. This means that there is a significantly different frequency selectivity of single and multiple onset adapters.

The data were separated into the single and multiple onset datasets and tested separately by two-way repeated measures ANOVAs, testing frequency separation vs duration/number of onsets. The multiple onset dataset showed a significant interaction of onsets with frequency separation ($F_{(3.2,51.8)}$=4.55, P=0.003), however for single onset adapters, adapter duration did not show a significant effect ($F_{(3.4,54.2)}$=1.09, P=0.369). This means that the multiple onset data will show increased frequency selectivity with increased number of adapters but the single onset data does not show increased frequency selectivity with increasing duration.

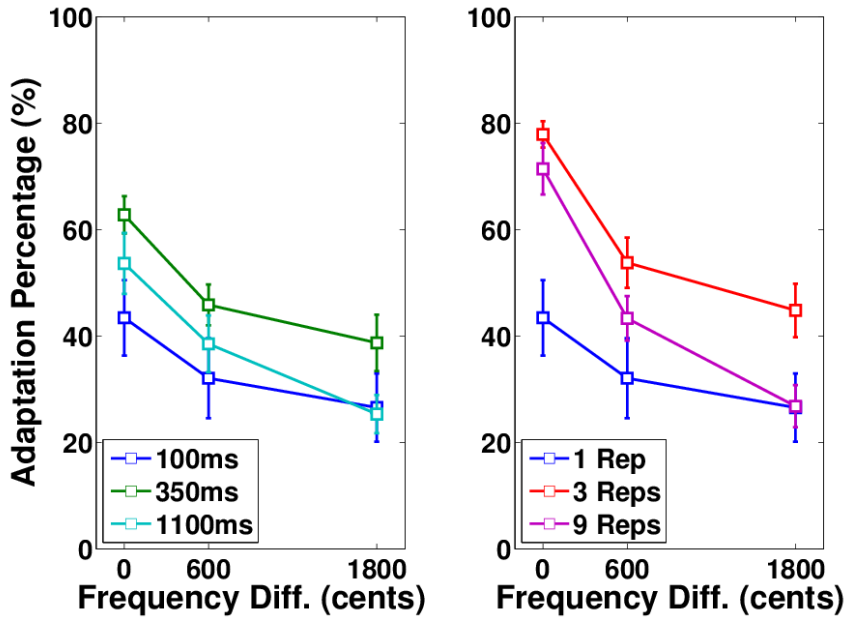

Figure 2.6: Effects of different adapter temporal parameters for single (left) and multiple (right) onset adapters on degree of adaptation with varying frequency separation between adapter and probe stimuli (n=18). Frequency selectivity of the response is represented by the gradient of the lines.

Another outcome of the experiment is the comparison between fast and slow adapter presentation rates. While there is a very significant effect of presentation rate on the degree of adaptation (two-way repeated measures ANOVA, $P = 2.5 \times 10^{-7}$), with the slower rate showing a much lower adaptation percentage, there does not appear to be an interaction between rate and frequency selectivity ($P=0.502$). Therefore the adapter presentation rate affects the amount of adaptation, with higher adapter rates leading to more adaptation, but does not have an effect on the frequency tuning. This effect leads to there being a larger release from adaptation for the slow 3 rep conditions than even the single adapter conditions.

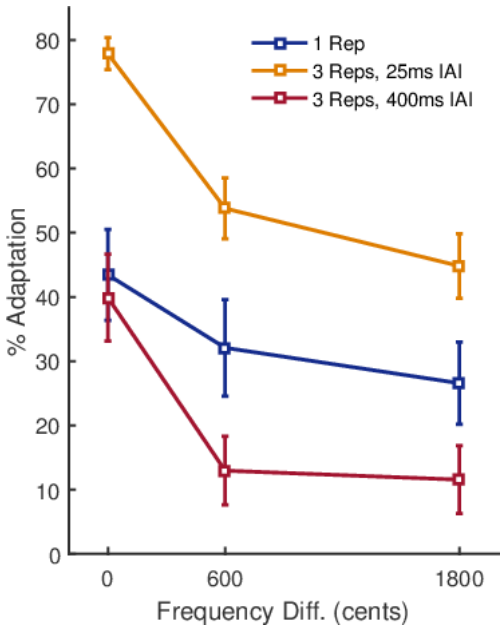

Figure 2.7: Effects of inter-adapter interval (IAI) for the two 3 onset adapter conditions on the level of adaptation

When looking at the waveforms for these conditions we can see in the slow 3 rep condition (Figure 2.8C) that the second and third adapters show considerable levels of suppression compared to the first adapter. This suppression of the preceding adapter could be a reason for the larger release from adaptation seen in the probe response. However if the recovery from adaptation was simply an exponential process then, even with a smaller adapter before it, it should show a similar or smaller amplitude than the adapter preceding it and here, even in the 0 cents condition, there is a release from adaptation. This could suggest that in sequences of adapters that the release from adaptation may not be a simple exponential recovery.

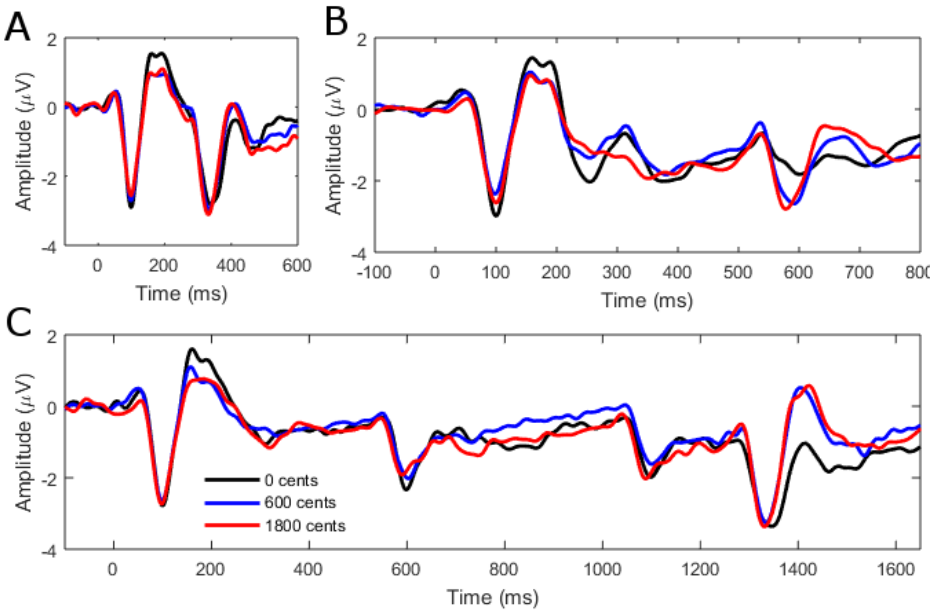

Figure 2.8: Grand average Cz waveforms for the 100ms/1Rep conditions (A), the 3 Reps, 25ms IAI conditions (B) and the 3 Reps, 400ms IAI conditions (C)

Using the grand average waveforms the topographic reconstructions of the probe response can be calculated. The response topography is a measure of the distribution of the voltage response over areas of the scalp. This has been calculated and visualised for each of the three inflection points (Figure 2.9).To estimate the topographic profile of the N1-P2 response the grand average is baselined to the latency of the N1 response and the voltage measurements at the P2 latency are used.

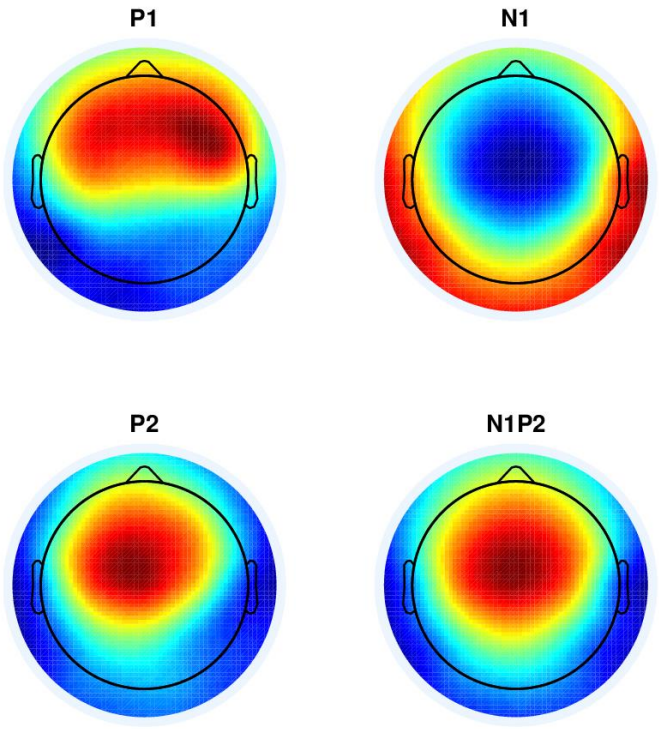

Figure 2.9: Signal topography of the three AEP peaks of the grand average unadapted response. The N1P2 map is the topography of the P2 peak when the electrodes are baselined to the N1 peak.

As an indicator of whether any additional brain regions are reacting to the adapting stimuli the topography of the adapted stimuli can be calculated and compared to the unadapted state using the global dissimilarity index (DISS). This is a measure of the similarity of two field configurations, independent of signal strength. DISS can range from 0 to 2 with 0 being topographic homogeneity and 2 being topographic inversion (Murray et al., 2008).

To determine whether there is a significant shift a multiple permutation distribution was determined by calculating the DISS for the grand average response after each subject's adapted and unadapted responses were randomly reassigned over 100,000 repetitions. This distribution suggests that the grand average DISS between the adapted and unadapted states is a statistically significant shift with $P<0.001$ although is still reasonably small at 0.21.

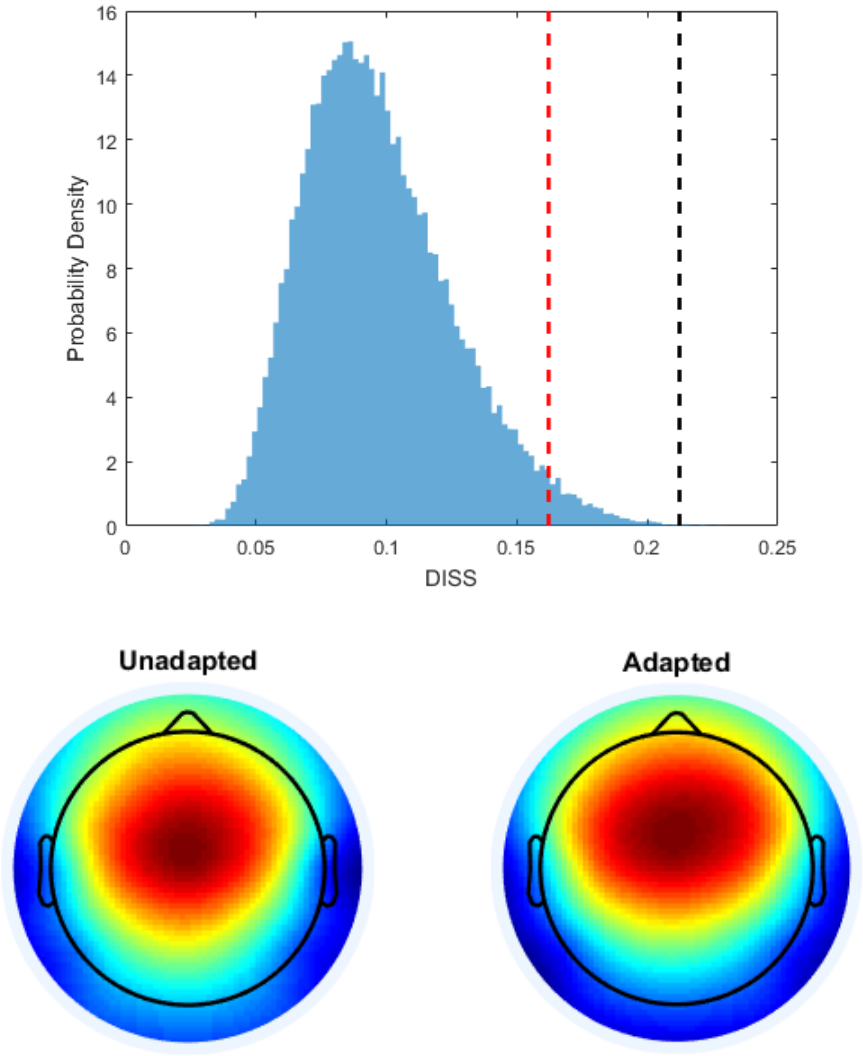

Figure 2.10: Top: Permutation testing of the DISS showing the 95th percentile (red) and the DISS of the grand average (black) indicating a statistically significant shift. Bottom: Grand average N1P2 topographies of the unadapted and adapted conditions.

By examining the topographies of each condition it does not appear there is any trends in the data that would suggest a progressive shift with either frequency, adapter duration or level of adaptation.

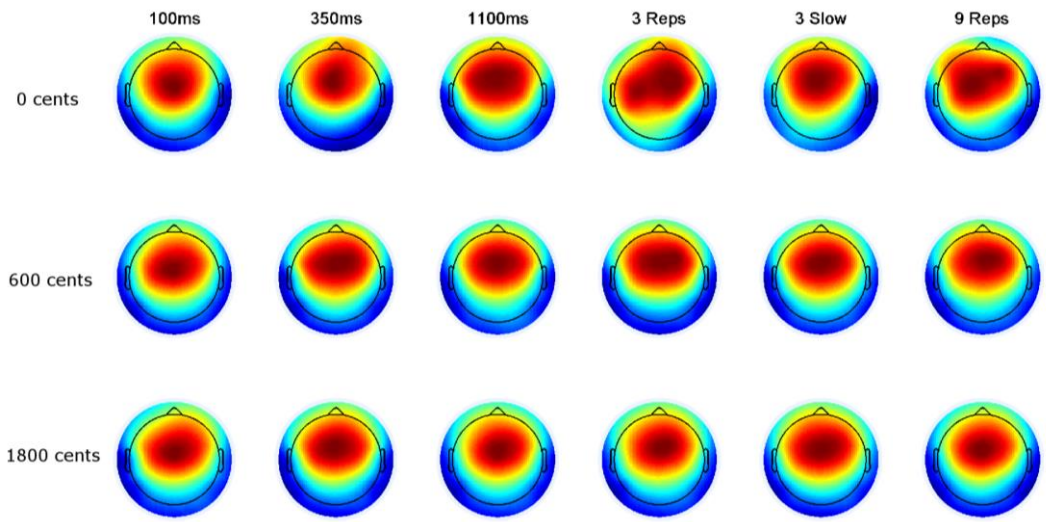

Figure 2.11: Signal topography of the N1P2 component of the grand average waveforms of each condition

The stability of the recordings over time was tested to rule out the main effects seen here being attributable to longer term adaptation effects or shifts in attention within the subjects as the experiment progressed. This was tested by comparing the degree of adaptation calculated from each subject's waveforms when using only the first two recording blocks or the last two blocks. These were tested using a four-way repeated measures ANOVA with factors block position, single vs multiple onsets, frequency separation and adapter duration. This test showed no main effect of block position (P=0.087) and no interaction between block position and any other factors including frequency separation (P=0.403).

2.3.3 Discussion

The main finding of this study is the importance of the number of tone onsets to the degree of adaptation specificity sharpening measured. This confirms the work of Briley (2013) where it was shown increased adapter number, for slow repeated adapters, would increase the degree of sharpening. We have also shown this effect is robust over different presentation rates, over a higher range of adapter repeat numbers and with a shorter ISI. Our results further show how these effects depend on number of repetitions and that no

sharpening is observed when adapters are prolonged rather than repeated. The repetition induced sharpening (RIS) also shows increase with increased number of adapters showing a robust effect.

With this experiment we've attempted to disentangle the effects of increased overall adapter duration and the effect of increasing the number of tone onsets that result from a repeated adapter. The results show that while increasing the duration of the adapting tone with a single onset may display a trend of increasing the sharpness of the adaptation specificity, this is not a statistically significant effect unlike increasing the number of onsets (Figure 2.6). This suggests that it is onsets and not exposure duration that conditions the probe response.

This onset induced sharpening appears to be mostly independent of rate or overall degree of adaptation, as shown by the comparison between the adapter rates, which, despite a ~40% difference in adaptation percentage and a substantial difference in presentation rate, still show comparable sharpening receptive field shapes.

To test if the multiple onsets could be resulting in some kind of deviance detection response the grand average waveforms were checked for an MMN response by creating a difference waveform between the 9 repetition and 1100ms duration conditions. The only noticeable difference between the two conditions was around the latency of the N1 with no significant effects in the 250-300ms latency range.

Another interesting trend seen in the data is a potential non-monotonicity in the level of adaptation with increasing duration in both the single and multiple onset conditions. This can be seen in both sets of data where the longest duration adapters show a lower adaptation percentage than the middle duration conditions for all frequency separations. This is perhaps most surprising for the 350ms vs 1100ms conditions at 0 cents where the longer duration condition produces ~15% less suppression. This goes against the

traditional assumption that long duration adapters will produce a monotonic, saturating level of adaptation with increasing duration (Lanting et al., 2013). With just three duration points this cannot be shown definitively though and a higher temporal resolution would be needed.

2.4 Experiment 2

It is possible that the results in experiment 1 contain a non-monotonicity in the level of adaptation with increasing duration or number of adapters. One potential explanation is that there are two separable processes occurring with different time constants. The onset of non-specific adaptation and the build-up of frequency sharpening. To better understand the time constants of the onset of these processes a higher temporal resolution of adapter durations than in experiment 1 is needed.

2.4.1 Method

Participants: 13 participants (8 male, 19-28 years, median 22 years) were recruited from the pool of subjects used for experiment 1 for retesting approximately 6 months after initial testing.

Parameters: Parameters were chosen as intermediary conditions to those tested previously and some outside the previous range tested. This resulted in the selection of 2, 6 and 15 repetitions and their single onset analogues, 225, 725 and 1850ms, along with the single 100ms adapter condition to act as a comparative measure between recording sessions.

EEG Data Acquisition, Stimulus Presentation and Analysis: Identical data acquisition, stimulus presentation methods and analysis methods were used to those in experiment 1 with the addition of source waveform analysis which was performed on both the experiment 1 and 2 data. Source waveforms were calculated using BESA Research 5.3, fitting dipole locations to the grand average unadapted response and then fitting vector orientations to the individual subject unadapted responses.

2.4.2 Results

This experiment is a continuation of experiment 1 to increase the temporal resolution of tested adapter durations. As such the two collected datasets are intended to be combined.

As a comparative measure between the experiment 1 and 2 recording sessions, the three frequency separations of the 100ms adapter condition were run in both (Figure 2.12). There was found to be no significant difference between the population means for these three conditions between the two experiments (two-way ANOVA, P=0.734). While the population means are comparable, when comparing individual subjects between recording sessions and looking at correlations between the two sessions there is less repeatability, producing correlation values of r=[0.19, 0.03, 0.04]. This demonstrates the noisy nature of EEG recordings and means that repeated measures statistics cannot be used to compare subjects between the two experiments. However, as the population means are not significantly different, it was deemed justifiable to combine the datasets for analysis.

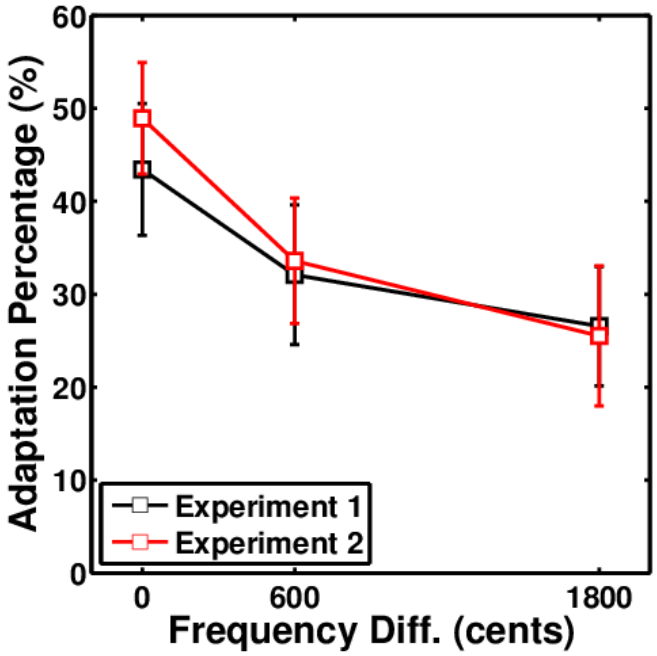

Figure 2.12: Comparison of the adaptation of the Cz waveform 100ms adapter conditions recorded in each session as a measure of test-retest reliability

Using the Cz waveform data, a three-way ANOVA comparing factors frequency separation, duration and single vs multiple onsets showed a significant interaction between frequency separation and single vs multiple onsets (P=0.028). From the visual trends seen in the data it was decided to split the dataset into the three adapter frequencies for post-hoc analysis (Figure 2.13).

The 0 cents and 600 cents conditions were found to have significant differences in adaptation percentage between the single and multiple onset conditions (two-way ANOVA, $P=9x10^{-9}$ and P=0.005 respectively) whereas at 1800 cents it did not reach significance (P=0.065).

While 600 cents reaches significance the effect size is reasonably small, with around a 5-10% increase in adaptation with multiple onsets over single onsets, a comparable degree to that of the 1800 cents condition, whereas the 0 cents conditions show an average 15-30% increase in adaptation. This shows that in the multiple onset conditions the 0 cents conditions are significantly more adapted than in the single onsets while the 1800 cents conditions do not change, increasing the adaptation gap between them and thereby showing an increase in the frequency selectivity.

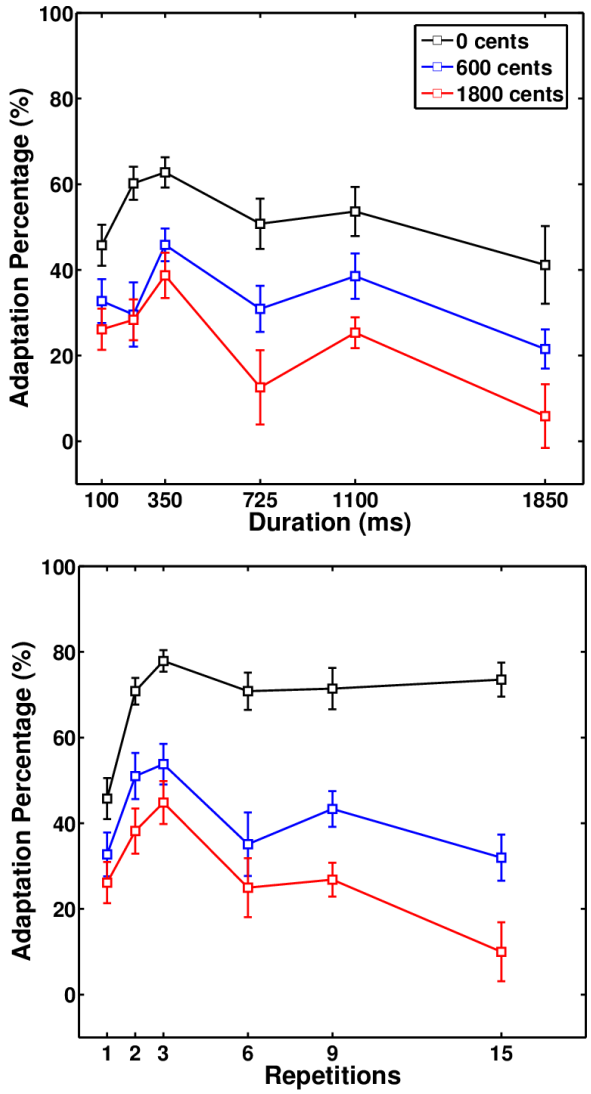

Figure 2.13: Effects of different adapter temporal parameters for single (top) and multiple (bottom) onset adapters on degree of adaptation of the Cz electrode AEP with varying frequency separation between adapter and probe stimuli

In experiment 1 it was shown there was a small but significant shift in the response topography between the unadapted and adapter conditions. As such, the Cz may not be a reliable measure as it could be reflecting a shift in the orientation of the current dipole of the response rather than the response size itself. To help rectify this and to validate the results, the data can be analysed the adaptation of the global field potential (GFP). The GFP is a measure of the activity of the whole brain. It is a calculation of the variance of the measured electrical fields, using all of the measurement electrodes and assuming their voltages sum to zero, based on the assumption the brain is a conservative

system whose sources and sinks will be the only contributors to the recordings (Lehmann and Skrandies, 1980). The GFP has been calculated with the following equations.

$$\omega_i(t) = V_i(t) - V_i(t_{N1}) \tag{2.2}$$

$$GFP(t) = \sqrt{\sum_{c=1}^{C} \frac{1}{C}\left(\omega_i(t) - \sum_{c=1}^{C} \frac{\omega_i(t)}{C}\right)^2} \tag{2.3}$$

Where $V_i(t)$ is the voltage measured by electrode i at time t, and t_{N1} is the latency of the N1 peak. By baselining to the N1 response the amplitude of the P2 peak can be used as the measure of adaptation and the recovery graphs can be calculated as they were for the Cz electrode and source waveforms.

As with the Cz recordings, the GFP results in the 0 cents and 600 cents conditions (Figure 2.14) were found to have significant differences between the duration and repetition conditions (two-way ANOVA, $P=3.8\text{x}10^{-8}$ and $P=0.015$ respectively) whereas at 1800 cents it did not reach significance ($P=0.139$).

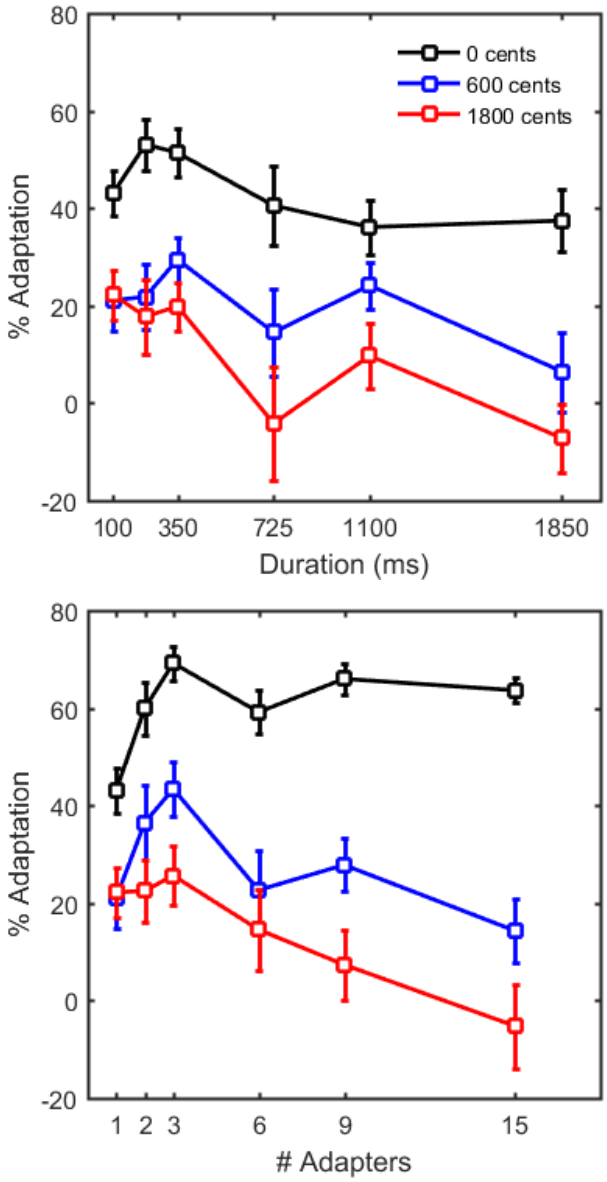

Figure 2.14: Effects of different adapter temporal parameters for single (top) and multiple (bottom) onset adapters on degree of adaptation of the GFP AEP with varying frequency separation between adapter and probe stimuli

To further show the robustness of the results the source waveforms from the auditory cortices were derived and the adaptation percentages calculated from the resulting waveforms. With these waveforms then in addition to the N1-P2 amplitude, the P1-N1 amplitude was also analysed as a measure of early cortical levels of adaptation.

The N1-P2 results show overall comparable trends to the Cz and GFP data, with increases in the 0 cents adaptation for the multiple onset data (two-way ANOVA, $P=7x10^{-8}$) but no significant change for 600 cents (P=0.176) or 1800 cents (P=0.302). These results also show an overall lower level of adaptation with some of the mean results showing facilitation of the response (% Adaptation<0) particularly those in the 1800 cents separation conditions (Figure 2.13).

However in the P1-N1 results there is no significant effect of single vs multiple onsets on the frequency selectivity of the response (three-way ANOVA, P=0.530). These results also show much smaller levels of adaptation and frequency selectivity throughout all conditions. This result suggests that the RIS effect is indeed generated in the cortex and is not inherited from subcortical processes.

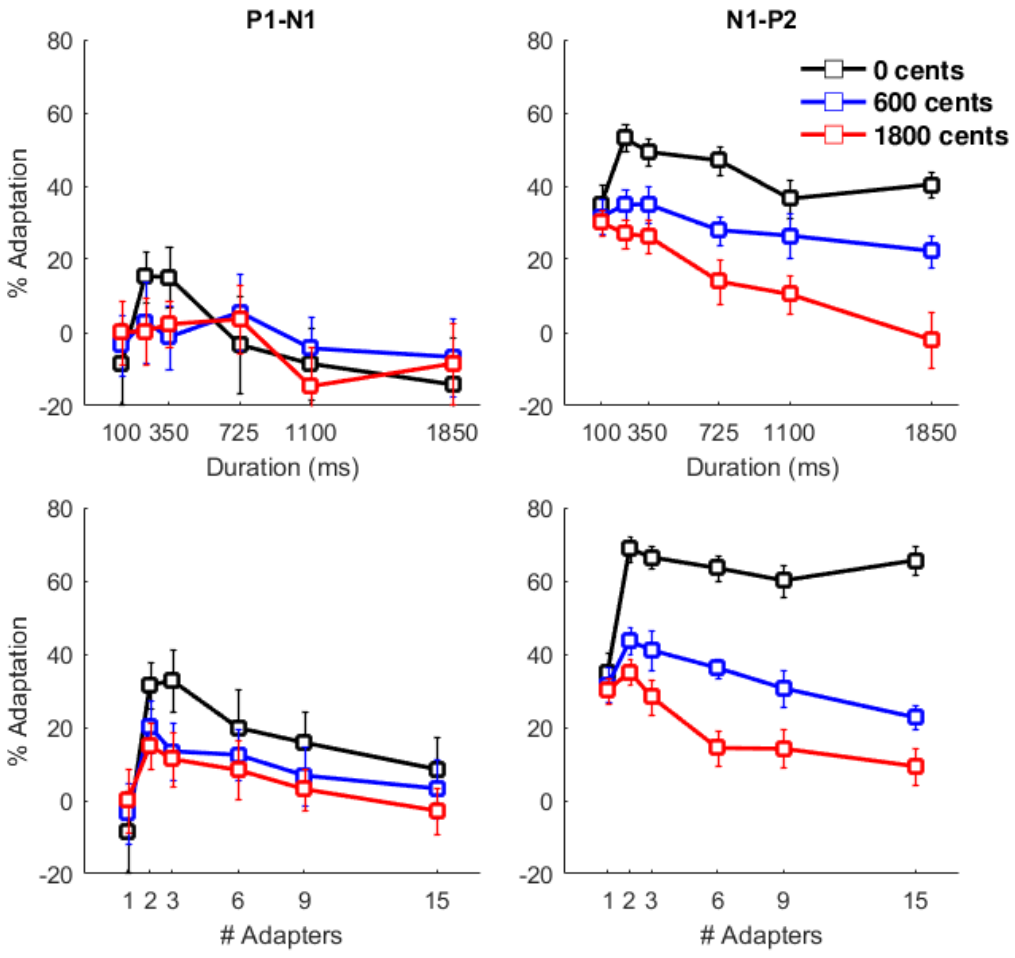

Figure 2.15: Effects of different adapter temporal parameters for single (top row) and multiple (bottom row) onset adapters on degree of adaptation of the source waveform P1-N1 (left column) and N1-P2 (right column) with varying frequency separation between adapter and probe stimuli

2.4.4 Discussion

Through these two experiments we have demonstrated that the temporal patterning of an adapting stimulus will affect the tuning of the resultant adaptation of a probe tone. This effect produces a significant sharpening of frequency selectivity in response to increasing numbers of tone onsets. This repetition induced sharpening (RIS) appears to be progressive with increasing number of adapter onsets, up to and potentially beyond 15 tone onsets.

This is a robust effect and can be demonstrated in the source waveforms, Cz channel and global field power. RIS is also reproducible at a population level as we are able to see clear trends and patterns in both halves of the dataset even though they are collected six months apart. However due to the inherent noise of collecting EEG data it appears adaptation is not reproducible at an individual subject level. This variability can also be seen in the results from the GFP and to a lesser extent the Cz waveforms where a zigzagging of results can be seen between the first and second experiment conditions. This effect seems to be mostly abolished in the source waveforms suggesting they will produce the most repeatable data.

Another main difference between the single and multiple onset conditions is that with increasing number of onsets the 0 cents condition appears to reach a steady state level whereas the degree of adaptation to single onset adapters begins to decay away with increasing duration. This effect demonstrates that, unlike in the visual system (Solomon and Kohn, 2014), auditory adaptation is a non-monotonic function of adapter length, with adapters of onset to offset duration of >350ms allowing some recovery resulting in a reduced level of adaptation. This non-monotonicity of auditory adaptation appears to be a

novel effect not previously reported in the literature. This could be due to other studies not using as broad range of adapter durations or for those that do, for example in the case of Lanting et al. (2013), using a shorter adapter-probe ISI which could lead to greater involvement of sub-cortical structures which may not show non-monotonic characteristics. It is not immediately obvious what neural mechanism would generate this non-monotonicity.

In the results for the source waveforms a number of conditions show facilitation (% Adaptation<0). As this source waveform is supposed to better represent the activity directly from the auditory cortex this could reflect a genuine increase in activity for those conditions. The conditions that demonstrate this phenomenon are primarily those with an 1800 cent frequency separation and a long duration adapter. That level of frequency separation would put it in the region where single neurons have been found to show facilitation (Brosch and Schreiner, 2000; Brosch and Scheich, 2008). This facilitation of the EEG response could represent a facilitation of the underlying neural spiking rate.

It has also been demonstrated that adaptation will cause a small but significant shift in the topography of the probe response. It could be possible this could represent activation of more frontal brain regions but due to the latencies involved (100-200ms) this is unlikely and it is more probable this shift reflects the variability in levels of adaptation of different primary and non-primary auditory regions.

It is generally assumed that, as subcortical neurons at the level of the auditory thalamus can maintain a following response to tones presented at a very high rate (~100-300Hz) compared to auditory cortex (~10Hz) (Froemke and Schreiner, 2015), that adaption will show a rate dependence in each brain region with higher presentation rates needed to affect more peripheral structures. By showing that sharpening will still occur with IAIs as large as 400ms (Figure 2.7) this suggests RIS is cortical in origin. This, combined with the lack of RIS seen in the earlier latency P1-N1 response and the fact that

adaptation has not been shown to have a significant corticofugal component (Antunes and Malmierca, 2011), comprising mainly a feedforward component, suggests there may not be any substantial changes in subcortical adaptation tuning.

This independence of the degree of adaptation and frequency selectivity also supports the idea that the non-monotonicity could be caused by a two-stage process. One component building up a rapidly developing and recovering non-frequency specific adaptation and another slower component, inducing an increased frequency selectivity.

Chapter 3

Modelling of Adaptation in Human EEG

3.1 Introduction

In the previous chapter we investigated the effects of adapter temporal parameters on the frequency tuning of adaptation. It was found that by using multiple onset adapters that a sharpening of the adaptation frequency selectivity could be induced but the same effect was not seen for single onset, long duration adapters. These results also displayed a non-monotonicity of adaptation with increasing adapter length. As these are novel effects it is not clear what neural processes could be causing them.

To further investigate the effects of the repetition induced sharpening (RIS) phenomenon discovered in Chapter 2 and to potentially reveal some of the underlying neural mechanisms, a computational model was developed. This neuro-computational network model is based on the model architecture of a previously published model designed to simulate SSA and MMN in auditory cortex (Mill et al., 2011). As this model had been designed for closely related phenomena to adaptation, simulates frequency specificity that can adapt over time and stimulus input and can show recovery over time it was considered to be a good starting point.

The model comprises of two layers of adapting synapses. The first layer comprises a bank of frequency selective neurons with varying characteristic frequency (CF) which will converge through independently adapting synapses to the second layer neurons. These second layer neurons then project directly to an output layer through a second adapting synapse.

This two stage, multi-channel architecture should be able to replicate some of the main phenomena seen in the EEG data for example frequency selectivity. If

an adapter is played this suppresses the synapses around the adapter frequency, if the probe is played at this frequency it produces a small response in the output layer. If it is played with a frequency separation the synapses are less suppressed and a larger response will propagate through the model (Figure 3.1A).

The two layers should also recreate the non-monotonicity of adaptation. With short adapters both layers will supress increasing the level of adaptation but with increasing duration adapters the first layer will adapt out. The second layer will no longer be active and will start to recover with longer adapters leading to a greater recovery.

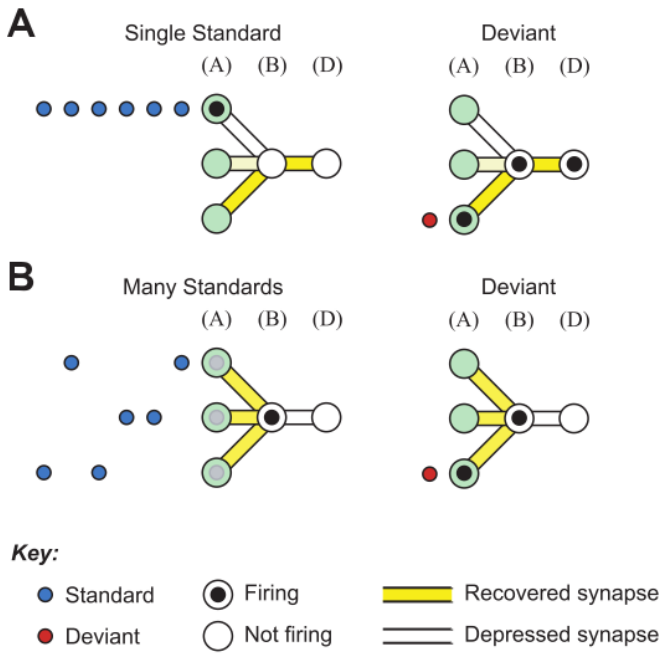

Figure 3.1: Schematic diagram of the initial model architecture showing the response to an oddball paradigm (A) or a many standards scheme (B). Figure from (Mill et al., 2011)

This model needed a modification from its initial form to be able to fit the EEG data. In its initial incarnation the model inputs were a binary time course with the tone either on or off with no special treatment for tone onsets. With the findings of the previous study it was necessary to include an onset selective component to be able to fit both the single and multiple onset data.

The model produces a good fit of the data and can simulate both the single and multiple onset conditions with the same parameter set. The purpose of this chapter is to investigate the underlying properties of the model.

In this chapter first a description of the full model is presented, which can replicate the patterns our data, and the rationale which led to its development. After that there is a parametric exploration of this model, to highlight the importance and effects of the different parameters. After that reduced versions of the model are considered, and how sacrificing different elements of the model impacts on the ability of the model to fit different aspects of the data.

3.2 Model Development and Description

As discussed earlier this model is based on the architecture of a previously published model (Mill et al., 2011) which comprises a two layer adaptation scheme, a schematic of which is shown in figure 3.2. In our setup this consists of our frequency selective layer (w) which will be active for the duration of a stimuli within their receptive field being played. These neurons converge toward the second layer neuron (y) through separately adapting synapses. Neuron y will combine the responses of multiple frequency response areas then project onto the output neuron (z) through another adapting synapse.

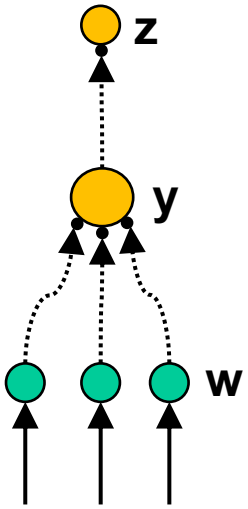

Figure 3.2: Schematic diagram of the initial model architecture from Mill et al. showing the convergent, adapting inputs of the first layer and the direct synaptic connection in the second

As it became evident that tone onsets were important for the build-up of RIS, and the model contained no onset selective components, this needed to be rectified. After several iterations of models the architecture in figure 3.3 was decided upon as this produced the best results and the majority of other versions tested were unstable or would not fit the data. This version includes an onset selective neuron (x) that will be responsive for 10ms following a tone onset and converges onto the second layer neurons using a transiently adapting synapse (Mill, R., personal communication). This synapse is treated as being non-adapting as it is considered to adapt and recover at a shorter timescale than is dealt with by this model.

In the single onset case the initial onset will activate both synapses and the sustained activity will keep both of them active. This is until the first synapse adapts out, therefore stops the stimulation of the second synapse allowing it to recover. This produces the non-monotonicity with increased adapter duration. For the multiple onset case however the x neuron will bypass the first synapse keeping the second stage adapted with the continued onset stimulation.

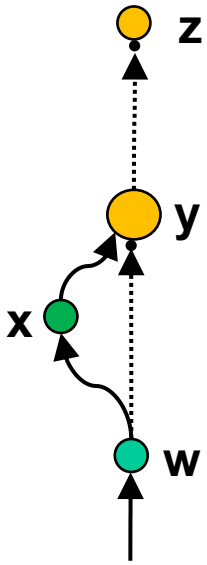

Figure 3.3: Schematic diagram of the onset neuron showing the non-adapting bypass of the first layer adapting synapse

These individual frequency channels can be stacked up into an interconnected network model. The model comprises 45 frequency channels with each neuron in the w layer having a characteristic frequency separated by 120 cents resulting in the model spanning a 4.5 octave gap. In the final fit, as discussed later, the onset neurons are narrowly tuned and will project to the y neuron within their channel but the adapting synapses are more broadly tuned, spreading to neighbouring channels in the *y* layer. The total response of the model is calculated as the summation of the activity of the *z* layer.

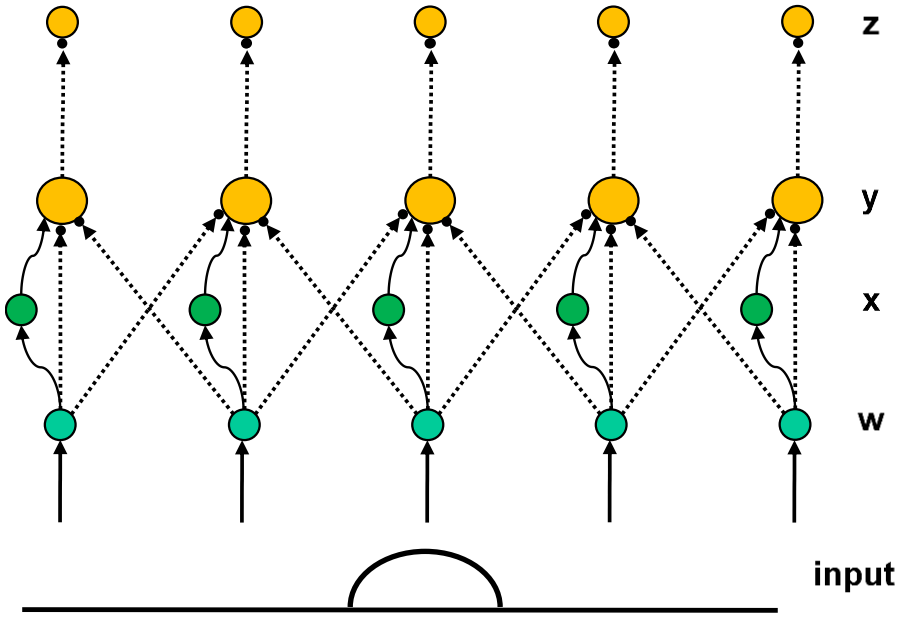

Figure 3.4: Schematic diagram of the full network model showing the distributed input, convergent first layer, directly connecting non-adapting onset neurons and the directly projecting second layer synapses

The model contains a total of eleven free parameters. Each of the two synapse layers have two variables for the time course of the onset (a) and recovery (b) from adaptation. The synapses have an activity threshold (ε) which will prevent inputs lower than that level not being propagated. The stimulus input, first stage synapse and the onset pathway each have a divergence parameter (σ) which represents the degree of spread of activity between channels from one layer to the next. A gain parameter (λ) will control the output level of the first layer. The model also incorporates a global inhibition module to act as an

overall normalisation of the level of adaptation with a tonic (I_t) and gain (I_g) parameter. This was necessary due to the facilitation seen in the experimental data as due to the constraints of the model it cannot produce facilitation without these additional parameters.

The output of the W synapses into the Y neurons is governed by the model inputs (C) and the synaptic signal strength (S), an analogue of neurotransmitter reserve, which is depleted while the synapse is active. This response is calculated for each frequency channel (n) and for each synaptic branch (j).

$$\frac{dS_{w,j}}{dt} = b_w\big(1 - S_{w,j}(t)\big) - a_w S_{w,j}(t) C_n(t) \tag{3.1}$$

$$W_n(t) = \lambda \sum_{j=1}^{J} S_w(t) C_n(t)\, G\big(n - j, \sigma_y\big) + \sum_{j=1}^{J} X_n(t)\, G(n - j, \sigma_x)\, - \varepsilon \tag{3.2}$$

$$(W_n \geq 0, otherwise\ 0)$$

The global inhibition comprises of two components. The tonic inhibition (I_t) is a measure of the degree of inhibition of the system at rest. The inhibition gain (I_g) interacts with an integrator of the first layer, freeing the system from inhibition as the first layer is stimulated.

$$\frac{dg_w}{dt} = \sum_{n=1}^{N} W_n(t) \tag{3.3}$$

$$g_i(t) = I_t(1 - I_g g_w(t)) \tag{3.4}$$

$$(g_i \geq 0, otherwise\ 0)$$

The second layer simply acts as a second in-line synapse with no interaction between different frequency channels.

$$\frac{dS_{y,n}}{dt} = b_y\left(1 - S_{y,n}(t)\right) - a_y S_{y,n}(t) W_n \tag{3.5}$$

$$Y_n = S_{y,n} W_n - \varepsilon - g_i \quad (Y_n \geq 0, otherwise\ 0) \tag{3.6}$$

The full model output is calculated as the summation of all of the layer Y outputs.

$$Z = \sum_{n=1}^{N} Y_n \tag{3.7}$$

The fitting procedure was progressive due to the number of free parameters. The fit was performed using a non-linear least squares fitting algorithm. Initially the model had all parameters constrained except the four synaptic adaptation, threshold and gain parameters, this was fit to the 0 cent separation conditions of the single onset conditions. The onset and sustained channel convergence parameters were then freed and the model was refit to all the single onset conditions. The final fit with all parameters freed was then performed on the full set of experimental data (Table 3.1).

$\mathbf{a_w}$	2.79	Build-up of first layer suppression
$\mathbf{b_w}$	3.36	Recovery of first layer suppression
$\mathbf{a_y}$	7.75	Build-up of second layer suppression
$\mathbf{b_y}$	1.82	Recovery of second layer suppression
$\boldsymbol{\varepsilon}$	0.633	Response threshold
$\boldsymbol{\sigma_x}$	0.104	Onset pathway frequency spread
$\boldsymbol{\sigma_y}$	4970	First layer synapse frequency spread
$\boldsymbol{\lambda}$	0.154	First layer gain
$\mathbf{I_t}$	0.135	Tonic inhibition
$\mathbf{I_g}$	0.0025	Inhibition gain
$\boldsymbol{\sigma_w}$	3.4	Input frequency spread

Table 3.1: Values of the model parameters of the model fitted to the experimental results

The final fit of the model produces a good quantitative fit to the experimental data. It displays all the patterns of adaptation seen in the human EEG results

including the frequency selectivity, RIS and non-monotonicity of adaptation with increasing duration.

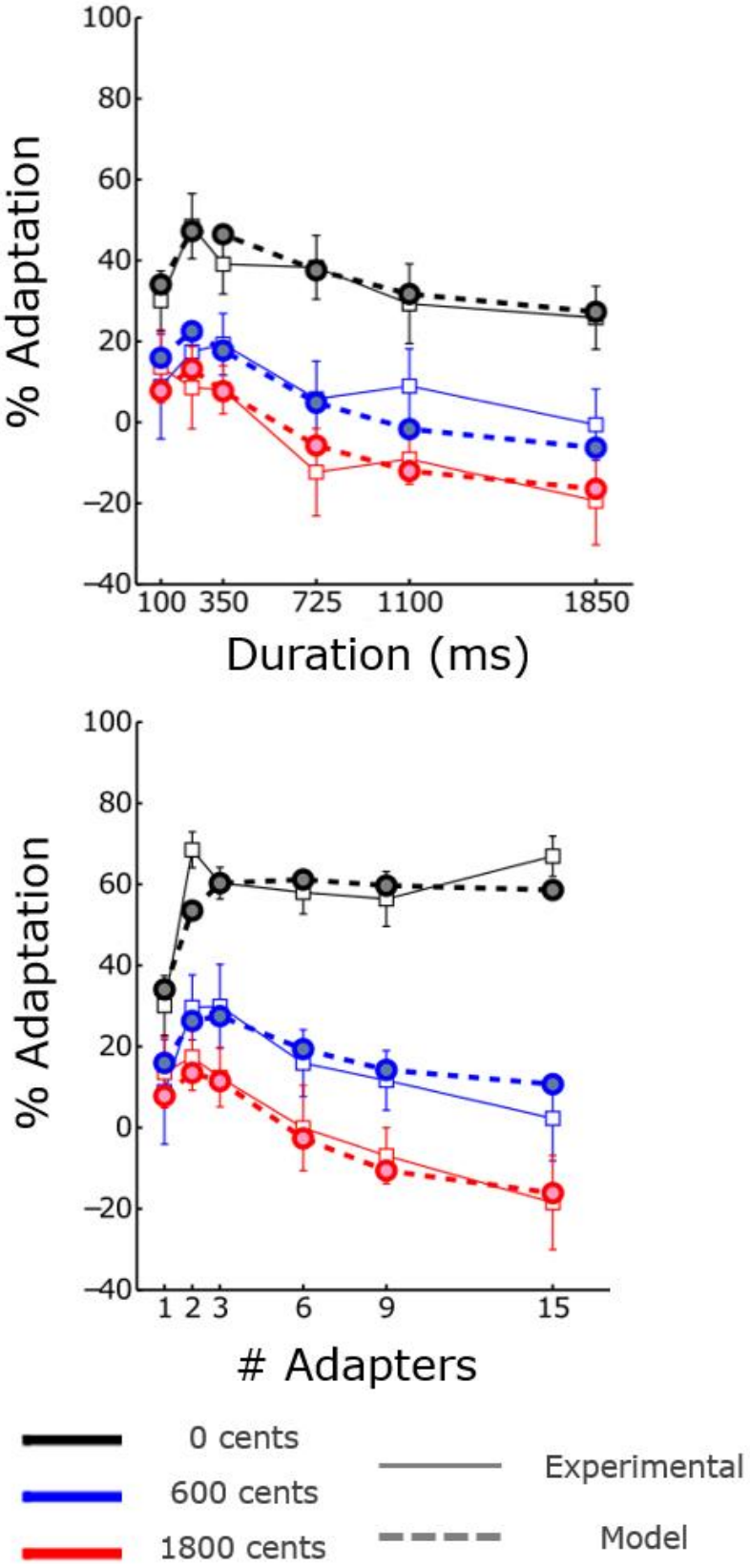

Figure 3.5: Overall fit of the two layer model to the human source waveform EEG experimental data

3.3 Evaluating the Model

3.3.1 Investigating the internal mechanisms

To see the responsiveness of the individual neurons simulated pure tones can be input to the model to see the excitation patterns. It appears from pure tone stimulation that the excitation spreads for an 8 channel/960 cent bandwidth centred about the stimulation frequency that as expected is identical for all of the input frequency channels. This response bandwidth of the frequency selective response is identical in both the first and second layers however the first layer, due to the broad convergent inputs shows a non-frequency selective response as shown by the shift in baseline. This degree of spread of excitation in the first layer appears to be a consequence of the bandwidth of the input and then propagated to the second layer by the narrow convergence of the onset pathway.

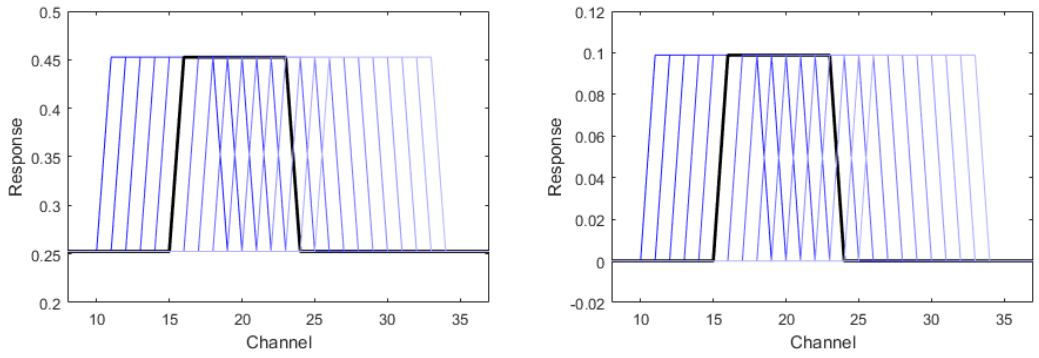

Figure 3.6: Response patterns of the first layer (top) and output layer (bottom) of the model in response to single channel stimulation from channels 15 to 30. Response to stimulation of channel 20 highlighted in black.

By looking into the model's internal workings the degree of adaptation can be derived at different stages of the model. For example the level of adaptation of the y layer neurons can be assessed and is showed compared to the full model outputs in figure 3.7. This shows that the first layer demonstrates a monotonically increasing level of adaptation with increasing duration and number of adapters. Without the second layer there is no recovery from adaptation and without the global inhibition component acting at this level

there is no facilitation. There appears to be little differentiation between the single and multiple onset conditions at this level with the multiple onset condition only showing a slightly lower level of adaptation, probably due to the silence gaps in these stimuli allowing a small amount of recovery.

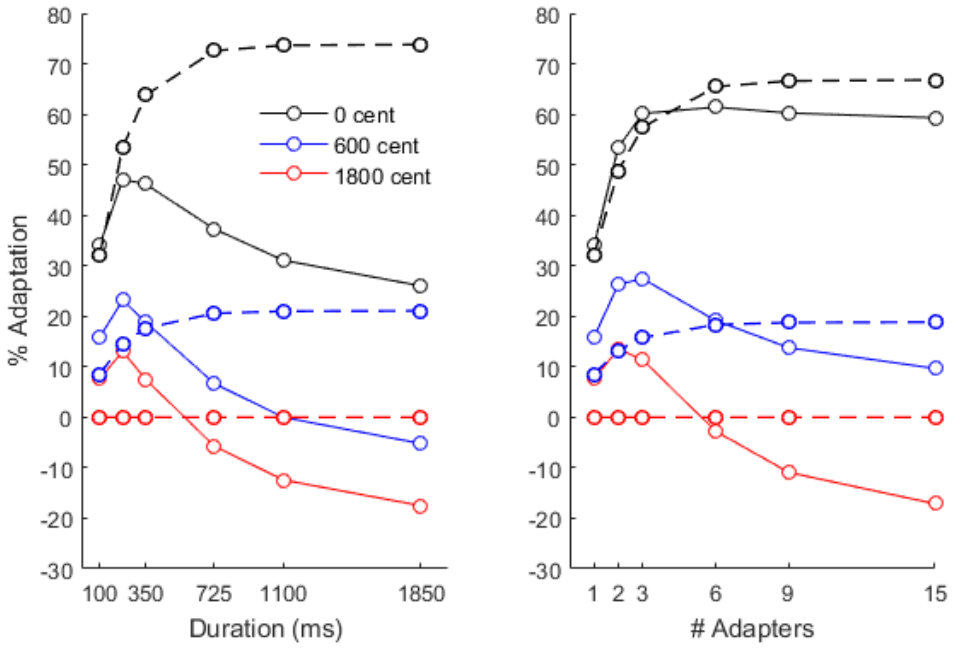

Figure 3.7: Level of adaptation of the output layer (solid line) and the first layer response (dashed line) in response to the experimental stimuli

By looking at the evolution of synaptic strength over time we can see that in the first layer synapses that the silence gaps between the multiple adapters do allow a recovery of the synapse whereas the single onset adapters will maintain their suppression. Also shown is the differentiation between the treatment of the second synapse between the single and multiple onset adapters. In the single onset condition the synapse strength is slowly suppressed over the first ~200ms before beginning to recover, this represents the first synapse's output degrading to a point where the build-up of adaptation in the second synapse is less than the recovery. By contrast, the multiple onset adapters will pass through the non-adapting onset neuron, bypassing the adapting first stage and maintaining the output through to the second synapse.

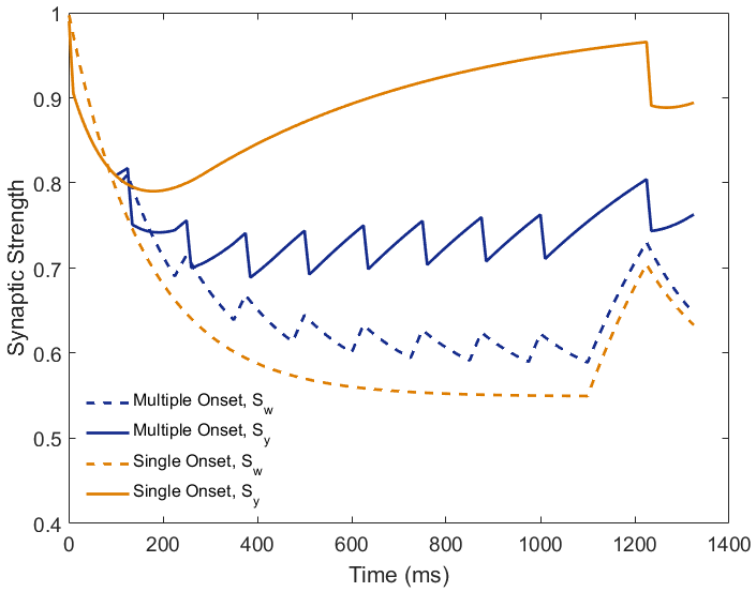

Figure 3.8: Synaptic strength of the first (dashed lines) and second (solid lines) layer synapses at the adapter frequency in response to the 0 cent frequency separation, single onset, 1100ms duration condition and the multiple onset, 9 adapter condition

At both of these levels we can also look at the frequency selectivity and the sharpening of response selectivity that occurs following the adapters. In the first layer results (Figure 3.9, Left) it appears selectivity will increase above the level of the standard 100ms adapter with a higher selectivity, shown by the gradient, of the continuous adapters over the multiple onset adapters. There appears to be no change in selectivity beyond around 1000 cents separation with no adaptation seen for any of the stimuli. However in the full model results (Figure 3.9, Right) it is the multiple onset adapters that show the larger increase in selectivity. It can be seen in the comparison between the 100ms and 350ms that the increasing duration will also create a small sharpening effect, much like the experimental results, but not of the same magnitude as the multiple onset conditions. Again much like the first layer results there appears to be no change in adaptation beyond 1000 cents separation.

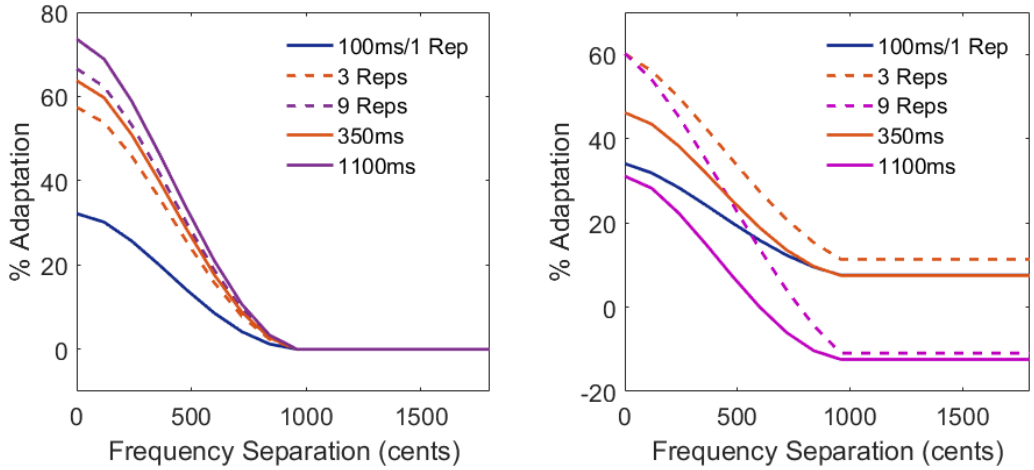

Figure 3.9: Level of adaptation of the outputs of the first (Left) and second (Right) layers with a range of adapter-probe frequency separations demonstrating the changes in frequency selectivity with different adapter types

3.3.2 Reponses of individual neurons in the model

The frequency selectivity can also be measured from individual neurons within the model. This model was developed to replicate evoked responses from large populations of neurons using a neurocomputational architecture. By investigating the contributions of individual neurons to this population response we can potentially relate these back to behaviours of neurons in the auditory cortex.

The neurons can be selected from either the first or second layer or either on the probe frequency or an off frequency neuron. When looking at the first layer neurons for both the on and off frequency neurons the frequency selectivity is identical and the patterns of change shown are identical to those in the whole layer results suggesting a homogeneous adaptation response across all the neurons in the first layer. However in the second layer neurons there appears to be differences between the on and off frequency neurons. Both show identical levels of adaptation for low frequency separations (<500 cents) but each shows a discontinuity, dropping to a lower level of adaptation. For the on frequency neuron this appears to happen around 500 cents but for the neuron 2 channels/240 cents higher in its CF this discontinuity happens around 750

cents. Apart from the heterogeneous discontinuities, the overall patterns of sharpening of the frequency selectivity appear similar to those seen in the whole second layer responses.

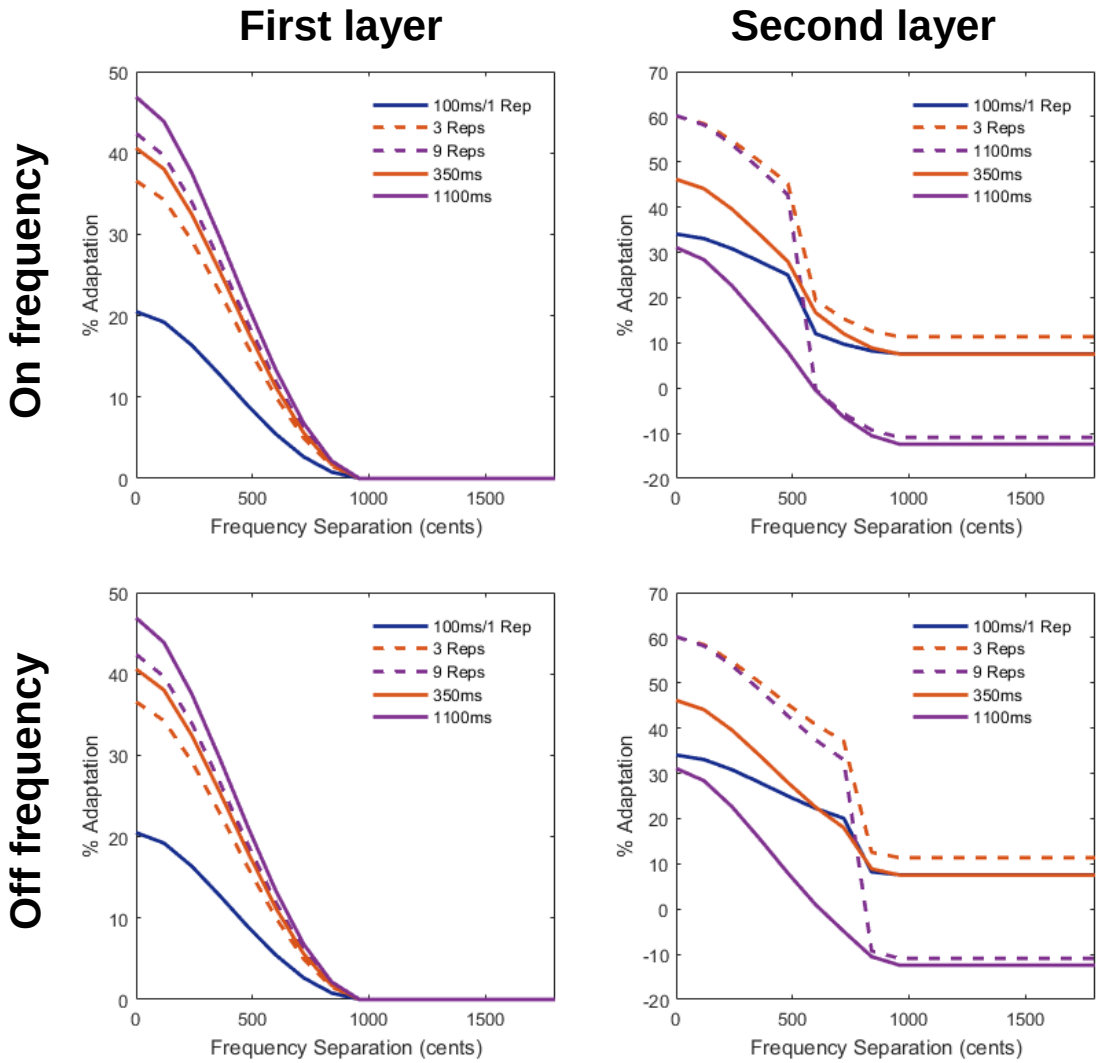

Figure 3.10: Single neuron frequency selectivity changes comparing the first layer (left column) and second layer (right column) and neurons with characteristic frequency on adapter frequency (top row) or 2 channels/240 cents higher (bottom row)

The causes for these changes in frequency selectivity can be seen in the adapted response profiles. For the first layer responses there is a global suppression of uniform magnitude over all channels. The magnitude of this suppression is relative to the degree of frequency separation of the adapter and probe. In the second layer however, there is a non-uniform level of adaptation over the channels and the channels closest to the adapter frequency will adapt

more strongly. This is the reason for the discontinuities in the frequency selectivity and the cause of the shift between channels. This adapter frequency specific suppression is very similar in nature to the frequency specific adaption (FSA) phenomenon discussed in section 1.2.2. With the global inhibition module working at this level this also produces a facilitation of the responses which is not seen in the first stage results.

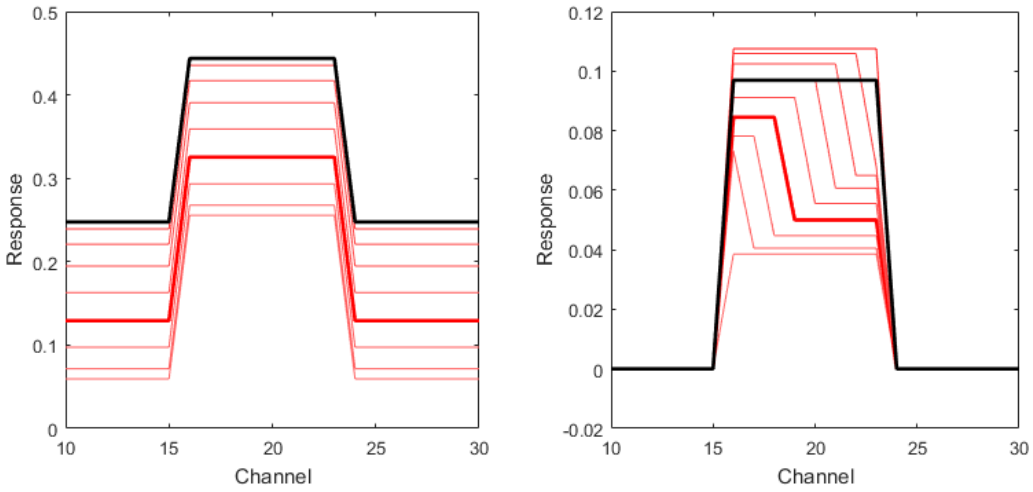

Figure 3.11: Response profile of the first layer (left) and output layer (right) of the model in response to a probe tone centred on channel 20, preceded by the 9 adapters condition with 0 to 15 channel separation above adapter to probe (light red). Unadapted response to the probe is shown in black and one condition, 3 channels/360 cents separation is highlighted in red

3.3.3 Time course of adaptation

Another test of the model is to apply it to data for which it hasn't been fitted to and from our initial experiments we have the 400ms IAI data. This dataset was testing the effect of using slower adapter rates on frequency selectivity. While the model fits the data for the 3 adapter, 25ms IAI conditions very faithfully, there is a large offset between the 3 adapter, 400ms IAI model and experimental conditions. The frequency selectivity of the conditions are comparable but the overall level of adaptation is ~40% too high. Due to the degree of facilitation seen in the slow rate adapters then it could be that the global inhibition parameters used in the model do not allow sufficient normalisation to allow the model to produce that degree of facilitation. It could

also be that the time course of the effects seen in the fast adapters cannot be extrapolated to longer timescales.

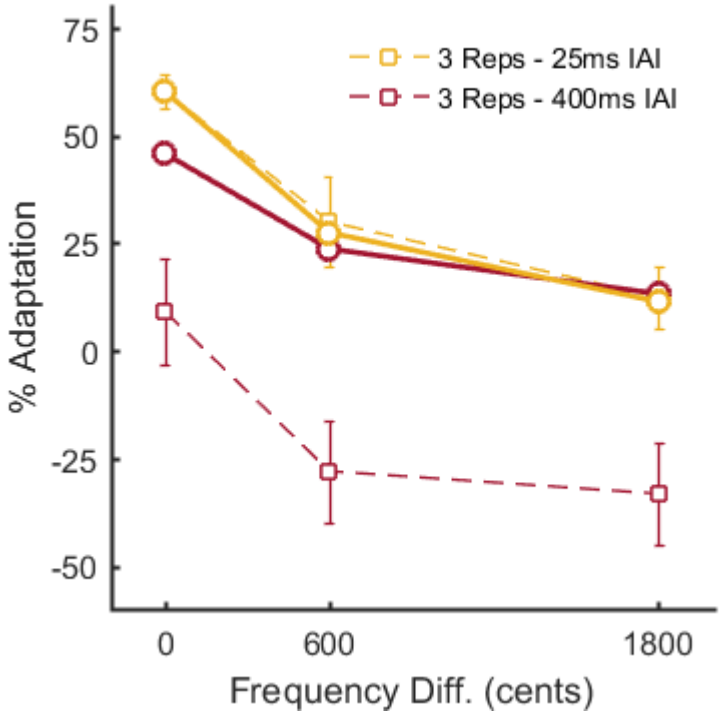

Figure 3.12: Fit of the model to the two 3 adapter conditions with varying inter-adapter interval (IAI). Experimental conditions are shown with dashed lines and model is shown solid.

3.3.4 Responses to Oddball stimuli

One of the properties of the initial Mills model was the ability to simulate responses to Oddball stimuli, Bernoulli sequences of two tone frequencies with different probabilities of occurring (Section 1.2.1). These sequences result in a difference in response size to the tones depending if they're played as a high probability standard or low probability deviant and using this difference the CSI can be calculated. For systems displaying SSA the CSI will be significantly different to 0.

The model was tested with sequences of 100 tones, with frequencies determined by a Bernoulli process with varying probabilities. This was repeated 100 times for each condition and the CSIs calculated (Equation 1.3).

The model in this form does show significant evidence of SSA for a variety of temporal conditions. With a tone duration and inter-stimulus interval of 100ms a highly significant SSA response can be elicited, with a magnitude proportional to the relative probabilities of the two frequencies. As the ISI is increased this pattern will hold but will show a decreasing CSI magnitude with increasing ISI (Figure 3.13).

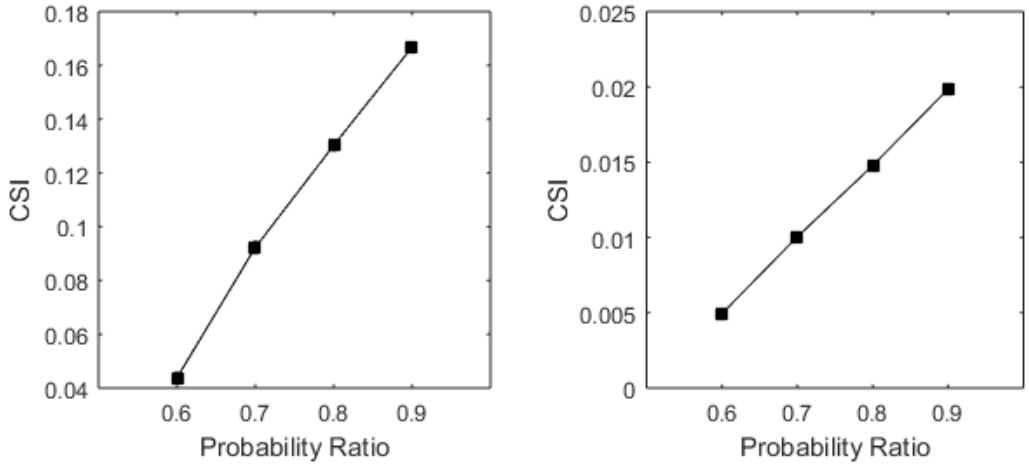

Figure 3.13: CSIs calculated from the model's response to Bernoulli sequences with varying probability of the standard response. Showing results for 100ms tone/ISI duration (left) and 100ms tone duration and 500ms ISI (right) with a 3 channel separation between the two frequencies.

3.3.5 Robustness of the fit

To assess the robustness of the fit, to help detect if it has reached a local rather than global minima and to detect if there are any significant non-linearities the model parameters can be varied and their effect on the quality of the fit can be assessed. The parameters were varied ±50% from the fitted values. For the four synaptic adaptation parameters there appears to be roughly parabolic changes to the RMS of comparable magnitude. The same can be seen of the global inhibition parameters. Both the threshold and onset spread parameters appear to show a sharp change in fit with increasing value but these changes reflect insignificant magnitude changes.

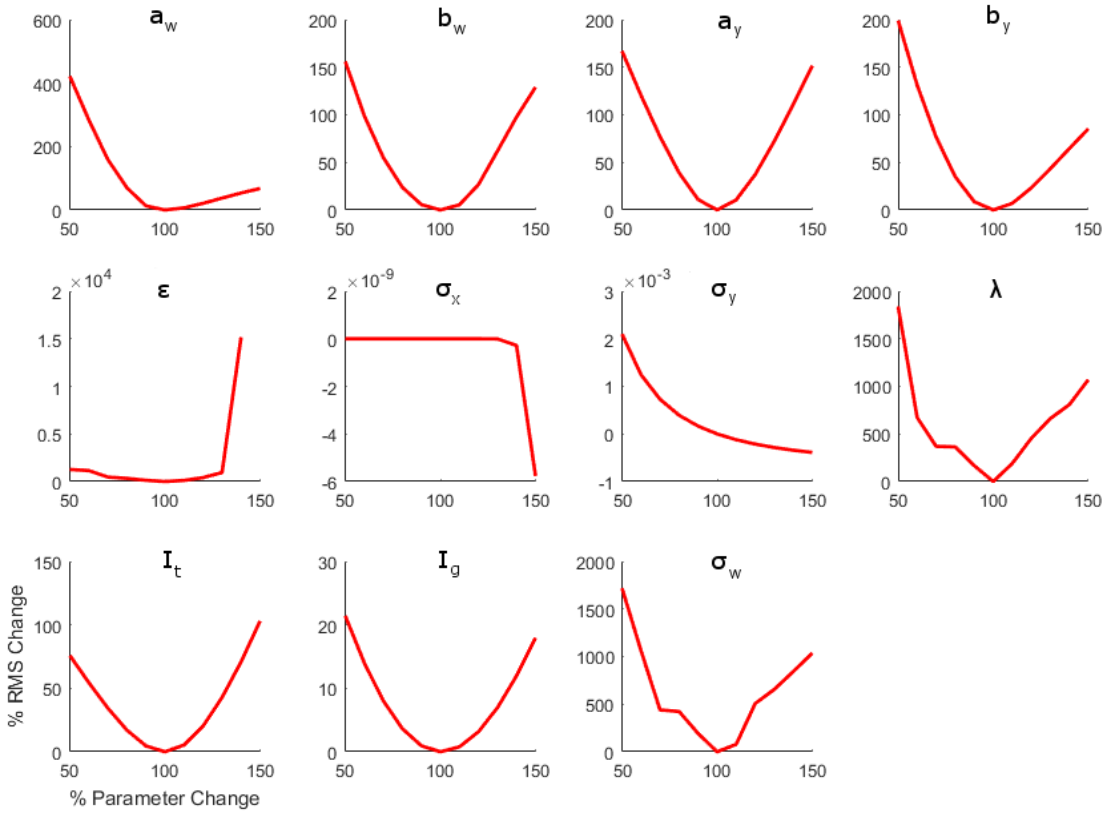

Figure 3.14: Effects of variations on the values of the fitting parameters on the quality of the model fit measured by a relative change in root mean squared error.

3.3.6 Testing reduced versions of the model

To test whether the model is overfitting the data the fits of several reduced model architectures can be tested. These models to be tested are first layer only (1), second layer only (2) and both layers without the onset pathway (3). To try to fit these each of the free parameters of these models were randomised with a large parameter range. Those that produced acceptable results (Unadapted response > 0, % Adaptation > 0) were used as initial parameters in the least squares fitting algorithm. The fits that produced the lowest RMS error were then selected.

The first one to be tested is the first layer only version. In this model the second layer synapse values were fixed such that their synapses would not suppress and simply acted to relay the activity of the first layer. The global inhibition parameters were also fixed to those seen in the full model as it was seen

through testing that these could be used by the fit to produce a non-monotonicity that was not produced by the synapses and not simply acting as a normalisation parameter as intended (Table 3.2). This model was easy to find potential parameters for with ~80% of the randomised parameters producing acceptable initial adaptation values. These models were fit to the single and multiple onset conditions separately. These fits produce qualitatively very similar results to those seen in the first layer results of the full model with a monotonic adaptation level with increasing duration and very little differentiation between the single and multiple onset conditions. When the model was fit using all the experimental conditions this produced results half way between those seen in the single and multiple fits with near identical levels of adaptation for both halves and a very poor fit for both (Figure 3.15).

	Single	**Multiple**
$\mathbf{a_w}$	11.5	0.0016
$\mathbf{b_w}$	12.7	6.75
$\mathbf{a_y}$	0.01	0.01
$\mathbf{b_y}$	$1 * 10^5$	$1 * 10^5$
$\boldsymbol{\varepsilon}$	2.71	2.48
$\boldsymbol{\sigma_x}$	0.104	0.104
$\boldsymbol{\sigma_y}$	$1 * 10^3$	$1.9 * 10^3$
$\boldsymbol{\lambda}$	1.302	0.817
$\mathbf{I_t}$	0.135	0.135
$\mathbf{I_g}$	0.0025	0.0025
$\boldsymbol{\sigma_w}$	3.4	3.4

Table 3.2: Parameters of the fitted model to each of the single and multiple onset conditions when the second stage is constrained to not suppress. Fixed parameters are shown in grey.

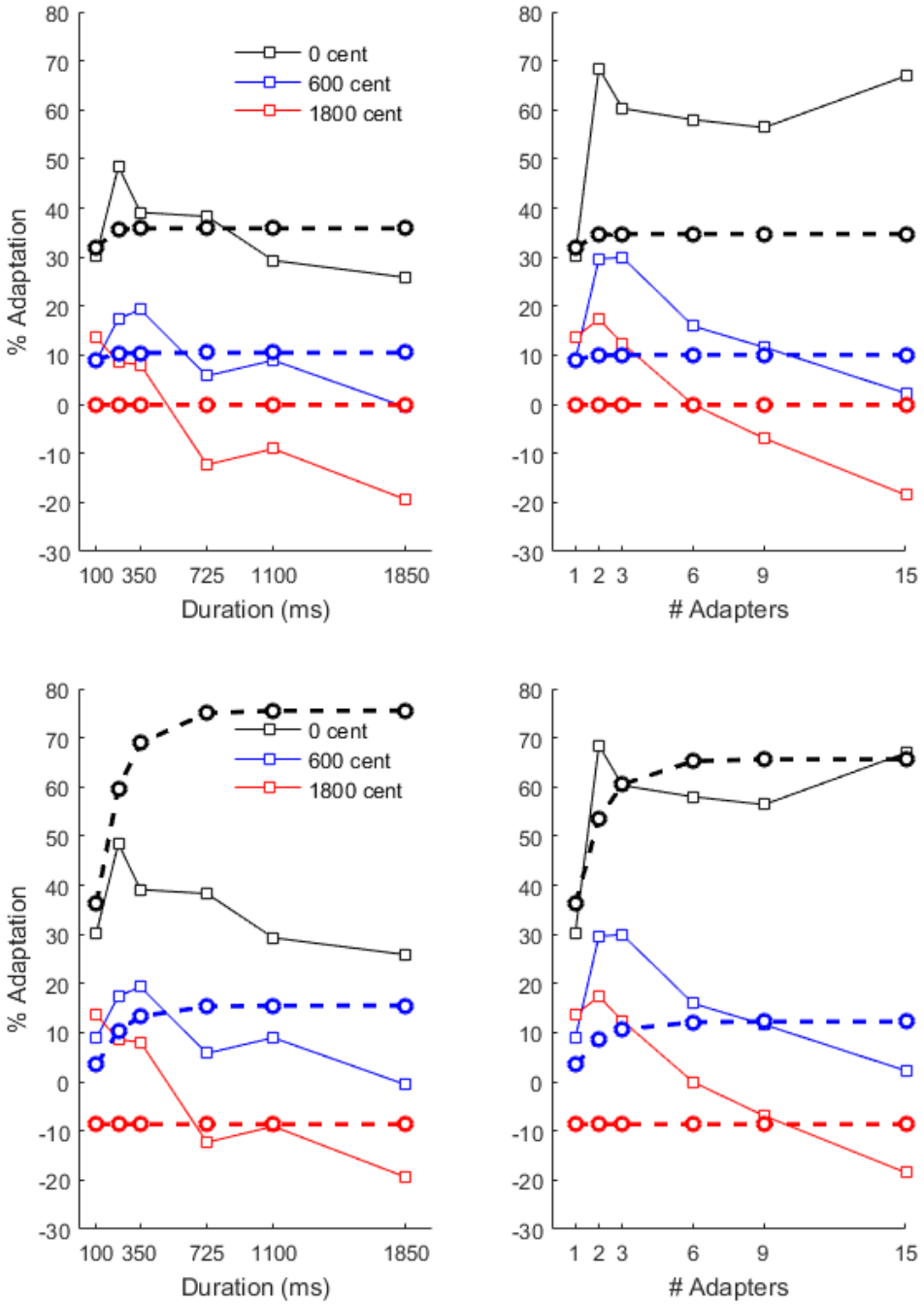

Figure 3.15: Level of adaptation of the fitted model to each of the single (top) and multiple (bottom) onset conditions when the second stage is constrained to not suppress

Next tested were the second layer version where the synapse values of the first layer were fixed such that their synapses would not suppress and as before the global inhibition parameters were also fixed. Much like the results from the fitting of the first stage only, the levels of adaptation are monotonically

increasing and therefore produce a reasonably poor fit to the experimental data (Figure 3.16).

	Single	Multiple
a_w	0.01	0.01
b_w	$1 * 10^5$	$1 * 10^5$
a_y	16.3	2.70
b_y	4.63	1.99
ε	1.39	6.43
σ_x	0.104	0.104
σ_y	5.09	3.57
λ	0.498	2.21
I_t	0.135	0.135
I_g	0.0025	0.0025
σ_w	3.4	3.4

Table 3.3: Parameters of the fitted model to each of the single and multiple onset conditions when the first stage is constrained to not suppress. Fixed parameters shown in grey.

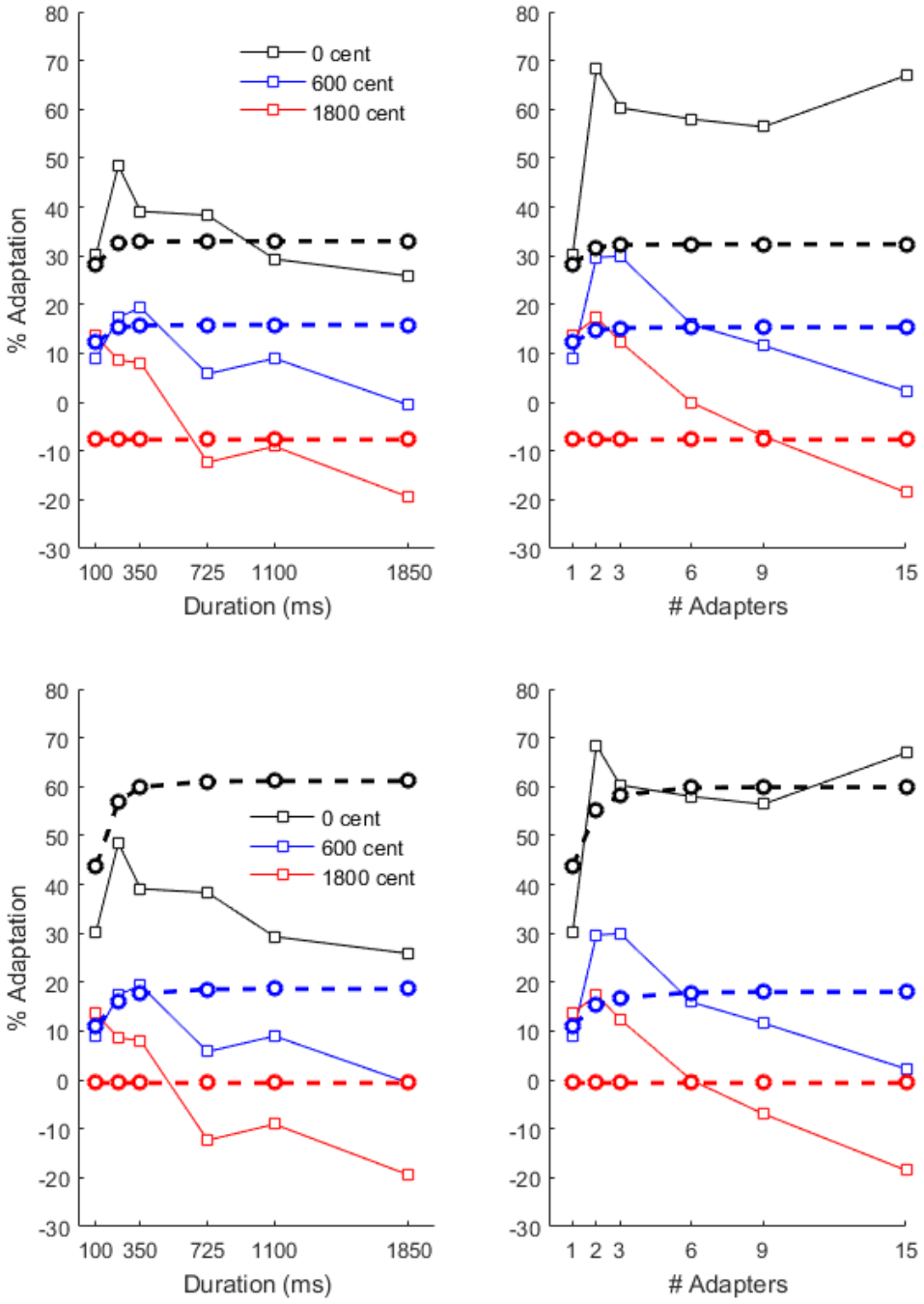

Figure 3.16: Level of adaptation of the fitted model to each of the single (top) and multiple (bottom) onset conditions when the second stage is constrained to not suppress

The last model tested was the two layer model with no onset pathway. As predicted, the two layer architecture is able to produce the non-monotonicity of the results without needing the onset pathway. With fits to each of the single and multiple onset conditions separately this model produces a very good fit

to each of the conditions. However as seen before there is no differentiation between the levels of adaptation between the single and multiple onset conditions within one parameter set. As seen in the previous partial models, when fitted to the entire dataset it produces a fit resulting in a rough average of the fits of the two onset conditions.

	Single	**Multiple**
$\mathbf{a_w}$	5.64	1.21
$\mathbf{b_w}$	7.07	4.64
$\mathbf{a_y}$	18.1	21.8
$\mathbf{b_y}$	1.52	1.09
$\boldsymbol{\varepsilon}$	0.554	1.89
$\boldsymbol{\sigma_x}$	0.104	0.104
$\boldsymbol{\sigma_y}$	277	327
$\boldsymbol{\lambda}$	0.149	0.360
$\mathbf{I_t}$	0.135	0.135
$\mathbf{I_g}$	0.0025	0.0025
$\boldsymbol{\sigma_w}$	3.4	3.4

Table 3.4: Parameters of the fitted model to each of the single and multiple onset conditions when the onset pathway is removed. Fixed parameters shown in grey.

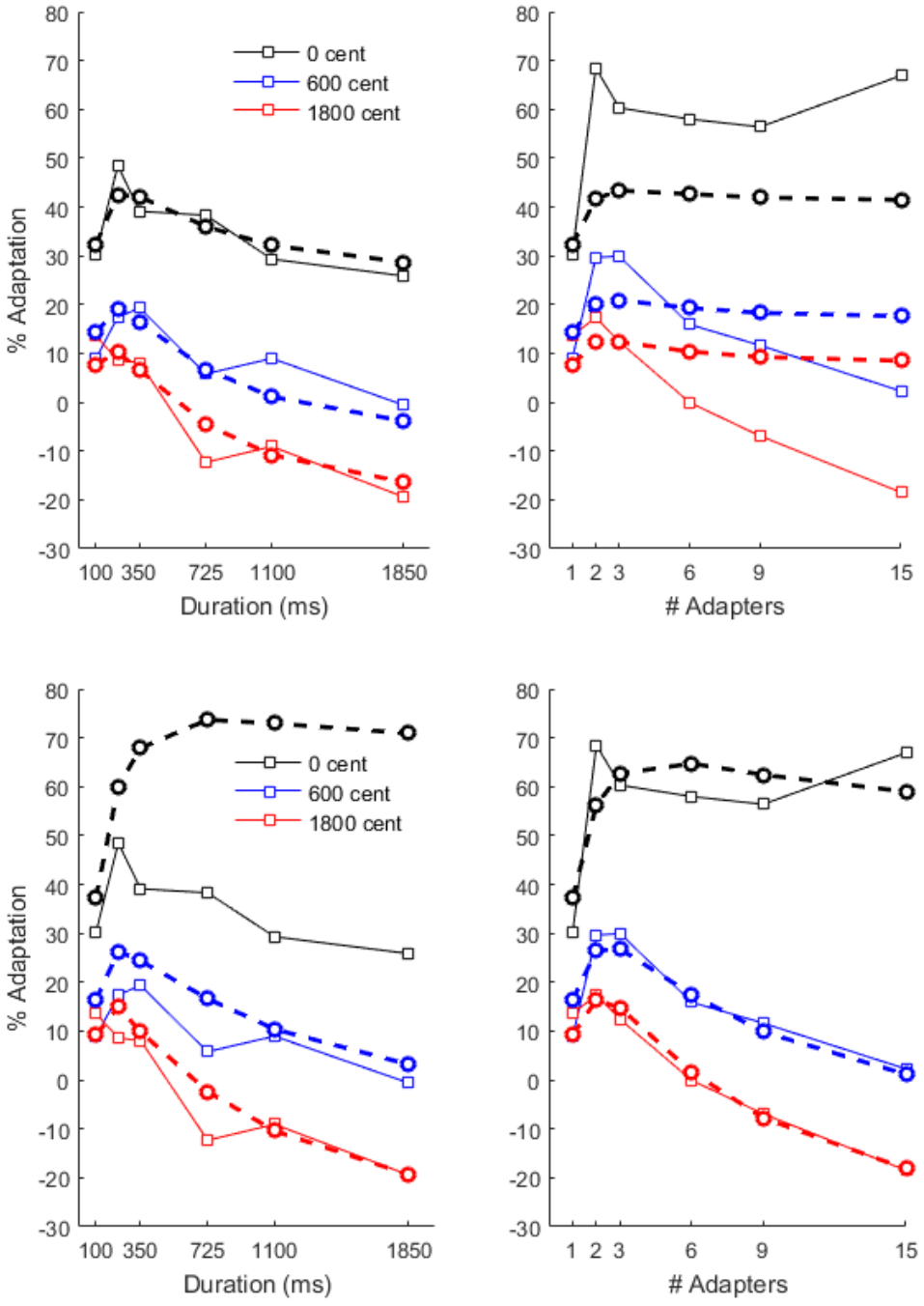

Figure 3.17: Level of adaptation of the fitted model to each of the single (top) and multiple (bottom) onset conditions when the onset pathway is removed

3.4 Discussion

The two-stage, adapting synapse model produces a good quantitative fit of the experimental data from Chapter 2. From the sensitivity analysis of the parameters this fit appears to be robust with parabolic variations in the RMS

error as the parameters are varied suggesting the parameters have reached their global optimum. Given the number of parameters there could be other potential parameter sets available by co-varying the parameters but these model parameters are stable for a wide range of initial fitting parameters.

In this model both of the two adapting stages are capable of displaying a sharpening response. In the first layer this is highly dependent on the tone duration as there is no onset selective component and appears to saturate reasonably early as there is not much progression of sharpening between the 3 and 9 adapter conditions relative to the difference between 1 and 3 adapters. It is also seen that in the first layer the degree of sharpening is independent of the neuron's CF as each neuron shows the same sharpening pattern as the layer as a whole. This is in contrast to the second layer neurons that show a modulation in the level of sharpening depending on their proximity to the adapter frequency.

With the behaviour of the individual neurons in this model this suggests the presence of two types of adapting neurons. One type that will display FSA, adapting most strongly around the adapter frequency with the rest of their response curve mostly unaffected and a second type that will show a less selective response, simply adapting in the presence of any auditory stimuli. As mentioned before there is evidence for FSA in the cortex (Scholes, 2009) so it could be possible to test for broader selectively adapting neurons in the data. This model begins to reconcile the differences seen between Scholes (2009) and Briley *et al.* (2013) as this model provides a neural architecture that can demonstrate population level sharpening of responses by neurons exhibiting FSA.

It has also been shown that in addition to the population level facilitation that individual neurons within the model can show facilitation (Figure 3.10). This is seen in the model when the adapter is far from the neuron's CF. This phenomenon is very similar to forward masking responses recorded from auditory cortex where an enhancement response area can be seen for adapter-

probe pairs that result in facilitation of the probe response, most prominently with an adapter-probe frequency separation of around an octave (Brosch and Schreiner, 2000; Brosch and Scheich, 2008).

This facilitation in the model is as a result of the global inhibition parameters. As mentioned earlier this is intended to act as a normalisation of responses by acting as an integrator of activity over time, increasing gain with increased activity to account for the increased suppression. This mechanism acts functionally similarly to contrast gain enhancement, a phenomenon which combines a decrease in the sensitivity of a system to stimuli with a small neural response, from an overall suppression, and enhancement of those responses that remain by an increase in response gain (Rabinowitz et al., 2013). Currently the global inhibition is implemented as a perfect integrator, in an attempt to minimise the number of free parameters in the model, but with additional parameters this could be made more biologically relevant by making it into a leaky integrator. This would mean the global inhibition could release over time during the silence gaps instead of being a monotonic function.

It appears from the results of the slow adapters that the results of this model are not immediately applicable to conditions with longer timescales. This could be a problem of training data, as the model is only fitted to results with fast repeating adapters so it could have found just one of several valid solutions that could fit the slow presentation rates. Alternatively there could be additional processes not captured in this model that will only have effects at a longer timescale and generate the experimental results seen in the slow adapter experiments. Potentially with a larger dataset, with a wider range of ISIs and IAIs, then a better parameter set could be found with greater external validity.

By using the partial models it can be shown that the two-stage architecture with the onset pathway is not an overly parameterised model. In both one-stage model variants the model is incapable of replicating the non-monotonicity of the results and can only increase the level of adaptation with

increasing adapter duration. In the two-stage model without the onset pathway the silence gaps between the repeating adapters are not sufficient to differentiate between the two datasets. The two-stage model is capable of fitting each of the datasets independently but is incapable of fitting both simultaneously, which requires the addition of the onset selective neuron pathway.

Chapter 4

Attentional Effects on Adaptation Tuning in Human Auditory Cortex

4.1 Introduction

As adaptation has previously been demonstrated to have beneficial effects on the neural coding of sensory stimuli, and potentially mediates a refinement of the cortical representation, then it would be reasonable to expect there may be a degree of attentive control of this phenomenon to further refine these effects. We can use experimental manipulations to investigate if this is an entirely pre-attentive phenomena, or whether attention can have modulatory effects on RIS. By using attention as a modulator this could also help show whether the RIS is generated cortically or inherited from more peripheral structures as attention generally does not show substantial effects on subcortical structures in the auditory pathway (Varghese et al., 2015).

It has been well established that attention will modulate frequency tuning in auditory cortex (Fritz et al., 2007; Okamoto et al., 2007, 2009; Connell et al., 2014). This is conjectured to be a method of the brain which attempts to better discriminate between attended, foreground sounds and background noise.

Two mechanisms have been suggested for this attentional modulation, an increased gain of attended, task relevant frequencies and a sharpening of responses to supress task-irrelevant neural signalling. The experimental evidence suggests a combination of these two mechanisms (Okamoto et al., 2007, 2009). There is still debate on the relative contributions of primary and non-primary auditory areas to the increase in frequency selectivity. Some fMRI studies have shown evidence for a non-primary region dominance (Jääskeläinen and Ahveninen, 2014) but growing numbers of invasive

electrode studies in humans (Bidet-Caulet et al., 2007) and macaques (Connell et al., 2014) are demonstrating the non-trivial effects attention has on frequency selectivity in primary auditory cortex. In single unit studies in macaque primary auditory cortex, it was found that attention modulates the sharpness of tuning of individual neurons without affecting their CF. This was done by enhancing the activity of the preferred frequencies while suppressing off-CF activity (Connell et al., 2014).

In Section 1.1.4 the potential links between adaptation and MMN were discussed and one aspect of the MMN is that it can be attentionally modulated (Restuccia et al., 2005; Sussman, 2007). This implies that if adaptation and MMN were linked, then it would be expected that adaptation is also attentionally modulated.

4.1.1 Hypotheses

Several hypotheses can be formed about the potential effects of attention on the adaptation tuning. The first two relate to its interaction with the repetition induced sharpening described in Chapter 2 and the second two on an effect that is independent of this phenomenon (Figure 4.1).

H_1: Repetition induced sharpening is enhanced by attention

The attentional effects interact with the effects of number of repetitions, enhancing the sharpening effects seen with increasing number of adapter onsets. To test this hypothesis an ANOVA can be used to look for interactions between number of repetitions, frequency selectivity and attentional state.

H_2: Repetition induced sharpening is enhanced by attention and the combined effect saturates early

The attentional effects interact with the effects of number of repetitions, enhancing the sharpening effects seen with increasing number of adapter onsets but this combined effect will reach a saturation point. If an attention effect were to be seen it would most likely be expected for a low number of

adapters before the increased stimulation leads to a saturation of the repetition induced effects which would prevent further sharpening. Similar to H_1 this would also show an interaction between repetitions, frequency and attention but would also feature an effect size inversely related to the number of adapters.

H_3: Attention sharpens the selectivity of cortical adaptation but does not interact with repetition induced sharpening

One prominent model of auditory selective attention (Fritz et al., 2007; Okamoto et al., 2007, 2009) postulates that when an auditory stimulus is attended to the neurons in auditory cortex will show sharper frequency tuning. If true, it might be plausible to expect that this would also sharpen the frequency tuning of adaptation. To test this hypothesis, an ANOVA would show interactions between frequency and attentional state but no interaction of frequency, attention and number of adapters. Additionally, when separating out the frequencies to test separately, attention would affect only frequency separations of >0 cents.

H_4: Attention causes a gross modulation of adaptation in a frequency independent manner

It is possible that attention will show an overall gain increase, independent of frequency, to produce a global release from adaptation to attended stimuli. To test this hypothesis, an ANOVA would show interactions between frequency and attentional state but no interaction of frequency, attention and number of adapters. Additionally, when separating out the frequencies to test separately, attention would affect both of the frequency separations.

H_0: Null Hypothesis

Attention has no effect on tuning of adaptation frequency selectivity. This will be accepted if no other hypotheses have sufficient evidence.

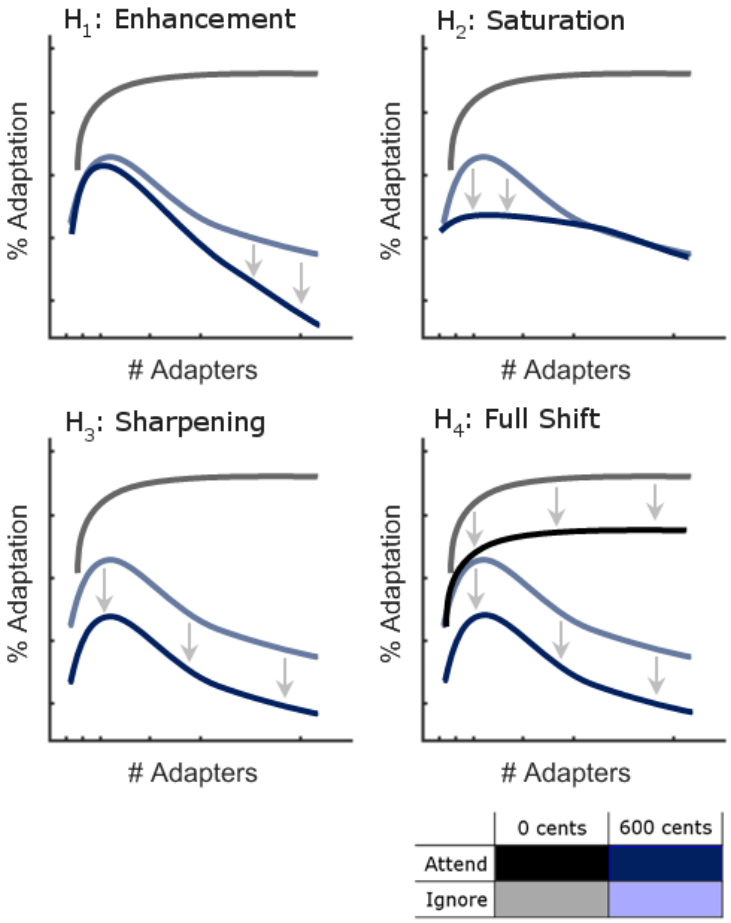

Figure 4.1: Potential effects of each hypothesis set out in section 4.1.1 on the probe response curves.

4.2 Method

Participants: 15 participants (11 male, 19-28 years, median 21 years, 3 left handed), naïve to the aims of the experiment, took part in the experiment after giving written, informed consent. All participants had normal hearing (pure tone thresholds below 20 dB HL between 0.25-8kHz) in both ears and no history of neurological or audiological disease. The experimental procedures used were approved by the School of Psychology Ethics Committee of the University of Nottingham and conformed to the Human Subjects Guidelines of the Helsinki Declaration (Version 6, 2008). They were not formally pre-registered online in accordance with the 2014 amendment to the declaration.

Attention Task: To modulate the participants' attention they performed a dichotic change detection task, with a tone task in one ear and a noise task in the other. The tone task used the adapter-probe stimuli from experiment 1 in Chapter 2 with 0 cent or 600 cent frequency separation between the adapter and probe stimuli. Participants were asked to determine if the frequency of the probe was the same as the preceding adapters or if it had changed. For the noise task, four amplitude modulated noise bursts were presented and participants had to determine if all four had the same amplitude modulation or if one was different from the other three (Figure 4.2). Participants were given a short (60 trials) training block of each task before the main experiment to acclimatise them to the tasks.

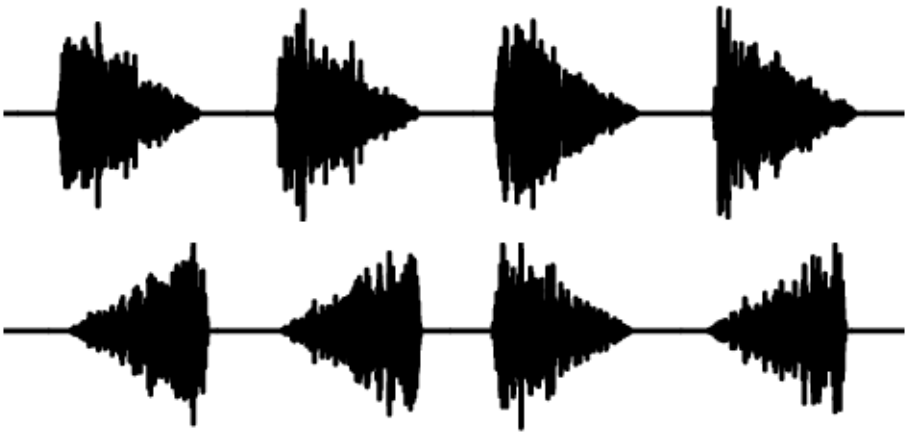

Figure 4.2: Waveforms of two of the noise task stimuli used, showing a 'Same' trial (top) with four falling modulations and a 'Change' trial (bottom) with three rising and one falling modulation

EEG Data Acquisition: Auditory evoked potentials were recorded with a 32-channel EEG amplifier system (BrainAmp DC, Brain Products, Gilching, Germany) and an EEG cap fitted with 32 Ag/AgCl ring electrodes, in the standard 10-20 electrode configuration, with a Cz reference electrode and grounded on the central forehead at AFz. Skin-to-electrode impedances were kept below 5kΩ. The data were recorded continuously at a sampling rate of 500Hz and band-pass filtered online between 0.1 and 250 Hz. The participants

were seated on a comfortable chair in a double-walled, sound-attenuating booth (Industrial Acoustics Company, Winchester, United Kingdom).

Stimulus Presentation: All stimuli were generated digitally at a sampling rate of 24.414 kHz by RPvdsEx (Tucker Davis Technologies, Alchua, FL), digital-to-analog converted with a 24-bit amplitude resolution using TDT System 3 (RP2.1 Real-Time Processor, HB7 Headphone Amplifier, Tucker Davis Technologies) and presented dichotically through Sennheiser HD280 headphones. The adapter and probe stimuli were gated on and off with 10ms cosine squared ramps and presented at an RMS level of 70dB SPL. They were presented in discrete trials of 3000ms duration with a pseudorandom, uniformly distributed ±200 cents jitter about the centre frequency to minimise longer term adaptation effects. The noise stimuli were presented to the contralateral ear with the onset uniformly jittered ±250ms about the first adapter onset. The noises were 200ms narrowband noise bursts, with a 100ms ISI, band pass filtered between 2-3kHz with a 4^{th} order Butterworth filter, gated on and off with 10ms cosine squared gates and amplitude modulated with either a rising or falling linear gate with a 100% modulation depth. The noise stimuli were subjectively loudness matched to the adapter-probe stimuli.

Parameter Variations: Adapter stimuli were either one, three or nine 100ms tones with 25ms IAI presented either 0 or 600 cents higher than the probe. Stimuli were presented to the participants in 4 (n=3) or 6 (n=12) blocks, each containing 50 repeats of each adapter-probe condition in a pseudorandom order. Participants were sequentially assigned to one of four groups starting with either the Attend or Ignore condition and tones played in the left or right ear. Attend/ignore target conditions were alternated for each block and sound presentation sides were switched every two blocks.

Analysis: Analysis was undertaken as in Chapter 2. In summary, the data was filtered, re-referenced to paired mastoids and epoched before being subjected to artefact rejection and ICA. The waveforms analysed are the EEG source waveforms with the dipole location set identically to that in Chapter 2 and the

orientations set to the unadapted responses for each subject, separating between the attend/ignore conditions.

4.3 Results

The unadapted response amplitude showed a significant increase of 30.3±9.9% in the attend condition vs the ignore condition (Two-tailed, paired sample t-test, P=0.0025). 11 out of the 15 subjects showed a greater than 5% increase in response size in the attend condition, with results ranging between 18% suppression to 90% enhancement.

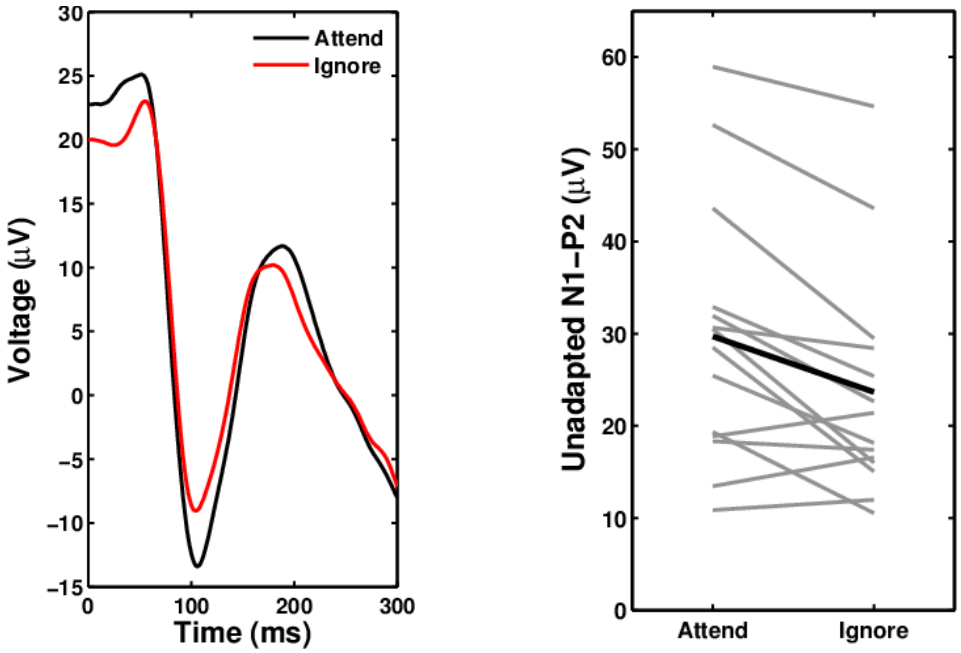

Figure 4.3: Grand average unadapted waveforms of the attend and ignore conditions (left) showing the overall attenuation of the unattended response. Individual subject unadapted response amplitudes (grey) and population average shift (black) between the attend and ignore conditions (right) are shown demonstrating a general overall trend of response size reduction within subject and a significant reduction at the population level.

Using a three-way, repeated measures ANOVA there was shown to be a significant interaction between attention and frequency ($F_{(1,13)}$=16.062, P=0.001). This shows there is a significant effect of the attentional modulation on the frequency selectivity of adaptation. However, there was no significant

interaction between attention, frequency and number of repetitions ($F_{(1.913,24.866)}$=0.186, P=0.822) showing no interaction between attention and RIS.

As a post-hoc analysis, two-way, repeated measures ANOVAs were used to test each frequency separately. For the 0 cents condition there was no significant main effect of attention (P=0.905) and showed no interaction between attention and number of repetitions (P=0.477) however attention did have a significant effect for the 600 cents conditions (P=0.006) as did the number of repetitions ($P=1x10^{-5}$). These results show that attention will only show a modulation of adaptation at the 600 cents separation, consistent with a sharpening effect. This effect leads to the 600 cents attend conditions showing considerable facilitation which increases with increased number of adapters.

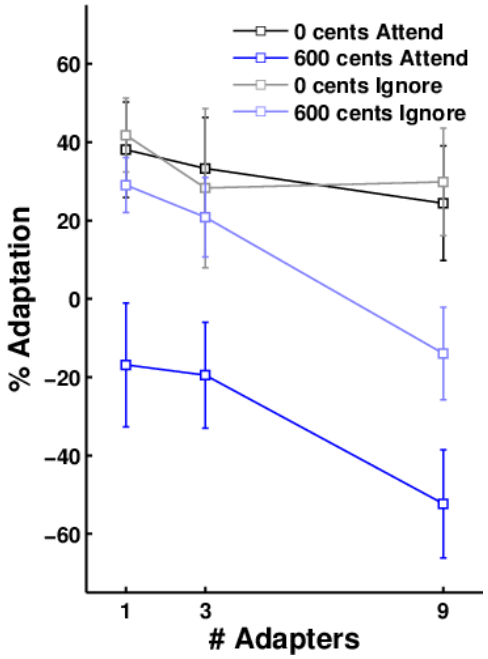

Figure 4.4: Effects of attentional modulation on the degree of adaptation of a probe tone preceded by multiple onset tonal adapters. Calculated from source waveforms.

The overall performance results in the two tests were 86.2±3.2% correct in the tone task and 88.5±4.2% in the noise task. The two tasks showed no significant difference in performance (two-sided, paired Wilcoxon signed rank test, P=0.091). Task performance also showed no correlation to the degree of

enhancement of the N1-P2 complex (r=0.1773). One subject performed at chance level in both tasks yet still showed a ~30% enhancement providing little evidence of a link between task performance and the effectiveness of the attentional modulation.

4.4 Discussion

This experiment looks into whether there is an interaction between attention and RIS of adaptation using a dichotic, auditory selective attention task.

As shown in figure 4.3 the attentional modulation shows a significantly larger amplitude of the unadapted AEP in the attend condition, a phenomenon regularly reported as a consequence of modulation of auditory selective attention. This demonstrates that the dichotic attention task used for this this experiment is successfully acting as an attentional modulator.

The results of this study show no significant shift in the level of 0 cents adaptation with attentional modulation but with a greater release from adaptation in attended stimuli. This effect showed no interaction with number of adapter repetitions suggesting that the attentional effects are independent of RIS. The results of this study most strongly support hypothesis 3, as outlined in Section 4.1.1.

By extension, accepting this hypothesis also supports the model of attentional receptive field sharpening. By narrowing the receptive fields of neurons in the auditory cortex then potentially a smaller population will respond to the adapting stimuli, which will adapt a smaller number of neurons and lead to an increased frequency selectivity of adaptation. One argument against this is that the unadapted response is larger, meaning the number of units responding is unlikely to have decreased. However, the larger response could potentially be either an increased firing rate of a smaller neural population or an increased firing coherence. This could be further explored by directly investigating changes in frequency selectivity of the probe response or by studies of single unit recordings in cortex.

Additionally, demonstrating that attention can have a significant effect on adaptation strongly suggests that multiple repeating stimuli induce a degree of cortical adaptation, and are not just acting sub-cortically. With no interaction between RIS and attention however, it cannot be proved whether this phenomenon is cortically generated or inherited from processes in the periphery.

The results of this experiment do not appear to show the same increase and saturation of adaptation of the 0 cents condition as those shown in chapter 2. As the attentional modulation does not appear to effect the 0 cents condition then this is could be due to the monaural presentation of the adapting stimuli while we record from both auditory cortices. It could be theoretically possible to isolate the responses from separate auditory cortices but the spatial resolution of the 32 channel recordings made here are unlikely to be sufficient to make meaningful conclusions.

Chapter 5

Neural Population Responses to Adapting Stimuli in Anaesthetised Guinea Pigs

5.1 Introduction

Now we have a characterisation of the effects of adaptation on frequency selectivity in human auditory cortex, as measured through EEG, we are now interested in looking at the underlying neural activity leading to this. To better understand the neural mechanisms generating RIS and the changes in adapter frequency selectivity then we need to look at a smaller neural scale than can be measured by EEG. This can be done by using an animal model, in our case guinea pigs (GPs) which will allow us to increase the resolution of our recordings to the single unit level to probe the underlying cortical representation. Firstly however we must confirm that GPs show similar trends to humans at a population level, especially given the conflicting results of the previous comparative studies discussed earlier (Section 1.1).

At a systems level, humans and other mammals show similar brain regions and comparable computational pathways but at a more fundamental level when comparing between species there are some significant differences. One of the most immediate differences is the physical size difference, resulting in faster transmission in smaller mammals as there is a shorter propagation distance for action potentials through the auditory pathway to the cortex.

Another important factor especially important to far-field electrophysiological measurement is that most rodent brains are lissencephalic, lacking the gyri and sulci found in human brains. In humans most of the primary auditory cortex is located in the lateral sulcus, extending into Heschl's gyrus and the superior temporal gyrus, this results in a range of orientations of cortical columns,

summing to produce a resultant current dipole. Because of the non-uniform orientation of the cortical columns it cannot be guaranteed the received signals are representative of the summation of all of the core and belt auditory regions. By comparison, the agyral brains of rodents will have neural columns aligned near-uniformly, perpendicular to the skull, meaning it is comparatively easy when making far-field measurements to pick up responses from the whole of auditory cortex.

Presented here are the results of an identical adaptation study to the human study in section 2.3, done in guinea pigs, recording global and local population responses along with accompanying characterisations of the guinea pig as a model of adaptation.

5.2 Method

Animal Preparation: Experiments were performed on 7 pigmented guinea pigs of both sexes that weighed 267-949 g (mean 686 g). Each guinea pig was anaesthetized with an intraperitoneal injection of urethane (4.5 ml kg^{-1} in a 20% solution) supplemented with intra-muscular injections of 0.2 ml ketamine/xylazine (ketamine 60 mg ml^{-1}, xylazine 8 mg ml^{-1}) whenever a pedal withdrawal reflex could be elicited. Each animal was tracheotomised, artificially respired and rectal temperature was maintained at 38°C by means of a heating blanket.

The animals were placed in a stereotaxic frame with hollow plastic specula replacing the ear bars, inside a sound-attenuating room. To equalize pressure across the tympanic membrane, the bulla on each side was vented with a polyethylene tube (22 cm long, 0.5 mm diameter), and the membrane overlying the foramen magnum was opened to release the pressure of the cerebrospinal fluid.

In all 7 animals, 8 burr holes were performed at the locations shown in figure 5.1 and ~0.5mm diameter silver ball electrodes (constructed in-house) were inserted into the holes and sealed in place with agar.

In 5 animals, a craniotomy with a diameter of about 6 mm was performed to expose the left primary auditory cortex (A1), the dura was removed. A linear multi-electrode array (Neuronexus A1x16-5mm-150-177-A16), consisting of 16 electrodes with 150µm spacing was advanced into A1 by a piezoelectric motor (Burleigh Inchworm IW-700 / 710) to a depth of 2200µm. In 1 animal a craniotomy was also made over inferior colliculus and a linear multi-electrode array was inserted. The craniotomy was then covered with a layer of agar. All experiments were performed in accordance with UK Home Office regulations under the Animal Scientific Procedures Act 1986.

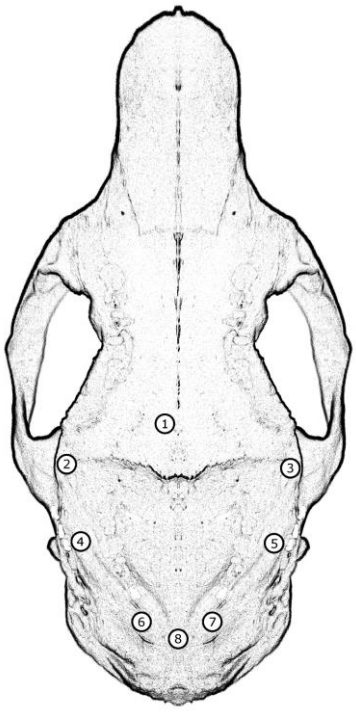

Figure 5.1: GP iEEG electrode placement

1. Vertex
2. Left Front A1
3. Right Front A1
4. Left Rear A1
5. Right Rear A1
6. ABR Left
7. ABR Right
8. Cerebellum

Acoustic stimuli and electrophysiological recording: Auditory stimuli were delivered diotically through sealed acoustic systems, consisting of modified Radio Shack 40-1377 tweeters coupled to damped probe tubes that fitted into the specula. The system was calibrated a few millimetres from the eardrum by a 1-mm probe tube that was attached to a microphone (Brüel & Kjaer 4134). This was to ensure that sound levels were consistent across experiments (± 3 dB).

All stimuli were generated by an array processor (TDT RX8, Alachua, FL, USA) and output at a sample rate of 100 kHz. Stimulus control was from a PC using Brainware (developed by J. Schnupp, University of Oxford). Responses from the electrodes were acquired using a Tucker Davis PZ5, sampled at 24.414 kHz with 16-bit resolution and amplified (approximately 40k) and filtered on-line between 20 Hz and 3 kHz.

Analysis: Unless otherwise stated, statistical results are presented as mean ± SE.

For analysis, recordings were down sampled from the recorded 24.414 kHz to 2 kHz and low pass filtered with a cut-off frequency of 250 Hz. Artefact rejection was undertaken using the root mean square (RMS) of the signal, rejecting trials with an RMS greater than 2.5 standard deviations above the mean for that channel. AEPs were obtained by averaging over electrodes 2-5 (Figure 5.1) and all remaining repeats of each condition, aligned by first adapter onset. AEP peaks were determined automatically as the maximal amplitude inflection points within the expected latency windows. The goodness of fit was assessed visually and peaks were reselected manually if necessary. Adaptation percentage was determined using equation 2.1, using the N1-P2 amplitude as the measure.

The results from two GPs' iEEG were excluded as the unadapted AEP amplitude was not sufficiently large to be reliably discriminated from background noise.

For multiunit activity an RMS measure was used, which has been shown to correlate well with thresholding measures (Niwa et al., 2013). The raw recordings were down sampled from the raw recordings to 6 kHz and high pass filtered at 300 Hz. RMS was calculated with a 10ms sliding window across each trial and the resulting envelopes averaged together. Active electrode channels were determined as channels whose RMS envelope in response to an unadapted stimulus crossed a threshold set as 2.5 standard deviations above the envelope amplitude of the spontaneous activity. Amplitudes for adaptation analysis were taken as the maximal value of the noise baselined RMS envelope in the window 15-60ms after stimulus onset.

Several strands of experiments were undertaken using the preceding methodology with varying stimuli.

Tuning of adaptation in guinea pig cortex: This experiment attempted to find the guinea pigs' adaptation frequency selectivity. Two 100ms duration, 10ms

cosine squared gated tones were presented with an ISI of 125ms and an inter-trial interval of 1000ms. Unless otherwise stated, the probe tone was presented at 1 kHz with the adapter having a frequency of 0-2400 cents higher than the probe.

Effects of adapter onsets and duration on adaptation tuning: This experiment used identical stimuli to those in the initial human EEG recordings (Section 2.3). In summary, adapting stimuli with either single onsets and variable duration (100, 350, 1100ms) or multiple 100ms adapters (1, 3, 9 repetitions) were presented 125ms before a 100ms, 1 kHz probe tone. The adapter frequencies were either 0, 600 or 1800 cents higher than the probe tone.

Laterality of adaptation: In this experiment the degree of cross hemispheric adaptation was investigated in two GPs with intracortical recording electrodes. Adapter and probe tones were presented either ipsilateral or contralateral to the recording electrode. Temporal parameters used were the same as the tuning experiment with frequency separations of 0, 600 and 1800 cents.

5.3 Results

Anaesthetised GPs appear to show a comparable morphology AEP to those seen in human EEG with a triple inflection waveform with the P1, N1 and P2 components (Figure 5.2), although it is unclear if these are directly comparable to the same generators and neuro-computational processes as the human response. By comparing the simultaneous recordings it appears the N1 component of the EEG primarily reflects the response of the primary auditory cortex. Given the latency of the P1 this may reflect a thalamic potential as it is between the latencies of the IC and A1. The divergence of the EEG and A1 LFPs from 40-75ms could represent the response of the belt regions of auditory cortex. The multiunit activity from A1 appears to follow the latency of the LFPs, as expected as they will both be generated from roughly the same sources.

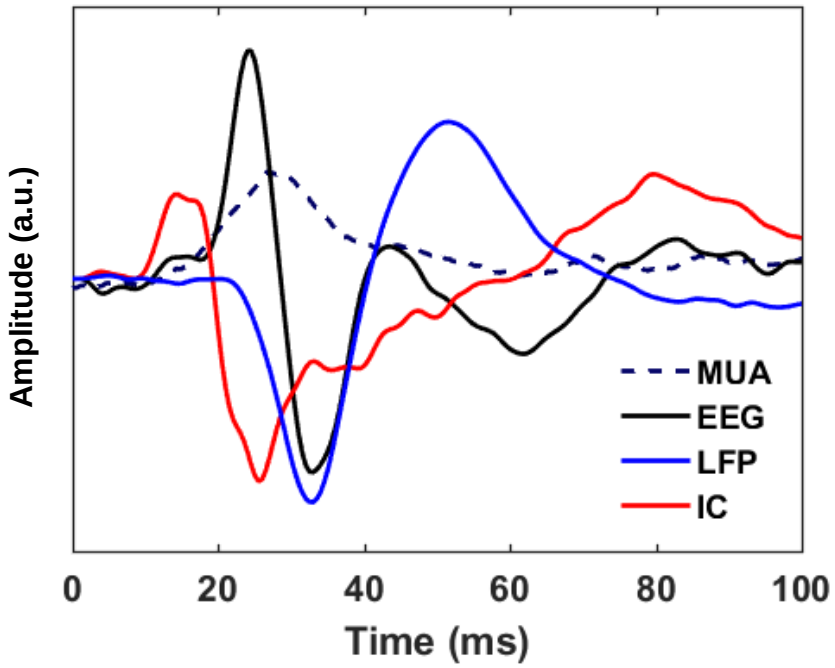

Figure 5.2: Multilevel GP grand average evoked potentials from EEG potentials, A1 local field potentials, A1 multiunit activity (MUA) and inferior colliculus local field potentials in response to a 100ms, 1 kHz, 70dB SPL tone, measured from tone onset

Initially the main difference seen between the human and GP AEPs is the latencies of the peaks (Table 5.1). The GP AEP lasts about a third the length of the human response and the P1 peak occurs ~25ms earlier. This could have significant effects on the time course of adaptation when comparing effects between humans and GPs as the 100ms tones used will have an offset around the latency of the human N1 but around 60ms after the GP P2.

Peak Latencies (ms)	Human EEG	GP iEEG	GP LFP
P1	45.2 ± 7.0	23.9 ± 0.6	15.3 ± 1.2
N1	100.9 ± 3.6	32.6 ± 1.2	28.0 ± 0.9
P2	170.9 ± 6.2	42.7 ± 2.0	42.6 ± 1.4

Table 5.1: Average peak latencies of evoked potentials, relative to tone onset, recorded in response to a 100ms, 1 kHz, 70dB SPL tone

With the type of electrodes used it is usually necessary to optimise positioning and stimulus frequency to be able to readily isolate single and multiunit spiking activity. In this experiment the electrode placement depth was chosen to

optimise the LFPs and the probe frequency was fixed at 1 kHz. Using the same filtering parameters as used for spiking activity (300-3000Hz) the RMS of the signal can be used as a measure of multiunit spiking activity in the vicinity of the electrode. To find sites responsive to the 1 kHz probe tone the unadapted probe response is thresholded (Figure 5.3). This yielded 92 electrode sites responsive to the 1 kHz probe tone.

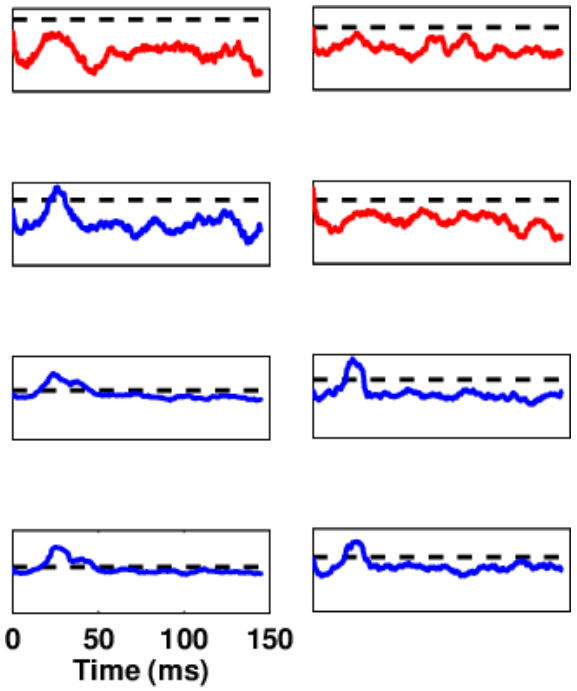

Figure 5.3: Mean, unadapted RMS response of eight electrode sites on one shank to a 1 kHz pure tone. Acceptance threshold for active units (dashed line) is set at 2.5 standard deviations of the spontaneous activity showing responsive (blue) and unresponsive (red) sites.

These sites showed frequency selectivity of adaptation much like the EEG and LFP responses though with a slightly broader tuning. The suppression of this multiunit activity appears to occur most strongly at a latency of around 25ms though there also seems to be a sustained suppression of activity thereafter (Figure 5.4).

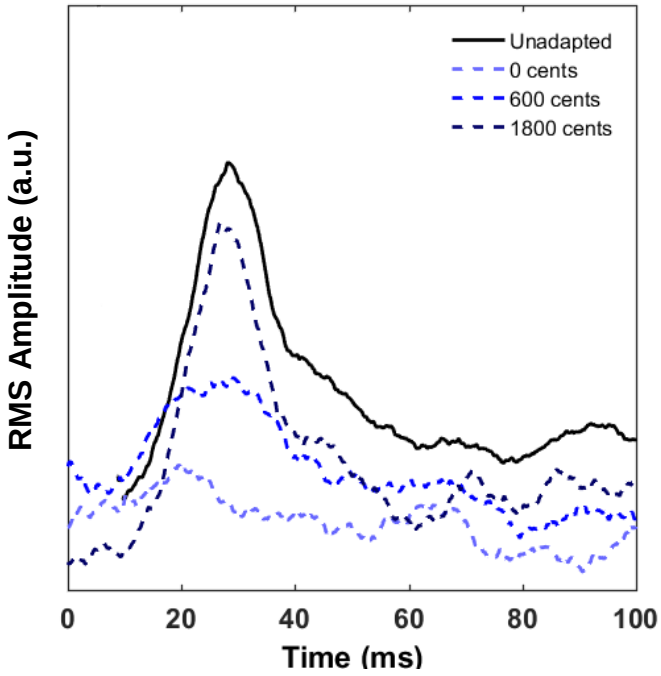

Figure 5.4: Grand average (n=92 electrode sites) RMS response showing the unadapted response and the effects of frequency separation following the nine adapter condition on the magnitude of the response

5.3.1 Tuning of adaptation in guinea pig cortex

As GPs have significantly broader tuning in the frequency selectivity of their cochlea when compared to humans (Evans et al., 1992) it is to be expected that they would show significant differences in their adaptation tuning. Results for single adapter tuning show strong agreement between the EEG and LFP recorded results with a near linear reduction of adaptation from 60% adaptation at 0 cents to near 0% adaptation at 2400 cents (Figure 5.5). The gradient of this reduction, from a least squares linear regression, is 27% and 32% per octave in the EEG and LFP respectively whereas the human data shows a reduction of 10% per octave. This effect of species on frequency tuning was tested and while the iEEG shows no significant difference in tuning from the human data (two-way ANOVA, $F_{(2,57)}$=1.337, P=0.271) there is a significant difference in LFP tuning from the human tuning ($F_{(2,72)}$=3.410, P=0.039). This could be an effect of the changing scales or it could be that the iEEG results do not have sufficient power to properly demonstrate this effect. These results could suggest that the GPs adaptation frequency selectivity is

sharper than in humans suggesting adaptation tuning in the cortex does not appear to reflect cochlear tuning.

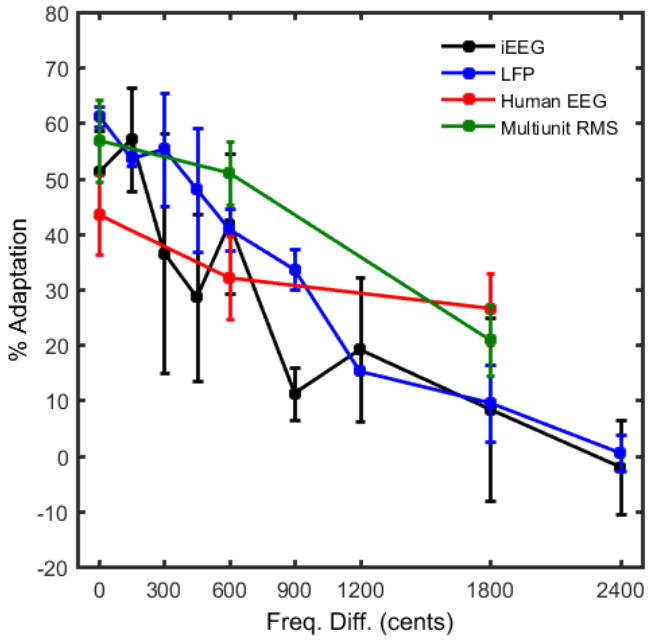

Figure 5.5: Adaptation of a probe tone preceded by a single, pure tone adapter with varying frequency separation. Measured through multiple methodologies. Human EEG (n=18, Chapter 2), GP iEEG (n=4), GP A1 LFPs (n=2) and GP Multiunit activity (n=5, sites averaged within each animal)

As a validation to show whether the probe frequency or direction of frequency separation will affect the sharpness of the measured selectivity tests were undertaken varying these parameters. When looking purely at the results where the adapter is higher than the probe (Freq. Diff. > 0 cents), there appears to be little effect of probe frequency on the selectivity of adaptation (Figure 5.6). However when looking at the conditions with a lower adapter than probe it does not appear to be symmetric about 0 cents. The 4 kHz probe condition shows broader tuning and the 1 kHz probe has sharper tuning than when the adapter is higher than the probe.

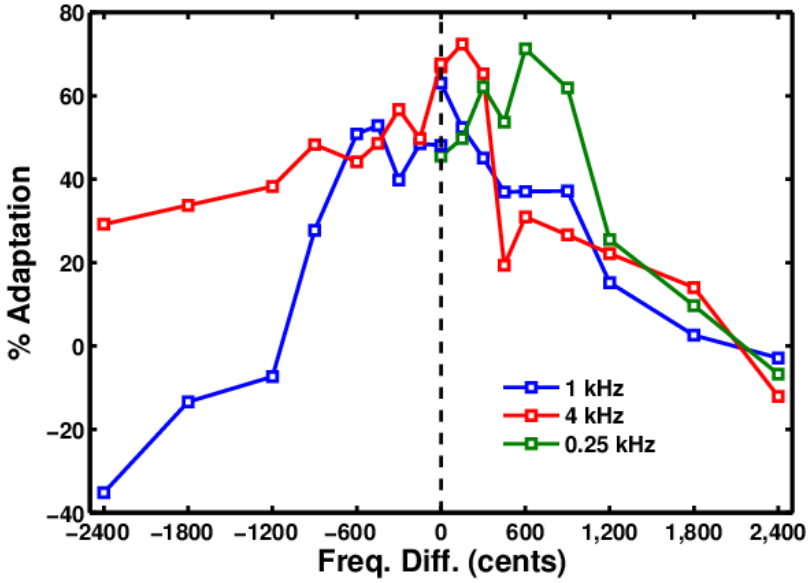

Figure 5.6: Changing the probe frequency has little effect of adaptation tuning for adapters higher than the probe however the tuning appears to be asymmetrical. Measured from LFPs (n=1)

5.3.2 Effects of adapter onsets and duration on adaptation tuning

Using an identical stimulus set to that used in the first human EEG study the effects of adapter onsets and duration were measured in GPs through iEEG, local field potentials and multiunit activity. Qualitatively the GPs do not show patterns of adaptation demonstrating the same characteristics as those found in humans.

In the LFP derived results in both the single and multiple onset conditions there is a slight (~10%) increase in adaptation between the 100-350ms adapters (Figure 5.7, middle row). For the 0 cents conditions, when comparing the results between the single and multiple onset conditions there appears to be no substantive difference between the two conditions, suggesting no RIS. This is confirmed in the statistics showing no significant interaction between single vs multiple onsets and frequency selectivity (three-way, repeated measures ANOVA, $F_{(1.93, 11.59)}$=1.05, P=0.379).

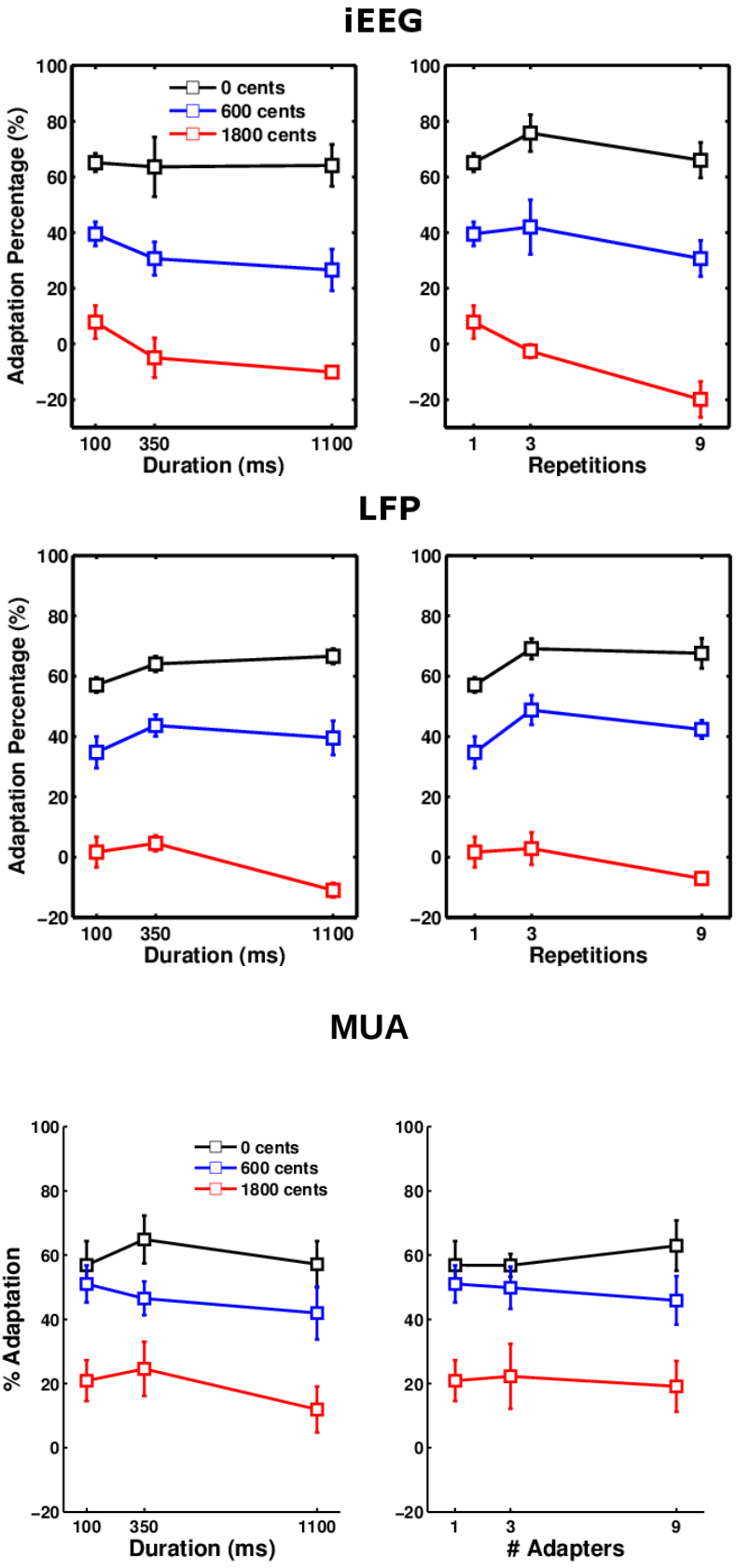
iEEG
0 cents
600 cents
1800 cents
Adaptation Percentage (%)
Duration (ms)
Repetitions
LFP
Adaptation Percentage (%)
Duration (ms)
Repetitions
MUA
0 cents
600 cents
1800 cents
% Adaptation
Duration (ms)
Adapters

Figure 5.7: Using single or multiple onset adapters has little effect on adaptation tuning in anaesthetised GPs. Measured via iEEG (n=5), LFPs (n=7 electrode sites in 5 animals) and MUA (n=5, sites averaged within each animal) in GPs

As with the human EEG data the 3 slow adapter condition was run to see the effects of adapter rate on the tuning and degree of adaptation (Figure 5.8). The results from this show no effect of adapter presentation rate on the amount of adaptation (two-way, repeated measures ANOVA, $F_{(1,6)}$=3.33, P=0.118), and a small but significant interaction between presentation rate and selectivity ($F_{(2,12)}$=4.354, P=0.04). This is in contrast to the human data where there is a ~40% reduction in adaptation at the slower rate. This could suggest that recovery from adaptation displays a longer lasting time course in GPs under anaesthesia or alternatively that it recovers fast enough that the first two adapters will have minimal effect on the probe response.

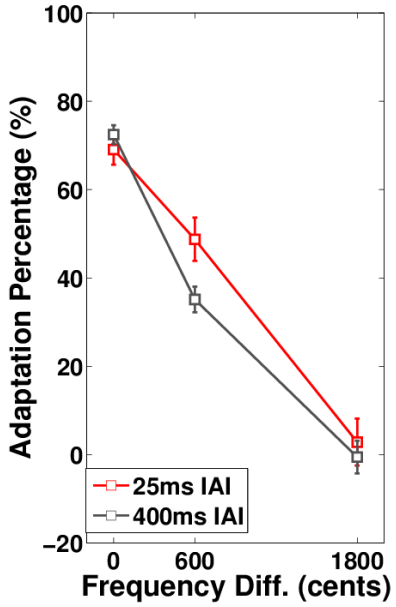

Figure 5.8: Adapter repetition rate has minimal effect on the degree or tuning of adaptation, recorded via LFPs in GPs (n=7 electrodes from 5 GPs)

5.3.3 Laterality of adaptation

To investigate the laterality of adaptation diotic and monaural adapter and probe stimuli were used ipsilateral and contralateral to the implanted electrode site (Figure 5.9). As expected the response to a probe tone

ipsilateral to the recording electrode produces a smaller AEP than one on the contralateral side and at a slightly longer latency. The unadapted contralateral response is also of comparable magnitude to that of the diotic stimuli.

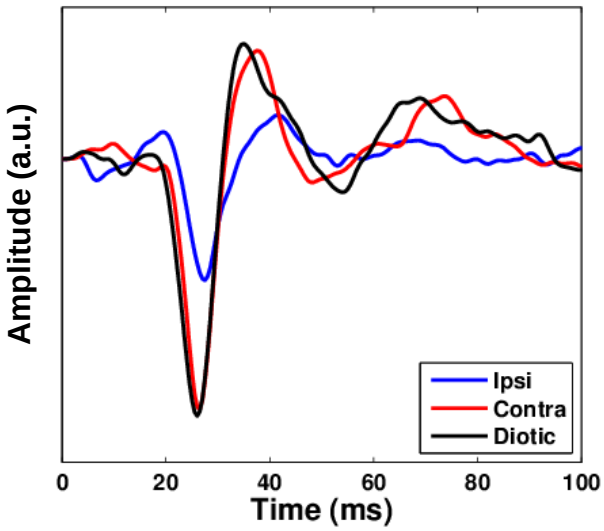

Figure 5.9: Grand average (n=2) unadapted LFPs in response to a 1 kHz, 70dB pure tone presented either diotically or in the ipsilateral or contralateral ear to the recording electrode.

Due to the low number of animals tested in this experiment (n=2) some of the conditions produce noisy results but some overall trends can be seen. As shown before with diotic adapters and probes a clear tuning is seen, peaking around 60% adaptation at 0 cents (Figure 5.10). This is comparable to the purely contralateral adapter-probe stimuli whereas the purely ipsilateral case appears to show an overall reduction in the degree of adaptation but still displays frequency selectivity. From these results it appears that using an ipsilateral adapter and contralateral probe will not result in any adaptation and in the inverse condition the 0 cents results may show the same, however the results of this condition with a frequency separation, comparing between subjects, is not consistent.

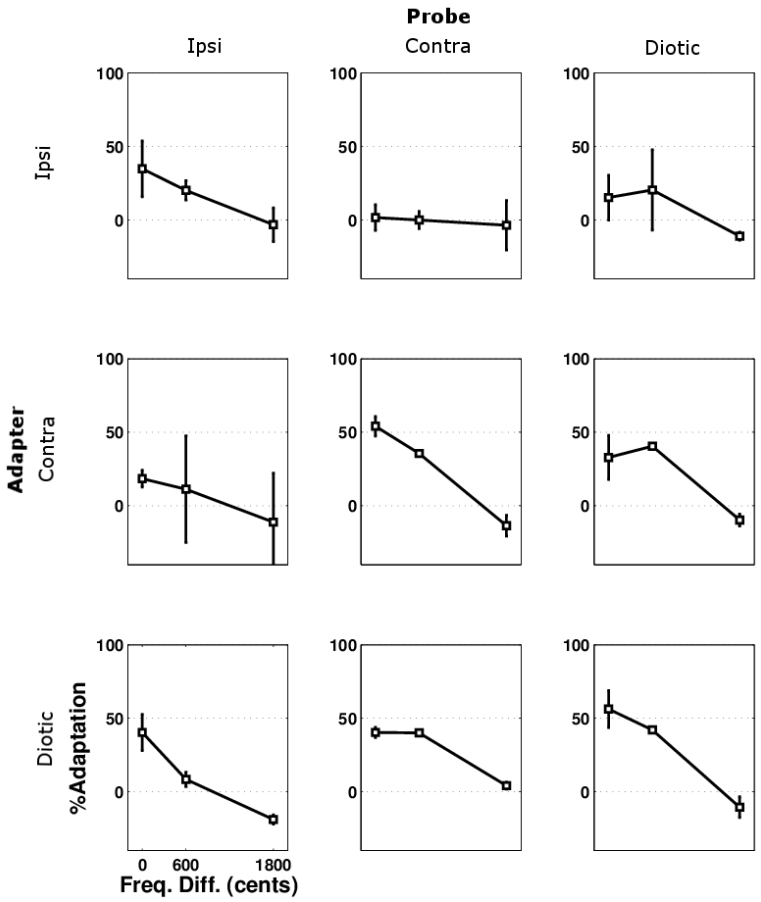

Figure 5.10: Changes to tuning of LFP adaptation with mono-lateral and bilateral adapter and probe tone presentation. Laterality references are stimulus presentation side relative to the side of the recording electrode (n=2)

5.4 Discussion

The results of these experiments demonstrate that overall the GPs show substantially different responses to adapting stimuli compared to those shown in the human data.

As predicted, one of the most immediate differences between the human and GP recordings is the significantly shorter latencies of the evoked potentials (Figure 5.2). This is a substantial difference when considering the GP AEP is concluded in about a quarter of the time of the human AEP (Table 5.1). This could be expected to have consequences about the effects of adapter repetition rate and the time constants of recovery from adaptation. The morphology of the EEG waveform is comparable to previously published literature of near

field measurements over auditory cortex in anesthetised GPs (Popelár et al., 1987; Syka et al., 1994).

By comparing the latencies of the peaks between the different recording methodologies then potential sources can be inferred. The N1 peaks of the EEG and LFP show the same latencies suggesting the source of the EEG's N1 response is primary auditory cortex. The P1 of the EEG appears roughly aligned with the N1 of the IC response. This could either be representative of this response with an inversed polarity due to the recording location or could be a thalamic potential, either way it is suggestive that the EEG P1's source is subcortical. There is a deflection in the EEG after the P2 (45-80ms) which is not evident in the other recording methodologies which could mean it is representative of higher, non-primary auditory regions.

5.4.1 Adaptation Tuning

For the single adapter condition, the GPs show a smooth, linear recovery from adaptation with increasing adapter-probe frequency difference that shows consistent gradient in both EEG and LFP recordings.

These results show that at both recording scales the GPs show consistently much sharper frequency selectivity than humans. This is quite surprising considering GPs have lower frequency resolution hearing than humans, due to wider cochlear filter bandwidths (Evans et al., 1992) and could mean that cortical tuning is not well correlated with cochlear tuning. This could instead represent the frequency selectivity seen at a cortical level but as cortical neurons will typically show receptive fields broader than a single auditory filter it is unlikely that GPs display naturally sharper cortical tuning than humans.

Data from other experiments (Merry et al., 2016) shows that anaesthesia has a substantial sharpening effect on notched noise derived frequency bands in both guinea pigs and ferrets for as yet unexplained reasons. These experiments were done under a variety of anaesthetic mixes including

ketamine/medetomidine and fentanyl/fluanisone/urethane and all showed sharper results than found in awake data. This could suggest the main difference in tuning observed here between the human and GP results is a result of anaesthesia rather than an inherent inter-species difference. There is literature supporting this as a potential mechanism as there is evidence of sharpening of cortical receptive fields under several anaesthetic agents (Gaese et al., 2001; Edeline, 2012).

While it is the standard procedure in the published literature, there is no published validation to show that using a single probe frequency with a one sided frequency separation is a valid representation of all frequencies and separations higher and lower than the probe, especially given the asymmetry of cochlear filters (Sumner et al., 2003). To test this the single adapter condition was run but with 3 different probe frequencies and testing frequency separations either higher or lower than the probe (Figure 5.6). As the data is from one subject there are no error bars but when comparing between probe frequencies, for adapters higher than the probe tone, there appears to be little change in the degree of adaptation or sharpness. When comparing the results of higher and lower separations, the 4 kHz probe condition is reasonably symmetrical but the 1 kHz tone shows more release from adaptation in the adapter lower than probe conditions. It is possible that these differences represent the asymmetries seen in auditory filters or, given the frequencies, could be an effect of the edges of the GPs hearing range.

5.4.2 Adapter Onsets and Duration

GPs were exposed to the same auditory stimuli used for the human experiments in section 2.3 to assess whether RIS can be elicited in non-human animals. It is evident in the recordings from iEEG, LFPs and multiunit activity that there is no evidence of substantial differences between the results recorded in the single vs multiple onset conditions meaning there is no RIS present in this study.

Several factors could account for the differences seen between the human and GP datasets. Firstly it could be simply that the GPs do not demonstrate RIS and the changes are not methodologically based but purely species driven. Alternatively it could be that due to differences in brain size and the neural response latencies that the GPs have a substantially different time course of adaptation compared to humans and therefore the stimulus parameters that were derived for using with humans are unsuitable for use with GPs. The repeating stimuli has a fast repeat rate with only a 25ms ISI. For example it could be suggested that these gaps are imperceptible to the GPs which would explain the lack of differences between the single and multiple onset data. However, previously published data from this lab has shown that in GP IC the mean single unit gap detection thresholds to pure tone stimuli are around 10ms, with ~80% of the 76 units recorded from having detection thresholds under 20ms (Berger et al., 2014). These recordings were made from GPs in the same colony as the ones used for this experiment and with an identical anaesthetic regime.

Another explanation could be that due to the differences in recording modality and cortical architecture between species that the GP recordings could be coming from more primary cortical regions than the human recordings which could be representing more higher-order brain regions. An additional explanation for the differences could be the anaesthesia used with the GP recordings, as the ketamine used will have effects on short term plasticity and could potentially prevent RIS. It is likely that it is a combination of these factors and as such potential further studies could include modifying the stimulus parameters to attempt to optimise them for use with GPs, recording from awake, unanaesthetised GPs or recording adaptation of mid-latency responses in humans to attempt to get a more response with a stronger influence from primary auditory cortex.

5.4.3 Adapter Laterality

In this experiment the GPs were exposed to monaural or diotic adapter and probe stimuli while responses were recorded from one auditory cortex. In the unadapted state, as expected, sound stimulation ipsilateral to the recording side will result in a much smaller evoked response than from contralateral stimulation. There is very little to distinguish the responses to contralateral and diotic stimulation.

When considering the conditions with an ipsilateral adapter the contralateral and diotic probes show very little adaptation suggesting very little overlap of cortical neurons responsive to both ipsi and contralateral stimulation. However using both ipsilateral adapter and probe a frequency selective adaptation response can be elicited.

With a contralateral adapter, the ipsilateral probe shows little adaptation but the contra-contra condition shows a level of adaptation and frequency tuning that is indistinguishable from the diotic-diotic condition. Comparably the ipsi-ipsi and diotic-ipsi conditions show very similar levels of adaptation and tuning.

This data all suggests that the two auditory cortices will adapt independently of each other, with little to no inter-hemispheric interaction, and potentially that the ipsilateral cortex will not adapt in response to monaurally presented sounds. This results in the stimulus delivered to the ipsilateral ear being effectively superfluous when compared to the contralateral response.

5.4.4 Summary

Overall the results of these experiments show exceptional differences between the responses of GPs to the RIS paradigm and those seen in the human EEG experiments. In the GPs there is no evidence for change in frequency selectivity with increased duration or number of adapters using this methodology.

The two most likely causes of these differences are the inter-species differences between humans and GPs or the effects of anaesthesia on adaptation. Investigating these differences forms the next two chapters of this thesis, first looking at adaptation in awake GPs then looking at the effects of anaesthesia on adaptation.

Chapter 6

Characteristics of Adaptation in Awake Guinea Pigs

6.1 Adaptation in GP EEG

6.1.1 Introduction

With the substantial differences of adaptation properties of humans and anaesthetised GPs shown in the previous chapter it is important to discover the cause of these discrepancies. The recordings were undertaken at a comparable neural scale which leaves two major differences, of species and anaesthesia. To disentangle these two effects we can make EEG recordings in awake GPs, removing the anaesthesia confound and leaving the primary difference as an inter-species one.

Our lab has developed a methodology for chronically recording intracranial EEG (iEEG) from ball electrodes in GPs. Outside of our lab, a comparable EEG methodology for GPs has not been demonstrated and within our lab iEEG has only very recently been used as part of a recovery surgery. Therefore a full characterisation of the recorded AEPs in awake GPs will be needed before they can be used to derive adaptation parameters.

This also means that the previous methodologies presented may not be best suited to characterise adaptation in this new model and the presented stimulus protocols used will need to be assessed and refined between experiments for optimal results.

6.1.2 Method

Animal Preparation: Experiments were performed on 6 pigmented guinea pigs (2 male, 4 female) in accordance with UK Home Office regulations under the Animal Scientific Procedures Act 1986. For the implantation of the iEEG array anaesthesia was induced with a ketamine/xylazine mixture injected

intraperitoneally and maintained with 2-3% isoflurane. Silver ball electrodes were implanted extradurally through burr holes made in the skull over auditory (See Section 5.2) and visual (4mm rostral of lambdoid suture, 4mm sagittal of midline) cortex (Nishimura and Song, 2012), referenced and grounded 2mm rostral of bregma. Electrodes were then secured with silicone elastomer and bone cement before recovering the animal.

Awake Recordings: Recordings were made inside a dark, sound-attenuating, electrically shielded booth. GPs were allowed to freely move around a custom made cage, surrounded by sound attenuating foam, to minimise sound reverberation. GPs were tethered to a cable, connected to their implant to allow data recording. Sounds were produced from a tweeter mounted directly above the cage.

Recording and Data Processing: Responses from the electrodes were acquired using a Tucker Davis RX7, sampled at 12.212 kHz with 16-bit resolution and amplified (approximately 50k). Evoked activity was filtered on-line between 10 Hz and 300Hz.

For analysis, recordings were down sampled to 2 kHz. Artefact rejection was undertaken using the root mean square (RMS) of the signal, rejecting trials with an RMS greater than 2.5 standard deviations above the mean for that channel. Where multiple sessions of activity were recorded over time within one animal, the waveforms were averaged over the multiple sessions within subject. AEP peaks were determined automatically as the maximal amplitude inflection points within the expected latency windows. The goodness of fit was assessed visually and peaks were reselected manually if necessary. Early responses were categorised as the negative deflection peaking at ~25ms latency and the late response with a negative deflection at ~50ms latency. Coloured patches around waveforms represent 95% confidence intervals derived from bootstrap resampling with 500 repeats.

Stimuli: Stimuli used include pure tones, broadband noise and band limited noise. Band limited noise was produced by low pass filtering a white noise signal with a cut-off frequency equal to the desired bandwidth. This signal was then multiplied by a pure tone with the desired noise centre frequency. Unless otherwise stated the stimuli were presented at 75 dB SPL, measured at the base of the cage.

6.1.3 Results

These experiments attempt to characterise the neural responses to auditory stimulation recorded from intracranial EEG in guinea pigs. This includes characterising and optimising the effects of using adapting stimuli to investigate frequency selectivity in the cortex.

6.1.3.1 Characterising Guinea Pig EEG

As seen in the previous chapter GPs show very short latency cortical responses in EEG recordings with the first major negative deflection having a latency of ~25ms, hereafter referred to as the early potential (Figure 6.1). In the awake GP there is also a late potential, at ~50ms, which was present in the previous recordings but was not as prominent. Considering the anaesthetised recordings this response is likely from auditory belt regions as this deflection was not present in A1 LFPs.

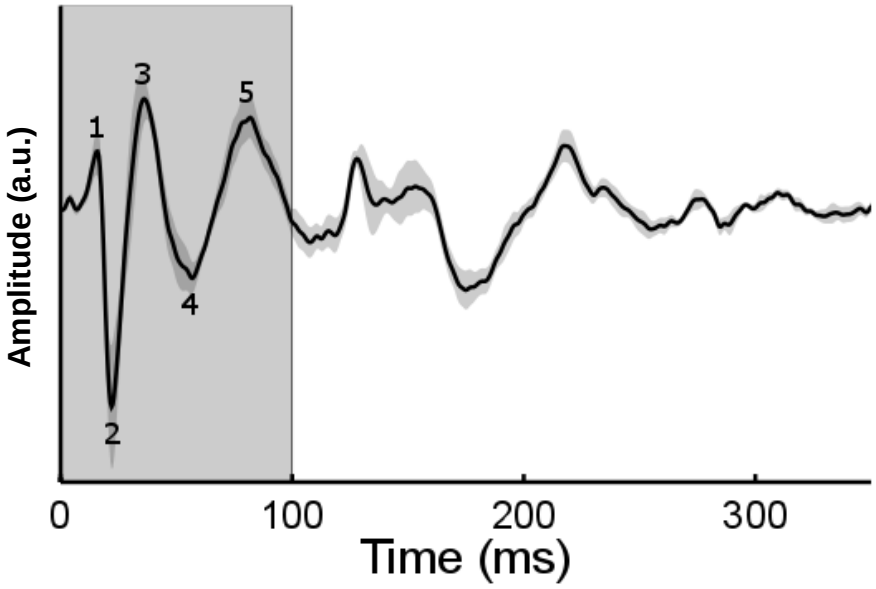

Figure 6.1: Grand average AEP in response to a 6 kHz, 100ms, 75 dB SPL pure tone. The AEP comprises of 5 inflection points making an early potential (1-2-3) and a late potential (3-4-5).

A new feature of the responses not seen in our anaesthetised recordings is offset responses to the tones (Figure 6.2). These are distinguishable with tones of 30ms or longer duration, for shorter tones they are likely present but are inseparable from the onset response. The offset responses have a longer latency than the onsets, peaking at ~40ms, this is possibly because the sound offset will be a less salient feature than the onset.

As stated earlier in humans there is an AEP integration window of ~72ms meaning a tone of this length or greater is required to elicit a maximal amplitude AEP. In the GPs using parameter variations this was found to be <20ms. This is demonstrated in figure 6.2 as all the tones with duration 20-100ms produce comparably sized onset responses.

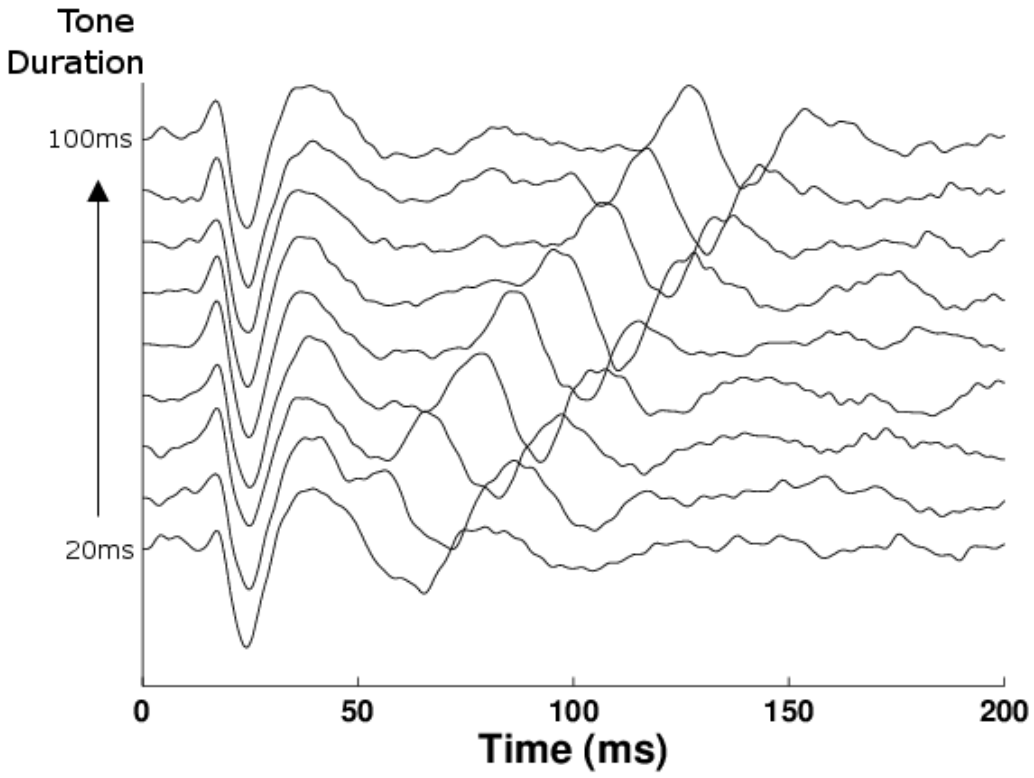

Figure 6.2: AEP montage for one subject, averaging over all electrodes, showing the effects of increasing tone duration on auditory cortex AEP morphology. The responses demonstrate the onset response with fixed latency and increasing offset response shift with increasing duration.

As the auditory responses are recorded across four electrodes it is worth analysing the between and within electrode variability in responses. Using bootstrapping it can be shown that the AEPs in response to a pure tone show a very low variability within each electrode and the primary variability is between electrodes. Figure 6.3 shows the simultaneously recorded responses from the four separate auditory electrodes from one subject. This demonstrates the changes in the ratio of the amplitude of the early and late onset components and the offset response between each electrode. This variability is likely to be as a result of electrode placement locations in relation to the related auditory structures.

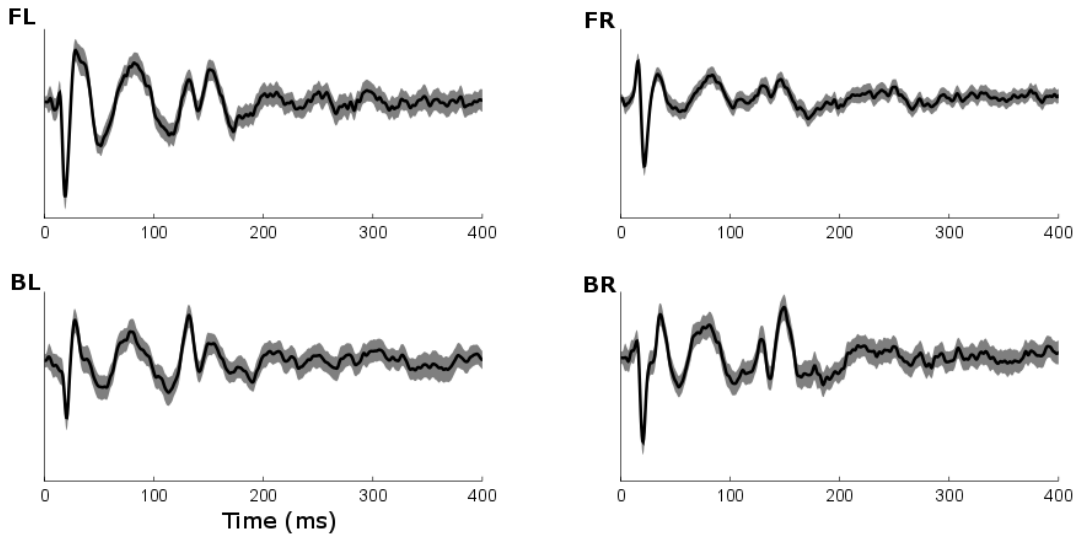

Figure 6.3: AEPs of the four auditory channels in one subject in response to a 100ms, 6kHz pure tone with bootstrapped, 95% confidence interval patches, demonstrating high repeatability within channel but morphology variations between channels. (FL: Front Left, BR: Back Right)

From initial experiments it was shown that the amplitude of pure tone responses was around 30% that of the amplitude of broadband clicks so it was decided to look into the amplitude vs bandwidth relationship as shown in figure 6.4. 100ms duration, band-limited noise bursts, centred about 6 kHz with between 75 and 2400 cents bandwidth were used. This demonstrated a sharp drop-off of response amplitude to band-limited noise when reducing the bandwidth from 2 octaves to 1 with a halving of response size.

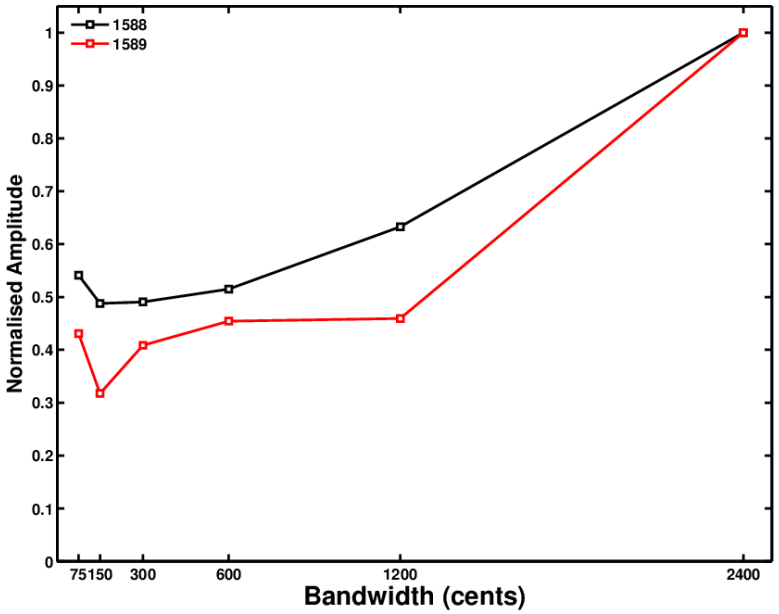

Figure 6.4: AEP amplitude scales with noise bandwidth. Responses of two subjects to variable bandwidth noise bursts centred about 6 kHz, normalised to the 2400 cents condition.

6.1.3.1 Adaptation

As we are attempting to find parameters that will allow an appropriate analogue of the human RIS study the characteristics of adaptation in GPs in both the temporal and frequency domains need to be determined.

Initial experiments attempted to look for a time course of adaptation recovery in GPs with a pure tone adapter-probe couple with a variable ISI however this resulted in some issues. 50ms duration, 6 kHz pure tone adapters were used with variable duration ISIs before a 100ms duration, 6 kHz probe, all presented at 80dB SPL. The 100ms probe duration was chosen to minimise the interaction between the probe's onset and offset responses. The results of the first four subjects are shown below, demonstrating that the results for conditions with an ISI<160ms show very noisy responses with poor repeatability between subjects.

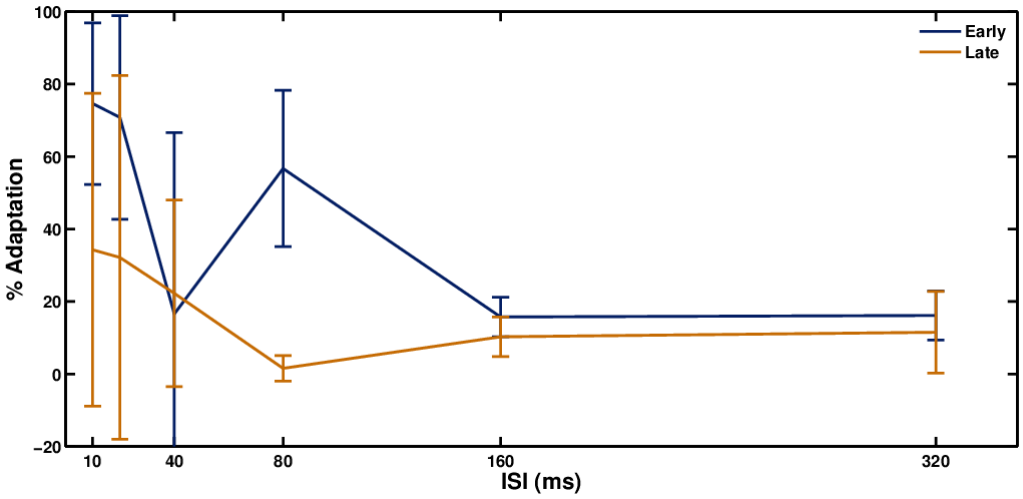

Figure 6.5: Pure tone adaptation in GPs results in highly noisy results for latencies <80ms. Adaptation shown separately for the early and late potentials of the AEP (n=4).

By analysing the raw waveforms of the responses a likely cause can be found. Figure 6.6 shows the responses of one subject's auditory cortex responses with the average AEP shown in black and a representative "baseline". This baseline condition is the waveform in the longest ISI condition to act as a surrogate for an adapter alone state, without a nearby probe response interacting, to see how much the adapter response is interfering with the probe response at short ISIs. This baseline response shows that the offset response of the adapter is overlapping with the early potential of the onset. When looking at the 10ms ISI condition it could be thought that a simple subtraction could remedy this but at the 20ms condition a subtraction would result in an almost doubling of response size. This suggests the combination offset-onset response is a non-linear summation of the two responses and as such would be difficult to disentangle.

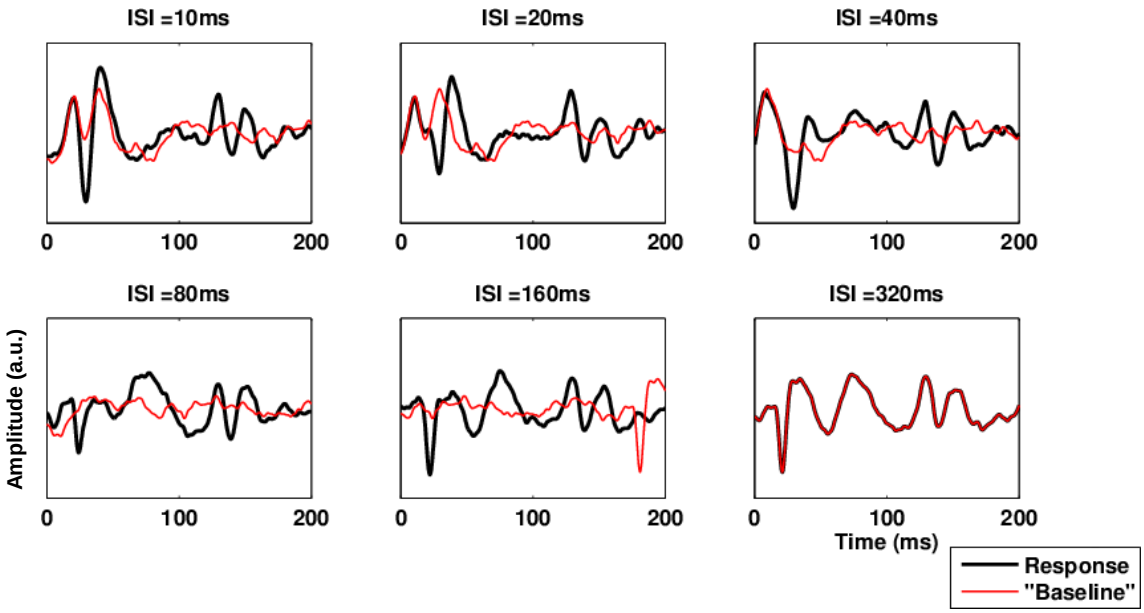

Figure 6.6: Responses (black) are shown compared to the adapter response of the longest ISI condition (red) time aligned to show a representative adapter only response. At short latencies (<80ms) probe onset responses overlap with adapter offset responses resulting in a non-linear combination response.

As an alternative to the pure tone adaptation time constant derivation method instead a broadband adapter-probe stimulus set can be used. All temporal parameters were identical to those in the previous experiment but the pure tones were replaced by broadband noise. This has two main advantages, firstly the response amplitude of broadband stimuli has a much more favourable signal to noise ratio (SNR) in the recordings allowing more accurate quantification of the most adapted conditions and secondly the broadband stimuli have much smaller amplitude offset responses relative to the onsets so will interfere less with the probe response. An unintended consequence of this switch to broadband stimuli means that cross modal responses in visual cortex can also be elicited and a time constant derived.

By using least squares fitting an exponential function was fit to the data in figure 6.7 and time constants determined. For the responses from auditory cortex this resulted in τ=60ms, compared to awake human EEG data with a τ of ~1200ms (Lanting et al., 2013). The auditory responses in visual cortex showed a longer recovery constant of τ=250ms (Figure 6.7).

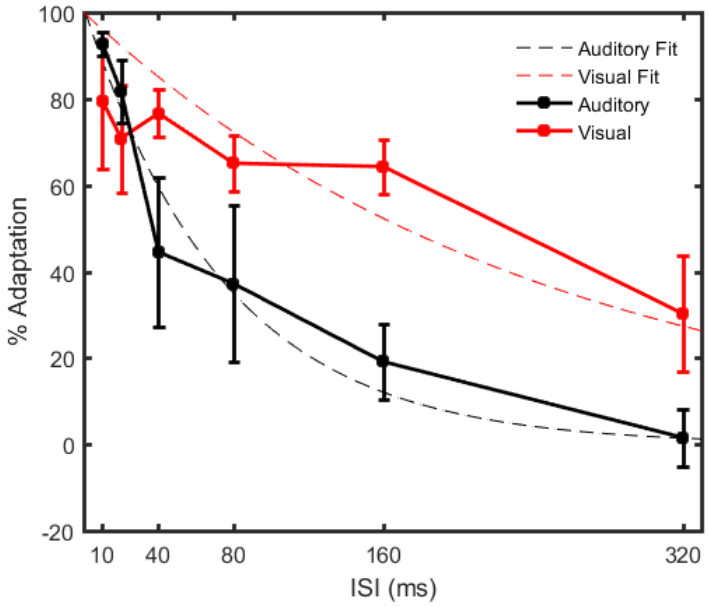

Figure 6.7: Time course of recovery from auditory adaptation of the early potential using broadband adapter and probe stimuli (n=4). Auditory and visual cortices show different adaptation recovery time constants

Figure 6.8 demonstrates the improvement to the signal quality with the effective attenuation of the adapter offset response and increase in unadapted response amplitude. The offset response of the adapter offset response is proportionally much smaller than the onset responses of the most adapted conditions compared to the pure tone conditions, contributing to a better SNR. This results in the much cleaner recovery curves seen above.

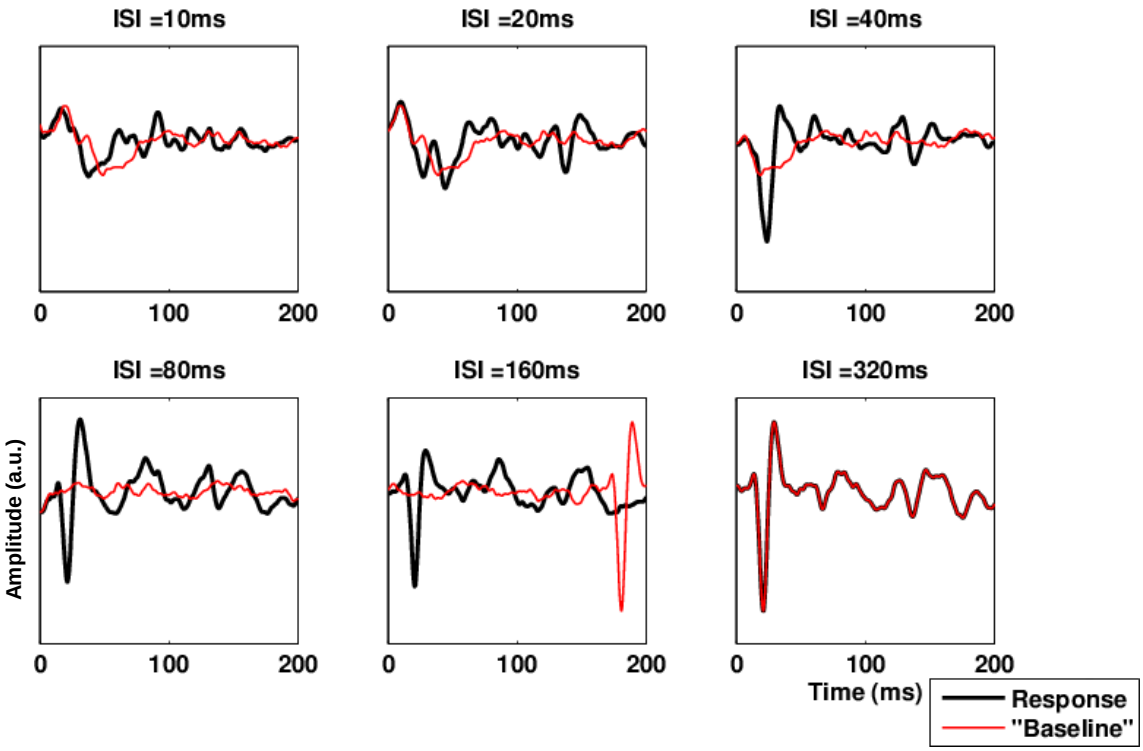

Figure 6.8: Responses (black) are shown compared to the response of the 320ms ISI condition (red) at an identical time point to show a representative adapter only response. Broadband adapters produce negligible offset responses resulting in less interaction with the probe onset response at short latencies

By using the broadband stimuli the time constant has been found but we are also interested in frequency selectivity of adaptation which entails using pure tone stimuli. As the previous experiments using pure tone stimuli were unsuccessful because of the adapter offset response a new stimulus protocol was devised to avoid eliciting an offset response. This is done by using a 0ms ISI between the adapter and probe stimuli. As with the original pure tone ISI experiment this uses a 50ms adapter and 100ms probe with no silence gap between them (figure 6.9). The probe was a 6 kHz pure tone with the adapter 0-300 cents higher. By removing the silence gap between adapter and probe then no offset response will be elicited.

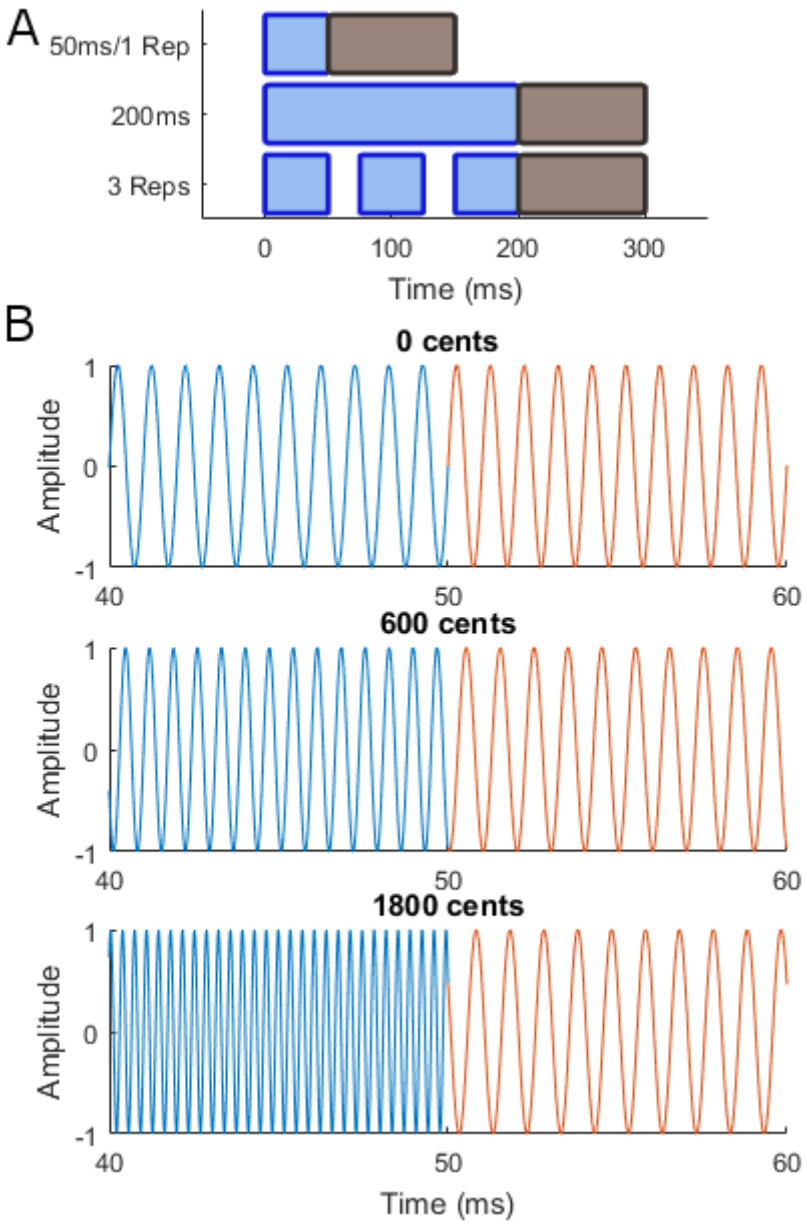

Figure 6.9: A: Example conditions using the 0ms ISI stimuli with the GP temporal parameters. In the single onset conditions the adapter and probe have no gap and in the multiple onset conditions there is no gap between the final adapter and the probe. B: Waveforms of the adapter-probe pair in the 50ms/1 Rep condition showing the frequency transition. The phase information is continued through the transition preventing any auditory artefacts.

Using this stimulus set produced an unexpectedly sharp tuning of adaptation with seemingly full adaptation range expended by 75 cents adapter-probe separation (Figure 6.10). This adaptation appears to asymptote around 45%, probably potentially due to the ungated onset of the unadapted condition. As there will be an abrupt transition between frequencies in the test conditions

the unadapted reference, assuming an identical waveform of the adapted probes, will have an ungated onset which results in a broadband spectral splatter. This will result in a larger unadapted AEP as a larger population of neurons will be recruited and therefore will shift the scaling of the resultant adaption percentage.

There was no directly comparable results readily available that would give an idea as to the sharpness of the tuning of human neural responses to these stimuli so as a comparative test a pilot study was run in human participants (n=3) with comparable stimuli. This was recorded using a 4 electrode EEG setup (Ground, AFz; Reference, TP9&10; Recording, Cz). The durations of the adapters and probes were scaled up for the humans with an adapter duration of 350ms and probe duration of 100ms. The probe for the human study was a 1 kHz pure tone. Data analysis was identical to that used in the pilot studies in Chapter 2.

These human results show a visually broader tuning in response to this stimulus than in the GP results with no clear asymptote present by 300 cents separation compared to the steady level of adaptation reached for separations of >75 cents in the GPs. However, possibly due to the low number of repeats of each condition, there is no statistically significant interaction between species and frequency selectivity in this dataset (two-way ANOVA, $F_{(9,50)}$=0.843, P=0.581).

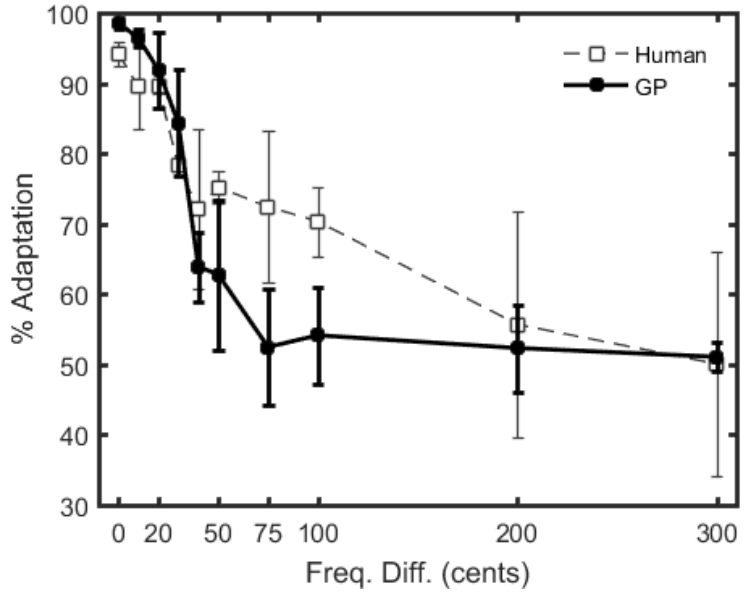

Figure 6.10: Frequency selectivity of pure tone adaptation measured with a 0ms adapter-probe ISI shows very sharp tuning in GPs (n=4) and slightly broader tuning in humans (n=3)

Using this method it is now possible to produce some measure of the frequency selectivity of adaptation in GPs. With this we can again try to replicate the RIS phenomenon seen in the human EEG data. The 0ms ISI method can be used with either a variable duration adapter or preceded by a train of multiple adapters. In this experiment durations of 50, 200 and 500ms were used and either the one 50ms adapter or a total of 3, 6 or 9 adapters, each 50ms duration and with an IAI of 25ms. Probes were 6 kHz pure tones with adapters 20 or 40 cents higher than the probe in both single and multiple onset conditions and 100 cents in the multiple onset conditions.

In this experiment sharpening is simply shown by a reduction in the level of adaptation, as by default the 0 cents separation condition is flat at 100% as there is no onset present (Figure 6.11). In both the single and multiple onset conditions there appears to be an increase in frequency selectivity with increasing adapter duration. There is a very similar reduction in percentage adaptation in both condition sets but despite the reductions, suggesting a greater selectivity from 0 cents, there does not appear to be any increase of selectivity between the different frequency conditions.

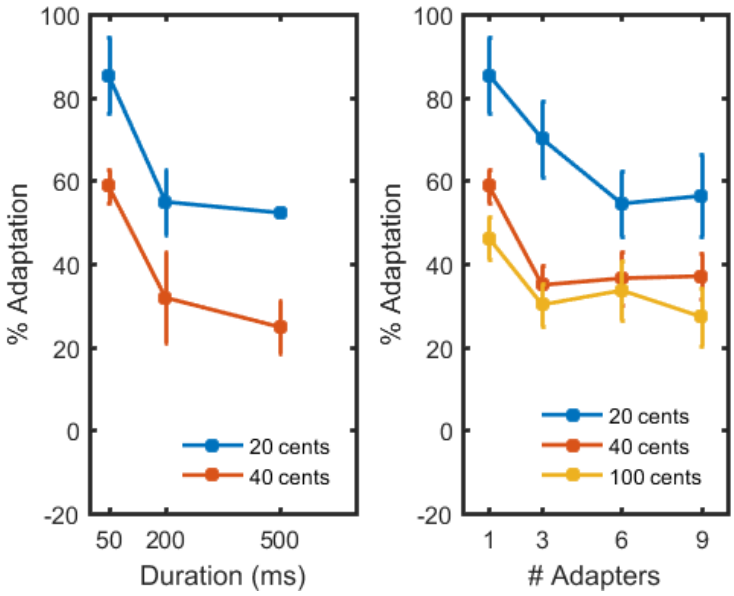

Figure 6.11: Frequency selectivity of pure tone adaptation measured with a 0ms adapter-probe ISI sharpens with both increased adapter duration and number of adapters (n=2)

6.1.4 Discussion

Initially the plan for these experiments was to be able to replicate RIS in our animal model to be able to use the awake GPs to investigate the underlying neural activity. However, due to the magnitude of the species specific differences between the adaptation characteristics of humans and GPs, this turned into a set of pilot studies to better understand how adaptation works in the GP brain and the best way to quantify this.

The iEEG recordings in the GPs showed robust responses to pure tones, broadband noise and band-limited noise that were highly repeatable between subjects. The waveform morphology and latency characteristics were all replicable and reliable within and between each animal. There was variation between electrodes within each animal suggesting that while these electrodes will pick up a large population of neurons they still show a somewhat local average response. As the positioning of the burr holes for the electrodes is based off the anatomy of the skull rather than the neural vasculature then there will be a greater variability in electrode placement over the auditory areas. While GP auditory areas cover a reasonably sized area of the cortical surface (~50mm^2) the primary auditory cortex only comprises around 40% of this, the

rest comprises of the, comparably sized, dorsocaudal belt region and other smaller non-primary regions like the dorsal and ventral rostral belts (Wallace et al., 2000). This means that although the cranial anatomical landmarks are a good guide for the location of the auditory areas meaning that auditory areas can be reliably found with these gross electrodes, the location of them within the auditory areas varies between implantations and therefore the relative contributions of each of these cortical areas to the recorded signal can vary.

One of the main confounding factors for the recording of the adaptation experiments that has been seen in these recordings but not in either the human EEG or anaesthetised GP recordings is the tone offset responses. These responses are seen reliably in all the tested GPs and display a longer latency and longer lasting response than the tone onsets. This long lasting response disrupts the ability to measure adaptation at short ISIs as the evoked activity from the adapter offset and probe onset will combine non-linearly and highly variably between subjects. It could be theoretically possible to derive some method of disentangling these responses but from these results it appears to be a non-trivial problem.

To circumvent these issues a methodology was developed that would not elicit this offset response by removing the silence gap between the adapter and probe. This stimulus set produces surprisingly sharp tuning, appearing to reach a maximum amplitude by 75 cents frequency separation. As this natural sharpness of the GPs was so unexpected the same experiment was replicated in humans. The results seen so far suggest the two more likely eventualities are also the least expected, that human and GP adaptation tuning is identical or that human tuning is broader. Given that GP cochlear tuning is broader than in humans it is generally assumed that neural tuning will follow this trend (Evans et al., 1992). From these results however, the statistics show no significant difference in adaptation frequency selectivity between the species. This could be accurate or could be as a result of the low number of subjects tested so far meaning there is not sufficient power to make a firm conclusion. From the

current trends in the data the humans may have a slightly broader tail to their tuning curve but this may disappear with more repeats. If it does emerge that human and GP adaptation tuning selectivity is directly comparable this invites the question of how, for example if it is that humans are processing frequency information sub-optimally or if GPs have neural mechanisms to compensate for their broader cochlear tuning.

This methodology is not an ideal solution as this experiment is unlikely to be activating the same neural pathways as those recorded with an ISI. As with the human experiments, the ISI was chosen to attempt to minimise the degree of subcortical adaptation. By removing this silence gap it is likely that most structures in the sub-cortical auditory pathway will show a reasonable degree of adaptation meaning the tuning seen will not be as heavily weighted toward the cortical tuning. This change in methodology also potentially means a shift away from measuring tuning of onset neurons, as the introduction of the probe is not strictly speaking an onset but rather a frequency transition, which progresses more toward the theories of neural change detection mechanisms (Ulanovsky et al., 2003).

Given we now have a method of discerning some form of adaptation tuning in GPs we attempted to find a correlate of RIS in the GPs. In the two GPs tested it appears there is a stimulus induced sharpening effect but this is not just limited to the repeating stimuli. Both the single and multiple onset adapters lead to a greater release from adaptation at each frequency separation with increasing adapter duration. As there is not the direct comparison between the human EEG experiments in Chapter 2 and this one in the GPs it is not yet clear whether this reflects an inter-species difference or if now the silence gap has been removed that this represents the adaptation effects on sub-cortical tuning.

To build on these experiments there are several follow ups that can be performed. Firstly, the power of the recovery and tuning experiments can be increased with further testing and increasing the number of repeats. Additionally the experiment looking into RIS in the 0ms ISI case can be

replicated in human test subjects to attempt to find whether this sharpening with both single and multiple onset adapters is present in humans in this methodology. Further from these experiments all of these experiments can be done while using invasive recordings of the auditory cortex to investigate which of these effects can be attributed to primary auditory regions and also to discover correlates of these population level recordings in single unit recordings.

6.2 Developing a method of chronically recording LFPs in awake guinea pigs

From the experiments presented in the previous section it can be shown that adaptation has quantitatively different characteristics in humans and guinea pigs, with substantial differences in time constants and frequency tuning. However, they show many of the same qualitative effects and should still be able to act as a model of the underlying neural mechanisms of adaptation. The differences have shown to be compounded by the effects of anaesthesia on auditory processing and therefore to produce the best quality experimental data on the underlying neural data ideally the experiments should be collected in awake animals. As this lab group has not previously recorded intracortical recordings in awake guinea pigs before then a new methodology was developed.

Building on previous experience of surgically implanting iEEG electrodes the methodology has been modified to allow the implantation of a silicon depth electrode to simultaneously measure at multiple cortical depths in awake, freely moving GPs.

6.2.1 Implantation

To limit the complexity of the experiment a prefabricated probe design was chosen, the Neuronexus A1x16-5mm-100-177-HZ16_21mm. This is a single shank silicon electrode with 16 linear electrode sites each with a 100μm spacing. With an implantation depth of 1600μm this will result in a spread of

recording sites from cortical layers I to V. With the HZ package, instead of there being a solid silicon link between the electrodes and the connector there is a flexible plastic ribbon cable which allows more flexibility for placement of the electrode and connector for implantation.

Developing this method blends the methodologies from the guinea pig EEG implants and a previously published methods paper using this style of probe (Gage et al., 2012). As with the EEG methodology a scalp resection is performed and screws are implanted into the skull, these act as mechanical stabilisers and as an electrical ground. A right sided craniotomy was performed over auditory cortex and the dura removed. The electrode shank was attached firmly to a micromanipulator using molten polyethylene glycol (PEG, Average molecular weight 1500). Implantation location was chosen based on the vasculature of the cortex (Wallace et al., 2000) and the electrode was advanced to 1600µm from the cortical surface before being secured by silicone elastomer and bone cement. The PEG was dissolved with warm saline, the micromanipulator removed, the connector cemented onto the midline of the skull and the skin sutured up around the base of the connector.

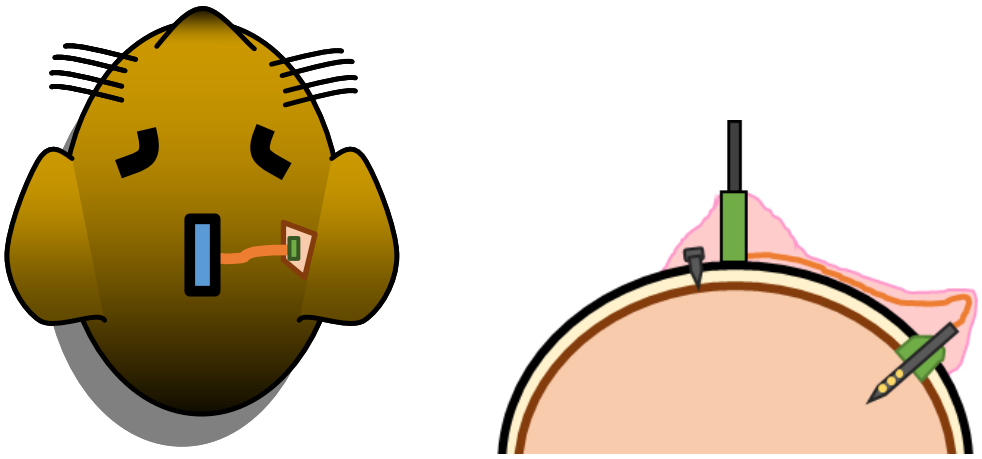

Figure 6.12: Schematic diagram of the layout of the electrode placement showing the approximate locations of the connector and electrode on the GP's head from an overhead (left) and transverse (right) view.

Early implantations encountered some problems, for example one instance of the silicon electrode shank snapping, corrected by building up above the silicon

with bone cement before manipulating the ribbon cable. There were also two instances of the bone cement shifting after electrode insertion which in both cases led to no auditory evoked activity being recorded, most likely from damage to the cortex, this was corrected by ensuring the bone cement is built up over the anchoring screws before removing the micromanipulator. In all cases the surgery was tolerated well and no adverse reactions to the implantation were observed. The longest implantation period so far has been just short of 2 months, with no substantial degradation of signal quality over time.

6.2.2 Recording Methodology

Animal Preparation: Successful implantation and recording took place in a total of 4 pigmented guinea pigs (all female). Procedures were performed in accordance with UK Home Office regulations under the Animal Scientific Procedures Act 1986. For the implantation of the LFP array anaesthesia was induced with a ketamine/xylazine mixture injected intraperitoneally and maintained with 2-3% isoflurane.

Awake Recordings: As in previous experiments with chronically implanted GPs recordings were made inside a dark, sound-attenuating, electrically shielded booth. GPs were allowed to freely move around a custom made cage, surrounded by sound attenuating foam, to minimise sound reverberation. GPs were tethered to a cable, connected to their implant to allow data recording. Sounds were produced from a tweeter mounted directly above the cage.

Recording and Data Processing: Responses from the electrodes were acquired using a Tucker Davis RX7, sampled at 12.212 kHz with 16-bit resolution and amplified (approximately 50k). Spontaneous activity and auditory steady state responses (ASSRs) were filtered on-line between 0.1Hz and 3000Hz. Other evoked activity was filtered on-line between 10Hz and 3000Hz.

For analysis of LFPs, recordings were down sampled to 2 kHz. Artefact rejection was undertaken using the root mean square (RMS) of the signal,

rejecting trials with an RMS greater than 2.5 standard deviations above the mean for that channel. For analysis of multiunit spiking activity the recordings were down sampled to 6 kHz and high pass filtered with a cut-off of 300Hz using a zero-phase digital filter. Spike detection was performed using a threshold for each channel, set at 2.5 standard deviations below the mean of all recordings within that experimental batch for that electrode channel.

6.2.3 Recording Results

As before, in Chapter 6, the responses recorded from these electrodes in response to auditory stimulation need to be characterised before they can be used to derive adaptation characteristics. The LFPs produce an AEP comparable to those seen in the anaesthetised recordings in Chapter 5 (Figure 6.13). The waveform morphology changes smoothly progressing down the cortical depth. In the most superficial layers the onset response has a large N1 and small P2. The N1 shrinks and P2 grows with increasing cortical depth. The offset shows a biphasic response in the superficial layers, with a positive and then negative deflection whereas the deepest electrodes show just a negative deflection.

When subjecting these waveforms to CSD analysis (Equation 1.1) this produces clear spatiotemporal patterns of current sources and sinks, the pattern of which matches previous literature in rodent auditory cortex (Szymanski et al., 2009). The largest current sink, representing local inward transmembrane currents which are taken as a correlate of excitatory activity, occurs at cortical depths from 500-1000μm from 20-30ms latency (Figure 6.13).

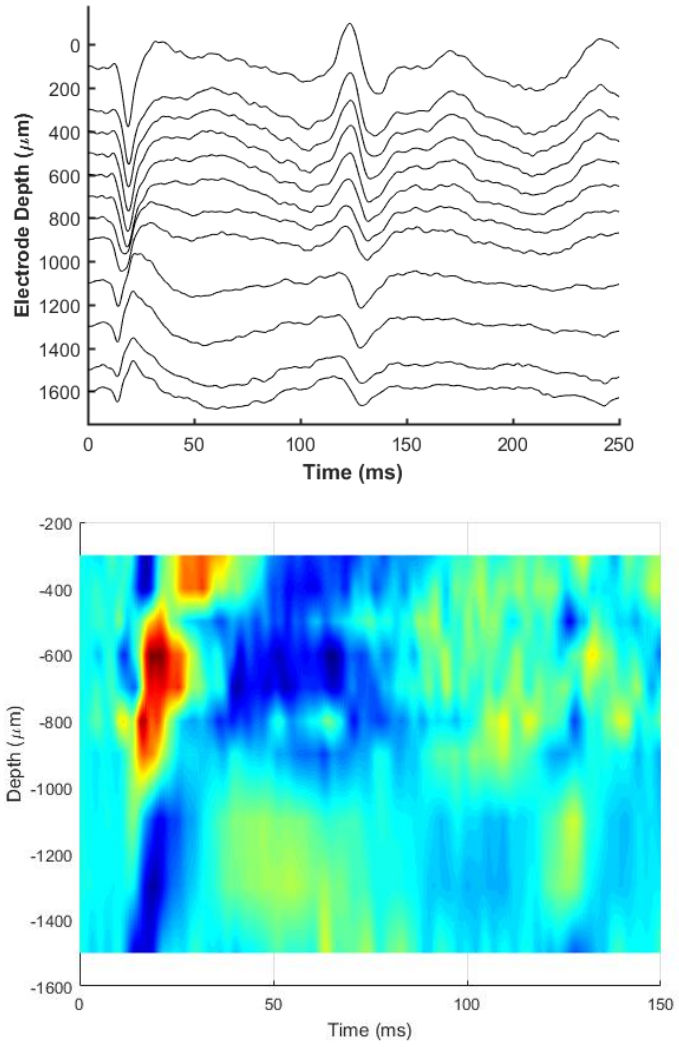

Figure 6.13: Representative example of an electrode purportedly implanted in primary auditory cortex. Top: Depth plot showing the change in waveform morphology through the cortical layers. Several unresponsive electrode channels were excluded. Bottom: CSD analysis of the above LFP signals showing current sinks in red, representing local excitatory activity, and current sources in blue.

To better characterise the properties of each electrode penetration receptive fields were determined, varying frequency and sound level. An example is given below of one penetration showing the tuning of the LFPs centring around 9 kHz (Figure 6.14, Top). The receptive fields of the multiunit spiking activity recorded at each electrode channel are also shown (Figure 6.14, Bottom). These results show that the deepest electrode channels show the broadest tuned units, with activity from 1.5-15 kHz compared to the relatively narrow tuning of the more superficial units between 9-15 kHz. This replicates effects

previously seen in auditory cortex in anaesthetised GPs (Wallace and Palmer, 2008).

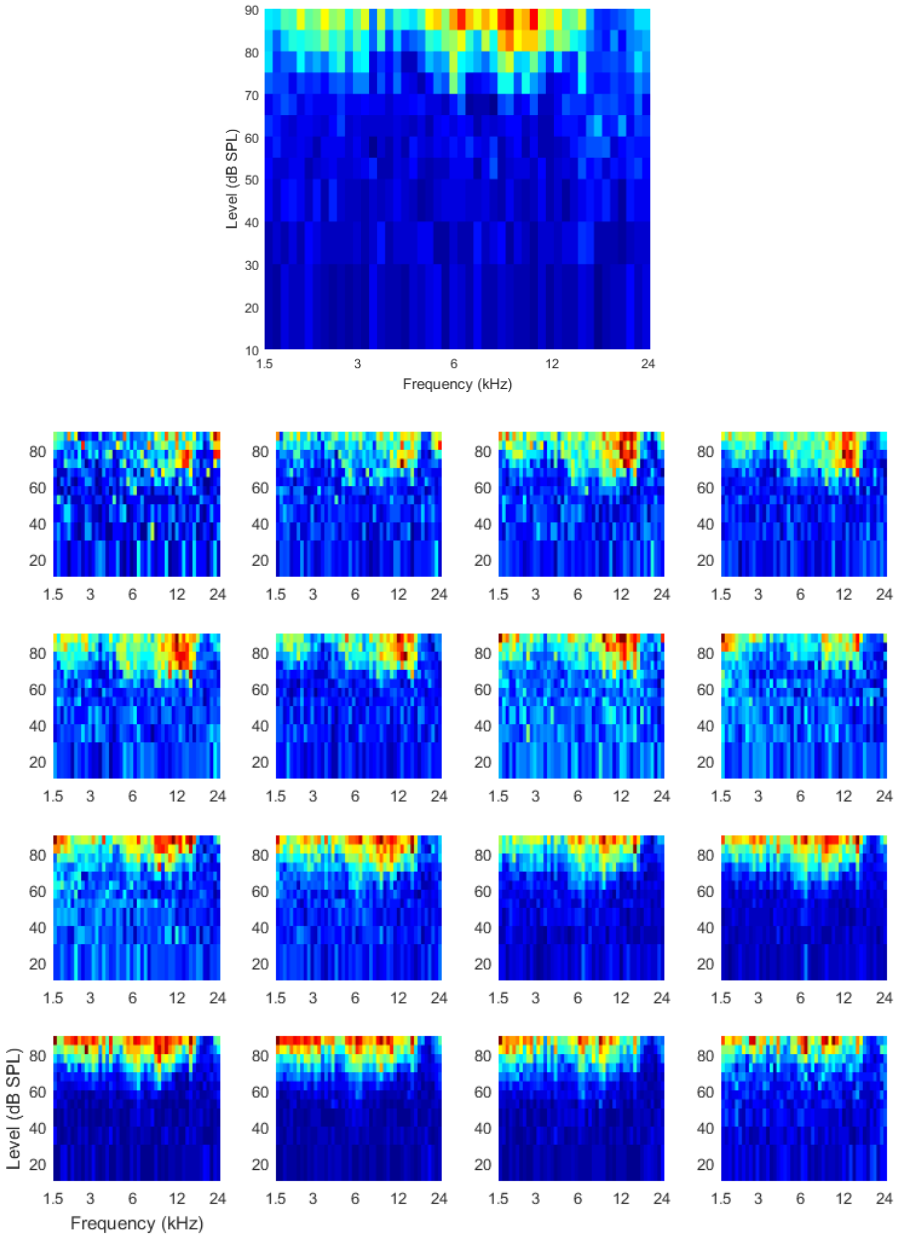

Figure 6.14: Receptive fields for one GP, derived from the all electrode average LFP (top) and individual channel multiunit spiking activity (bottom). Most superficial electrode is top left and deepest is bottom right, progressing sequentially deeper along the rows.

These multiunit clusters also demonstrate changes in their response type with cortical depth, as shown by their post-stimulus time histogram (PSTH). The deepest electrodes are picking up units with a large onset response and

sustained activity for the duration of the tone, followed by an offset response (Figure 6.15). The more superficial sites show just an onset response with no sustained activity of offset response. They also appear to show a higher proportional spontaneous rate.

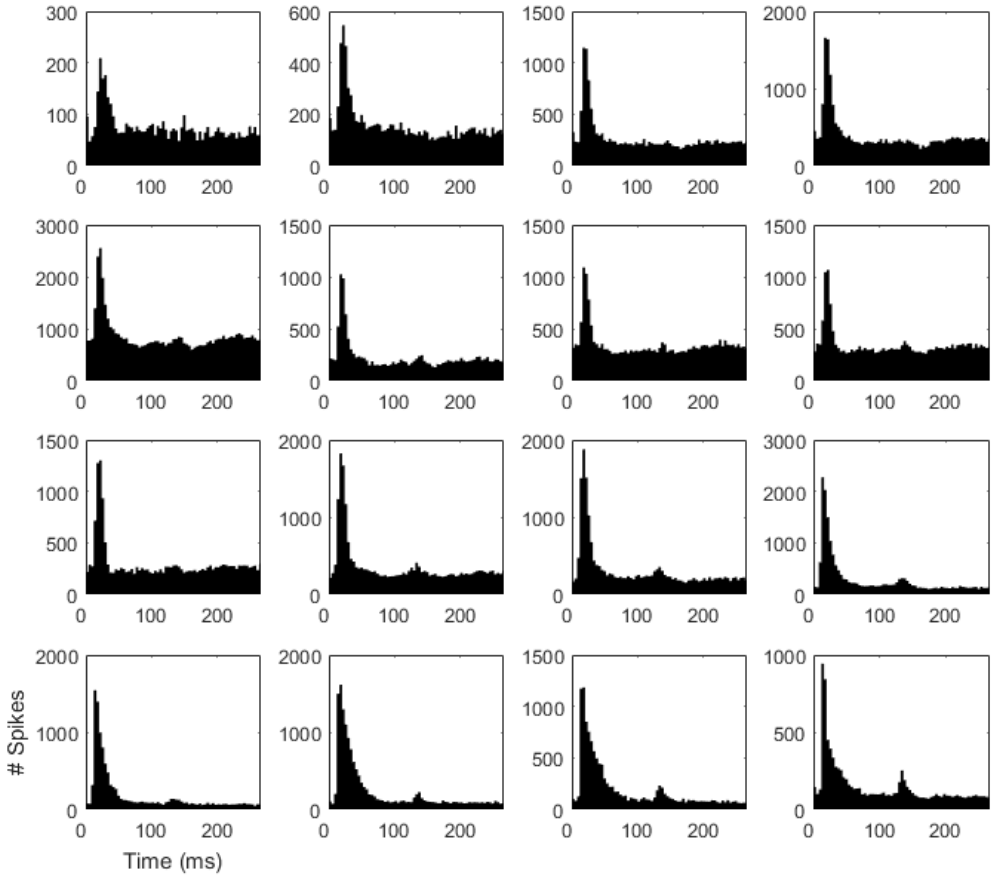

Figure 6.15: Multiunit PSTH from all 16 electrodes of one GP (Same as previous figure), showing combined responses from all receptive field conditions. Most superficial electrode is top left and deepest is bottom right, progressing sequentially deeper along the rows.

6.3 Cortical Adaptation of LFPs and Single Neurons

In Chapter 5 we investigated the neural correlates of RIS in anaesthetised GPs. This produced results that were qualitatively very different to those seen in the humans in Chapter 3. In this chapter we tried these experiments again in awake GPs, recording population responses and managed to find more suitable parameters to be able to quantify adaptation in GPs and began to see initial signs of RIS. To build on this previous research we can now investigate adaptation and RIS intracortically in auditory cortex of awake GPs. This allows

us to find single neuron correlates of the effects seen in previous chapters and investigate which of these effects can be attributed to primary auditory cortex or if any of these phenomena are generated in higher order regions.

A new addition to the methodologies in this chapter is using auditory steady state responses (ASSRs). These are frequency following responses that are seen in response to amplitude modulated (AM) tones or noise that can be seen as an increase in oscillatory power at the frequency of the amplitude modulation. ASSRs are used clinically to test hearing objectively in neonates as an alternative to ABRs which will test earlier in the auditory pathway. For our purposes ASSRs can be used to investigate temporal processing of complex sounds and also can be used to look at frequency tuning. As the rates of adaptation at different levels of the auditory pathway are sometimes quoted as being correlated with their maximum frequency following rates (Froemke and Schreiner, 2015) then comparing the frequency following rates in GPs and humans may give further comparative information about adaptation temporal processing between the two species.

6.3.1 Methods

The majority of the methods in this section are identical to those used in chapter 6. The recordings were performed in the same testing booth and in most cases identical stimuli were used and data analysis performed.

Adaptation recovery: Stimuli used are identical to those used in Chapter 6. In summary, a 50ms adapter and 100ms probe tone are used with a variable ISI of 10-320ms. Both adapter and probe are broadband noise bursts of equal level at 80 dB SPL.

Adaptation tuning: Stimuli used are identical to those used in Chapter 6. In summary, a 50ms adapter and 100ms probe tone are used with 0ms ISI between them. Both adapter and probe are pure tones, the probe is at 6 kHz with the adapter 0-300 cents higher.

Multiunit Adaptation: For both the preceding adaptation experiments the probe response was taken as the number of spikes recorded in the window of 0-50ms after the probe tone onset to capture the onset response of the multiunit clusters. Adaptation percentage was calculated, as before, using equation 2.1.

Steady state responses: ASSRs are elicited using long duration AM tones. AM tones with a carrier frequency of 6 kHz and modulation frequency of between 2.5 and 320Hz were used, each presented for 10s, gated on and off with a 10ms cosine squared gate. The period from 2-10s from onset was used for analysis to remove the effect of the onset response and leave the steady state response. LFPs were analysed by fast Fourier transform (FFT) analysis. Amplitudes of the ASSR responses were taken as the magnitude of the power at the frequency of the presented tone, baselined to the mean of the two neighbouring frequency channels.

Steady state multiunits: Frequency following ability of the multiunit clusters was tested by windowing over each period of the AM tone. Each period was divided into 50 equally sized bins of $\pi/25$ radians each to create a spike histogram as a function of phase. To quantify vector strength of the phase locking ability of the units two analysis methods were used, synchronisation coefficient (Goldberg and Brown, 1969) and a method using an FFT of the spike histogram (Shackleton et al., 2009). Synchronisation coefficient (SC) is calculated from the phase PSTH using the following equations.

$$X = \int_0^{2\pi} g(x)\cos(x)\,dx \tag{6.1}$$

$$Y = \int_0^{2\pi} g(x)\sin(x)\,dx \tag{6.2}$$

$$SC = \sqrt{X^2 + Y^2} \tag{6.3}$$

Where g is the normalised PSTH, expressed as a function of phase, x, such that $\int_0^{2\pi} g(x)dx = 1$ (Ashida and Carr, 2010).

The FFT method is calculated by taking an FFT of the phase PSTH and normalising the magnitudes by the zero frequency bin, representing the DC shift. The first frequency bin will represent the vector strength of the fundamental frequency, the second bin that of the first harmonic and so on.

For both measures the vector strength can vary between 0 and 1, with 0 representing no phase locking and 1 represents a perfect phase locked response.

6.3.2 Results

As shown earlier in this chapter, adaptation recovery in GP cortex can be tested using pairs of broadband noise bursts with a variable ISI. The results of the LFP responses follow a very similar time course to those seen in the EEG responses with an overall 10-15% shift toward more release from adaptation. The only significant deviation between the EEG and LFP results is at 20ms ISI where the EEG results show ~80% adaptation whereas the LFP shows only 35%. There is a shift of the derived time constant of recovery between the EEG results (τ=60ms) and LFP results (τ=30ms).

When looking at the multiunit spiking the level of adaptation of the firing rates can be compared. This analysis produces a very similar time course again for ISIs 20ms or greater, with almost identical results shown from 40-160ms. At 10ms ISI there is a substantially reduced adaptation percentage. This could either be a genuine retention of firing activity or could be picking up the offset response of the adapter as has been seen before.

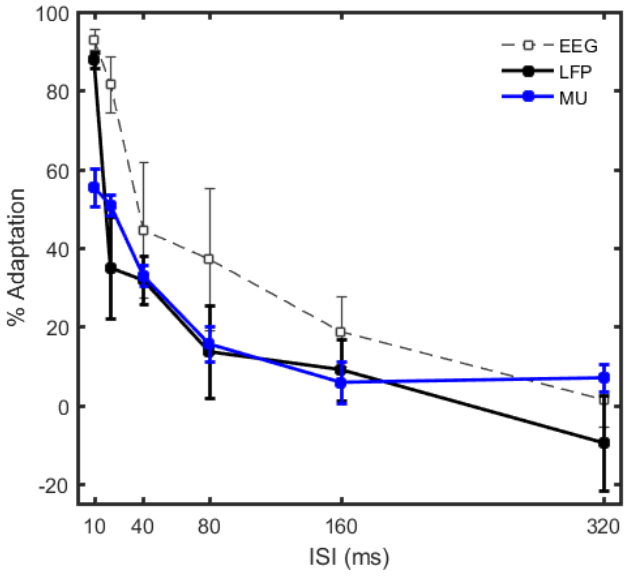

Figure 6.16: Time course of recovery from auditory adaptation of the early potential using broadband adapter and probe stimuli. Results are shown from recordings of EEG (n=4), LFPs (n=2) and spiking activity (n=16 multiunit clusters)

Previously, in our iEEG experiments, we have used pure tone adapter-probe stimuli with 0ms ISI to as a measure of adaptation tuning. Again, there is a very good agreement between the results seen in the EEG and LFP results as both appear to reach a steady state level beyond 75 cents, with similar selectivity at lower separations (Figure 6.17). The LFPs show overall more adapted results, probably representing the greater levels of adaptation in primary auditory cortex relative to the non-primary regions. The multiunit spiking activity shows very close agreement again with equal tuning, very reliably between different multiunit sites. One potential deviation is that between 100 to 300 cents frequency separation there appears to be an increase in adaptation. Tests at wider frequency separations would be needed to see if this trend continues.

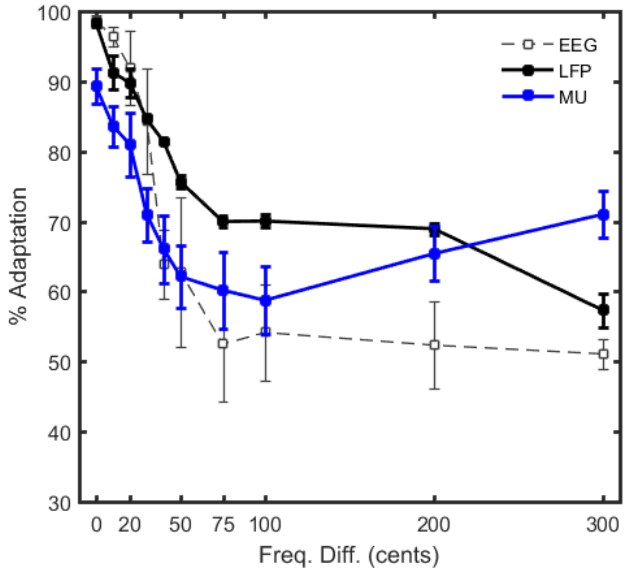

Figure 6.17: Frequency selectivity of pure tone adaptation measured with a 0ms adapter-probe ISI. Results are shown from recordings of EEG (n=2), LFPs (n=2) and spiking activity (n=13 multiunit clusters)

Earlier it was shown there is evidence for adapter induced sharpening in GP cortex as measured through EEG. Unlike in humans where this sharpening seems to be mainly induced by tone onsets, in GPs this effect was seen with both single and multiple onset adapters. With an n=2 the results are still reasonably noisy but it can be seen there is a reduction in the level of adaptation for most conditions. In the 20 cents separation condition for the multiple onset conditions it appears there is an increase in adaptation with increased adapter duration in a deviation from the EEG results. The effects of the 20 cents separation on the single onset conditions are unclear in this experiment as it was not as repeatable between subjects.

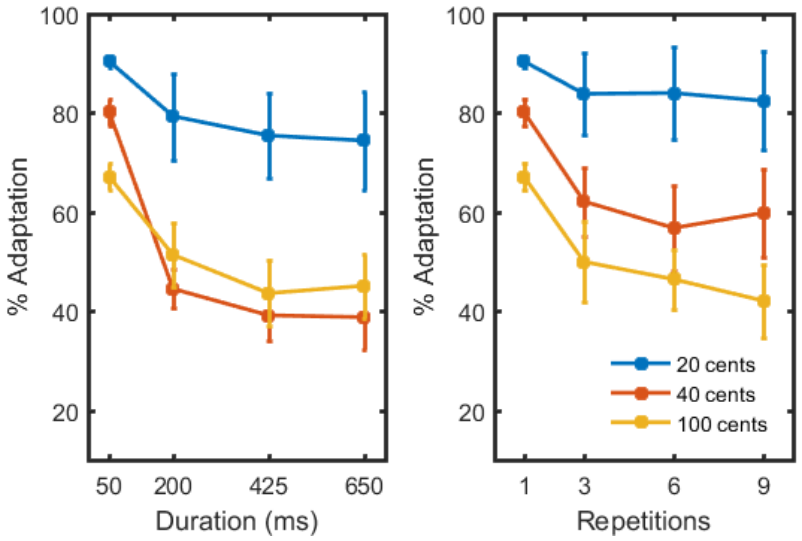

Figure 6.18: Frequency selectivity of LFP measured, pure tone adaptation measured with a 0ms adapter-probe ISI sharpens with both increased adapter duration and number of adapters (n=4)

When playing AM tones the oscillations in the auditory cortex will follow the frequency of modulation. In the FFT of the oscillations, sharp peaks can be seen both at the fundamental frequency of the modulation rate and several harmonics at multiples of the fundamental. The ASSR power decays with higher harmonics. It can also be shown that the ASSR response is highly frequency specific as 1Hz differences in modulation rate are resolvable in the FFT, as shown in figure 6.19 between 20/21Hz, and were also seen at 10/11Hz and 40/41Hz.

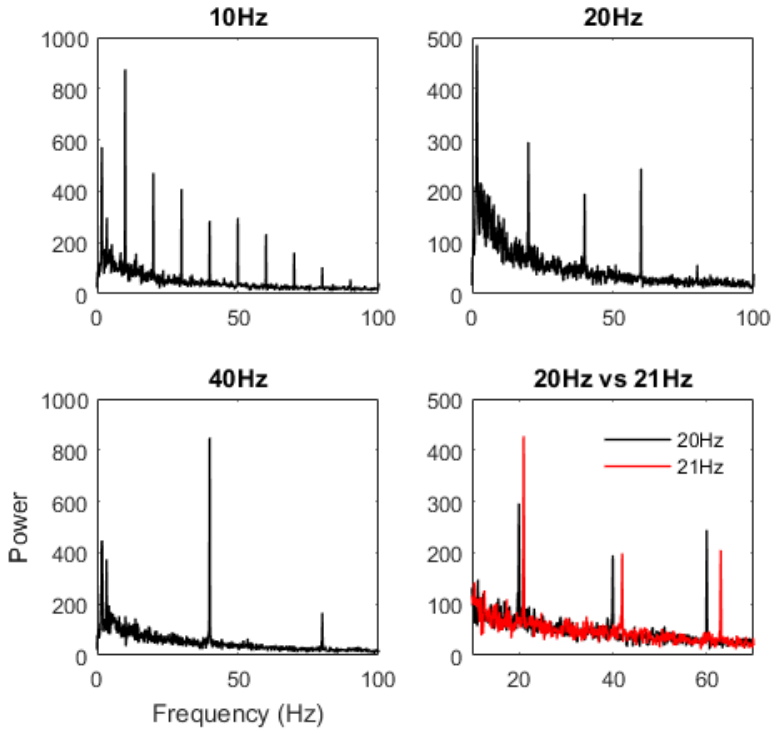

Figure 6.19: FFTs of the neural response to AM tones from one GP with different modulation rates showing the increases in power at the fundamental frequency of the modulation and several harmonics. Also shown (Bottom right) is a display of the frequency resolution of this response, easily able to distinguish a 1 Hz difference at 20/21Hz modulation rates.

The fundamental frequency (f_0) of the ASSR shows reasonably level power with modulation rates from 2.5-40Hz. This will reduce at higher frequencies as the cortex can no longer accurately follow the speed of oscillation. By a modulation rate of 320Hz the ASSR is no longer detectable above baseline activity. By contrast the first harmonic (f_1) will peak at 10Hz modulation rate, decreasing in power with increasing or decreasing modulation rate. The first harmonic will disappear earlier than the fundamental, at 160Hz, which is not unexpected as 160Hz's first harmonic is at 320Hz.

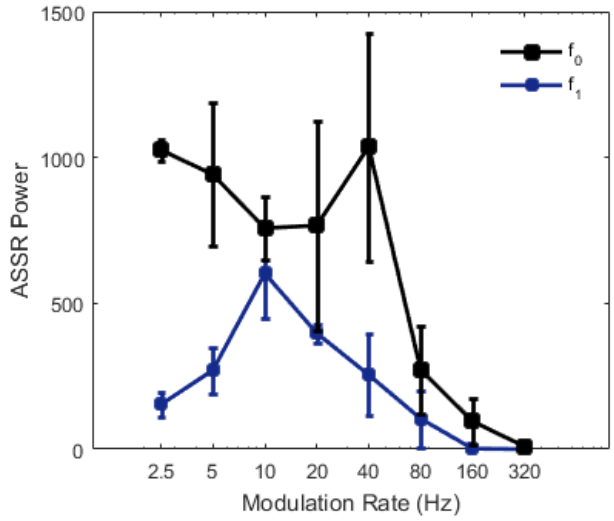

Figure 6.20: Effects of modulation rate on power of the ASSR fundamental frequency. Recorded from LFPs in GP primary auditory cortex

Further analysis has be undertaken and the underlying multiunit activity has been assessed for its ability to lock to the ASSR modulation. This phase locking behaviour can be seen in the pooled activity (Figure 6.21). The PSTHs for 10, 20 and 40Hz show distinct peaks at various points in the ASSR phase, indicative of the units being entrained to fire at the stimulus frequency. At 5Hz there is a small peak but there is a much less pronounced locking response.

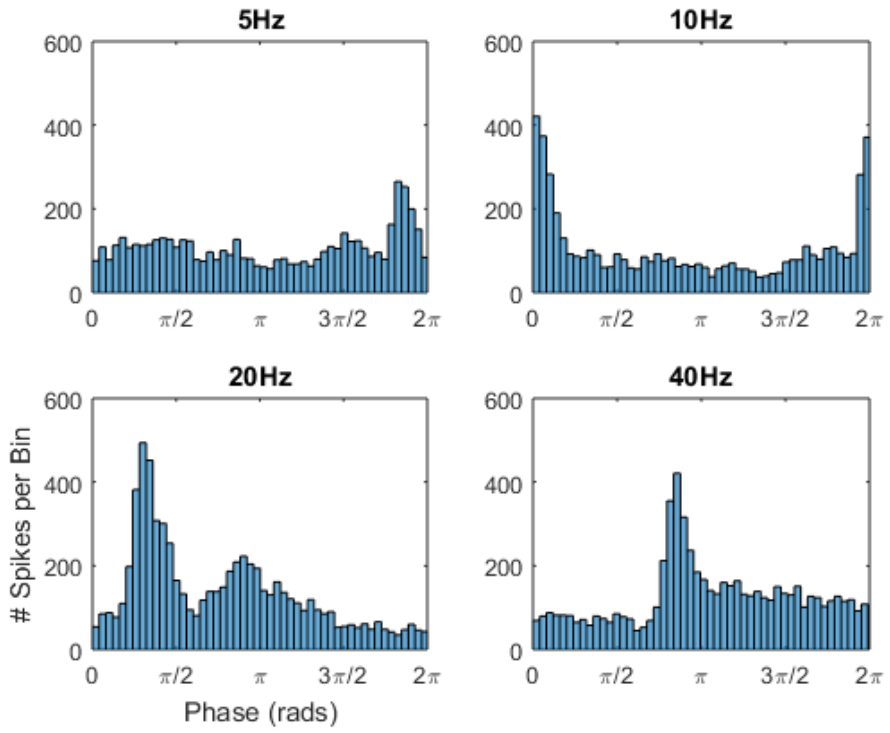

Figure 6.21: Multiunit PSTHs for multiple modulation rates, aligning responses to the phase of the modulation

To quantify the strength of these phase locking responses the vector strength of the responses was calculated using two different methods. It was unclear *a priori* whether this analysis would be more representative of the LFP activity if run on a combination of the population spiking activity of all the sites, or as a mean of the properties of each separate site so both were analysed.

When analysing the population spiking activity this produces a V-shaped curve in both analysis methods, peaking at 20Hz with the SC method and 10Hz with the FFT method. In the single site analysis however it shows a pattern more similar to the LFP. Using the SC method there is a stable vector strength from 2.5 to 40Hz before decaying away at higher frequencies. The FFT method shows something similar but with a weaker vector strength relative to the peak value at lower frequencies.

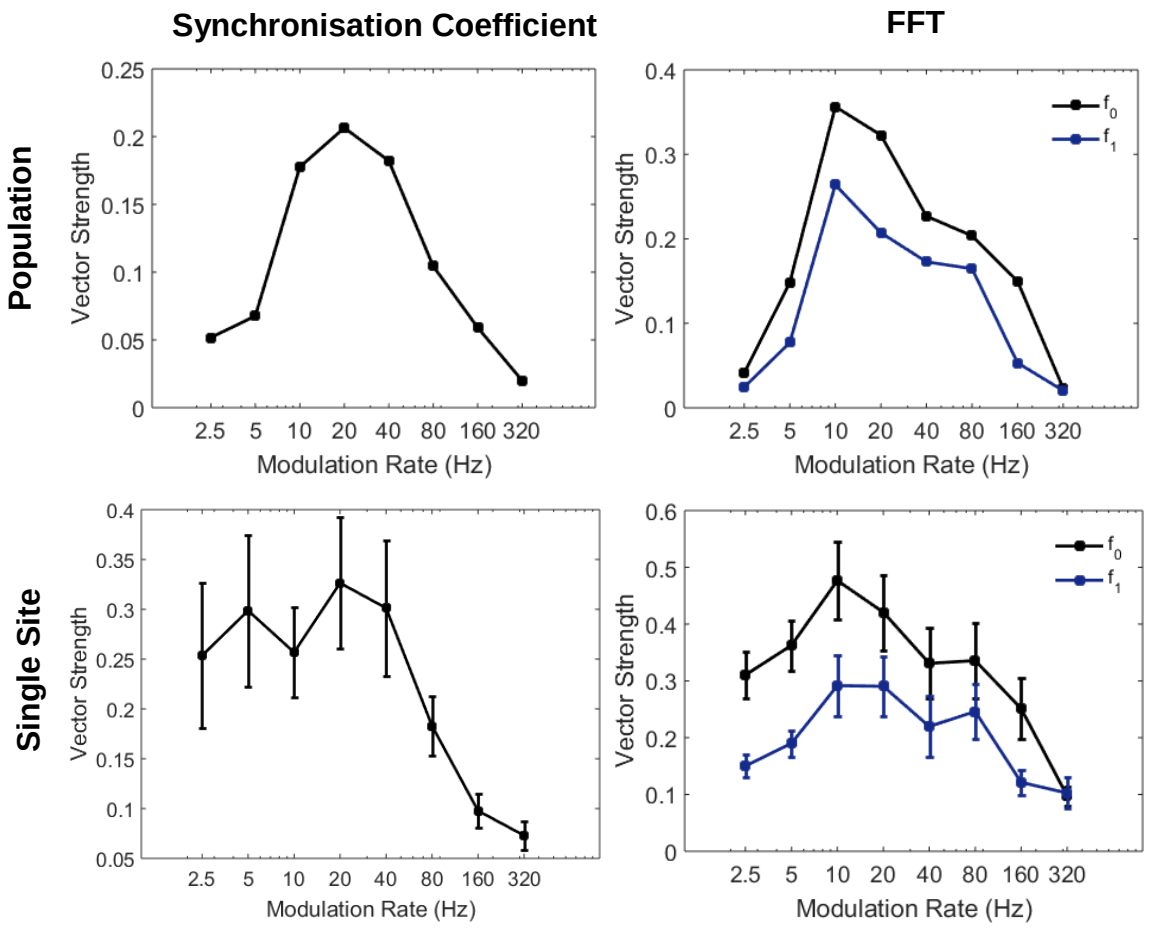

Figure 6.22: Phase-locking vector strength of the multiunit clusters measured by two different analysis methods, applied to the pooled activity over all sites (Top) and within each site (Bottom). Synchronisation coefficient (Left) and FFT method (Right) of the multiunit clusters at

6.3.3 Discussion

This section has dealt with finding intracortical and neural correlates of the far field potentials measured in the previous section, looking into the characteristics of adaptation in GPs, and built on this by investigating ASSRs in GP primary auditory cortex.

In both the studies of recovery from adaptation with separation of adapter and probe in time and frequency there is a remarkable consistency between the recording methodologies of EEG, LFPs and multiunit spiking. The time constant experiment shows, for most conditions, there is very little difference between the levels of adaptation measured by LFP and multiunits. The main exception to this is the result at 10ms ISI which shows a much lower level of

adaptation. Given the latency this is likely to be a similar effect to that seen earlier where the offset of the adapter acts as a confound to measuring the onset of the probe.

Even with the close agreement of the LFPs and multiunits there seems to be a deviation between these results and those seen in the EEG recordings. The LFP results show a much shorter time constant (τ=30ms) than the EEG results (τ=60ms). It is unclear yet if this is a genuine difference in recovery constant or as a result of the slightly noisier data or under-sampling at low ISIs but this could reflect the faster recovery of primary auditory regions relative to the surrounding belt areas. These non-primary regions could be expected to have a slower recovery due to the trends of slower adaptation recovery up the auditory pathway from the auditory nerve to the primary auditory cortex (Froemke and Schreiner, 2015) and there is some evidence from the two non-primary implanted GPs to suggest this is true.

For the frequency selectivity experiment the opposite is true, with greater levels of adaptation in the LFP recordings. In this case it could be A1's greater affinity for pure tones over other non-primary regions that led it to have a greater than average level of adaptation (Wallace et al., 2000). As non-primary regions will have a lower responsiveness to pure tones and often non-contiguous receptive fields they are unlikely to show as substantial an adaptation response to this stimuli. However the results from the multiunits may contradict this as they show a very similar level of adaptation to the EEG.

So far the results of the effects of single and multiple onset adapters on the 0ms ISI adaptation tuning of LFPs are not overly informative beyond what was seen in the EEG results. In these results it is shown again that wider frequency separations will show a sharpening effect with both increased duration and number of adapters. Unlike the EEG results these show a stable level of adaptation for narrow (20 cents) frequency separations in the multiple onset condition. With an n=2 the statistics performed on these data

were uninformative and a greater number of repeats would be needed to make any firm conclusions about these results.

Neural responses to AM tones were recorded to better characterise the temporal properties of GP auditory cortex as the temporal properties of adaptation are frequently linked to the frequency following abilities of the brain structure being investigated (Froemke and Schreiner, 2015).

The results in figure 6.20 show the power of the baselined, LFP-derived, ASSRs at different modulation rates. The ASSR at the fundamental frequency of the AM stimulus shows a consistent amplitude from 2.5-40Hz and is easily discernible from the background up to around 80Hz. These results appear to agree well with previous literature on the responses to AM tones in GP auditory cortex with a flat response at low frequencies, tapering off toward 100Hz modulation rate (Feng et al., 2009).

The first harmonic shows a more selective response, peaking at 10Hz modulation rate and decaying away at higher and lower rates. This is to be expected at the higher frequencies as this mirrors the inability of the cortex to follow the higher rates but the disappearance of the harmonics at low frequencies is unexpected, especially as humans will retain their ASSR fundamental and harmonics down to rates as low as 1.25Hz (Tlumak et al., 2011).

In the multiunit responses the data were analysed by two different methods and for both a combined population response summing all the units within one GP or analysed at each site independently. The population responses in both analysis methods show a V-shaped profile, peaking at 20Hz in the SC method and 10Hz in the FFT method for both the fundamental frequency and first harmonic. Both methods show comparable patterns of vector strength as a function of modulation rate. The single site results also seem to show the same trends overall but maintain their vector strength better at lower modulation rates than the population response.

The drop in vector strength at low modulation rates in the population level analysis compared to the individual site analysis could represent a loss of firing synchrony between sites at the lower rates. When combining across sites for the population PSTH this loss of synchrony would flatten the PSTH and thereby make it appear the population doesn't follow the frequency although the individual multiunits do.

These results contrast with the findings from human EEG recordings of ASSRs which display a preference for 40Hz AM tones (Galambos et al., 1981; Plourde and Victoria, 1996; Plourde et al., 1997; Ross et al., 2003), compared to the 10-20Hz preference seen in the GP LFP and MU responses. This preference can also be contrasted with comparable experiments earlier in the auditory pathway, looking at the phase locking ability of units in GP IC, which showed a preferred frequency of 71Hz and the ability to lock at and above 400Hz (Shackleton et al., 2009).

Overall there is generally good agreement between the patterns of adaptation seen in the EEG, LFPs and MUs when separating the adapter and probe in time or frequency. Any differences can potentially be explained by different behaviours of surrounding brain regions. In addition it's been shown ASSRs can reliably be evoked in GP cortex and can be recorded and analysed from LFP and MU activity.

Chapter 7

Effects of Anaesthesia on Electrophysiological Recordings

7.1 Anaesthesia Effects on GP EEG

7.1.1 Introduction

Anaesthesia is widely used in *in vivo* studies of sensory neural processing. Previous studies of the effects of systemic general anaesthesia on neurons in the auditory cortex have shown significant changes to frequency tuning of individual neurons (Gaese et al., 2001) and responses to basic features within the stimulus such as onsets and offsets (Zurita et al., 1994). Studies of this nature have typically used a single anaesthetic agent, comparing a wake and anaesthetised states. The majority of studies when two or more anaesthetics are compared have no baseline or control conditions. It remains unclear to what extent the choice of anaesthetic agent will affect basic response properties of neurons to sensory stimulation.

The main current theory on the mechanism by which the majority of anaesthetics cause a loss of consciousness is their modulation of ligand-gated ion channels. This can be through various pathways, for example ketamine is an NMDA antagonist which noncompetitively binds to NMDA receptors decreasing the activity of the excitatory neurotransmitter glutamate. This is in contrast to diazepam, a benzodiazepine, which potentiates $GABA_A$ activity by increasing the total conduction of chloride ions across the $GABA_A$ receptor, thereby increasing the power of inhibitory GABAergic neurons. Urethane is a long-acting injectable anaesthetic but does not show as strong affinity for any single ion channel as many other anaesthetics but instead shows a distributive effect, potentiating GABA and antagonising NMDA channels to a much smaller

degree than other anaesthetics with specific target channels. Opioid derivatives, such as fentanyl, target opioid receptors. Fentanyl preferentially binds with the μ-opioid receptor which will in turn cause a reduction in intracellular calcium currents, inhibiting the ability of neurons to release neurotransmitter vesicles.

Most experiments into the effects of anaesthesia on humans are done using participants who are undergoing surgery so the choice of anaesthetic agent is determined by medical rather than experimental need which results in the majority of literature in humans being conducted under sevoflurane and/or propofol which are both GABA potentiators. Under these anaesthetics it has been shown there are increases in power in low frequency oscillations and a decrease in high frequency power. Additionally it has been shown these effects will have a rapid onset at loss of consciousness. It has also been observed that AEPs recorded under propofol anaesthesia will reduce in amplitude compared to when awake (Simpson et al., 2002). This relationship has been investigated as a potential metric for assessing depth of anaesthesia during surgery (Horn et al., 2009).

Another neural metric that has been proposed as a measure of depth of anaesthesia is criticality. There is a growing body of evidence that suggests that the cortex operates near criticality (Solovey et al., 2012; Shew and Plenz, 2013; Arviv et al., 2015). A critical system is defined as operating at a phase transition, in the case of the cortex this transition will be between damped and undamped propagation of neural activity (Figure 7.1). Criticality has been shown to have functional benefits to sensory neural coding by increasing dynamic range, information transmission and information capacity of neural networks (Shew and Plenz, 2013; Gautam et al., 2015) and therefore modulation of this network property will have implications for sensory processing. Previously published work has suggested that anaesthesia will tend to move the cortex into a subcritical state representing a stabilization of activity (Solovey et al., 2015).

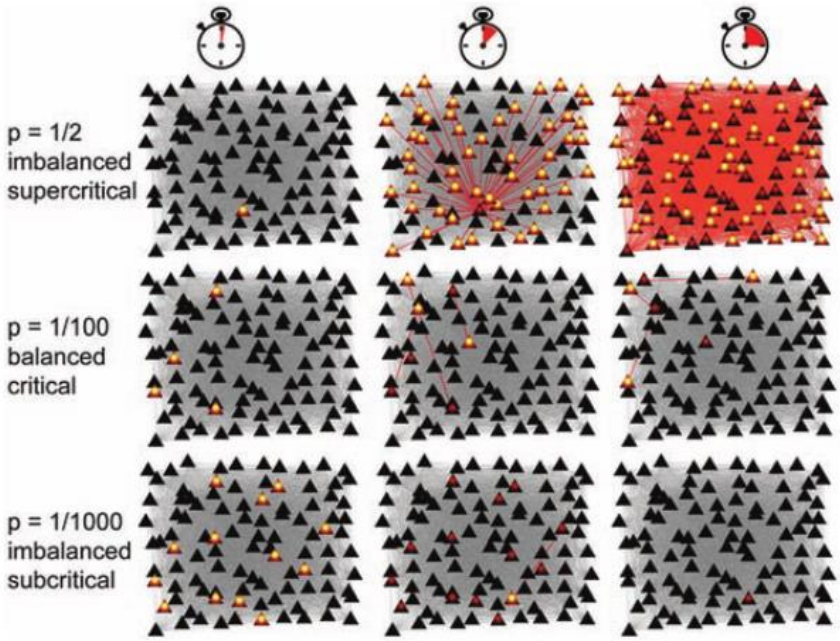

Figure 7.1: Criticality demonstrated in a representative population of 100 fully interconnected model neurons with a value p that represents the probability of a neuron firing given a connected neuron fires. If p=1/2 this will lead to a supercritical state of explosive growth reaching steady state with all neurons firing. With p=1/1000 the system will be subcritical and the activity will die down and stop firing whereas for p=1/100 the neurons will be in a critical state and maintain a stable level of activity (Shew and Plenz, 2013)

As mentioned previously our adaptation experiments in guinea pig cortex showed significant differences compared to those made in humans and it is unclear the relative contributions of anaesthesia and inter-species differences. Recordings made in awake guinea pigs have allowed us to compare the inter-species effect (Chapter 6) but it is also unknown to what degree anaesthesia will affect the recordings.

These experiments will attempt to assess the different effects of multiple anaesthetic regimes on spontaneous, sensory and cross-modal evoked activity recorded from guinea pig cortex.

7.1.2 Method

Animal Preparation: (See Section 6.2)

Awake Recordings: Recordings were made inside a dark, sound-attenuating, electrically shielded booth. GPs were allowed to freely move around a custom made cage, surrounded by sound attenuating foam, to minimise sound reverberation. GPs were tethered to a cable, connected to their implant to allow data recording. Sounds were produced from a tweeter mounted directly above the cage. Visual stimulation was from an array of white LEDs mounted directly above the cage.

Anaesthetic Recordings: Anaesthesia was induced intraperitoneally with medetomidine (0.2 mg kg^{-1}) combined with either ketamine (60 mg kg^{-1}/20 mg), diazepam (3 mg kg^{-1}/ 1 mg), fentanyl (0.35 mg kg^{-1}) or urethane (4.5 ml kg^{-1} in 20% solution) (induction/maintenance). A maintenance dose was administered intramuscularly if a pedal withdrawal reflex could be elicited. After loss of consciousness the GPs were transferred onto a heating blanket to help maintain their core body temperature. After recordings were complete then the medetomidine reversal agent atipamozole (0.25 mg kg^{-1}) was administered intramuscularly. A washout period of at least 72 hours between anaesthetic administrations to baseline recordings was maintained and there was at least a week between each anaesthetic administration. Order of anaesthetics was varied between animals, except for urethane which can only be used for non-recovery procedures so was used last. Time from implantation to final anaesthetic was ~30 days.

Recording and Data Processing: Oscillatory activity was filtered online between 0.1-300Hz. Evoked activity was filtered online between 10-300Hz. Recordings were made at 12.212kHz sampling rate and were down sampled to 2kHz for analysis. Where multiple sessions of activity were recorded over time within one animal, the waveforms were averaged over the multiple sessions within subject. To estimate signal power spectra the signal was separated into windows of length 0.5s comprising 1000 data points. The multi-taper method was used as it has previously been shown to work well on neural data (Magri et al., 2012) with a good trade-off between bias and variance. A time-

bandwidth parameter of NW=2 was used. It was chosen over traditional Fourier analysis as it has been shown to be more stable at analysing non-stationary signals and shows a better time-frequency resolution (Vugt et al., 2007).

To determine which frequency bands showed a significant effect a non-parametric, cluster based test was used (Maris and Oostenveld, 2007). In short, the individual trials of each animal were randomly assigned to either the control or anaesthetic condition before being averaged within animal. Paired sample t-tests were then used at each frequency band. Clusters were defined as contiguous regions with $t>3.356$. Each cluster was integrated and the largest positive and negative clusters were recorded. This was repeated 10,000 times to create a two-tailed, non-parametric distribution to test the experimental clusters against. Clusters were accepted at significance of $P<0.01$.

Autoregressive stability analysis was used on the oscillatory data. Trials were split into 0.5s epochs and were fit by a multivariate autoregressive model (Neumaier and Schneider, 2001) and the coefficients produced underwent eigendecomposition. The stability indices, λ, are the absolute values of the eigenvalues where a value of $0<\lambda<1$ represents a stable oscillatory mode and $\lambda>1$ will be an unstable one.

Stimuli: All stimuli were generated by an array processor (TDT RX8, Alachua, FL, USA) and output at a sample rate of 100 kHz. Stimulus control was from a PC using Brainware (developed by J. Schnupp, University of Oxford). Recordings were either made in silence, in response to 60-110dB, 20ms, broadband auditory clicks, 80dB, 100ms, 6 kHz pure tones or 20ms, 300 lux, wide-field light flashes.

7.1.3 Results

7.1.3.1 Oscillatory Activity

Oscillations were recorded in silence while awake and under each anaesthesia and the power spectra of the signals calculated.

For all anaesthetics tested, low frequency power (<10Hz) shows an increase and power at 20-40Hz shows a slight decrease. Low frequency activity under ketamine, fentanyl and urethane all show practically identical power spectra in the <40Hz region whereas diazepam shows a smaller increase on average.

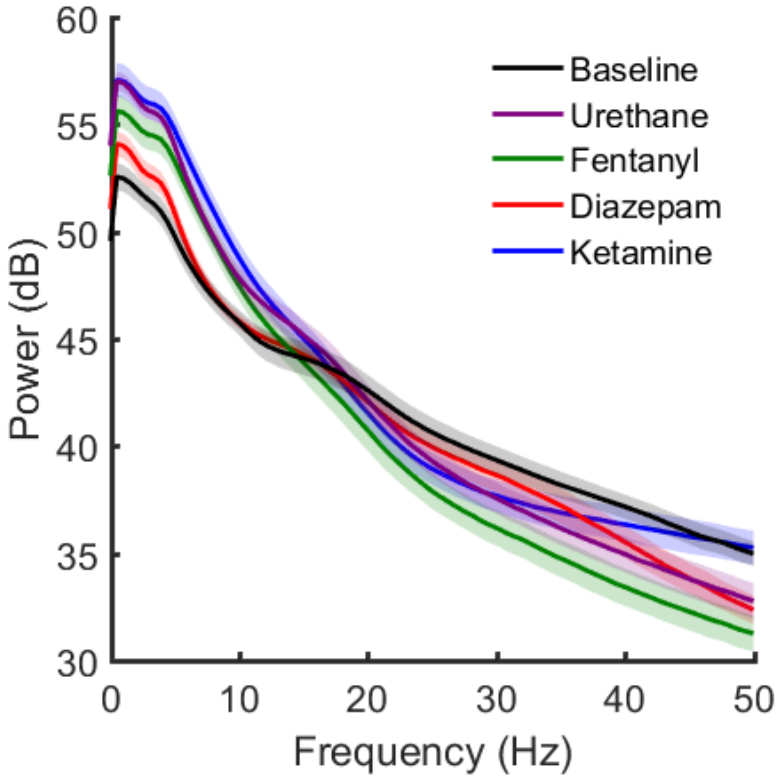

Figure 7.2: Power spectral density of spontaneous oscillations recorded in silence, averaged over all electrodes. Results under each anaesthetic are shown ± standard error.

Each anaesthetic was tested for regions of significant change in frequency using a method which has no preconceptions about neural frequency bands (alpha, gamma, etc.) (Figure 7.3). With the changes seen in previous chapters between human and GP neural processing it was decided to take an agnostic approach to regions of frequency change. All anaesthetics tested except diazepam showed a significant increase in low frequency (~15Hz) power, peaking at a 5-7dB increase. Diazepam, fentanyl and urethane all show significant reductions in power of high frequency (>30Hz) oscillations whereas ketamine displays an enhancement of high frequency activity (50-120Hz).

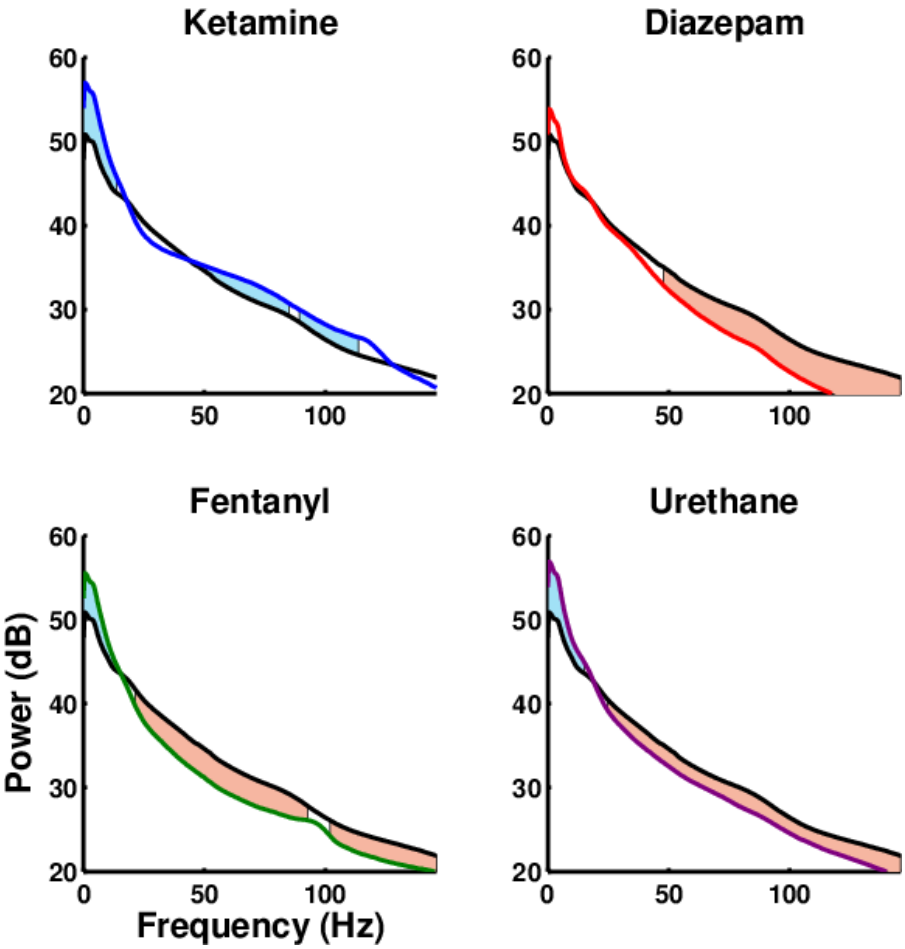

Figure 7.3: Power of spontaneous oscillations under each anaesthetic compared to awake recordings (black) showing regions of significant increase (blue) and decrease (red) in power

Recordings of spontaneous activity were made, following injection of anaesthetic agents, during loss of consciousness (LOC) to investigate the transition in brain states. The results were analysed with a temporal resolution of 1s allowing the change of frequency components over time to be assessed. These results showed a large, rapid increase in low frequency (<8Hz) power occurring in <1s (Figure 7.4). This can also be seen visually in the raw electrode traces where stable, high frequency oscillations are disrupted by large baseline shifts at LOC.

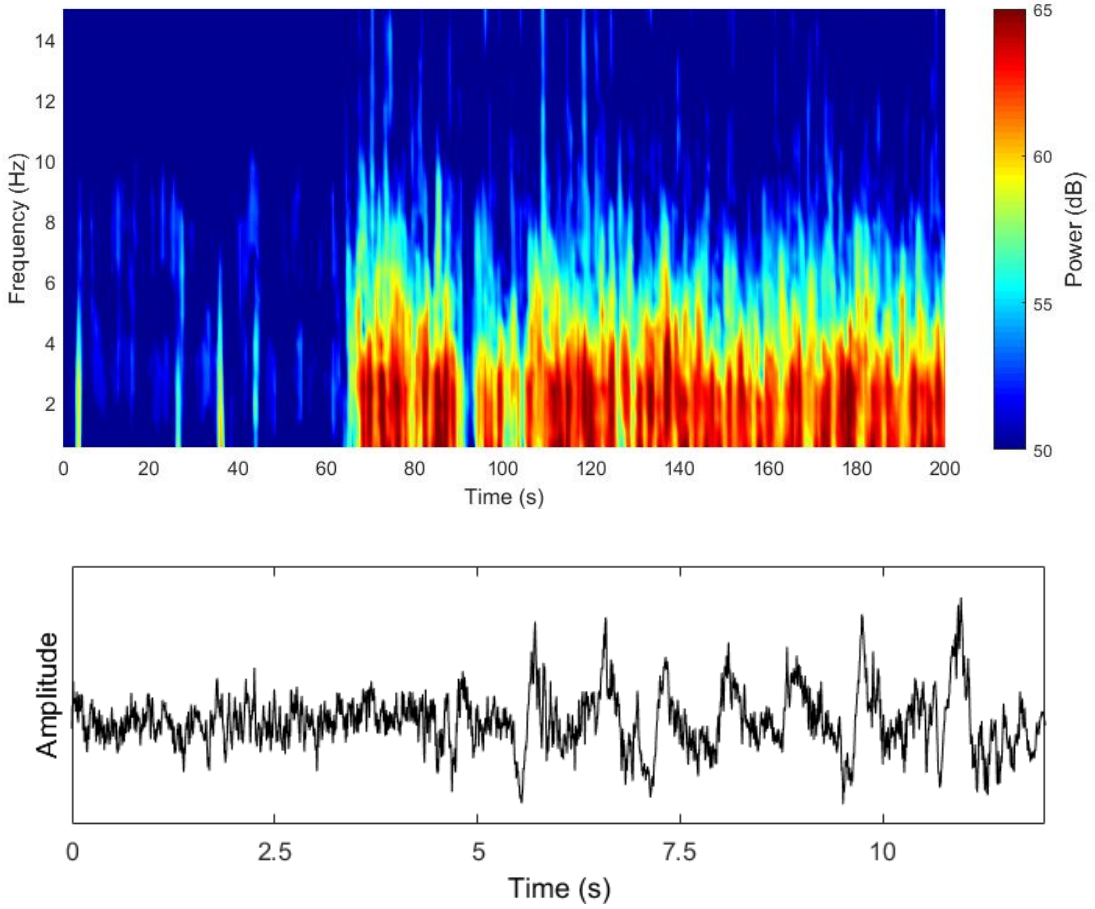

Figure 7.4: Top: Power spectral density over time of spontaneous oscillations in visual cortex following injection of urethane/medetomidine. t=0 represents start of recording, not time of injection. Bottom: Raw trace from a visual cortex electrode, following injection of ketamine/medetomidine, demonstrating the sudden onset of low frequency oscillations at ~5s. Each recording from one session, representative of all anaesthetics tested.

Autoregressive stability analysis, a method of measuring criticality in large scale neural recordings, was used on the spontaneously recorded activity. The distribution of autoregression eigenmodes shows a shift toward criticality under all anaesthetic conditions, all showing a very similar distribution. This shift is accompanied with an increase in the proportion of eigenmodes deemed unstable ($\lambda>1$) which is highly significant in all conditions with a shift from ~0.25% to around 2%.

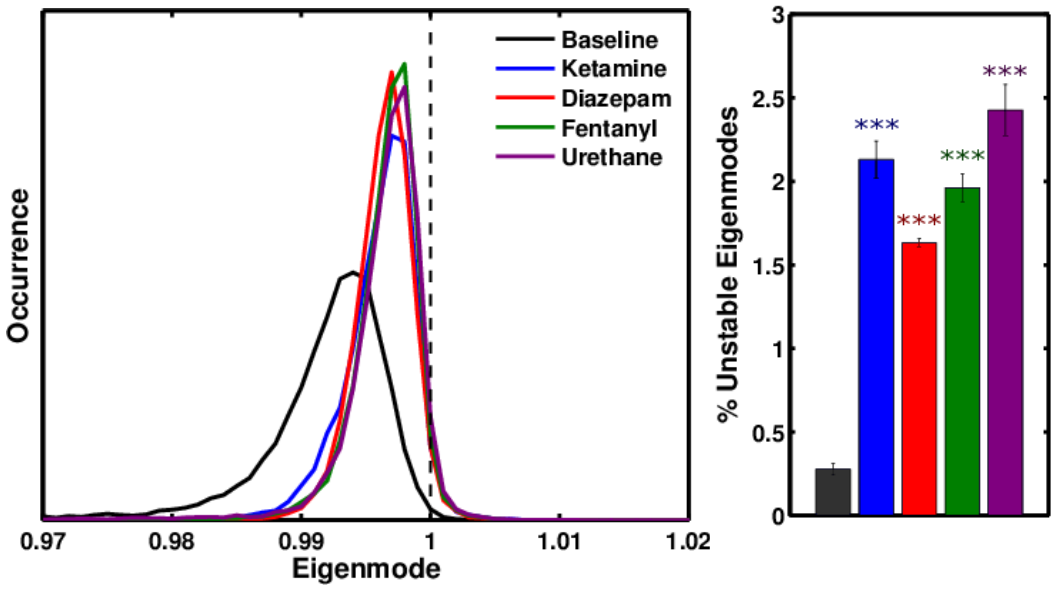

Figure 7.5: Dynamic stability profile of spontaneous oscillations showing the probability distribution of eigenmodes (left). The rightward shift in the eigenmode distribution shifts a greater number of modes into the unstable region (eigenmode >1, right).

7.1.3.2 Evoked Activity

The response to 100dB clicks produced large AEPs in both auditory and visual cortex. Unlike AEPs from human auditory cortex which show a single prominent negative voltage deflection, the GPs show two deflections in auditory cortex, an early component (~25ms latency) and a late component (~50ms latency). In awake GPs, a cross-modal response is also seen in visual cortex in response to auditory stimulation (Figure 7.6). In auditory cortex the overall waveform morphology is maintained under all anaesthetics but with shifts in some of the peak latencies. By contrast, the morphology of the cross-modal response in the visual cortex is completely removed.

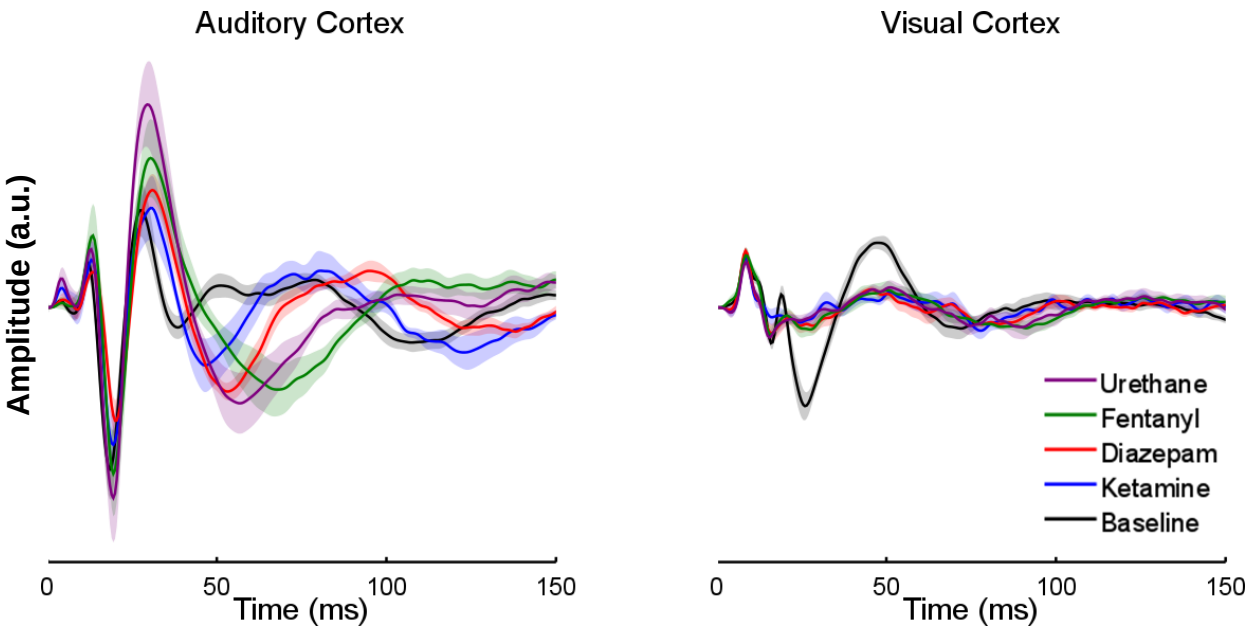

Figure 7.6: Auditory evoked potentials in response to 100dB broadband clicks, recorded from both auditory and visual cortex under multiple anaesthetics. Response amplitudes in auditory and visual cortex shown on the same scale.

In auditory cortex both ketamine and diazepam show little effect on the amplitude of the early peak of the AEP whereas fentanyl and urethane increase this component. The late component is suppressed by ketamine but enhanced by the other three anaesthetics. This component also seems to have had its latency shifted by all of the anaesthetics, most substantially by fentanyl which represents a >20ms delay. By comparison the main response from visual cortex is substantially supressed under all anaesthetics tested. A very early response (<10ms) in the visual cortex electrodes does not seem to be affected but given the latency this is likely to be the electrode picking up responses from a nearby sub-cortical auditory structure such as the auditory brainstem.

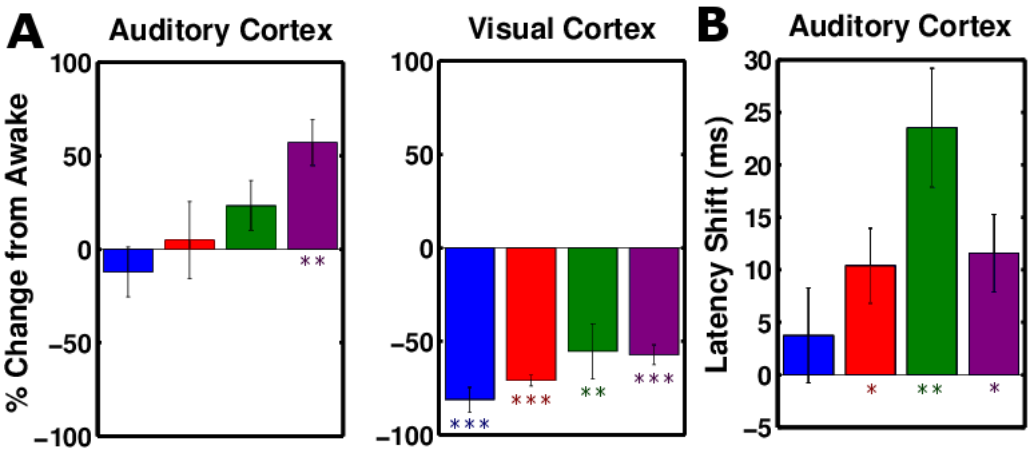

Figure 7.7: (A) Percentage change in peak-to-peak amplitude of the early potential and visual response relative to the awake condition. (B) Latency shift of the late potential's negative peak relative to awake

In response to a flash of light there was a visually evoked potential in the visual cortex, characterised by a negative deflection at ~40ms (Figure 7.8). There was not a large enough cross-modal response from the auditory cortex electrodes to reliably characterise the response. Under every anaesthetic tested this negative deflection was entirely abolished and instead replaced by a positive deflection at ~60ms and a slow negative deflection with a trough at ~90ms. The responses under each anaesthetic are very different from the awake condition but are all very similar to each other, suggesting an effect of unconsciousness rather than a direct effect on any individual neurotransmitter.

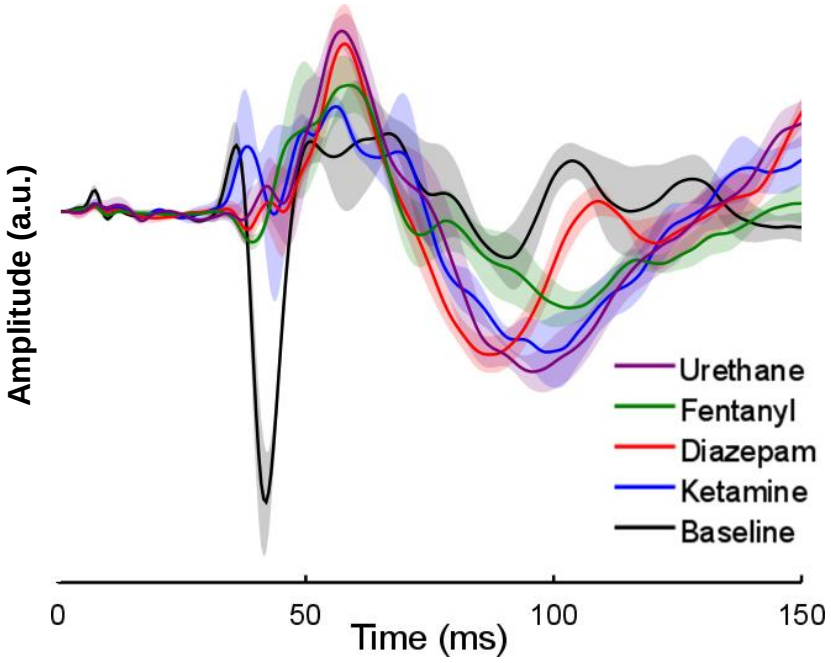

Figure 7.8: Flash evoked potentials in response to 20ms, 300 lux light flashes, recorded from over visual cortex under multiple anaesthetics.

Pure tone responses do not show as prominent late potentials but will demonstrate offset responses for tones longer than 30ms. Similar to the click evoked responses, urethane shows a significant increase in response size of ~100%, comparable to that shown under fentanyl. Ketamine and diazepam however do not show a significant change. The only anaesthetic agent to show significant changes to the offset response is fentanyl which shows a six-fold increase of response size compared to the awake condition.

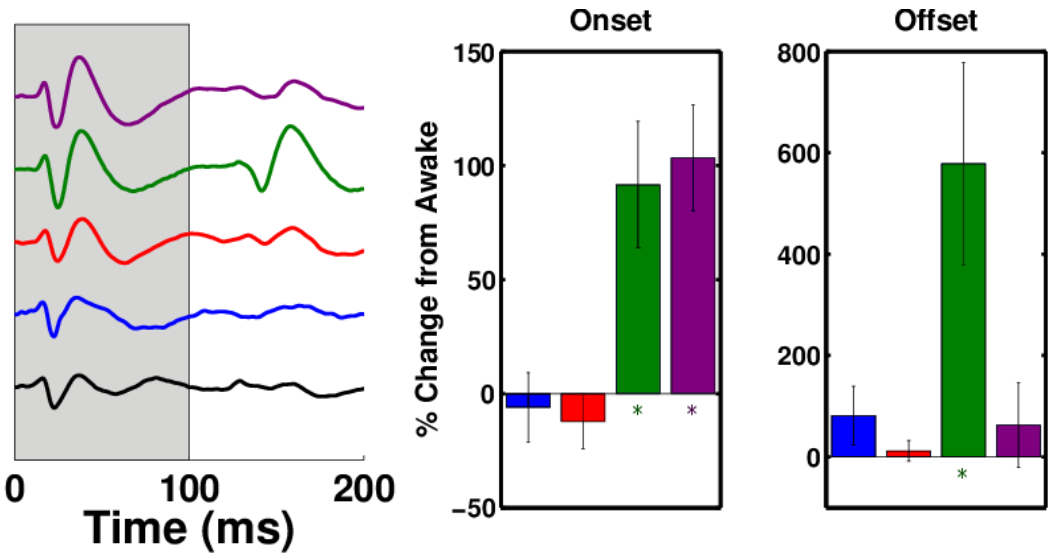

Figure 7.9: All-subject average waveform for the 100ms tone duration condition for each anaesthetic and the awake condition (left). The effects of each anaesthetic on the amplitude of the early potential and offset response have been calculated (right)

When looking at the fentanyl on variable duration tones the increase in offset response amplitude can be seen clearly at all durations from 20-100ms (Figure 7.10). For all of these responses as well as enhancing the response the latency is also shifted quite considerably. It is also seen at all the tested durations that fentanyl will enhance the response size. For durations 20-90ms however there only appears to be an increase in the P1 and P2 amplitude, with only the 100ms condition showing an increased N1 response.

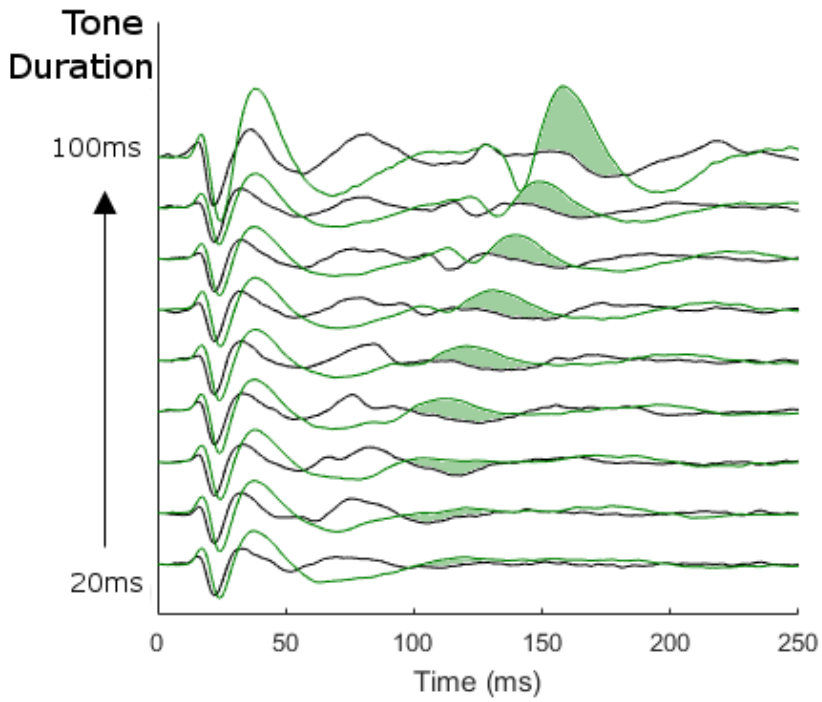

Figure 7.10: Effects of fentanyl (green) on the neural response to increasing duration tones compared to awake (black), averaged over all GPs. Bottom waveform is the response to a 20ms, 6 kHz tone. Duration increases by 10ms up to 100ms for the top waveform. Enhancement of the P2 response and a latency shift are seen in short duration tones with longer tones showing greater enhancement to the N1 and the offset response amplitude. Regions of offset P2 enhancement highlighted in light green.

7.1.3.3 Adaptation

GPs were played pairs of broadband noise tokens with variable ISIs. To determine a recovery time constant for adaptation an exponential function was fit to the derived adaptation data. From our data the recovery time constant while awake (τ=60ms) is substantially slowed by diazepam (τ=250ms) and sped up by ketamine (τ=40ms). Fentanyl and urethane show smaller increases in recovery time than diazepam, at τ=180ms and τ=150ms respectively.

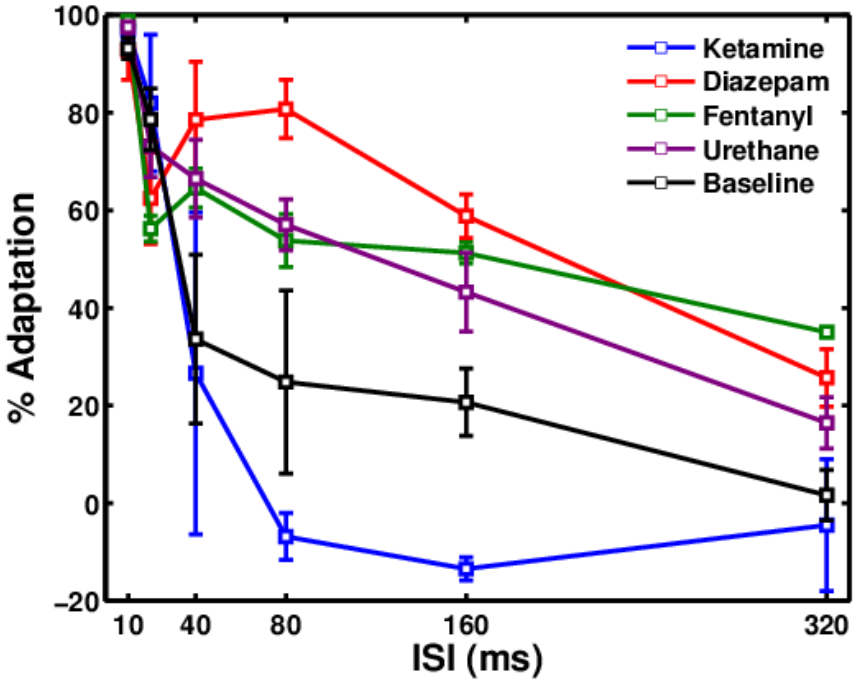

Figure 7.12: Adaptation percentage derived from the amplitude of a broadband probe stimulus preceded by a broadband adapter with a variable ISI. Anaesthesia has a strong modulatory effect on the recovery time following an adapter

7.1.4 Discussion

The results of these experiments demonstrate that the choice of anaesthetic agent for studies of auditory evoked activity in cortex will have a significant and substantial effect on the recorded population activity.

The recordings of spontaneous activity appear to replicate the results found in humans with increases in low frequency power with a rapid onset. This effect seems to be mostly independent of the anaesthetic used. Diazepam potentially shows a smaller increase in oscillatory power as at the dose used it will only reach a plane of deep sedation while the other anaesthetic agents will be able to achieve a full surgical plane of anaesthesia.

The increase in high frequency oscillations under ketamine is not a novel effect and has been reported before in the literature and is one of the reasons ketamine is used as an analogue of schizophrenia. This response is most commonly attributed to cortical disinhibition, a phenomenon caused by

ketamine's apparent targeting of excitatory connections innervating inhibitory cells causing a net reduction in inhibitory activity (Miller et al., 2016).

The loss of consciousness recordings show similar results to those shown in humans, with a rapid onset of low frequency oscillations, the onset of which happens in under 1s. Along with the other oscillatory activity recorded this appears to be independent of the anaesthetic agent used. This supports and builds on previous studies in humans studying LOC under propofol (Lewis et al., 2012; Mukamel et al., 2014).

The main finding of this experiment is the degree of variability between different anaesthetic agents in the processing of auditory stimuli. Especially with the identical effects on spontaneous activity between the different agents it is surprising that they would have such varied effects on AEP morphology. It is unclear, as it is generally assumed that in a state of anaesthesia the brain will be less active, why some of the anaesthetics would increase the magnitude of the evoked response. These effects are however robust and the places where there is overlap with published literature appear to replicate the effects found such as the increase in AEP amplitudes under fentanyl (Antunes et al., 2003). More experimentation would be needed, recording single unit responses to determine whether this was caused by an increase in neural firing rate or an increase in firing synchrony.

Combined with this result is the finding that all anaesthetics will attenuate AEPs generated in visual cortex. This disconnect between the effects on auditory and visual cortex suggests that visual areas may not be receiving their cross-modal input from sub-cortical structures and instead are receiving them from cortico-cortical connections which will be more strongly influenced by anaesthesia. This finding is not necessarily surprising as some literature suggests that anaesthesia will knock out long range connections between disparate brain regions, resulting in functional systems having to work as isolated networks without reliable input from other areas (Lewis et al., 2012). However with the reduction of responsiveness of visual cortex to visual

stimulation it may just be that the visual cortex is more susceptible to anaesthesia than auditory cortex.

When looking at the effects of anaesthesia on adaptation it is shown there is a big divide between the three anaesthetics that will have direct effects on GABA signalling, diazepam, fentanyl and urethane, and the one that doesn't, ketamine. The three GABA modulators all show a slowing of recovery from adaptation whereas the NMDA blocker does not and instead appears to show a faster recovery. These effects on adaptation would appear to support the findings of other groups looking into the effects of GABA on SSA (Pérez-González et al., 2012; Duque et al., 2014). These studies in IC and MGB found that by introducing GABA there would be a stronger adaptation of their Oddball stimuli. As the mechanisms of adaptation are still not that well defined in terms of neurotransmitters then a direct causal link is not possible but it appears it is possible to modulate its time course with GABA and potentially NMDA.

The only main section of this chapter to contradict any published literature is the effects of anaesthesia on criticality. In the study by Solovey *et al.* (2015) they found that at loss of consciousness that criticality would reduce, representing a stabilisation of neural activity. In our data however it appears the opposite happens and the instability increases. The analysis of these data differ in that here we have compared steady state activity whereas Solovey focussed around LOC. By analysing the figures from their paper it can be seen there is indeed a stabilisation of activity around the time of LOC, however looking at further ahead in the recordings during steady unconsciousness the proportion of unstable eigenmodes appears to be higher than baseline (Figure 7.13). If this is accurate this would indeed agree with our data. This can be backed up with single unit recordings as the population recordings used for this are just an indirect method of measuring criticality and by measuring firing characteristics a more direct measure can be taken.

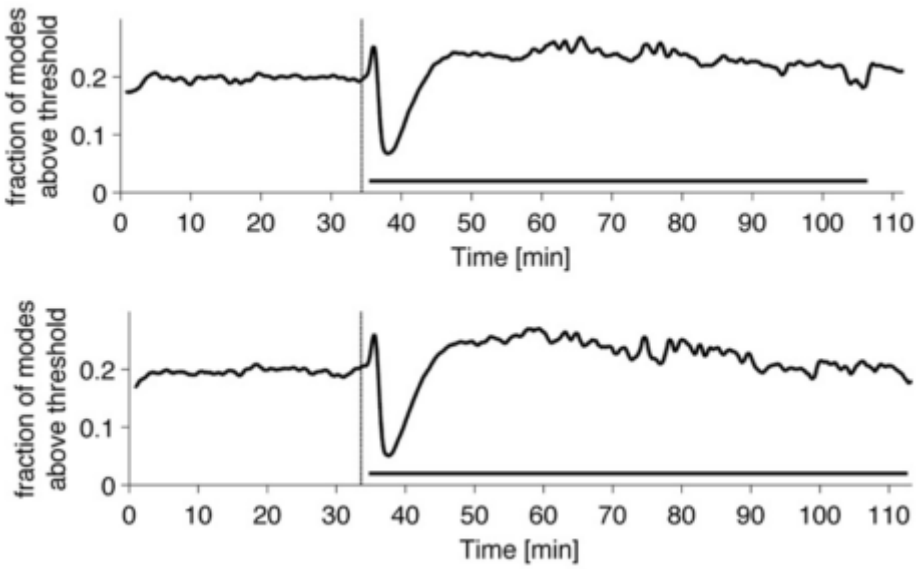

Figure 7.13: Cortical activity appears to stabilise around loss of consciousness but within ~10 minutes appear to increase above baseline. Plots show the proportion of unstable eigenmodes in ECoG recordings from macaques. Vertical line shows point of drug injection and horizontal bar shows period of unconsciousness (Solovey et al., 2015)

These results together show that anaesthesia has significant effects on systems level sensory processing and that the choice of anaesthetic used for recording can have grossly different effects on the response to even simple sensory stimuli. Both clicks and tones will have their amplitudes and waveform morphologies modified and adaptation time constants will be altered. The effects being repeatable between animals and easily determinable for each anaesthetic means for simple experiments it should be possible to account for these changes and interpret the results with the anaesthesia caveat. However combining these effects together will compound problems if investigating complex auditory stimuli and the responses in the anaesthetised brain may not be so easily relatable to awake animals. This is further compounded if investigating multisensory phenomena, given the degree of modulation of both visual processing and cross-modal signalling.

7.2 Effects of Anaesthesia on LFPs and Single Units

7.2.1 Introduction

In the previous section we investigated the effects of anaesthesia on sensory processing in GP cortex. In the EEG results this showed substantial changes compared to the awake baseline conditions. This included shifts in oscillatory power, changes in response size to auditory stimulation and modulation of adaptation recovery time constants. These experiments have shown the extent of the changes in population response to auditory stimulation under anaesthesia but as this was from a gross recording it is unclear if these changes are representative of primary auditory cortex and if they can be directly related to the underlying neural activity. Here we have investigated the main effects seen previously to attempt to find their neural correlates.

7.2.1 Methods

The majority of the methods in this section are identical to those used in the previous section and Section 6.2.2. The recordings were performed in the same testing booth and in most cases identical stimuli were used and data analysis performed. The anaesthetic regimes were identical to those used in previous animals.

7.2.2 Results

As with the iEEG GPs, oscillations were recorded in silence while awake and under each anaesthesia and the power spectra of the signals calculated. For all anaesthetics tested, the changes in oscillatory power are comparable to those seen in the previous results. For diazepam, fentanyl and urethane this results in an increase in low frequency power (<20Hz) and suppression of high frequency power (>40Hz). This effect is smaller for diazepam than the other anaesthetics. Ketamine is again shown to increase power in both low and high frequency oscillations. These results were tested by the same non-parametric cluster analysis method as the EEG results but due to the low power (n=2) no regions of significance were detected.

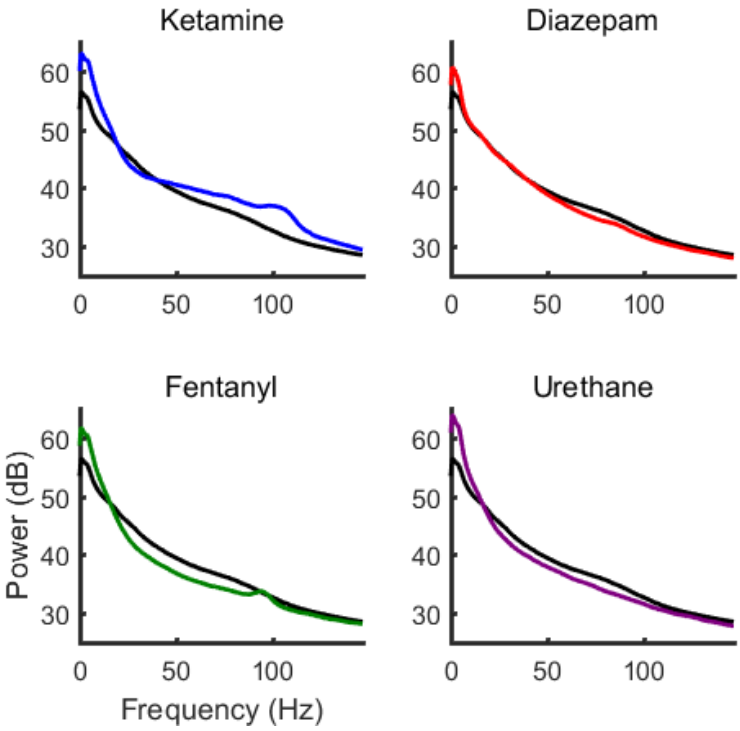

Figure 7.14: Power of spontaneous oscillations under each anaesthetic compared to awake recordings (black)

The responses to broadband clicks were also recorded. Unlike the results in the previous chapter it appears there is a universal suppression of responses in the primary auditory cortex under all of the tested anaesthetics. Ketamine, diazepam and urethane all show ~40% suppression of AEP amplitude and fentanyl shows a less reliable ~20% decrease in peak to peak amplitude. The shifts of both diazepam and urethane are significant even with an n=2. In all of these waveforms there is a suppression of both the N1 and P2 amplitude, with all but diazepam demonstrating a total removal of the P2 response and any longer latency responses.

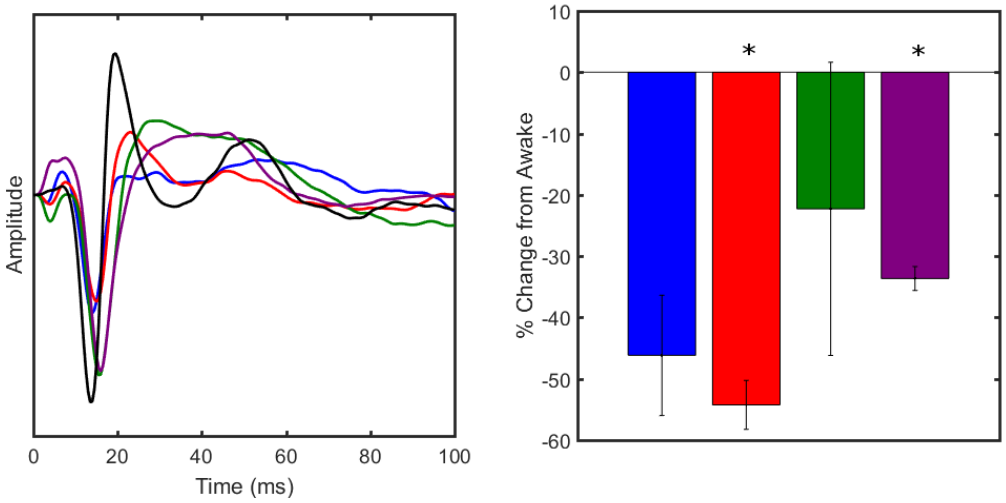

Figure 7.15: Auditory evoked potentials in response to 100dB broadband clicks, recorded from auditory cortex under multiple anaesthetics (Left). Percentage change in peak-to-peak amplitude of the response relative to the awake condition (Right)

Pure tone responses were also tested for variable duration, 6 kHz pure tones. Unlike the clicks there appears to be an overall agreement between the results seen in the iEEG and LFP results. From the waveforms in response to a 100ms tone it can easily be seen that under both fentanyl and urethane there is an increase in onset response size. Ketamine appears to show a delayed P2 response in the onset and diazepam does not appear to show any substantial changes. In the offset responses both ketamine and diazepam show little change however both urethane and fentanyl will enhance offset responses.

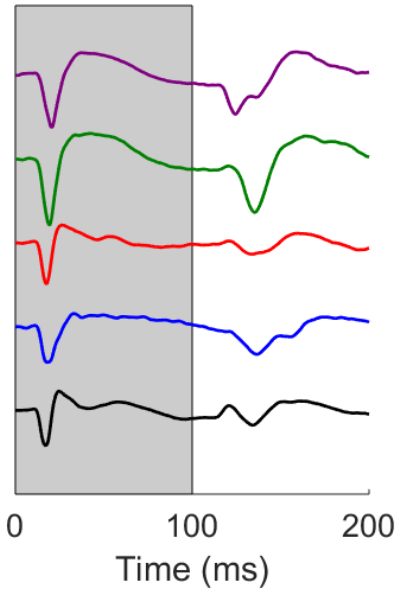

Figure 7.16: All-subject (n=2) average waveform in response to a 6 kHz, 100ms tone for each anaesthetic and the awake condition

When looking at the peak to peak measures these visual trends are confirmed. The onset responses for the fentanyl and urethane show average increases but with a high standard error. The offset responses however show roughly 200% increases in offset responses amplitude for both fentanyl and urethane. These results also show a latency shift in the N1 response of the onset response for all of the anaesthetics with all but diazepam showing a reliable 1.5-2ms shift. This shift can also be seen in all but urethane in the offset response, most prominently and reliably under ketamine with a ~5ms increase.

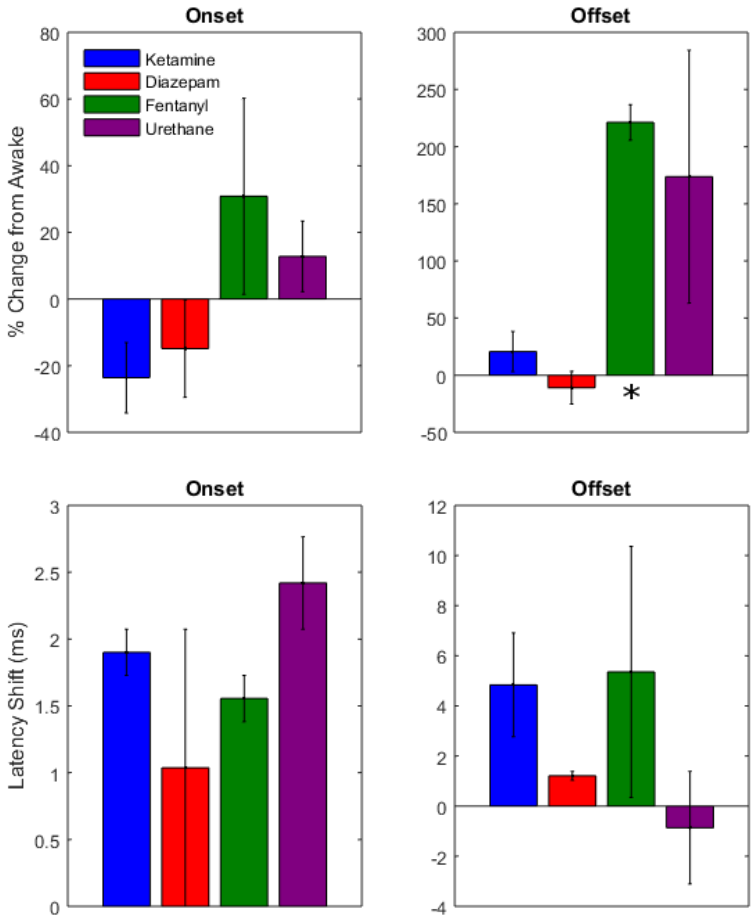

Figure 7.17: Percentage change in peak-to-peak amplitude of the LFP response to both the tone onset and offset of a 6 kHz, 100ms pure tone relative to the awake condition (Top). Latency shift in the N1 of the LFP response to both the tone onset and offset of a 6 kHz, 100ms pure tone relative to the awake condition (Bottom)

The changes in LFP amplitude under these anaesthetics represent changes in the underlying neural firing activity. An increase in response will most commonly represent either an increase in firing rate or an increased coherence of spike timings. For this experiment the multiunit spiking activity recorded simultaneously with the EP data can be analysed and it can be seen, as predicted, that the onset responses to the tone will be enhanced under fentanyl. This increase in firing rate could easily be an explanation for the increase in the negative deflection in the LFP signal. However, it can be seen that in all of the duration conditions there does not appear to be a substantial increase in the amount of spikes in response to the tone offset. There is a visible

increase in the two longest durations but not of the magnitude of the difference between the awake and fentanyl conditions in the LFP.

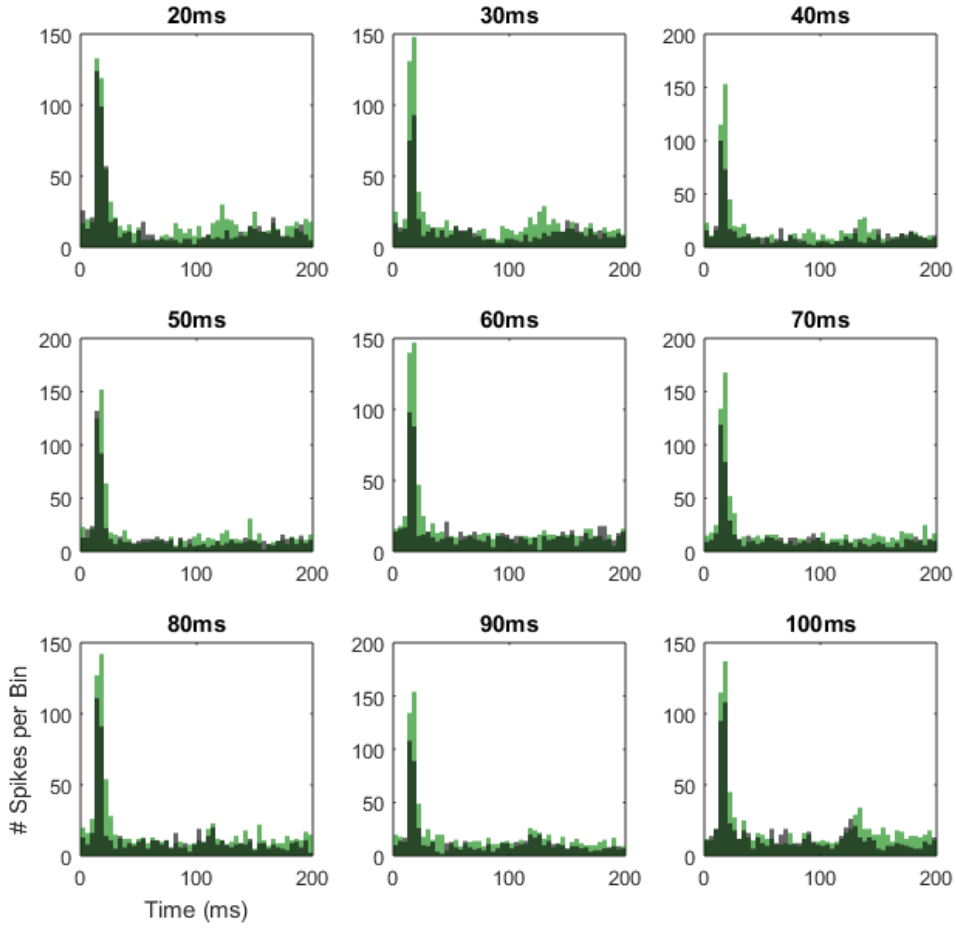

Figure 7.18: Combined PSTHs of all electrode sites within one GP in response to variable duration 6 kHz pure tones. Responses while awake (grey) and under fentanyl (green) are shown.

GPs were played pairs of broadband noise tokens with variable ISIs to measure their recovery from adaptation. As with the previous EEG experiments, adaptation appears to be modulated strongly by anaesthesia. Ketamine does not appear to have a large effect on the degree of adaptation but the other three anaesthetics tested all show a large increase in the degree of adaptation.

As before time constants were derived by fitting an exponential function to the mean data. The awake GPs showed a faster recovery in the LFPs than the earlier EEG recordings (τ=30ms). Unlike the previous recordings ketamine did not speed up recovery of adaptation but instead showed a slight increase

(τ=70ms). Diazepam, fentanyl and urethane all showed large increases in recovery time constant (τ=180, 160 and 210ms respectively).

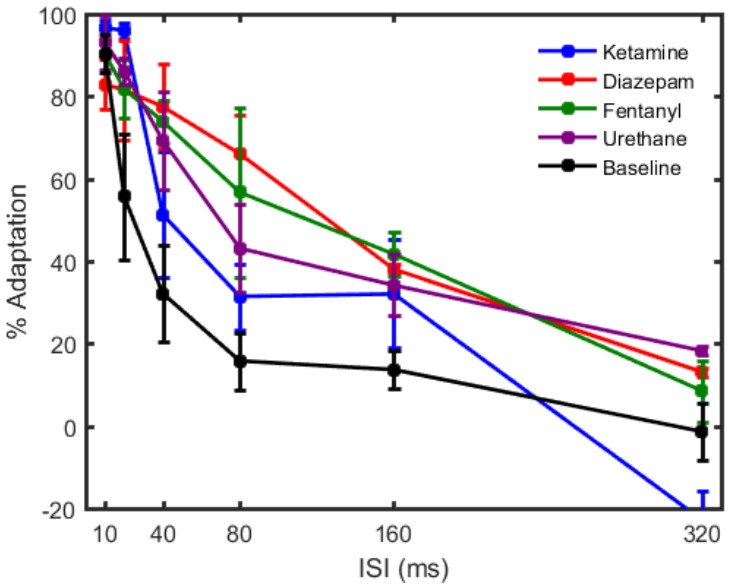

Figure 7.19: Adaptation percentage derived from the amplitude of a broadband probe stimulus preceded by a broadband adapter with a variable ISI. Recorded from GP LFPs while awake and under various anaesthetics

The GPs were also tested using the 0ms ISI pure tone adapter-probe methodology to assess the effects of anaesthesia on neural tuning. Overall there appears to be little effect of anaesthesia on the tuning measured by this technique. Ketamine, urethane and fentanyl show very little difference between 0-75 cents and at wider frequency separations there is just a small increase in degree of adaptation. Surprisingly, considering its effects on the time course of recovery, diazepam appears to show a universal release from adaptation compared to the awake condition.

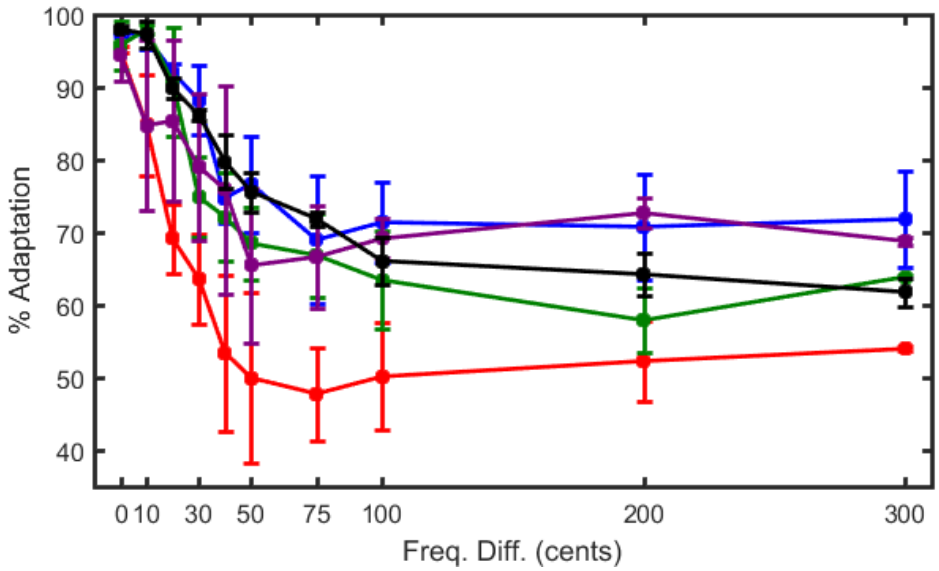

Figure 7.20: Frequency selectivity of pure tone adaptation measured with a 0ms adapter-probe ISI under multiple anaesthetics measured from local field potentials.

AM tones were played to the anaesthetised GPs to assess the effect on the frequency following ability of the auditory cortex. For urethane, diazepam and fentanyl there appears to be an overall effect of enhancing the power of LFP ASSRs in response to low modulation rates (<20Hz) and all anaesthetics show an attenuation of the responses to higher modulation rates (<20Hz).

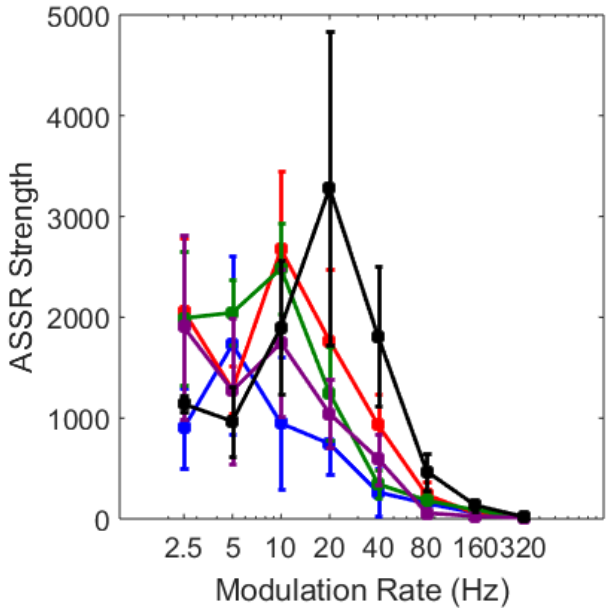

Figure 7.21: Anaesthesia will modulate the power of the ASSR response to AM tones with varying effects depending on the modulation rate

The multiunit activity in response to the ASSRs was analysed using the population and single site SC methods presented earlier in the chapter. This analysis is a measure of the ability of the cortex to phase lock to the modulation frequency of the AM tones. In the population response, unlike the LFP results, this analysis shows a universal abolishment of cortical population phase locking under all anaesthetics tested. In the analysis of the individual sites however only diazepam shows a complete suppression whereas ketamine shows a partial suppression at all frequencies. Fentanyl shows no effect at the two lowest frequencies, an enhancement at 10Hz then a suppression at higher frequencies.

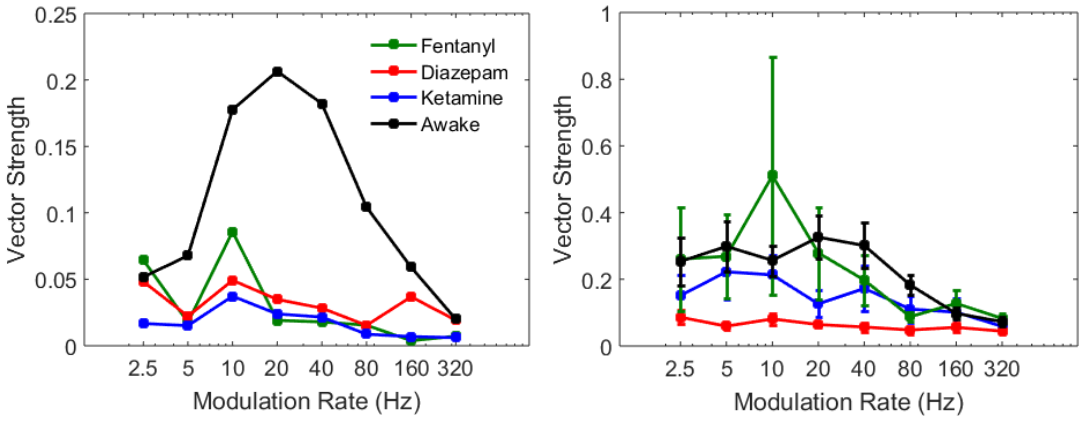

Figure 7.22: Population (Left) and individual site (Right) SC of spiking units in GP primary auditory cortex, measured under multiple anaesthetics within one GP

7.2.3 Discussion

This section has dealt with finding intracortical and neural correlates of the far field potentials measured in the previous section, looking into the effects of anaesthesia on basic auditory processing and adaptation in GP cortex.

In the previous literature there has not been many papers looking directly at the effects of anaesthesia on intracortical recordings in auditory cortex so the majority of the effects seen here are novel.

The changes in oscillatory power under each anaesthetic recorded in these GPs show almost identical patterns to those seen previously in Chapter 6.

This is a positive sign to see in terms of robustness and replicability as the patterns can be replicated in two separate batches of GPs using different recording techniques. As oscillatory activity is grossly comparable across large areas of the brain it is not unexpected that the LFPs would correlate so strongly with the EEG recorded results. This suggests the same regions of significant change would be seen in the LFPs once a greater number of GPs are tested.

The effects of anaesthesia on the neural response to broadband clicks demonstrates the first major deviation in results between the EEG and LFP recorded potentials. In the EEG results both ketamine and diazepam showed very little effect on click evoked AEP amplitude, fentanyl showed a non-significant change, trending towards an increase in amplitude, and urethane showed a significant amplitude increase of ~50% over the awake amplitude. In the LFPs however there is a universal suppressive effect on click evoked AEP amplitude across all anaesthetics. As primary auditory cortex in GPs is more responsive to pure tones than clicks (Wallace et al., 2000) it might be expected that the retention of its responsiveness to clicks under anaesthesia may be less robust than that in response to tones. As it is the long latency components, such as the P2 and the late potential, that appear to be most strongly attenuated by anaesthesia in these recordings it could be expected this represents a suppression of activity in the higher order belt regions. However this also leaves the question of what brain area is contributing to the increases in AEP amplitude seen in the EEG. This would need further investigation into the changes in amplitude at different sources.

The tone evoked responses are more consistent when comparing between the LFPs and EEG responses. This is as expected as the primary auditory cortex is characterised by its high responsiveness to pure tones so any changes in response to pure tones are likely to originate here. Again ketamine and diazepam show small effects on the amplitude of both the onset and offset and fentanyl shows a large enhancement of the response to both onsets

and offsets. Urethane however shows the opposite response in the LFPs to those seen in the EEG, having little effect on the onset and a large increase to the offset. This could either be due to the comparatively large variability in comparison to the other anaesthetics or could represent effects happening outside of primary auditory cortex.

To try to better understand the large enhancement seen in the LFPs in response to tone onsets and offsets under fentanyl the underlying multiunit activity was analysed. As expected for the onset response there is a consistent increase in firing rate across all the duration conditions. For the offset however there is no visible increase in offset response at the population level, especially not at a size relative to the increase in LFP amplitude, and very few individual units showing an increase in offset responsiveness. There could be several reasons for this, firstly it could be a problem of under-sampling and just more units need to be analysed. It could also be a temporal blurring effect by comparing either between multiunits or the single units within the multiunit clusters that the offset may not be as temporally consistent between units and disappear by averaging into the PSTH. This is supported by the longer and more spread out offset EP. Additionally, it is plausible the majority of the offset response could originate from a different region of cortex. The LFP can pick up sources >600μm laterally from the electrode placement (Kajikawa and Schroeder, 2011) so it is still possible the offset responses could originate outside of primary auditory cortex.

The results of the adaptation recovery experiment mostly replicate those seen in the EEG results. Diazepam, fentanyl and urethane will all increase the recovery time constant of adaptation above that of the awake animal but in these results more consistently between the anaesthetics than was seen before. In the EEG results ketamine showed a reduction of the adaptation recovery time, allowing faster recovery than when awake but in these results it shows no substantial change from the awake condition. The results seen here for both ketamine and diazepam mirror previously published results

about the effects of adaptation on units in primary auditory cortex (Wehr and Zador, 2005).

The close agreement between the EEG and LFP results, combined with the analysis earlier about the change in the baseline time constants, suggests potentially that anaesthesia will affect primary auditory cortex and the surrounding belt regions in a similar manner in terms of adaptation recovery. This could be aided by the fact that the broadband noise used for this experiment will activate broader areas of cortex than pure tone stimuli.

The 0ms ISI adaptation tuning experiment was developed in the late stages of the experiments so it was not possible to collect data under multiple anaesthetics for the EEG experiments so this data does not yet have an EEG version to compare with. These results however show that for all the tested anaesthetics show little to no effect on tuning in this experiment. For responses with a 0-100 cent frequency separation there is no meaningful difference between the results. Beyond this, at higher frequency separations, there may be a slight increase in adaptation but this is not shown to be shown as significant at this time. This lack of effect when previous studies have shown sharpening of frequency selectivity with anaesthesia (Gaese et al., 2001; Merry et al., 2016) could add evidence to the possibility that this experiment is measuring sub-cortical tuning. In general, anaesthesia has smaller effects on the properties of sub-cortical neurons in the auditory system (Smith and Mills, 1989; van Looij et al., 2004; Ruebhausen et al., 2012) and has been shown to have no effect on tuning in GP IC neurons (Astl et al., 1996) and the avian auditory midbrain (Schumacher et al., 2011).

The LFP derived ASSRs show stable power in the awake GPs between 2.5 to 40Hz. It appears this will be enhanced at 5-10Hz under ketamine and fentanyl and at 10Hz by diazepam. At frequencies >40Hz there is a suppressive effect on the ASSR power compared to when awake. It could be thought this is a correlate of the oscillatory activity as most of the anaesthetics show an enhancement of low frequency power and suppression of high frequencies

but with one exception, ketamine. In the oscillatory power shifts, ketamine shows an enhancement of high frequency oscillations but here still shows suppression of the high frequency ASSRs.

Several previous studies have looked into the effects of anaesthesia on ASSRs in human EEG. These studies found that ketamine enhances the amplitude of ASSRs (Plourde et al., 1997) whereas ASSRs were supressed under a fentanyl derivative (Plourde and Boylan, 1991) and propofol (Plourde and Victoria, 1996). The methodology used makes it slightly harder to make a direct comparison as all of these were tested at 40Hz modulation rate as this is the maximal frequency in humans so this could relate directly to 40Hz in the GP or to the GP's preferred frequency of 10Hz. If considering either of these then the results are not replicated as all three of the analogues in this study show roughly similar results at each individual frequency. The species difference in oscillatory frequencies and maximal ASSR frequency may therefore be the reasons for these differences.

As a comparison the multiunit phase locking strength was also tested under each anaesthesia to see the effects. Using the SC method on the population response it was shown there was a universal elimination of phase locking when combining the PSTHs of all 16 multiunit clusters. When considering each site separately there is more of a differentiation between the anaesthetics. Diazepam shows a universal elimination of the phase locking response, from the raw results likely due to a generalised suppression of spiking activity. Ketamine shows a less complete suppression, reducing the vector strength by around 50% at all frequencies. Fentanyl shows the closest response in its multiunit responses compared with its LFP, with an enhancement of vector strength at 10Hz modulation but a suppression at high frequencies. As all three of these anaesthetics showed enhancement of the LFPs at 10Hz and only one shows it in the multiunit its possible this could be an issue of under-sampling and more units need to be recorded from. Less

likely would be that the anaesthetics cause the LFP enhancement from different sources within the auditory cortex.

It could be said that the suppression under ketamine and diazepam could be due to a reduced signal quality over time in this animal losing the ability to record from multiunit spiking but the anaesthetic order for this GP was ketamine, fentanyl, diazepam so at minimum the ketamine and fentanyl results appear genuine. By checking the multiunit spiking response to pure tones in the same diazepam recording session it's shown most of the sites still demonstrate a robust onset response countering this argument.

Overall it can be shown that anaesthesia will for the most part show the same effects for the LFP derived results as those from the EEG recordings. The main deviation from this is the click evoked responses, for which their primary source may be outside the spatial range of our recordings. The effects on oscillations, pure tones and adaptation are however replicable between the two methodologies. It has also been shown anaesthesia may have implications for temporal processing of complex sounds as it will impair the frequency following abilities of the auditory cortex.

Chapter 8

Conclusions

8.1 Adaptation and Frequency Selectivity

In this thesis we have looked into the effects of adaptation on frequency selectivity in auditory cortex. This has included human EEG, GP EEG, LFPs and spiking activity and is complimented by computational modelling work.

8.1.1 Repetition Induced Sharpening

Our initial EEG experiments looked into the effects of the temporal patterning of adapters on the frequency selectivity of the probe response. These experiments demonstrated an onset driven sharpening of frequency selectivity, termed repetition induced sharpening (RIS), and a non-monotonic level of adaptation with increasing adapter duration. Further experiments also showed that by using an attentional manipulation that adaptation frequency selectivity can be attentionally modulated.

The RIS effect found here is mostly novel and while Briley *et al.* (2013) originally showed a sharpening with increased number of adapters we have demonstrated that this is an onset driven effect which will build up over time, is long lasting and is independent of attention.

A computational model capable of replicating the experimental results using a neurocomputational architecture was tested and found to contain neurons within it that replicate, frequency specific adaptation (FSA) (Scholes, 2009). This model helps reconcile Briley's experiments and the findings of Scholes by providing a framework where neurons displaying FSA can result in a population response displaying RIS. While this model can replicate most of the data it has been fit to it does not appear to be able to replicate results using a

different timescale to those it has been trained on so will need further development.

Continuing this work, to better characterise the phenomenon and to provide further fitting data for the computational model a greater range of temporal parameters can be tested. In Briley's paper they found altering the gap between a single adapter and probe had no effect of tuning however Lanting *et al.* (2013) found that the time constant of recovery from adaptation changed with the number of preceding adapters. This could suggest the frequency tuning would change at different adapter-probe ISIs. We have shown the sharpening effect is robust to changing rates of adapters but the silence gap from the final adapter to the probe is always constant in these experiments so it is as yet unclear the full relationship between tuning and recovery from adaptation so this is an area to potentially be investigated.

8.1.2 Adaptation in Guinea Pigs

The effects of adaptation on GP auditory cortex were assessed and major differences between them and the humans were found, primarily in the temporal domain. In human EEG a time constant of recovery from adaptation was derived as 1200ms (Lanting et al., 2013). In our awake GP EEG results this was found to be 60ms. This means GP adaptation will last a twentieth of the time it does it humans and, as such, major changes are needed between the temporal parameters used in experiments between humans and GPs. This could simply be an effect of species as with a smaller brain the GP may be able to signal faster and recover faster but also this could be an effect on where on the brain it is recorded from. In human EEG the primary auditory cortex does not make a large contribution in our measure of adaptation as we, and Lanting, use the N1-P2 complex to quantify adaptation whereas primary auditory cortex mainly affects the P1 peak of the AEP in humans (Godey et al., 2001). In the GP's lissencephalic brains we can easily pick up the primary auditory cortex and from our experiments it was found to be the most likely generator for the N1 peak. This means identical brain regions are not being recorded from in

each species meaning this could be a contributing factor. However due to the magnitude of the difference between the two species it is unlikely this is the only cause.

Other changes seen between the humans and GPs include changes to frequency selectivity where in all recordings so far it appears as though GPs potentially have sharper adaptation tuning than the humans. Initially this was thought of as potentially being caused by the effects of anaesthesia sharpening receptive fields but in the awake recordings this trend continued (Figure 6.10). Given the broader tuned cochlear filters in GPs it has been unclear how the cortical tuning of GPs could be sharper than that in humans. The easiest explanation would be the difference in recording type and scale, much like in the temporal recovery experiments, where the brain regions being recorded from are not directly comparable. This could be tested by either taking recordings from human mid-latency responses which have more contribution from human primary auditory cortex or recording from higher order GP auditory areas.

A combination of these changes in temporal and frequency differences between humans and GPs led to us being unable to record RIS in GPs. Using the same stimuli in anaesthetised GPs as the humans led to no effect of repetition or duration being seen, simply seeing the same tuning at all time points. In the awake GPs the confound of the offset response of the adapter interacting with the onset of the probe meant it wasn't possible to quantify adaptation using the same methods as in the humans. A new method was developed that was not directly comparable but gave a measure of adaptation tuning. Using this method it was shown that we could produce a stimulus induced sharpening of adaptation in GPs but this was not onset selective like in the humans but occurred with both increases of duration and number of adapters.

While the GPs do not produce all the same responses as humans and operate on different timescales they can still be used as a model of basic auditory adaptation mechanisms.

8.1.3 ASSRs

It was shown that ASSRs can be reliably evoked in awake GP cortex, measurable through LFPs. These responses can be evoked with AM tones with modulation rates from 2.5-160Hz and produce peaks at the fundamental frequency and harmonics of the modulation rate. This response is sensitive to frequency changes with 1Hz differences in modulation rate being easily resolvable.

AM tones can also induce a phase locking response in cortical neurons in the auditory cortex. This response mostly aligns with results seen in the LFPs but strength of measured phase locking in low frequency modulation rates appears to vary depending on analysis method. This phase locking appears to be strongest around 10Hz modulation rate as compared to the 40Hz preference in humans (Ross et al., 2003).

These results act as foundation work for an additional comparative method of measuring adaptation in both humans and GPs. By playing two simultaneous AM tones with similar, fixed modulation rates the carrier frequency of one can be varied and the change in power of the oscillations of the other can be measured (Ross et al., 2003). This method allows another way to potentially measure adaptation frequency tuning in both humans and GPs. By using reasonably low modulation rates sub-cortical adaptation can be mostly avoided. This method does however have the problems of not being able to investigate repetition or duration however as it is a steady state measure.

8.2 Relating Neural Activity to EEG

In this thesis we have also covered making neural recordings from multiple scales, comparing results recorded from EEG, LFPs and spiking activity.

8.2.1 Local Field Potentials

Through this project we have recorded LFPs in awake GPs and simultaneous LFPs and EEG in anaesthetised GPs. In our GPs with simultaneously recorded EEG and LFP we saw that we can attribute certain sources to the separate parts of the EEG waveform. The P1 component appears to be primarily generated by the IC whereas the N1 represents the primary auditory cortex. The later components such as the P2 and late potential appear to be generated by the auditory belt regions.

In almost every experiment so far there is a very close agreement between the EEG and LFPs, both within one animal and also comparing between EEG GPs and LFP GPs. This suggests that, depending on the stimulus set, using EEG in GPs could be a quicker and simpler methodology to determine the activity of the auditory cortex than LFPs with comparable results.

The only major deviation seen between the EEG and LFPs in these experiments was comparing the effects on click evoked responses under different anaesthetics. The EEG click evoked AEPs showed a range of different modulations under the anaesthetics, from slight suppression to large enhancements but in the LFPs there was a universal suppression under all anaesthetics. This demonstrates some of the variability of responses of different spatial regions of the auditory cortex. This being the only major difference seen is probably biased by the majority of other stimuli used in this project being pure tone stimuli, meaning the largest response will be from primary auditory cortex where we recorded from. The click evoked responses however will result in the largest responses coming from non-primary regions which will be picked up in the EEG but not the LFPs. This potentially suggests that more differences would be seen between the EEG and LFPs when recording the pure tone based experiments from non-primary auditory regions.

8.2.2 Multiunit Activity

Multiunit activity was recorded both from acutely implanted anaesthetised GPs and chronically implanted GPs while awake and anaesthetised. All these recordings were made with linear silicon shank depth electrodes.

In early recordings the stimulus parameters had not been optimised in frequency and therefore reliable spiking activity was not seen in the recordings made. This led to using an RMS measure of neural activity in the 300-3000Hz frequency band. This MUA showed similar tuning and temporal properties to the EEG and LFP activity

In later recordings in awake GPs the time course of the parameters was shifted and the stimulation frequency was moved closer to the centre of the GPs hearing range which evoked larger LFPs and resulted in the ability to record neural spike trains. These multiunits were tuned similarly to the LFPs of the same electrodes. Their tuning changed with depth, with the deepest electrodes showing broad tuning, responding to frequencies in a ~3.5 octave bandwidth, and the most superficial electrodes showing sharper tuning with a ~1 octave bandwidth.

This spiking activity was analysed for the time and frequency separation adaptation experiments and for the most part showed very close agreement with the results derived from both EEG and LFPs. This is also true for the analysis of phase locking to AM tones when comparing to the ASSRs recorded from LFPs. The first real deviation seen between the recordings of multiunits and LFPs was the changes between awake and anaesthetised states under fentanyl, looking at the tone offset responses. Under fentanyl both onset and offset responses in EEG and LFPs are enhanced, when investigating this in the spiking activity there was a visual increase in the onset response but no substantial difference in the offset response. In the CSD (Figure 6.13) it can be seen there is a large spatio-temporal area of activity seen during the tone onset but very little seen during the offset, even though there is a large deflection in the LFP. This could reflect the large spatial reach of the LFPs compared to the

very narrow range of recording multiunits meaning LFPs can pick up responses from nearby brain areas not reflected in the spikes.

So far the units have been analysed as all spiking activity within each electrode site as a multiunit but to gain higher quality data this can be spike sorted, attempting to separate out the individual neurons' responses. This may also help denoise some of the recordings as it is possible in these recordings that some detected spikes may be artefactual. Additionally all the analysis used so far on the multiunits has combined their properties to look at a population average response. For a greater insight into the underlying coding of the phenomena the range of properties of the individual neurons should be investigated.

8.3 Anaesthesia and Auditory Cortex

Sections of this thesis have looked into the effects of anaesthesia on sensory processing in GP cortex, both auditory and some visual with some investigation of their cross modal interaction.

8.3.1 Spontaneous Oscillations

Recordings of spontaneous neural activity were made in awake and anaesthetised animals. Under most of the anaesthetics tested there was an identical pattern of changes compared to the awake recordings, namely an increase in power of low frequency activity (<15Hz) and a suppression of high frequency power (>40Hz). The only exception to this was ketamine which showed an enhancement of high frequency activity (50-120Hz) due a phenomenon called cortical disinhibition (Miller et al., 2016).

This study replicated the effects of previous studies of loss of consciousness (LOC) in humans under propofol anaesthesia showing that the onset of the increase in low frequency oscillatory power has a sudden, rapid onset taking <1s to establish (Lewis et al., 2012; Mukamel et al., 2014). We have built on their work showing this effect will also occur in GPs and showing that is an effect independent of anaesthetic agent.

To build on this work further the effects of anaesthesia on the spontaneous rates of spiking activity can be investigated. This can help analyse the baseline excitability of the network and should be reasonably easy to analyse from the recordings made already.

Another effect found from the oscillatory activity was a modulation of the brain closer to a state of criticality. Criticality is a network property based on the stability of propagation of events through the system and has been demonstrated theoretically and experimentally to have benefits to sensory neural coding (Shew and Plenz, 2013; Gautam et al., 2015). Under all the anaesthetics tested there was an overall shift toward criticality, making the network more unstable. This appeared to contradict the conclusions of previous published results (Solovey et al., 2015) but further analysis of their data showed this experiment appears to replicate a section of their data that was not analysed as part of their main conclusion.

This method of measuring criticality from population recordings is a reasonably gross measure and could be backed up by further analysis of the spontaneous firing activity during these recordings. Criticality in single units can be shown by the statistics of neural avalanches, burst firing sessions where multiple single units will spontaneously fire together (Dehghani et al., 2012; Lombardi et al., 2016). In a critical system the frequency of occurrence of the sizes of these events will be power law distributed and the quality of fit of the system dynamics to a power law distribution is taken as a measure of how close to criticality the system is. This analysis could take place on the recordings already made of spontaneous activity.

8.3.2 Auditory Evoked Potentials

Auditory evoked potentials were recorded from either chronically implanted EEG electrodes or LFP depth electrodes in GP auditory cortex while awake and under a range of anaesthetics.

Tone evoked AEPs were most strongly affected by fentanyl and urethane, both of which caused significant increases in response amplitude to both onsets and offsets. Given their mechanisms of action it is uncertain how they could be achieving this directly but may be altering network properties such as the balance of excitation and inhibition. This can be investigated by further analysing the spiking activity in response to these stimuli. For example, one potentially informative analysis to perform would be to assess the different effects on excitatory and inhibitory cells. It is possible to putatively characterise single neurons as excitatory or inhibitory based on their spike morphologies (Barthó et al., 2004). Using this it could be possible to track the balance of excitation and inhibition through the course of the system.

As discussed earlier, the click evoked responses show different modulations by anaesthesia in the EEG and LFP recorded results, indicative of variable responses in different regions of the auditory cortex. One way of investigating the effects of the anaesthesia induced changes on multiple regions of the auditory cortex at once could be to use voltage sensitive dyes to better localise which regions contribute to the amplitude changes in response seen (Nishimura and Song, 2012). These dyes will fluoresce in areas of the brain that are locally active and using a camera mounted above the area being recorded from this can be tracked over time and space. The main issue with this is due to the need for stability of the image it would be difficult to get an awake baseline condition.

In this thesis the majority of neural tuning metrics used to assess tuning were using indirect measures such as adaptation. A more direct measure would be to analyse the receptive fields of the LFPs and multiunit sites under each anaesthetic and measure directly changes in bandwidth of their RF. It has previously been shown anaesthesia under a pentobarbital/chloral hydrate mix can lead to tuning changes in the RF of single units (Gaese et al., 2001). Given the variety of effects seen in these experiments these tuning changes may also not be constant between anaesthetics.

8.3.3 Visual Cortex

With two electrodes in the chronically implanted EEG GPs over visual cortex this allowed the ability to record both auditory and visually evoked responses in visual cortex.

VEPs were evoked in visual cortex using brief, wide field flashes of white light and showed a reliable response with a longer latency than the AEPs in auditory cortex. Under all the anaesthetics tested the response seen while awake was abolished entirely and replaced with a much slower waveform with an N1 peak at 100ms instead of 40ms when awake. It is unclear how this change occurs, potentially due to effects of anaesthesia on the retina or optic nerve, but due to the invariance between the anaesthetics this could be simply an effect of unconsciousness rather than specifically from the anaesthetics.

While no visually evoked response could be detected in auditory cortex, an AEP could easily be seen in visual cortex in the awake GPs. This response even adapted in the temporal separation experiments, showing a recovery constant of 250ms. Under the anaesthetics however, like the VEPs, there was a universal abolishment of cross-modal responses. This could either represent the separation of disparate brain regions due to fragmentation of neural networks under anaesthesia (Lewis et al., 2012) or, due to the large effects of anaesthesia on VEPs, it could be that the visual cortex is more susceptible to anaesthesia than auditory cortex.

8.3.4 Adaptation

In GPs with either EEG or LFP implants we recorded responses to adapting stimuli under multiple anaesthetics. In the temporal separation experiments it was shown diazepam, fentanyl and urethane, the three anaesthetics with direct effects on GABA signalling would all dramatically slow the recovery from adaptation as recorded in both the EEG and LFP results. Ketamine however showed no effect in the LFP results and an increase in recovery speed in the EEG results. As before with results seen with differences between the LFP and

EEG results then it is likely there may be another brain region outside primary auditory cortex that is the cause for these differences.

In the adapter-probe frequency separation experiments recordings were only made in the LFP GPs. From the results so far it appears most of the anaesthetics show no changes to the adaptation tuning. The one potential exception is urethane which in this experiment showed a dramatic broadening of frequency selectivity. So far this has only been shown in a single test so could be artefactual so more repeats are needed but if it were a genuine effect would raise questions as to the mechanism.

8.4 Summary

(1) Humans display repetition induced sharpening (RIS) of frequency selectivity in auditory cortex when presented with a sequence of adapters with multiple onsets but not for long duration, single onset adapters.

(2) Adaptation in human auditory cortex is a non-monotonic function of adapter length.

(3) RIS can be simulated by a neurocomputational model with individual components within it that display FSA characteristics.

(4) RIS does not interact with attention but attention will independently sharpen frequency selectivity of adaptation.

(5) There is currently no evidence that RIS occurs in GP auditory cortex.

(6) GPs show dramatically more rapid recovery from adaptation than seen in humans.

(7) Anaesthetic choice will substantially alter the population response of auditory cortex to basic auditory stimuli.

(8) Anaesthesia modulates recovery from adaptation. Most notably with anaesthetics enhancing GABA signalling which will substantially slow recovery.

Chapter 9

References

Abbott LF, Dayan P (1999) The Effect of Correlated Variability on the Accuracy of a Population Code. Neural Comput 11:91–101.

Adibi M, Clifford CWG, Arabzadeh E (2013a) Informational basis of sensory adaptation: entropy and single-spike efficiency in rat barrel cortex. J Neurosci 33:14921–14926.

Adibi M, McDonald JS, Clifford CWG, Arabzadeh E (2013b) Adaptation improves neural coding efficiency despite increasing correlations in variability. J Neurosci 33:2108–2120.

Anderson LA, Christianson GB, Linden JF (2009) Stimulus-specific adaptation occurs in the auditory thalamus. J Neurosci 29:7359–7363.

Antunes FM, Malmierca MS (2011) Effect of auditory cortex deactivation on stimulus-specific adaptation in the medial geniculate body. J Neurosci 31:17306–17316.

Antunes FM, Nelken I, Covey E, Malmierca MS (2010) Stimulus-specific adaptation in the auditory thalamus of the anesthetized rat. PLoS One 5.

Antunes LM, Roughan J V, Flecknell PA (2003) Excitatory effects of fentanyl upon the rat electroencephalogram and auditory-evoked potential responses during anaesthesia. Eur J Anaesthesiol 20:800–808.

Arviv O, Goldstein A, Shriki O (2015) Near-Critical Dynamics in Stimulus-Evoked Activity of the Human Brain and Its Relation to Spontaneous Resting-State Activity. J Neurosci 35:13927–13942.

Ashida G, Carr CE (2010) Effect of sampling frequency on the measurement of phase-locked action potentials. Front Neurosci 4:1–9.

Astl J, Popelar J, Kvasnak E, Syka J (1996) Comparison of Response Properties of Neurons in the Inferior Colliculus of Guinea Pigs Under Difference Anesthetics. Audiology 35:335–345.

Avissar M, Furman AC, Saunders JC, Parsons TD (2007) Adaptation Reduces Spike-Count Reliability But Not Spike-Timing Precision of Auditory Nerve Responses. J Neurosci 27:6461–6472.

Ayala YA, Malmierca MS (2015) Cholinergic Modulation of Stimulus-Specific Adaptation in the Inferior Colliculus. J Neurosci 35:12261–12272.

Ayala YA, Pérez-González D, Duque D, Nelken I, Malmierca MS (2013) Frequency discrimination and stimulus deviance in the inferior colliculus and cochlear nucleus. Front Neural Circuits 6:119.

Ayala YA, Pérez-González D, Malmierca MS (2015) Stimulus-specific adaptation in the inferior colliculus: The role of excitatory, inhibitory and modulatory inputs. Biol Psychol.

Barlow H, Foldiak P (1989) Adaptation and Decorrelation in the Cortex. In: The Computing Neuron (Durbin R, Miall C, Mitchison G, eds), pp 54–72. Addison-Wesley Publishing Company.

Barthó P, Hirase H, Monconduit L, Zugaro M, Harris KD, Buzsáki G (2004) Characterization of neocortical principal cells and interneurons by network interactions and extracellular features. J Neurophysiol 92:600–608.

Bartlett EL, Wang X (2005) Long-Lasting Modulation by Stimulus Context in Primate Auditory Cortex. J Neurophysiol 94:83–104.

Bauerle P, Behrens W Von Der, Kossl M, Gaese BH (2011) Stimulus-Specific Adaptation in the Gerbil Primary Auditory Thalamus Is the Result of a Fast Frequency-Specific Habituation and Is Regulated by the Corticofugal System. J Neurosci 31:9708–9722.

Benucci A, Saleem AB, Carandini M (2013) Adaptation maintains population homeostasis in primary visual cortex. Nat Neurosci 16:724–729 Available

at: http://dx.doi.org/10.1038/nn.3382.

Berger JI, Coomber B, Wells TT, Wallace MN, Palmer AR (2014) Changes in the response properties of inferior colliculus neurons relating to tinnitus. Front Neurol 5.

Bidet-Caulet A, Fischer C, Besle J, Aguera P-E, Giard M-H, Bertrand O (2007) Effects of Selective Attention on the Electrophysiological Representation of Concurrent Sounds in the Human Auditory Cortex. J Neurosci 27:9252–9261.

Briley PM, Breakey C, Krumbholz K (2013) Evidence for Pitch Chroma Mapping in Human Auditory Cortex. Cereb Cortex 23:2601–2610.

Briley PM, Krumbholz K (2013) The specificity of stimulus-specific adaptation in human auditory cortex increases with repeated exposure to the adapting stimulus. J Neurophysiol 110:2679–2688.

Brosch M, Scheich H (2008) Tone-sequence analysis in the auditory cortex of awake macaque monkeys. Exp Brain Res 184:349–361.

Brosch M, Schreiner CE (2000) Sequence sensitivity of neurons in cat primary auditory cortex. Cereb Cortex 10:1155–1167.

Burkard RF, Don M (2007) The Auditory Brainstem Response. In: Auditory Evoked Potentials: Basic Principles and Clinical Applications (Burkard RF, Don M, Eggermont JJ, eds), pp 229–253.

Buzsáki G, Anastassiou C a, Koch C (2012) The origin of extracellular fields and currents--EEG, ECoG, LFP and spikes. Nat Rev Neurosci 13:407–420.

Calford MB, Semple MN (1995) Monaural inhibition in cat auditory cortex. J Neurophysiol 73:1876–1891.

Carlson NR (2006) Audition, the Body Senses, and the Chemical Senses. In: Physiology of Behaviour, pp 210. Pearson.

Cederholm JME, Froud KE, Wong ACY, Ko M, Ryan AF, Housley GD (2012)

Differential actions of isoflurane and ketamine-based anaesthetics on cochlear function in the mouse. Hear Res 292:71–79.

Chechik G, Anderson MJ, Bar-Yosef O, Young ED, Tishby N, Nelken I (2006) Reduction of Information Redundancy in the Ascending Auditory Pathway. Neuron 51:359–368.

Chen C, Read HL, Escabi MA (2012) Precise Feature Based Time Scales and Frequency Decorrelation Lead to a Sparse Auditory Code. J Neurosci 32:8454–8468.

Connell MNO, Barczak A, Schroeder CE, Lakatos P (2014) Layer Specific Sharpening of Frequency Tuning by Selective Attention in Primary Auditory Cortex. J Neurosci 34:16496–16508.

Dean I, Harper NS, McAlpine D (2005) Neural population coding of sound level adapts to stimulus statistics. Nat Neurosci 8:1684–1689.

Dehghani N, Hatsopoulos NG, Haga ZD, Parker RA, Greger B, Halgren E, Cash SS, Destexhe A (2012) Avalanche analysis from multielectrode ensemble recordings in cat, monkey, and human cerebral cortex during wakefulness and sleep. Front Physiol 3 AUG:1–18.

Duncan CC, Barry RJ, Connolly JF, Fischer C, Michie PT, Näätänen R, Polich J, Reinvang I, Van Petten C (2009) Event-related potentials in clinical research: guidelines for eliciting, recording, and quantifying mismatch negativity, P300, and N400. Clin Neurophysiol 120:1883–1908.

Duque D, Malmierca MS, Caspary DM (2014) Modulation of stimulus-specific adaptation by GABAA receptor activation or blockade in the medial geniculate body of the anesthetized rat. J Physiol 592:729–743.

Edeline J-M (2012) Beyond traditional approaches to understanding the functional role of neuromodulators in sensory cortices. Front Behav Neurosci 6:1–14.

Eggermont JJ (2007) Electric and Magnetic Fields of Synchronous Neural

Activity. In: Auditory Evoked Potentials: Basic Principles and Clinical Applications (Burkard RF, Don M, Eggermont JJ, eds), pp 2–21. Lippincott Williams and Wilkins.

Ehrlichman RS, Maxwell CR, Majumdar S, Siegel SJ (2008) Deviance-elicited changes in event-related potentials are attenuated by ketamine in mice. J Cogn Neurosci 20:1403–1414.

Einevoll GT, Kayser C, Logothetis NK, Panzeri S (2013) Modelling and analysis of local field potentials for studying the function of cortical circuits. Nat Rev Neurosci 14:770–785.

Evans E, Pratt S, Spenner H, Cooper N (1992) Comparisons of physiological and behavioural properties: auditory frequency selectivity. In: Advances in the Biosciences Vol. 83 (Cazals Y, Horner K, Demany L, eds), pp 159–170. Pergamon Press, Oxford.

Feng Y, Yin S, Wang J (2009) Cortical responses to amplitude modulation in guinea pigs and the effects of general anesthesia by pentobarbital. Hear Res 247:40–46.

Finlayson PG (1999) Post-stimulatory suppression, facilitation and tuning for delays shape responses of inferior colliculus neurons to sequential pure tones. Hear Res 131:177–194.

Franke F, Fiscella M, Sevelev M, Roska B, Hierlemann A, da Silveira RA (2015) Structures of Neural Correlation and How They Favor Coding. Neuron 89:409–422.

Friauf E, Fischer AU, Fuhr MF (2015) Synaptic plasticity in the auditory system: a review. Cell Tissue Res 361:177–213.

Fritz JB, Elhilali M, Shamma SA (2007) Adaptive changes in cortical receptive fields induced by attention to complex sounds. J Neurophysiol 98:2337–2346.

Froemke RC, Schreiner CE (2015) Synaptic plasticity as a cortical coding scheme.

Curr Opin Neurobiol 35:185–199.

Gaese BH, Ostwald J, Carrasco A, Kok M a, Lomber SG (2001) Anesthesia Changes Frequency Tuning of Neurons in the Rat Primary Auditory Cortex. J Neurophysiol 86:1062–1066.

Gage GJ, Stoetzner CR, Richner T, Brodnick SK, Williams JC, Kipke DR (2012) Surgical Implantation of Chronic Neural Electrodes for Recording Single Unit Activity and Electrocorticographic Signals. J Vis Exp:3–5.

Galambos R, Makeig S, Talmachoff PJ (1981) A 40-Hz auditory potential recorded from the human scalp. PNAS 78:2643–2647.

Gautam SH, Hoang TT, McClanahan K, Grady SK, Shew WL (2015) Maximizing Sensory Dynamic Range by Tuning the Cortical State to Criticality. PLoS Comput Biol 11:1–15.

Godey B, Schwartz D, De Graaf JB, Chauvel P, Liégeois-Chauvel C (2001) Neuromagnetic source localization of auditory evoked fields and intracerebral evoked potentials: A comparison of data in the same patients. Clin Neurophysiol 112:1850–1859.

Goldberg JM, Brown PB (1969) Response of binaural neurons of dog superior olivary complex to dichotic tonal stimuli: some physiological mechanisms of sound localization. J Neurophysiol 32:613–636.

Grill-Spector K, Henson R, Martin A (2006) Repetition and the brain: neural models of stimulus-specific effects. Trends Cogn Sci 10:14–23.

Gunduz-Bruce H, Reinhart RMG, Roach BJ, Gueorguieva R, Oliver S, D'Souza DC, Ford JM, Krystal JH, Mathalon DH (2012) Glutamatergic modulation of auditory information processing in the human brain. Biol Psychiatry 71:969–977.

Hara K, Harris RA (2002) The anesthetic mechanism of urethane: the effects on neurotransmitter-gated ion channels. Anesth Analg 94:313–318.

Harris DM, Dallos P (1979) Forward masking of auditory nerve fiber responses. J Neurophysiol 42:1083–1107.

Heekeren K, Daumann J, Neukirch A, Stock C, Kawohl W, Norra C, Waberski TD, Gouzoulis-Mayfrank E (2008) Mismatch negativity generation in the human 5HT2A agonist and NMDA antagonist model of psychosis. Psychopharmacology (Berl) 199:77–88.

Heinke W, Kenntner R, Gunter TC, Sammler D, Olthoff D, Koelsch S (2004) Sequential effects of increasing propofol sedation on frontal and temporal cortices as indexed by auditory event-related potentials. Anesthesiology 100:617–625.

Horn B, Pilge S, Kochs EF, Stockmanns G, Hock A, Schneider G (2009) A combination of electroencephalogram and auditory evoked potentials separates different levels of anesthesia in volunteers. Anesth Analg 108:1512–1521.

Jääskeläinen IP, Ahveninen J (2014) Auditory-cortex short-term plasticity induced by selective attention. Neural Plast 2014:216731.

Jääskeläinen IP, Pekkonen E, Hirvonen J, Sillanaukee P, Näätänen R (1996) Mismatch negativity subcomponents and ethyl alcohol. Biol Psychol 43:13–25.

Javitt DC, Steinschneider M, Schroeder CE, Arezzo JC (1996) Role of cortical N-methyl-D-aspartate receptors in auditory sensory memory and mismatch negativity generation: implications for schizophrenia. PNAS 93:11962–11967.

Kajikawa Y, Schroeder CE (2011) How local is the local field potential? Neuron 72:847–858.

Khan ZP, Ferguson CN, Jones RM (1999) Alpha-2 and imidazoline receptor agonists. Their pharmacology and therapeutic role. Anaesthesia 54:146–165.

Kohn A (2007) Visual adaptation: physiology, mechanisms, and functional benefits. J Neurophysiol 97:3155–3164.

Lanting CP, Briley PM, Sumner CJ, Krumbholz K (2013) Mechanisms of adaptation in human auditory cortex. J Neurophysiol 110:973–983.

Lehmann D, Skrandies W (1980) Reference-free identification of components of checkerboard-evoked multichannel potential fields. Electroencephalogr Clin Neurophysiol 48:609–621.

Lewis LD, Weiner VS, Mukamel E a, Donoghue J a, Eskandar EN, Madsen JR, Anderson WS, Hochberg LR, Cash SS, Brown EN, Purdon PL (2012) Rapid fragmentation of neuronal networks at the onset of propofol-induced unconsciousness. PNAS 109.

Lieder F, Daunizeau J, Garrido MI, Friston KJ, Stephan KE (2013) Modelling trial-by-trial changes in the mismatch negativity. PLoS Comput Biol 9.

Liegeois-Chauvel C, Musolino A, Badier JM, Marquis P, Chauvel P (1994) Evoked potentials recorded from the auditory cortex in man: evaluation and topography of the middle latency components. Electroencephalogr Clin Neurophysiol Evoked Potentials 92:204–214.

Linden JF, Schreiner CE (2003) Columnar Transformations in Auditory Cortex ? A Comparison to Visual and Somatosensory Cortices. Cereb Cortex 13:83–89.

Lombardi F, Herrmann HJ, Plenz D, de Arcangelis L (2016) Temporal correlations in neuronal avalanche occurrence. Sci Rep 6.

Loquet G, Meyer K, Rouiller EM (2003) Effects of intensity of repetitive acoustic stimuli on neural adaptation in the ventral cochlear nucleus of the rat. Exp Brain Res 153:436–442.

Magri C, Mazzoni A, Logothetis NK, Panzeri S (2012) Optimal band separation of extracellular field potentials. J Neurosci Methods 210:66–78.

Makeig S, Jung TP, Bell AJ, Ghahremani D, Sejnowski TJ (1997) Blind separation

of auditory event-related brain responses into independent components. PNAS 94:10979–10984.

Marblestone AH, Zamft BM, Maguire YG, Shapiro MG, Cybulski TR, Glaser JI, Amodei D, Stranges PB, Kalhor R, Dalrymple D a, Seo D, Alon E, Maharbiz MM, Carmena JM, Rabaey JM, Boyden ES, Church GM, Kording KP (2013) Physical principles for scalable neural recording. Front Comput Neurosci 7:137.

Maris E, Oostenveld R (2007) Nonparametric statistical testing of EEG- and MEG-data. J Neurosci Methods 164:177–190.

May PJC, Tiitinen H (2010) Mismatch negativity (MMN), the deviance-elicited auditory deflection, explained. Psychophysiology 47:66–122.

Merry D, Wells T, Adjamian P, Palmer AR, Sumner C (2016) Frequency Selectivity of Neurons in the Ferret Auditory Cortex measured using Notched Noise Masking. In: Association for Research in Otolaryngology 39th MidWinter Meeting, pp PS718. San Diego, CA.

Metherate R, Ashe JH (1994) Facilitation of an NMDA receptor-mediated EPSP by paired-pulse stimulation in rat neocortex via depression of GABAergic IPSPs. J Physiol 481:331–348 Available at: http://www.pubmedcentral.nih.gov/articlerender.fcgi?artid=1155933&tool=pmcentrez&rendertype=abstract.

Mill R, Coath M, Wennekers T, Denham SL (2011) A neurocomputational model of stimulus-specific adaptation to oddball and Markov sequences. PLoS Comput Biol 7.

Miller OH, Moran JT, Hall BJ (2016) Two cellular hypotheses explaining the initiation of ketamine's antidepressant actions: Direct inhibition and disinhibition. Neuropharmacology 100:17–26.

Mukamel EA, Pirondini E, Babadi B, Wong KFK, Pierce ET, Harrell PG, Walsh JL, Salazar-Gomez AF, Cash SS, Eskandar EN, Weiner VS, Brown EN, Purdon PL

(2014) A Transition in Brain State during Propofol-Induced Unconsciousness. J Neurosci 34:839–845.

Murray MM, Brunet D, Michel CM (2008) Topographic ERP analyses: a step-by-step tutorial review. Brain Topogr 20:249–264.

Näätänen R, Paavilainen P, Rinne T, Alho K (2007) The mismatch negativity (MMN) in basic research of central auditory processing: a review. Clin Neurophysiol 118:2544–2590.

Neumaier A, Schneider T (2001) Estimation of parameters and eigenmodes of multivariate autoregressive models. ACM Trans Math Softw 27:27–57.

Nishimura M, Song WJ (2012) Temporal Sequence of Visuo-Auditory Interaction in Multiple Areas of the Guinea Pig Visual Cortex. PLoS One 7.

Niwa M, Johnson JS, O'Connor KN, Sutter ML (2013) Differences between primary auditory cortex and auditory belt related to encoding and choice for AM sounds. J Neurosci 33:8378–8395.

Okamoto H, Stracke H, Wolters CH, Schmael F, Pantev C (2007) Attention improves population-level frequency tuning in human auditory cortex. J Neurosci 27:10383–10390.

Okamoto H, Stracke H, Zwitserlood P, Roberts LE, Pantev C (2009) Frequency-specific modulation of population-level frequency tuning in human auditory cortex. BMC Neurosci 10:1.

Pérez-González D, Hernández O, Covey E, Malmierca MS (2012) GABA(A)-mediated inhibition modulates stimulus-specific adaptation in the inferior colliculus. PLoS One 7.

Pfurtscheller G, Cooper R (1975) Frequency Dependance of the Transmission of the EEG from Cortex to Scalp. Electroencephalogr Clin Neurophysiol 38:93–96.

Plourde G, Baribeau J, Bonhomme V (1997) Ketamine increases the amplitude of

the 40-Hz auditory steady-state response in humans. Br J Anaesth 78:524–529.

Plourde G, Boylan JF (1991) The auditory steady state response during Sufentanil anaesthesia. Br J Anaesth 66:683–691.

Plourde G, Victoria R (1996) The Effects of Propofol on the 40-Hz Auditory Steady-State Response and on the Electroencephalogram in Humans. Anesth Analg 82:1015–1022.

Popelár J, Syka J, Berndt H, Popelar J (1987) Effect of noise on auditory evoked responses in awake guinea pigs. Hear Res 26:239–247.

Pressnitzer D, Sayles M, Micheyl C, Winter IM (2008) Perceptual Organization of Sound Begins in the Auditory Periphery. Curr Biol 18:1124–1128.

Quiroga RQ, Nadasdy Z, Ben-Shaul Y (2004) Unsupervised spike detection and sorting with wavelets and superparamagnetic clustering. Neural Comput 16:1661–1687.

Quiroga RQ, Panzeri S (2009) Extracting information from neuronal populations: information theory and decoding approaches. Nat Rev Neurosci 10:173–185.

Rabinowitz NC, Willmore BDB, King AJ, Schnupp JWH (2013) Constructing Noise-Invariant Representations of Sound in the Auditory Pathway. PLoS Biol 11.

Restuccia D, Della Marca G, Marra C, Rubino M, Valeriani M (2005) Attentional load of the primary task influences the frontal but not the temporal generators of mismatch negativity. Cogn Brain Res 25:891–899.

Ross B, Draganova R, Picton TW, Pantev C (2003) Frequency specificity of 40-Hz auditory steady-state responses. Hear Res 186:57–68.

Ruebhausen MR, Brozoski TJ, Bauer C a (2012) A comparison of the effects of isoflurane and ketamine anesthesia on auditory brainstem response (ABR) thresholds in rats. Hear Res 287:25–29.

Samra SK, Lilly DJ, Rush NL, Kirsch MM (1984) Fentanyl Anesthesia and Human Brain-stem auditory Evoked Potentials. Anesthesiology 61:261–265.

Sanna E, Mascia MP, Klein RL, Whiting PJ, Biggio G, Harris RA (1995) Actions of the general anesthetic propofol on recombinant human GABAA receptors: influence of receptor subunits. J Pharmacol Exp Ther 274:353–360.

Schneider G, Hollweck R, Ningler M, Stockmanns G, Kochs EF (2005) Detection of Consciousness by Electroencephalogram and Auditory Evoked Potentials. Anesthesiology 103:934–943.

Scholes C (2009) Investigations of the Effects of Sequential Tones on the Responses of Neurons in the Guinea Pig Primary Auditory Cortex.

Scholes C, Palmer AR, Sumner CJ (2011) Forward suppression in the auditory cortex is frequency-specific. Eur J Neurosci 33:1240–1251.

Schumacher JW, Schneider DM, Woolley SMN (2011) Anesthetic state modulates excitability but not spectral tuning or neural discrimination in single auditory midbrain neurons. J Neurophysiol 106:500–514.

Schwender D, Conzen P, Klasing S, Finsterer U, Poppel E, Peter K (1995) The Effects of Anesthesia with Increasing End-Expiratory Concentrations of Sevoflurane on Midlatency Auditory Evoked Potentials. Anesth Analg 81:817–822.

Schwender D, Rimkus T, Haessler R, Klasing S, Poppel E, Peter K (1993) Effects of increasing doses of alfenanil, fentanyl and morphine on mid-latency auditory evoked potentials. Br J Anaesth 71:622–628.

Schwindt PC, Spain WJ, Foehring RC, Chubb MC, Crill WE (1988) Slow conductances in neurons from cat sensorimotor cortex in vitro and their role in slow excitability changes. J Neurophysiol 59:450–467.

Sculthorpe LD, Ouellet DR, Campbell KB (2009) MMN elicitation during natural sleep to violations of an auditory pattern. Brain Res 1290:52–62.

Shackleton TM, Liu LF, Palmer AR (2009) Responses to diotic, dichotic, and alternating phase harmonic stimuli in the inferior colliculus of Guinea pigs. J Assoc Res Otolaryngol 10:76–90.

Shew WL, Plenz D (2013) The Functional Benefits of Criticality in the Cortex. Neurosci 19:88–100.

Shim SS, Grant ER, Singh S, Gallagher MJ, Lynch DR (1999) Actions of butyrophenones and other antipsychotic agents at NMDA receptors: relationship with clinical effects and structural considerations. Neurochem Int 34:167–175.

Simpson TP, Manara AR, Kane NM, Barton RL, Rowlands CA, Butler SR (2002) Effect of propofol anaesthesia on the event-related potential mismatch negativity and the auditory-evoked potential N1. Br J Anaesth 89:382–388.

Sloan T, Sloan H, Rogers J (2010) Nitrous oxide and isoflurane are synergistic with respect to amplitude and latency effects on sensory evoked potentials. J Clin Monit Comput 24:113–123.

Smith DI, Mills JH (1989) Anesthesia effects: auditory brain-stem response. Electroencephalogr Clin Neurophysiol 72:422–428.

Solomon SG, Kohn A (2014) Moving sensory adaptation beyond suppressive effects in single neurons. Curr Biol 24:1012–1022.

Solovey G, Alonso LM, Yanagawa T, Fujii N, Magnasco MO, Cecchi G a., Proekt A (2015) Loss of Consciousness Is Associated with Stabilization of Cortical Activity. J Neurosci 35:10866–10877.

Solovey G, Miller KJ, Ojemann JG, Magnasco MO, Cecchi G a. (2012) Self-Regulated Dynamical Criticality in Human ECoG. Front Integr Neurosci 6:1–9.

Stronks HC, Aarts MCJ, Klis SFL (2010) Effects of isoflurane on auditory evoked potentials in the cochlea and brainstem of guinea pigs. Hear Res 260:20–29.

Sumner CJ, O'Mard LP, Lopez-Poveda EA, Meddis R (2003) A nonlinear filter-

bank model of the guinea-pig cochlear nerve: Rate responses. Acoust Soc Am 113:3264–3274.

Sussman ES (2007) A New View on the MMN and Attention Debate: The Role of Context in Processing Auditory Events. J Psychophysiol 21.

Syka J, Rybalko N, Popelář J (1994) Enhancement of the auditory cortex evoked responses in awake guinea pigs after noise exposure. Hear Res 78:158–168.

Szymanski FD, Garcia-Lazaro JA, Schnupp JWH (2009) Current Source Density Profiles of Stimulus-Specific Adaptation in Rat Auditory Cortex. J Neurophysiol 102:1483–1490.

Tlumak AI, Durrant JD, Delgado RE, Boston JR (2011) Steady-state analysis of auditory evoked potentials over a wide range of stimulus repetition rates: profile in adults. Int J Audiol 50:448–458.

Ulanovsky N, Las L, Nelken I (2003) Processing of low-probability sounds by cortical neurons. Nat Neurosci 6:391–398.

Umbricht D, Schmid L, Koller R, Vollenweider FX, Hell D, Javitt DC (2000) Ketamine-Induced Deficits in Auditory and Visual Context-Dependent Processing in Healthy Volunteers. Arch Gen Psychiatry 57:1139–1147.

van Looij M a J, Liem S-S, van der Burg H, van der Wees J, De Zeeuw CI, van Zanten BG a (2004) Impact of conventional anesthesia on auditory brainstem responses in mice. Hear Res 193:75–82.

Varghese L, Bharadwaj HM, Shinn-Cunningham BG (2015) Evidence against attentional state modulating scalp-recorded auditory brainstem steady-state responses. Brain Res 1626:146–164.

Vugt MK van, Sederberg PB, Kahana MJ (2007) Comparison of spectral analysis methods for characterizing brain oscillations. J Neurosci Methods 162:49–63.

Wallace MN, Palmer AR (2008) Laminar differences in the response properties of

cells in the primary auditory cortex. Exp Brain Res 184:179–191.

Wallace MN, Rutkowski RG, Palmer AR (2000) Identification and localisation of auditory areas in guinea pig cortex. Exp Brain Res 132:445–456.

Wark B, Lundstrom BN, Fairhall A (2007) Sensory adaptation. Curr Opin Neurobiol 17:423–429.

Wehr M, Zador AM (2005) Synaptic mechanisms of forward suppression in rat auditory cortex. Neuron 47:437–445.

Woods DL (1995) The component structure of the N1 wave of the human auditory evoked potential. Electroencephalogr Clin Neurophysiol 44:102–109.

Yamakura T, Bertaccini E, Trudell JR, Harris RA (2001) Anesthetics and ion channels: molecular models and sites of action. Annu Rev Pharmacol Toxicol 41:23–51.

Yamakura T, Harris RA (2000) Effects of Gaseous Anesthetics Nitrous Oxide and Xenon on Ligand-gated Ion Channels. Anesthesiology 93:1095–1101.

Zurita P, Villa AEP, de Ribaupierre Y, de Ribaupierre F, Rouiller EM (1994) Changes of single unit activity in the cat's auditory thalamus and cortex associated to different anesthetic conditions. Neurosci Res 19:303–316.